UNIVERSIDAD NACIONAL DEL LITORAL

DOCTORADO EN INGENIERÍA

Degradación De Contaminantes Emergentes Presentes En Aguas Reales Empleando Reactores Solares A Escala Planta Piloto

Bárbara Natalí Giménez

FICH
FACULTAD DE INGENIERÍA Y CIENCIAS HÍDRICAS

INTEC
INSTITUTO DE DESARROLLO TECNOLÓGICO PARA LA INDUSTRIA QUÍMICA

CIMEC
CENTRO DE INVESTIGACIÓN DE MÉTODOS COMPUTACIONALES

sinc(*i*)
INSTITUTO DE INVESTIGACIÓN EN SEÑALES, SISTEMAS E INTELIGENCIA COMPUTACIONAL

Tesis de Doctorado **2024**

UNIVERSIDAD NACIONAL DEL LITORAL
Facultad de Ingeniería y Ciencias Hídricas
Instituto de Desarrollo Tecnológico para la Industria Química
Centro de Investigación de Métodos Computacionales
Instituto de Investigación en Señales, Sistemas e Inteligencia Computacional

DEGRADACIÓN DE CONTAMINANTES EMERGENTES PRESENTES EN AGUAS REALES EMPLEANDO REACTORES SOLARES A ESCALA PLANTA PILOTO

Bárbara Natalí Giménez

Tesis remitida al Comité Académico del Doctorado
como parte de los requisitos para la obtención
del grado de
DOCTOR EN INGENIERIA
Mención Ambiental
de la
UNIVERSIDAD NACIONAL DEL LITORAL

2024

Secretaría de Posgrado, Facultad de Ingeniería y Ciencias Hídricas, Ciudad Universitaria, Paraje “El Pozo”, S3000, Santa Fe, Argentina

UNIVERSIDAD NACIONAL DEL LITORAL
Facultad de Ingeniería y Ciencias Hídricas
Instituto de Desarrollo Tecnológico para la Industria Química
Centro de Investigación de Métodos Computacionales
Instituto de Investigaciones en Señales, Sistemas e Inteligencia Computacional

DEGRADACIÓN DE CONTAMINANTES EMERGENTES PRESENTES EN AGUAS REALES EMPLEANDO REACTORES SOLARES A ESCALA PLANTA PILOTO

Bárbara Natalí Giménez

Lugar de Trabajo:
INTEC
Instituto de Desarrollo Tecnológico para la Industria Química
Facultad de Ingeniería y Ciencias Hídricas
Universidad Nacional del Litoral

Director:
Leandro Oscar Conte INTEC (CONICET-UNL)

Co-director:
Agustina Violeta Schenone INTEC (CONICET-UNL)

Jurado Evaluador:
Dr. Roberto CANDAL (USAM - Conicet)
Dr. Ricardo TORRES PALMA (UDEA. Colombia)
Dr. Enelton FAGNANI (UNICAMP, Brasil)

2024

(1994–2024) 30 años de la Consagración Constitucional de la Autonomía y Autarquía Universitaria en Argentina.

UNIVERSIDAD NACIONAL DEL LITORAL
Facultad de Ingeniería y Ciencias Hídricas

Santa Fe, 26 de Julio de 2024.

Como miembros del Jurado Evaluador de la Tesis de Doctorado en Ingeniería titulada ***"Degradación de contaminantes presentes en aguas reales empleando reactores solares a escala piloto"***, desarrollada por la Lic. Bábara Natalí GIMÉNEZ, en el marco de la Mención "Ambiental", certificamos que hemos evaluado la Tesis y recomendamos que sea aceptada como parte de los requisitos para la obtención del título de Doctor en Ingeniería.

La aprobación final de esta disertación estará condicionada a la presentación de dos copias encuadernadas de la versión final de la Tesis ante el Comité Académico del Doctorado en Ingeniería.

Dr. Roberto Candal	Dr. Ricardo Torres Palma	Dr. Enelton Fagnani

Santa Fe, 26 de Julio de 2024.

Certifico haber leído la Tesis, preparada bajo mi dirección en el marco de la Mención "Ambiental" y recomiendo que sea aceptada como parte de los requisitos para la obtención del título de Doctor en Ingeniería.

.....	.....
Dra. Agustina Schenone	Dr. Leandro Conte
Codirector de Tesis	Director de Tesis

Mg. Virginia Margenet
Subsecretaria de Posgrado FICH
Coordinadora Académica
EGA - MGA - FICH - UNL

Dependencia
Dirección postal
Código postal, Ciudad, Argentina
Teléfono
Correo electrónico

DECLARACIÓN DEL AUTOR

Esta Tesis ha sido remitida como parte de los requisitos para la obtención del grado académico Doctorado en Ingeniería, Mención Ambiental, ante la Universidad Nacional del Litoral y ha sido depositada en la Biblioteca de la Facultad de Ingeniería y Ciencias Hídricas para que esté a disposición de sus lectores bajo las condiciones estipuladas por el reglamento de la mencionada Biblioteca.

Citaciones breves de esta Tesis son permitidas sin la necesidad de un permiso especial, en la suposición de que la fuente sea correctamente citada. Solicitudes de permiso para la citación extendida o para la reproducción parcial o total de ese manuscrito serán concebidos por el portador legal del derecho de propiedad intelectual de la obra.

TESIS POR COMPILACIÓN

La presente tesis se encuentra organizada bajo el formato de Tesis por Compilación, aprobado en la resolución N% 255/17 (Expte. N% 888317-17) por el Comité Académico de la Carrera Doctorado en Ingeniería, Facultad de Ingeniería y Ciencias Hídricas, Universidad Nacional del Litoral (UNL). De dicha resolución:

"En el caso de optar por la Tesis por Compilación, ésta consistirá en una descripción técnica de al menos 30 páginas, redactada en español e incluyendo todas las investigaciones abordadas en la tesis. Se deberán incluir las secciones habituales indicadas a continuación en la Sección Contenidos de la Tesis. Los artículos científicos publicados por el autor, en el idioma original de las publicaciones, deberán incluirse en un Anexo con el formato unificado al estilo general de la Tesis indicado en la Sección Formato. El Anexo deberá estar encabezado por una sección donde el tesista detalle para cada una de las publicaciones cuál ha sido su contribución. Esta sección deberá estar avalada por su director de Tesis. El documento central de la Tesis debe incluir referencias explícitas a todas las publicaciones anexadas y presentar una conclusión que muestre la coherencia de dichos trabajos con el hilo conceptual y metodológico de la tesis. Los artículos presentados en los anexos podrán ser artículos publicados, aceptados para publicación (en prensa) o en revisión."

AGRADECIMIENTOS

En primer lugar, deseo expresar mi agradecimiento al Estado Argentino, por la Educación Pública y el apoyo al Desarrollo de la Ciencia y la Tecnología en los diferentes ámbitos, sin los cuales este proyecto de investigación y de vida, no hubieran existido. En especial al Consejo Nacional de Investigaciones Científicas y Técnicas (CONICET) por la beca otorgada en estos años de estudio e investigación. Asimismo, mi gratitud hacia la Universidad Nacional del Litoral (UNL), institución que me ha acogido desde la educación secundaria hasta mi formación de posgrado, y en particular a la Facultad de Ingeniería y Ciencias Hídricas (FICH), por brindarme la oportunidad de realizar este Doctorado. Finalmente, mi agradecimiento al Instituto de Desarrollo para la Industria Química (INTEC), por brindarme el espacio para desarrollar mis tareas de investigación, y a todos los que son parte de él, por su constante colaboración con mi persona, cada vez que lo requería.

Deseo agradecer sinceramente y de corazón a todas las personas que han colaborado, directa o indirectamente, para la elaboración de esta tesis.

A mis directores, Leandro y Agustina, les agradezco no solo por su orientación y apoyo constantes en la realización de esta tesis, sino también por su confianza en mí, su aliento para superarme constantemente y su paciencia al guiarme. Además, agradezco a mi quien fue mi primer director, Orlando, por siempre estar atento a mi formación y a mi desempeño durante todos estos años.

A mis padres, María Eva y Jorge, quienes me han acompañado durante toda mi vida, nunca han dejado de apoyarme y han luchado incansablemente para que pueda alcanzar mis sueños, les expreso mi más profundo agradecimiento. También quiero agradecer a mis hermanos, Bruno y Bautista, y a mi primo Julián.

A todos mis amigos, de la escuela, la facultad y de la vida, y a las nuevas amistades que surgieron en este recorrido que fue la realización del doctorado, les agradezco por su constante compañía, sus risas, sus ánimos y, simplemente, por su incondicional amistad.

Por último, quiero agradecer a los miembros del Jurado, por su interés y dedicación en la evaluación de esta tesis.

ÍNDICE GENERAL

ÍNDICE DE FIGURAS

ÍNDICE DE TABLAS

RESUMEN

Los Contaminantes de Preocupación Emergente (CPEs) abarcan una amplia variedad de compuestos químicos (pesticidas, fármacos, compuestos perfluorados, etc.) que no son en la mayoría de los casos eficientemente degradados por las plantas de tratamiento de aguas residuales convencionales. En este sentido, los Procesos Avanzados de Oxidación (PAOs), representan una alternativa de depuración muy atractiva.

Esta tesis doctoral propone el estudio sistemático, modelado y optimización del proceso foto-Fenton (PFF), principalmente a pH cercano a la neutralidad, utilizando Ferrioxalato como catalizador (proceso foto-Fenton/Ferrioxalato, PFF/FeOxa), aplicado a la remoción de paracetamol (PCT, modelo de contaminante) presente en medios acuosos reales, empleando reactores a escala laboratorio y planta piloto, activados con radiación artificial o solar natural.

En una fase inicial de investigación, se emplearon herramientas de diseño de experimentos y superficie de respuesta para analizar la influencia de las principales variables operacionales sobre la efectividad del PFF/FeOxa. Esto es, temperatura, radiación, pH, concentración de especies activas, entre las más significativas.

Posteriormente, se procedió al modelado de los PFF y PFF/FeOxa bajo diversas condiciones de reacción, empleando reactores fotoquímicos con múltiples geometrías y fuentes de radiación. Para todos los modelos desarrollados se obtuvo una correcta representación de las medidas experimentales realizadas para las principales especies reactivas presentes.

Considerando que el peróxido de hidrógeno es uno de los principales reactivos químicos del PFF/FeOxa, se evaluó la intensificación del proceso empleando diversas estrategias de dosificación de agente oxidante (puntual, continua y combinaciones de ambas). Estas estrategias operativas fueron analizadas en reactores de laboratorio, y escaladas a reactores solares escala planta piloto empleando matrices acuosas reales.

Se demostró la efectividad de los PFF y PFF/FeOxa estudiados en la eliminación no sólo del contaminante modelo y sus intermediarios de reacción, sino también en la reducción de la toxicidad de los efluentes tratados (*Vibrio fischeri* y células VERO), incluso en el tratamiento de matrices acuosas reales empleando fotorreactores activados con luz solar.

ABSTRACT

Contaminants of Emerging Concern (CECs) include a wide variety of chemical compounds (pesticides, pharmaceuticals, perfluorinated compounds, etc.) that, in most cases, are not efficiently degraded by conventional wastewater treatment plants. In this sense, Advanced Oxidation Processes (AOPs) represent a highly attractive purification alternative.

This doctoral thesis proposes the systematic study, modelling, and optimization of the photo-Fenton process (PFP), primarily at near-neutral pH, using ferrioxalate as a catalyst (photo-Fenton/Ferrioxalate process, PFP/FeOxa). This process is applied to the removal of paracetamol (PCT, a model contaminant) present in real aqueous media, employing laboratory-scale and pilot-scale reactors, activated with artificial or natural solar radiation.

In the initial phase of this research, the design of experiments and response surface methodology were employed to analyze the influence of the main operational variables on the effectiveness of the PFP/FeOxa. These variables include temperature, radiation, pH, and concentration of active species, among the most significant.

Subsequently, PFP and PFP/FeOxa modelling was conducted under various reaction conditions, employing photochemical reactors with multiple geometries and radiation sources. All developed models provided a satisfactory representation of the experimental measurements conducted for the main reactive species.

Considering that hydrogen peroxide is one of the main chemical reagents in PFP/FeOxa, the intensification of the process was evaluated using various oxidant dosing strategies (punctual, continuous, and combinations of both). These operational strategies were analyzed in laboratory reactors and scaled to solar reactors at the pilot plant scale using real aqueous matrices.

The effectiveness of the studied processes (PFF and PFF/FeOxa) was demonstrated in the removal not only of the model contaminant and its reaction intermediates but also in the reduction of the toxicity of the treated effluents (Vibrio fischeri and VERO cells), even in the treatment of real aqueous matrices employing solar-activated photoreactors.

Capítulo 1. INTRODUCCIÓN

1.1. Presentación de la problemática

1.1.1. Disponibilidad y calidad del agua

El agua, un recurso vital escaso, es esencial para la supervivencia humana y el equilibrio ambiental. Aproximadamente el 70% de las extracciones de agua dulce a nivel mundial están destinadas a la agricultura, seguida de la industria (casi un 20%) y los usos domésticos (o municipales; en torno al 12%). Las aguas subterráneas proporcionan alrededor del 25% de toda el agua utilizada para el riego y la mitad del agua dulce para fines domésticos. Sin embargo, estas cifras varían considerablemente en función del nivel de desarrollo económico de un país, siendo que los países de ingresos más altos utilizan más agua para la industria, mientras que los países de ingresos más bajos utilizan el 90% (o más) de su agua para el riego agrícola (United Nations 2024). En Argentina, los porcentajes de agua dulce dedicados a cada área son los siguientes: agricultura y ganadería 80% (en especial el riego), doméstico (y municipal) 13%, e industria 7% (Ministerio de Salud 2024).

Aunque el uso del agua se ha estabilizado en países de América del Norte y Europa desde principios de la década de 1980, la demanda mundial de agua dulce ha estado aumentando en poco menos del 1% por año hasta la fecha. La demanda creciente está impulsada principalmente por una combinación de desarrollo socioeconómico y cambios relacionados en los patrones de consumo, de modo que la mayor parte de este aumento se encuentra en regiones que experimentan un rápido desarrollo económico, especialmente en economías emergentes (Ritchie y Roser 2024). La evidencia disponible

sugiere que la demanda de agua del sector municipal (o doméstico) ha experimentado un aumento considerable en comparación con los otros sectores y es probable que continúe creciendo a medida que las poblaciones urbanas aumenten y los sistemas de suministro de agua y saneamiento que atienden estas ciudades se expandan (Otto y Schleifer 2020).

No existe una relación clara entre el producto interior bruto (PBI) per cápita de un país y su disponibilidad de agua. Aunque se estima que el 80% de los puestos de empleo de los países con bajos ingresos dependen del agua, esencialmente debido a la predominancia de la agricultura, que es el principal sector de empleo (Connor y Chaves Pacheco 2024). A su vez, en estos países, la mala calidad del agua ambiental se debe principalmente a los bajos niveles de tratamiento de las aguas residuales (urbanas, industriales, agrícolas y ganaderas), pudiendo incluso extender la contaminación hasta las fuentes de agua potable (Szopińska et al. 2022) . Desafortunadamente, en estos países los datos sobre la calidad del agua siguen siendo escasos (United Nations 2023).

Al respecto, en un estudio que abarcaba 258 ríos del mundo, se hallaron altas concentraciones de antimicrobianos (por encima de los límites de seguridad), originadas a partir de aguas residuales domésticas tratadas insuficientemente, cría de ganado y acuicultura (Wilkinson et al. 2022). Mientras que los efectos exactos en la salud humana y la biodiversidad no se conocen completamente, la evidencia sugiere que este tipo de contaminación probablemente aumentará la resistencia a los antimicrobianos, entre otros inconvenientes (Reichert et al. 2019).

El escaso o nulo tratamiento de aguas residuales se debe, en parte, a la falta de políticas regulatorias y sistemas de monitoreo robustos que permitan promover el uso responsable del agua (Sandoval et al. 2024). Incluso en Argentina, la población está expuesta constantemente a diversos contaminantes presentes en el agua, que no son

monitoreados habitualmente debido a la obsolescencia de las normas vigentes (Aparicio y De Gerónimo 2024).

Por lo tanto, la creciente demanda de agua, principalmente en países en desarrollo, y la aparición de nuevos contaminantes subrayan la necesidad de seguir investigando para proteger la salud humana y el medio ambiente.

1.1.2. Contaminantes de Preocupación Emergente (CPEs)

En las últimas décadas, los avances científicos y tecnológicos han impulsado el crecimiento urbano, industrial y la explotación de recursos a nivel global, lo que ha generado desafíos significativos en la gestión de residuos y la aparición de nuevos contaminantes ambientales. Este fenómeno se manifiesta en la detección de una amplia gama de compuestos químicos previamente no identificados, así como de compuestos que, si bien son conocidos, comparten la característica común de no estar contemplados en las normativas regulatorias en cuanto a la calidad del agua (Sandoval et al. 2024). Estos contaminantes, conocidos como Contaminantes de Preocupación Emergente (CPEs), incluyen una amplia gama de compuestos químicos, como pesticidas, productos farmacéuticos, disruptores endócrinos, productos de cuidado personal, entre otros. Su presencia plantea riesgos para la salud ambiental, requiriendo una identificación y monitoreo adecuados para desarrollar estrategias efectivas de gestión y mitigación (Khan et al. 2022).

Según la sección de “Control y Monitoreo Ambiental” del Ministerio del Interior de la República Argentina los CPEs “son compuestos de distinto origen y naturaleza química que con el avance de las técnicas y el instrumental de detección están siendo ampliamente detectados en los cuerpos de agua y suelo, y que tienen el potencial de

impactar negativamente sobre el ambiente, así como causar efectos adversos sobre la salud animal y de las personas" (Ministerio del Interior 2024).

La detección de CPEs en vertidos residuales, aguas superficiales y subterráneas se ha vinculado con actividades domésticas, comerciales, industriales y agrícolas, siendo estas últimas una fuente importante debido a la lixiviación de contaminantes hacia los cuerpos de agua (Mukhopadhyay et al. 2022). Es fundamental destacar que la persistencia y capacidad de desplazamiento a largas distancias de los CPEs han dado lugar a su detección en áreas donde nunca antes se habían utilizado. La complejidad y diversidad de estas fuentes de contaminación subrayan la necesidad de abordar de manera integral el problema de los CPEs en el agua, considerando tanto sus orígenes domésticos como industriales (Hale et al. 2020).

Numerosos estudios indican que los procesos de tratamiento de aguas residuales convencionales (tratamientos fisicoquímicos, biológicos y de desinfección) no son eficientes en la remoción de la mayoría de los CPEs (Rizzo et al. 2019; Gosset et al. 2021). Por lo tanto, la descarga de efluentes tratados deficientemente por parte de las plantas de tratamiento convencionales contribuye a la contaminación de ríos, aguas subterráneas, cuencas hidrográficas y, en última instancia, agua potable (Mukhopadhyay et al. 2022). El destino de los CPEs en el medio ambiente está determinado por sus propiedades fisicoquímicas y su interacción con el entorno. Una vez que alcanzan el ambiente, pueden experimentar diversos fenómenos, como absorción, dilución, hidrólisis, fotólisis, biodegradación, volatilización, oxidación o formación de diferentes complejos con otras sustancias (Starling et al. 2019). Además, los CPEs pueden ejercer impactos negativos en la salud humana y los ecosistemas acuáticos, incluso en bajas concentraciones, debido a su capacidad para interactuar con organismos vivos y provocar efectos adversos como feminización, alteraciones en el comportamiento de peces,

cánceres y desarrollo de genes resistentes a antibióticos. Más aún, la mezcla de estos contaminantes puede aumentar su toxicidad debido al sinergismo o al antagonismo, y su capacidad de bio-acumulación en la cadena alimentaria representa una preocupación adicional para la salud humana (Lajmanovich et al. 2019).

1.1.3. El paracetamol como contaminante

El Paracetamol (PCT), también conocido como acetaminofén, es un ácido orgánico débil (pKa = 9,5), altamente soluble en agua (14 mg mL^{-1} a 20 °C) y, en el rango de pH fisiológico, está en gran parte no ionizado. Dichas características le permiten penetrar rápidamente las membranas celulares (Ayoub 2021). Es un fármaco analgésico y antipirético de venta libre que goza de un amplio uso a nivel global. En la actualidad, se ha consolidado como el tratamiento convencional primario para diversas condiciones, y está disponible en múltiples formas de dispensación sin prescripción médica, principalmente destinadas para su administración vía oral (Ayoub 2021).

El consumo de este medicamento ha experimentado un incremento continuo en las últimas décadas, el cual se ha visto potenciado con la llegada del SARS-COV-2 (Nason et al. 2021). Durante la pandemia de COVID-19, las autoridades sanitarias desaconsejaron el uso de otros fármacos como el ibuprofeno y el diclofenac, promoviendo en su lugar el uso del PCT, lo que conllevó a un aumento del 198% en su consumo (Galani et al. 2021), representando una amenaza potencial para el medio ambiente.

Como consecuencia del elevado consumo, el paracetamol se ha convertido en uno de los fármacos más comúnmente detectados en aguas naturales e incluso en suministros de agua potable (Pacheco-Álvarez et al. 2022). Se han registrado concentraciones elevadas de paracetamol (hasta 300 mg L^{-1}, Peralta-Hernández y Brillas 2023) en los efluentes de instalaciones hospitalarias (Ulvi et al. 2022), aguas residuales de la industria

farmacéutica (Okeke et al. 2022) y en plantas de tratamiento de aguas residuales urbanas (Jiménez-Bambague et al. 2023). En países en desarrollo, la falta de recolección y tratamiento adecuados de efluentes industriales, aguas residuales municipales, residuos hospitalarios y efluentes de tanques sépticos, ha resultado en la presencia generalizada de paracetamol en cuerpos de agua superficiales (Pacheco-Álvarez et al. 2022). En Argentina, si bien los reportes en cuanto a este compuesto son escasos, se ha detectado en concentraciones de hasta 9.62 μg L^{-1} en aguas superficiales (Mastrángelo et al. 2022; Bertrand et al. 2023; Salgado Costa et al. 2023). Además, se evidencia su bio-acumulación en diferentes organismos acuáticos autóctonos (Carrizo et al. 2022; Salgado Costa et al. 2023).

Entonces, dada su presencia ubicua en diferentes tipos de aguas y compartimentos ambientales, se concluye que los métodos de tratamiento de aguas residuales convencionales resultan insuficientes para el tratamiento de este tipo de contaminantes (AL Falahi et al. 2022; Beamud et al. 2024), convirtiendo al PCT en un contaminante pseudo-recalcitrante. Por este motivo, en los últimos años, se ha promovido la investigación y desarrollo de diversas tecnologías alternativas que permitan el tratamiento eficiente de aguas contaminadas con PCT, así como con otros contaminantes considerados de interés emergente.

1.2. Motivación de la Investigación

La contaminación y la escasez del agua son desafíos ambientales cruciales que requieren soluciones efectivas y sostenibles. Con el aumento de la urbanización y la industrialización, ha aumentado la presencia de CPEs en el medio ambiente, por lo que es imperativo investigar y desarrollar tecnologías avanzadas para el tratamiento de aguas

residuales.

Los Procesos Avanzados de Oxidación, como los procesos foto-Fenton (PFF) y foto-Fenton/Ferrioxalato (PFF/FeOxa), han surgido como alternativas prometedoras a los métodos convencionales de tratamiento de aguas residuales. Estas tecnologías poseen la capacidad de degradar eficazmente una amplia gama de CPEs, ya que, a diferencia de otros métodos de depuración que simplemente transfieren los contaminantes de una fase a otra, estos procesos pueden transformar a los contaminantes en compuestos más biodegradables y/o reducir sus niveles de toxicidad. Su eficiencia y versatilidad los hacen aptos para tratar diversas matrices de aguas residuales, desde las municipales hasta las industriales altamente contaminadas (Pandis et al. 2022; Kulišťáková 2023).

Por lo tanto, investigar los PFF y PFF/FeOxa como tecnologías alternativas para el tratamiento de aguas residuales es fundamental para avanzar hacia una gestión más sostenible de nuestros recursos hídricos. El proceso PFF/FeOxa tiene la capacidad de incorporar la radiación solar en su funcionamiento, aprovechando así su carácter de fuente de energía natural y de bajo costo. De esta forma, se considera una tecnología con muy alto potencial de desarrollo, pudiendo proporcionar soluciones innovadoras y ambientalmente responsables a los desafíos actuales de contaminación y escasez del agua, contribuyendo así a la protección de la salud humana y la conservación del medio ambiente. Además, esta perspectiva abre nuevas vías de investigación para optimizar aún más la eficiencia y la viabilidad económica de estos procesos (Oller y Malato 2021; Machado et al. 2023).

Sin embargo, para que estas tecnologías puedan ser realmente empleadas de forma habitual para el tratamiento de aguas residuales, es necesario, en primer lugar, estudiar las características intrínsecas de los PFF y PFF/FeOxa, para comprender su

funcionamiento frente a diferentes condiciones operacionales controladas. Luego, es necesario evaluar su comportamiento y eficiencia cuando son empleados bajo condiciones operacionales reales, con el fin de superar las limitaciones actuales de estas tecnologías. Además, se deben atender las demandas concretas que implica el saneamiento de matrices acuosas contaminadas, para que puedan ser aprovechadas por industrias regionales, y organismos gubernamentales en el tratamiento terciario de los efluentes que generen, o en la potabilización del agua. De esta forma, se consolidaría esta tecnología como una solución ambiental y económicamente viable en la remoción de los CPEs en aguas contaminadas.

Por lo tanto, teniendo en cuenta la problemática planteada anteriormente, y la motivación en relación al tema de investigación, a continuación, se describen los objetivos planteados al momento de dar inicio al desarrollo de esta tesis.

1.3. Objetivos de la Tesis

1.3.1. Objetivo general

La eliminación de diversos contaminantes mediante los procesos Fenton y foto-Fenton ha sido ampliamente estudiada a pH ácido. Sin embargo, existe un interés creciente en desarrollar estrategias operativas para abordar los inconvenientes asociados con el funcionamiento del sistema en condiciones ácidas. En este contexto, la operación del proceso a pH cercano a la neutralidad, utilizando ferrioxalato como catalizador, ha demostrado ser una alternativa eficiente. No obstante, es necesario profundizar las investigaciones sobre las condiciones operacionales y los mecanismos cinéticos de estos procesos (PFF y PFF/FeOxa). Además, se requiere demostrar la eficiencia de estas

tecnologías cuando se aplican a matrices acuosas reales (presencia de diversas especies orgánicas e inorgánicas interferentes) que representan un desafío para el funcionamiento del proceso foto-Fenton solar.

Por lo tanto, la presente tesis tiene como objetivo estudiar sistemáticamente, modelar y optimizar el proceso foto-Fenton, utilizando principalmente Ferrioxalato como catalizador y operando a pH cercano a la neutralidad. Se pretende aplicar dicho proceso a la remoción del PCT (modelo de contaminante pseudo-recalcitrante) presente en medios acuosos reales, empleando reactores a escala laboratorio y planta piloto, activados con radiación artificial o solar natural.

1.3.2. Objetivos específicos

- Desarrollar modelos cinéticos asociados a la degradación foto-Fenton y foto-Fenton/Ferrioxalato del PCT. Estos modelos deberán incorporar los principales efectos que influencian el comportamiento del sistema, como ser: diferentes configuraciones de los sistemas experimentales, distintas fuentes y niveles de radiación, variaciones en el pH, diversas concentraciones de agente oxidante, y distintas temperaturas de operación.

- Estimar los parámetros cinéticos resultantes de los modelos planteados previamente, empleando algoritmos de optimización no lineales. Esto requerirá la resolución de los balances de materia para las especies reactivas involucradas. Además, será esencial realizar una evaluación precisa del campo de radiación incidente sobre la ventana del reactor, así como comprender la variación espacial de la radiación absorbida en el medio reaccionante.

- Emplear diferentes herramientas quimiométricas. Diseño de Experimentos (como el D-Optimal) para planificar adecuadamente los ensayos a realizar, disminuir la cantidad

de experimentos requeridos, y obtener información de calidad. Superficies de Respuesta, para optimizar el PFF/FeOxa estudiado (maximizando la conversión del PCT, minimizando el consumo de HP) en función de diferentes variables operacionales claves: radiación, temperatura, concentración de agente oxidante y dosificación de peróxido de hidrógeno.

- Estudiar el comportamiento de los PFF/FeOxa y/o PFF/FeOxa Solar bajo diferentes escenarios operativos complejos reales, tales como la presencia del PCT en concentraciones extremadamente bajas (del orden de μg L^{-1}) y presencia de diversas especies interferentes (cationes y aniones, y otros componentes orgánicos) presentes en efluentes industriales reales.

- Evaluar la eficiencia de los PFF y PFF/FeOxa en la descontaminación, mediante la determinación de la materia orgánica contenida en el efluente tratado y la toxicidad remanente (utilizando bacterias *Vibrio fischeri* y células VERO), incluso en matrices acuosas reales.

1.4. Organización de la Tesis

Esta tesis se encuentra organizada bajo el formato de Tesis por Compilación de la siguiente forma:

- En el capítulo 1 se introducen los conceptos necesarios para la comprensión del problema describiendo la implicancia de los CPEs, entre ellos el paracetamol, en el deterioro de la calidad de los recursos acuáticos. Luego, se describe la motivación de la investigación realizada y los problemas a abordar, estableciendo así los objetivos dentro del marco de esta tesis.

- En el capítulo 2 se presenta el estado del arte de los PAOs, con un enfoque particular en el sistema foto-Fenton/Ferrioxalato, tecnología propuesta para la remediación de aguas contaminadas con CPEs.

- En el capítulo 3 se detallan los dispositivos experimentales utilizados, tanto a escala laboratorio como planta piloto. Además, las diversas técnicas analíticas empleadas; las herramientas quimiométricas implicadas en la obtención, recopilación y el análisis de los datos; y, finalmente, la metodología adoptada para el modelado de los fotorreactores.

- En el capítulo 4 se recopilan los principales resultados obtenidos en los trabajos de investigación presentados en los Anexos de esta tesis. En primer lugar, se presenta el modelo cinético desarrollado para describir el proceso PFF a pH ácido empleando un reactor anular concéntrico a escala de planta piloto, con una lámpara germicida como fuente de radiación. A continuación, se muestra el modelado empírico (empleando la metodología de superficie de respuesta) realizado para estudiar la influencia de las principales variables operacionales sobre la efectividad del PFF/FeOxa, analizado en condiciones de pH neutro. Posteriormente, se describe el modelo cinético desarrollado para el PFF/FeOxa utilizando un reactor de placa plana iluminado lateralmente por un simulador solar. Seguidamente, se analiza el desempeño del PFF/FeOxa en la eliminación del contaminante (PCT) a muy baja concentración, considerando los niveles hallados en cuerpos de agua naturales. Por último, se presentan diferentes estrategias de dosificación del agente oxidante (puntual, continua o una combinación de ambas) para la intensificación del PFF/FeOxa, utilizando diversas matrices acuosas reales. Además, se analiza la toxicidad remanente de los efluentes generados (Microtox®), considerando el empleo de un reactor solar a escala de planta piloto.

- En el capítulo 5 se resumen e integran las conclusiones derivadas de los resultados obtenidos en las distintas publicaciones científicas realizadas que conforman esta tesis.

- Finalmente, en los Anexos se presentan todos los trabajos de investigación en los que se basa la presente tesis.

Capítulo 2. ESTADO DEL ARTE

2.1. Procesos Avanzados de Oxidación (PAOs)

El enfoque en la aplicación de métodos para el tratamiento de aguas residuales reside en comprender la naturaleza y las propiedades fisicoquímicas de los efluentes. El agua contaminada, usualmente resultado de la actividad humana, puede ser tratada eficientemente mediante tratamientos biológicos, adsorción en carbón activado o tratamientos químicos convencionales. Sin embargo, estos métodos tradicionales no siempre logran los niveles de pureza exigidos por las regulaciones o los usos posteriores que se le dará al agua tratada (Manna y Sen 2022). Por lo tanto, la utilización de PAOs está ganando terreno en la mayoría de los países industrializados (Priyadarshini et al. 2022).

Los PAOs, concebidos inicialmente en 1987 (Glaze et al. 1987), comprenden un conjunto de técnicas capaces de generar especies altamente oxidantes in situ. Aunque los oxidantes primarios son los radicales hidroxilo ($HO^{\bullet}$), recientemente el concepto de PAO se ha ampliado para incluir procesos oxidativos con radicales sulfato ($SO_4^{\bullet -}$) (Lee et al. 2020). Las propiedades reactivas de los $HO^{\bullet}$ son beneficiosas para completar la mineralización de los contaminantes o degradarlos en sustancias fácilmente biodegradables, lo que generalmente produce como productos finales CO_2, agua e iones inorgánicos (Ma et al. 2021). Los PAOs pueden clasificarse en métodos fotoquímicos y no fotoquímicos, siendo los más utilizados en los últimos años las reacciones tipo Fenton (procesos Fenton y foto-Fenton), la fotocatálisis heterogénea con TiO_2, la ozonización y los sistemas de H_2O_2 (Pandis et al. 2022). Los PAOs presentan varias ventajas comparativas frente a otros procesos de depuración. En lugar de simplemente transferir

los contaminantes de una fase a otra (como ocurre por ejemplo en tratamientos convencionales con carbón activado), éstos los transforman químicamente en compuestos más simples, lo que reduce en muchos casos sus niveles de toxicidad e incluso puede llevar a su completa mineralización. Además, los PAOs son altamente eficaces para tratar numerosos contaminantes refractarios que son resistentes a métodos de tratamiento tipo biológicos. Finalmente, estos procesos se caracterizan por su naturaleza no selectiva, lo que permite degradar no solo el contaminante principal, sino también los subproductos de degradación que puedan formarse a partir de éste (Pandis et al. 2022; Kumari y Kumar 2023). Sin embargo, el uso de PAOs también conlleva algunas desventajas, principalmente el costo operativo elevado, por lo que deben explorarse alternativas que permitan el desarrollo de procesos más robustos, eficientes y menos costosos.

De acuerdo a Machado et al. (2023) la producción científica sobre PAOs entre 2000 y 2022 comprendió alrededor de 9940 artículos, publicados principalmente en los campos de Ciencias Ambientales (~ 4276), Ingeniería Ambiental (~ 3543) e Ingeniería Química (~ 2816), donde la producción anual reveló un gran aumento en los artículos publicados en la segunda década (2011–2021). Precisando la búsqueda con las palabras clave "Fenton" y "foto-Fenton", se contabilizaron aproximadamente 5.530 artículos publicados, es decir, un 55% del total de trabajos publicados sobre PAOs. Considerando la amplia variedad que existe de PAOs, el número de publicaciones que involucran a las tecnologías Fenton es significativo y puede atribuirse al hecho de que estos procesos son atractivos por su simplicidad y bajo costo operativo en comparación con otros (Ameta et al. 2018), por lo que han llamado la atención de muchos grupos de investigación. De hecho, el proceso foto-Fenton es considerado una de las tecnologías más prometedoras y más eficientes para degradar compuestos recalcitrantes en el tratamiento de aguas residuales (Velo-Gala et al. 2017; Maniakova et al. 2020; Singh y Garg 2021).

2.2. Proceso foto-Fenton

La oxidación tipo Fenton es una de las tecnologías representativas de los PAOs, aplicada principalmente en el tratamiento de aguas residuales que contienen contaminantes orgánicos no biodegradables. Esta tecnología se basa en la reacción de Fenton, que se refiere a la reacción del ion ferroso (Fe(II)) con peróxido de hidrógeno (HP) para generar radicales hidroxilos (HO•). La reacción de Fenton puede producir rápidamente una cantidad estequiométrica de HO• mediante la reacción equimolar del Fe(II) con el HP (ecuación (*2.1)*). El Fe(III) resultante se puede reducir nuevamente a Fe(II) mediante su reacción con el HP (ecuación (*2.2)*), pero esta reacción es muy lenta en comparación con la reacción de Fenton (Ziembowicz y Kida 2022). Por lo tanto, la producción de HO• no puede depender únicamente de la descomposición catalítica del HP mediante el ciclo Fe(II)/Fe(III). Luego, es que resulta necesario emplear altas dosis de catalizador (Fe(II)), lo que genera gran cantidad de barros como subproductos después del tratamiento al precipitar el exceso de hierro. El proceso Fenton se opera a un pH ácido (aproximadamente 2.8) donde el Fe (II) es mayoritariamente soluble, luego el Fe (III) resultante se elimina en forma de precipitados de $Fe(OH)_3$ (el lodo de hierro) a medida que se neutraliza el agua tratada. El tratamiento secundario necesario para eliminar los lodos de hierro aumenta el costo operativo del proceso Fenton (Chen et al. 2023).

$$Fe^{2+} + H_2O_2 \xrightarrow{k1} Fe^{3+} + OH^- + HO^{\bullet} \quad (2.1)$$

$$Fe^{3+} + H_2O_2 \xrightarrow{k2} Fe^{2+} + H^+ + HO_2^{\bullet} \quad (2.2)$$

Para superar estos problemas, se ha sugerido como alternativa metodológica el proceso foto-Fenton. En este proceso, se utiliza una cantidad relativamente pequeña de Fe(II), y el Fe(III) resultante se regenera continuamente a Fe (II) mediante luz UV-Vis (ecuación *(2.3)*). De esta manera, la producción de lodos de hierro se puede reducir

significativamente. En particular, el proceso de foto-Fenton tiene el potencial de ser una tecnología limpia y energéticamente eficiente porque puede utilizar la luz solar, prescindiendo así del uso de lámparas costosas y la electricidad necesaria para su funcionamiento (Bah et al. 2023). La eficiencia del sistema foto-Fenton en la degradación de contaminantes del agua está determinada principalmente por la cinética de las reacciones fotoquímicas de los complejos de Fe(III) y de los factores que afectan éstas, tales como el pH, la temperatura y los tipos de ligandos que determinan la especiación de los complejos de Fe(III) (López-Vinent et al. 2022).

$$Fe^{3+} + H_2O \xrightarrow{h\upsilon} Fe^{2+} + H^+ + HO^{\bullet} \quad (2.3)$$

Dentro de los ligandos orgánicos posibles de emplear como catalizadores del proceso foto-Fenton se destaca el oxalato de hierro (principalmente el complejo de $Fe(C_2O_4)_3^{3-}$, Ferrioxalato) (Ahile et al. 2020).

Este sistema foto-Fenton/Ferrioxalato (incluido dentro de los procesos foto-Fenton-*like*) presenta varias ventajas sobre los sistemas tradicionales:

- Muestra un rendimiento fotocatalítico superior, ya que los complejos de Fe(III)-oxalato tienen valores de absortividad molar (ε) y rendimientos cuánticos (ϕ) más altos que los acuo-complejos de Fe(III) en la región UV-Vis del espectro de radiación. De hecho, la absorbancia de los complejos de Fe(III)-oxalato es más de dos veces superior que la del complejo $Fe(OH)^{2+}$ en la región UV-Vis (Conte et al. 2014). De esta forma, se podría obtener un mayor aprovechamiento de las fracciones UV-Vis incidentes del sol (foto-Fenton solar).

- El complejo $Fe(C_2O_4)_3^{3-}$, especie soluble en agua que es dominante en el rango de pH < 8.5, lo que posibilita trabajar a pH neutro reduciendo los costos operativos del proceso, ya que no son necesarios los ajustes de pH antes y después del proceso (Teutli-

Sequeira et al. 2020).

- La formación del complejo hierro-oxalato puede minimizar las interferencias causadas por aniones quelantes de hierro que podrían estar presentes en el agua. El oxalato añadido al sistema compite por la quelación de Fe(III) con otros ligandos (Lee et al. 2022).

Cabe mencionar, que diversos contaminantes han sido degradados exitosamente con el sistema foto-Fenton/Ferrioxalato Solar, tales como herbicidas, fármacos y lixiviados de vertederos (Durán et al. 2018; Rebolledo et al. 2019; Teutli-Sequeira et al. 2020). Aun así, es una tecnología prometedora que puede ser mejorada tanto en su rendimiento como a nivel de costos.

2.3. Dosificación de Peróxido de Hidrógeno

El peróxido de hidrógeno (HP) desempeña una función fundamental en la remediación de aguas residuales cuando se emplea el proceso foto-Fenton, debido a que es uno de los parámetros determinantes en la generación catalítica del HO•, afectando la eficiencia global del proceso. Por ello, la cantidad óptima para cada sistema reaccionante debe determinarse experimentalmente, ya que el HP puede limitar la velocidad de degradación del contaminante si se aplica en concentraciones demasiado bajas y, por el contrario, a una concentración muy alta, este reactivo puede competir con los contaminantes por los HO• generados, afectando la velocidad de degradación de dichos contaminantes, así como también puede malgastarse al auto-descomponerse en oxígeno y agua (Ziembowicz y Kida 2022).

Como se mencionó en la **sección 2.2**, operando el sistema a un pH natural y empleando radiación solar, el agente oxidante a utilizar puede considerarse entonces la principal fuente de costos (Rodríguez-García et al. 2023). Por lo tanto, su utilización en

exceso, además de provocar un consumo improductivo, resultaría en un reactivo residual no convertido que no puede ser recuperado y debe ser eliminado antes de descargar el efluente final ya que posee efectos tóxicos para el medio ambiente. Esto también resulta relevante en el caso de que el proceso foto-Fenton sea empleado como un pretratamiento de aguas residuales para mejorar su biodegradabilidad, dado que el HP podría tener un efecto adverso en la reactividad de los microorganismos que se utilizan en los biotratamientos subsiguientes (Shokri y Fard 2022).

De acuerdo a la bibliografía, una solución a estos inconvenientes, y que además podría mejorar la efectividad del proceso, es la dosificación del agente oxidante al medio de reacción, para que de esta forma sea aprovechado de manera más eficiente por el sistema (Yu et al. 2021; Shokri y Fard 2022).

Si se realiza una búsqueda actual en Scopus empleando como palabras clave "*photo-fenton*", "*hydrogen peroxide*" y "*dosage*" se observan 214 publicaciones entre los años 2000-2023, de los cuales casi un 75% fue publicado en los últimos 9 años, con un máximo de publicaciones (32 trabajos) en el año 2021, demostrando un creciente interés de los investigadores en esta temática y enfoque en particular.

En la literatura pueden encontrarse varios trabajos donde se analizó la dosificación de peróxido de hidrógeno en el sistema foto-Fenton, utilizando sales de sulfato de hierro en un medio ácido (Audino et al. 2019; Gamaralalage et al. 2020; Yu et al. 2020; Nasr Esfahani et al. 2022). Por el contrario, se encuentran pocos artículos donde se aplique la dosificación del HP en el proceso foto-Fenton con ferrioxalato como catalizador (Monteagudo et al. 2010; Soares et al. 2015).

Estudios previos sobre el uso del concepto de dosificación del HP en el proceso Fenton han adoptado diferentes estrategias:

- Dividir la cantidad total de HP en varias porciones y añadirlas en diferentes tiempos pre-establecidos (Yamal-Turbay et al. 2012; Munoz et al. 2014; Polo-López et al. 2014).
- Dosificación continua del HP a velocidad constante a lo largo del tiempo de reacción (Prato-Garcia y Buitrón 2012; Gamaralalage et al. 2020).
- Utilizar la variación del oxígeno disuelto (OD) para regular el suministro de HP durante el tiempo de reacción (Prieto-Rodríguez et al. 2011; Ortega-Gómez et al. 2012; Saldaña-Flores et al. 2021), dado que el aumento o disminución del OD en el medio de reacción, podría indicar un exceso o un déficit de la cantidad de HP administrada, respectivamente (mecanismo de Dorfman) (Xiangwei et al. 2021).

Recientemente, algunos autores han desarrollado modelos y estrategias de dosificación, donde la dosificación del HP es dinámica, empleando modelos tipo *fed-batch*, para determinar el mejor perfil de suministro del HP al medio de reacción (Yu et al. 2021; Nasr Esfahani et al. 2022)

2.4. Modelado de los procesos Fenton y foto-Fenton

El carácter complejo de los sistemas foto-Fenton y foto-Fenton/Ferrioxalato implica un arduo trabajo para identificar los mecanismos de reacción que permiten comprender y predecir el comportamiento de estos tratamientos. Aunque el modelado de estos procesos se lleva a cabo empleando diferentes enfoques, el objetivo es, en general, la optimización de dichos procesos. Específicamente, se pueden identificar dos grandes tipos de modelos, cada uno con sus metodologías y propósitos definidos (Malato et al. 2020):

- Modelos Empíricos: son modelos que dependen completamente de un enfoque

experimental y no contemplan las características fisicoquímicas del proceso, por lo que es esencial un trabajo extenso en el tratamiento de datos. Para la obtención de estos modelos se emplean diseños experimentales adecuados, para posteriormente aplicar enfoques de optimización como la metodología de la superficie de respuesta. Son modelos sencillos que resultan útiles para determinar tendencias, y posibles interacciones entre las variables operacionales del sistema evaluado. El principal inconveniente de este enfoque es que los modelos desarrollados no capturan la complejidad de los procesos fotoquímicos, y los resultados obtenidos no pueden ser extrapolados cuando se cambia la configuración del sistema experimental (Pérez-Moya et al. 2011; Nascimento et al. 2020).

- Modelos Mecanísticos: son enfoques meticulosos basados en balances de masa y energía. Se realiza una descripción completa del proceso, utilizando información del dispositivo experimental empleado y de las diferentes reacciones químicas involucradas, lo cual se complementa con la modelización de la radiación en el fotorreactor, resolviendo la Ecuación de Transferencia Radiativa (Cassano et al. 1995) para el cálculo de la tasa volumétrica local de absorción de fotones (LVRPA), variable que se considera fundamental dentro del estudio de la cinética y el diseño de fotorreactores (Alfano y Cassano 2008; Grčić et al. 2021). Si bien son modelos complejos, tanto de construir como de resolver, son una herramienta fundamental para la optimización y el diseño de reactores y procesos más eficientes, dado que su principal ventaja radica no solo en su capacidad de realizar predicciones asociadas al comportamiento de los sistemas de reacción sino también en la posibilidad de extrapolar los resultados a escalas de operación mayores (planta piloto y reactores industriales) (Hincapié Mejía et al. 2022).

En el **Capítulo 3** (Materiales y Métodos) se proporciona información detallada sobre las herramientas quimiométricas utilizadas para desarrollar los modelos empíricos

(**sección 3.3**), así como la metodología empleada para la elaboración de los modelos mecanísticos (**sección 3.4**) presentados en esta tesis.

De acuerdo a la bibliografía existente, y tomando como ejemplo la degradación Fenton y foto-Fenton del paracetamol, la gran mayoría de los artículos de investigación presentados hasta la fecha, han propuesto modelos empíricos (Rad et al. 2015a; Shokry et al. 2015; Villota et al. 2018; Audino et al. 2019b). Por el contrario, solo unos pocos artículos han abordado el tema de la cinética de reacción en sus trabajos de investigación (Cabrera Reina et al. 2015; Audino et al. 2019a).

Capítulo 3. MATERIALES Y MÉTODOS

3.1. Dispositivos Experimentales

3.1.1. Reactor de Placa Plana

Este reactor (**Figura 3.1**) es de vidrio borosilicato, de sección transversal circular y está inserto en un sistema de reciclo externo que incluye un tanque de almacenamiento de 3000 cm3, equipado con un sistema para la toma de muestra, un termómetro y un medidor de pH. Además, esta configuración experimental presenta un intercambiador de calor conectado a un baño termostático que permite mantener constante la temperatura durante la reacción, y una bomba centrífuga que permite lograr un alto caudal de recirculación que asegure las condiciones de mezclado óptimas.

Figura 3.1. Fotografía del reactor de placa plana y el simulador solar.

El fotorreactor se encuentra irradiado desde un lateral por un Simulador Solar (**Figura 3.1**) marca ORIEL modelo 9600 (Rad UV-Vis). Dicho dispositivo cuenta con una lámpara de xenón libre de ozono de 150 W, y genera un haz colimado de 33 mm de

diámetro. Sobre el colimador del equipo pueden acoplarse distintos filtros, como ser: filtros de aire, filtros líquidos y filtros de atenuación, los cuales poseen diferentes funciones y cuyas combinaciones otorgan la posibilidad de simular diversas condiciones solares y atmosféricas, obteniendo diferentes niveles de radiación.

En la **Figura 1** del **Anexo B**, se muestra un esquema del dispositivo experimental aquí descrito y en la **Tabla 3.1** se presentan sus dimensiones y principales características.

Tabla 3.1. Dimensiones y principales características del dispositivo experimental.

Reactor	*Volumen Irradiado*	69,94 cm^3
	Diámetro	4,40 cm
	Longitud	4,60 cm
Simulador Solar (lámpara de Xenón)	*Potencia Nominal*	150 W
	Potencia de Salida (sin filtros)	230-280 nm: 11,5 mW
		280-320 nm: 27 mW
		320-400 nm: 85 mW
		400-700 nm: 430 mW
Bomba de recirculación	*Caudal*	85 cm^3/s
Volumen Total de Líquido		3000 cm^3

3.1.2. Reactor anular concéntrico

Este sistema experimental escala planta piloto comprende un reactor anular concéntrico (**Figura 3.2**), un depósito de almacenamiento de Pyrex, un sistema de recirculación que asegura condiciones óptimas de mezclado y un sistema integrado de adquisición de datos en línea. El fotorreactor anular consta de dos cilindros dispuestos concéntricamente, uno de vidrio Pyrex en el exterior y otro de cuarzo en el interior. Además, una lámpara actínica Philips TL-DK 36W/10 (con una potencia de salida de 7,4 W y un rango de longitud de onda de 315-400 nm) se sitúa en el eje del cilindro interior. El volumen total de reacción es de 15 L, mientras que el volumen irradiado es de 1.5 L. El esquema del dispositivo experimental y una tabla con sus dimensiones y características

principales se presentan en la **Figura S1** del **Material Suplementario** del **Anexo C**. Además, la distribución espectral de potencia de salida de la lámpara actínica Philips mencionada anteriormente (con un pico de emisión cercano a los 370 nm), se muestra en la **Figura S2** del **Material Suplementario** del **Anexo C**.

Figura 3.2. Fotografía del sistema experimental compuesto por el reactor anular concéntrico.

3.1.3. Fotorreactor Solar

Este fotorreactor escala planta piloto es de tipo placa plana aislado y no concentrador, y está diseñado para capturar radiación solar UV/visible e infrarroja cercana (patente INPI P-080103697). Todo el sistema de reacción opera dentro de un circuito cerrado de recirculación impulsado por una bomba centrífuga de alto caudal, y un tanque de almacenamiento bien agitado que completa el sistema experimental (**Figura 3.3**). El tanque de almacenamiento está equipado con un medidor de pH y un sensor de OD. Además, se utilizan termocuplas tipo J para monitorear las variaciones de temperatura en diferentes posiciones del sistema a lo largo del tiempo. Dentro de este

fotorreactor, la solución a tratar ingresa a un canal inferior para su precalentamiento. Posteriormente, el fluido circula hacia un canal superior donde continúa calentándose, y donde absorbe la radiación solar UV/visible, la cual es empleada en la degradación de los contaminantes. Para medir los flujos de radiación solar, UV y Total, incidentes en la ventana del reactor, se emplearon dos radiómetros: CUV3 y CM11 (Kipp and Zonen). El volumen irradiado del reactor es de 6.1 L, mientras que el volumen total de líquido es de 35 L. Este dispositivo consta además de una placa de adquisición de datos, la cual permite registrar datos on-line de diferentes variables asociadas al comportamiento del reactor solar (temperatura, radiación UV y Total, pH y Oxígeno Disuelto) en intervalos de tiempos del orden de segundos. Pueden encontrarse más detalles de este fotorreactor en el trabajo publicado por Conte et al. (2017).

Figura 3.3. Fotografía del Reactor Solar escala planta piloto.

3.1.4. Bomba dosificadora

Este dispositivo es una bomba de tipo electromagnética a diafragma y opera de manera intermitente. La regulación del caudal es electrónica y actúa sobre el número de inyecciones de la bomba dosificadora. Puede dosificar hasta 1.5 L h^{-1}, ya que la serie MA-CP (Acquatron S.A.) fue especialmente diseñada para dosificación de caudales pequeños.

Esta bomba dosificadora puede acoplarse tanto al dispositivo experimental del reactor de placa plana, como al reactor solar, y fue empleada para realizar la dosificación del agente oxidante, en el trabajo de investigación presentado en el **Anexo F**.

3.2. Determinaciones Analíticas

En todas estas determinaciones analíticas, a excepción de los ensayos de toxicidad, se elaboraron curvas de calibrado para los rangos de concentraciones de trabajo, empleando las sustancias estándares correspondientes. Luego, las concentraciones de las diferentes especies en el medio de reacción se determinaron indirectamente utilizando dichas curvas de calibrado.

3.2.1. Cromatografía líquida

Esta técnica analítica se utilizó para cuantificar diferentes especies en el medio reaccionante, empleando diferentes equipos y diferentes configuraciones de los mismos, como se detalla a continuación.

La cuantificación del PCT al igual que la de sus intermediarios de reacción (HQ y BQ), en los trabajos presentados en los **Anexos A**, **B**, **D**, **E** y **F** se realizó mediante cromatografía líquida de alta resolución utilizando un cromatógrafo Waters (modelo

1525) equipado con una columna analítica YCM-Triart C18 (250 x 4.6 mm, 5 µm) y, un detector de absorbancia dual (Waters 2489) o un detector UV-DAD (Waters 2898). Se utilizó un eluente compuesto por agua y metanol en una proporción 75:25, siendo, además, la velocidad de flujo de eluente (método isocrático) de 1 mL min^{-1}. La detección se realizó a 220 y 243 nm. Estas condiciones permiten una perfecta separación de los picos correspondientes al PCT, la HQ y la BQ, y su óptima cuantificación. Cabe aclarar que las muestras para este análisis, son pre-tratadas con metanol grado HPLC para "congelar" la reacción.

En el caso del trabajo presentado en el **Anexo C**, el PCT, la HQ y la BQ fueron determinados utilizando un cromatógrafo líquido Agilent (serie 1200) con detector DAD, equipado con una columna Akady C-18 de 5 µm de 150×4.6 mm. La detección se realizó a 243 nm. El eluente utilizado fue una mezcla de metanol:agua (25:75) con un flujo de 0.4 mL min^{-1} (isocrático). Las muestras (20 µL) fueron inyectadas manualmente, y fueron previamente tratadas con metanol 0.1 M, en una proporción de 50:50, para detener la reacción.

El equipo utilizado para determinar los iones oxalato (Oxa) fue un cromatógrafo Waters (modelo 1525) combinado con un detector de conductividad (Waters 432) y una supresora (Dionex ERS 500). La fase estacionara fue una columna analítica de intercambio aniónico IonPac AS22 y una pre-columna IonPack AS22. Como eluente se utilizó una solución de 7,2 mM Na2CO3/ 3,2 mM NaOH, y el caudal de flujo fue de 1.2 mL min^{-1}. Esta misma metodología fue empleada para el monitoreo de los aniones (Cl^-, SO_4^{2-}) presentes en el agua subterránea y la matriz de aniones, empleadas en los trabajos presentados en los **Anexos E** y **F**.

3.2.2. Técnicas colorimétricas

Para todas las determinaciones basadas en reacciones colorimétricas, en los trabajos presentados en los **Anexos A**, **B**, **D**, **E** y **F** se empleó un espectrofotómetro UV-Vis Lambda 35 (Perkin-Elmer).

La concentración de peróxido de hidrógeno se obtuvo empleando una técnica yodométrica modificada (Allen et al. 1952). Este método se basa en la cuantificación del yodo generado a partir de la oxidación de un yoduro metálico por el peróxido de hidrógeno presente en solución, catalizada por el molibdato de amonio. La medición se realiza a 350 nm.

Para la cuantificación del hierro, se aprovecha la capacidad del ion Fe^{2+} disuelto de formar un complejo de color rojizo con tres moléculas de 1,10-fenantrolina. Para asegurar la formación cuantitativa de dicho complejo es necesario mantener el pH entre 3 y 3,5, por lo que, para lograrlo, se agrega una solución buffer de Acetato de Sodio. Así, la absorbancia del complejo Fe^{2+}-1,10-fenantrolina, medida a 510 nm, es proporcional a la concentración de ion ferroso. Para la determinación del Hierro Total en solución se emplea el mismo principio, pero se reduce previamente todo el hierro existente en la muestra utilizando ácido ascórbico como agente reductor. Luego, el Fe^{3+} se determina por diferencia entre el Hierro Total y el Fe^{2+} cuantificados de cada muestra. Cabe aclarar que este método funciona satisfactoriamente en los ensayos donde se empleó ferrioxalato como catalizador para el proceso.

En el trabajo presentado en el **Anexo C** se empleó un espectrofotómetro UV-Vis U-2001 (Hitachi) para realizar las determinaciones colorimétricas. Para la cuantificación de Hierro total y Fe^{2+} se empleó el mismo método colorimétrico con 1,10-fenantrolina explicado anteriormente. Para la cuantificación del peróxido de hidrógeno se empleó un

método basado en la reacción del HP con metavanadato de amonio en medio ácido, lo que da como resultado la formación del catión peroxovanadio (VO_2^{3+}) de color rojo-anaranjado, con máxima absorbancia a 450 nm. Por estequiometría, la concentración final del catión peroxovanadio es igual a la concentración inicial de peróxido de hidrógeno.

3.2.3. Determinación del Carbono Orgánico Total

Se determinó el Carbono Orgánico Total (TOC, por sus siglas en inglés) para evaluar el grado de mineralización alcanzado durante el proceso de degradación. Para tal fin, en la presente tesis se emplearon dos equipos: el analizador de TOC vario cube de Elementar (**Anexos A**, **B**, **D** y **F**) y el analizador de TOC VCHS/CSN de Shimadzu (**Anexo C**). Esta determinación se basa en la oxidación total de la muestra, cuantificándose en primer lugar el Carbono Total y luego el Carbono Inorgánico, por lo que es posible determinar el TOC por diferencia entre las mediciones anteriores. La diferencia al momento de determinar el CI radica en que la muestra es mezclada con una solución de ácido fosfórico, lo que permite la determinación del contenido de carbono que se encuentra en la forma de carbonatos y bicarbonatos. Finalmente, las muestras para este análisis fueron pre-tratadas con Sulfito de Sodio, que reduce rápidamente todos los posibles compuestos oxidantes presentes en el medio, deteniendo instantáneamente la reacción.

3.2.4. Ensayos de Toxicidad

En el caso de los trabajos presentados en los **Anexos A** y **F**, los ensayos para el monitoreo de la toxicidad aguda fueron realizados empleando el bioensayo de toxicidad Microtox®, el cual es ampliamente utilizado por sus bondades en cuanto a sensibilidad, poder discriminante, reproducibilidad y fácil aplicación para contaminantes orgánicos e

inorgánicos. Además, los resultados obtenidos con el sistema Microtox® se han correlacionado bien con las toxicidades agudas medidas a través de otros métodos estándar. Este método ha mostrado una gran sensibilidad y correlación con resultados obtenidos en peces y en *Daphnia magna*, siendo recomendado por la EPA para la evaluación de la toxicidad aguda en muestras de agua (ISO11348-3:2007, 2022). El fundamento del método Microtox® radica en la capacidad de la bacteria marina *Vibrio fischeri* para producir bioluminiscencia, la cual se reduce en presencia de agentes contaminantes. La reacción de bioluminiscencia bacteriana está ligada al sistema de transporte de electrones en la respiración celular, de modo que la disminución de la bioluminiscencia indica una disminución en la respiración celular debido a la presencia de contaminantes físicos, químicos o biológicos. La toxicidad de la muestra analizada puede expresarse como porcentaje de inhibición de la actividad bioluminiscente para distintos tiempos de exposición (5 o 15 minutos) (Hernando et al. 2007).

En el caso del trabajo presentado en el **Anexo C** se llevaron a cabo pruebas de citotoxicidad basadas en el cultivo de líneas celulares. Específicamente, se seleccionaron y evaluaron las células VERO, línea celular aislada de riñón de mono verde africano, cuya morfología corresponde a células epiteliales (ATCC®, Manassas, VA, USA). La citotoxicidad se evaluó midiendo la viabilidad de las células expuestas al contaminante evaluado (PCT) y sus subproductos (HQ y BQ). El ensayo MTT fue el seleccionado para tal fin, el cual es un ensayo colorimétrico para medir la actividad metabólica celular. El MTT es un tinte de tetrazolio que puede ser reducido por enzimas celulares, reflejando así el número de células viables presentes. Los ensayos MTT han sido utilizados con frecuencia para detectar citotoxicidad después de la exposición a sustancias tóxicas, y la validez de este método ha sido probada en varias líneas celulares (Mecha et al. 2017).

3.2.5. Flujo de Radiación

Para cuantificar la radiación incidente sobre la ventana de los dispositivos experimentales utilizados, se empleó la Espectroscopia UV-Vis. Para tal fin se utilizó un Espectrómetro Portátil modelo USB 2000+UV-Vis-ES (Ocean Optics) acoplado con una fibra óptica para la colección de la luz. Este instrumento permite obtener medidas de absorbancia y transmitancia, reflexión, emisión, irradiancia, etc. en un rango de longitudes de onda desde los 200 a los 880 nm. A partir de los espectros de emisión obtenidos tanto para el simulador solar, como para la luz solar, se calcularon los flujos de radiación incidentes entre las longitudes de onda de interés.

3.2.6. Extracción en Fase Sólida

En el trabajo presentado en el **Anexo D** se optimizó y aplicó una técnica de pre-concentración en fase sólida para la posterior detección y cuantificación del PCT en niveles de $\mu g\ L^{-1}$. La extracción en fase sólida (SPE, por sus siglas en inglés) es una técnica alternativa al método clásico de extracción líquido-líquido, que requiere menos tiempo y menor cantidad de solventes, y es capaz de extraer muchas sustancias difíciles de concentrar de otra manera. Además, tiene la ventaja de purificar la muestra generando una matriz con menor cantidad de interferentes. Se realizaron pruebas con los cartuchos Strata C18-U 500mg/3mL (Phenomenex) y un colector de vacío para cartuchos SPE de 12 posiciones (Phenomenex), para la pre-concentración en fase sólida del PCT. La optimización del protocolo de SPE se realizó empleando un diseño experimental factorial multiniveles donde se evaluaron distintos solventes de lavado, solventes de elución, volúmenes de lavado y volúmenes de elución. Finalmente, en base a conocimientos previos de la técnica y los resultados obtenidos del diseño experimental y su posterior evaluación empleando la metodología de la superficie de respuesta (ver siguiente

sección), se optimizó el método de extracción en fase sólida para el PCT, obteniendo el siguiente protocolo (**Tabla 3.2**):

Tabla 3.2. Protocolo de Extracción en Fase Sólida para el PCT.

Acondicionamiento	3 mL Metanol
	3 mL H_20
Muestra	15 mL (500 μg L^{-1} PCT) con Sulfito de sodio. Flujo 1 mL min^{-1}
Lavado	3 mL H_20
Secado	2 min con vacío
Elución	3 mL MeOH/ACN (50:50). Flujo 1 mL min^{-1}

En los ensayos de degradación presentados en el **Anexo D**, se empleó una concentración inicial de PCT de 500 μg L^{-1}. Con el protocolo de SPE antes presentado (**Tabla 3.2**), se obtiene un factor de concentración de 5 y un porcentaje de recuperación superior al 97%. Cabe resaltar que se hicieron ensayos sobre el efecto matriz que puedan tener las diferentes especies presentes en el sistema de reacción durante la degradación foto-Fenton/Ferrioxalato del PCT (hierro, peróxido de hidrógeno, oxalato, etc.), descartándose dicho efecto sobre la recuperación del proceso de SPE para el PCT.

3.3. Diseño Experimental y Metodología de la Superficie de Respuesta.

Se emplearon diseños experimentales que permitieron evaluar, de manera eficiente, los múltiples factores que influyen en el proceso foto-Fenton, maximizando la calidad de la información obtenida, minimizando, a la vez, el tiempo y los costos involucrados en los análisis. Para tal fin, los métodos de diseño experimental multivariado resultan ventajosos ya que, además de requerir menos tiempo y recursos, permiten obtener un

conocimiento global del sistema y facilitan la construcción de modelos matemáticos (Parra-Marfil et al. 2023).

El diseño experimental empleado en los trabajos presentados en los **Anexos A** y **E** de esta tesis es un Diseño D-Optimal. Este procedimiento genera diseños de criterio óptimo para experimentos multi-factor con factores tanto cuantitativos (continuos), como cualitativos (discretos). Además, permite que los factores tengan un número mixto de niveles.

Respecto al proceso foto-Fenton/Ferrioxalato, se evaluaron factores cuantitativos tales como: la temperatura y la concentración de peróxido de hidrógeno; y factores cualitativos tales como: el nivel de radiación y la dosificación del agente oxidante, con diferente número de niveles por cada factor.

Por otro lado, los diseños D-optimal son útiles cuando se tienen limitaciones en el número de experimentos que es posible realizar, ya sea por cuestiones temporales o económicas, o bien, en casos en los que cualquier combinación de los valores de las variables experimentales no es posible. Al respecto, para evitar la precipitación del hierro, se evitó realizar ensayos empleando conjuntamente altas temperaturas y elevadas concentraciones de hierro (Conte et al. 2012).

Luego de ejecutados los diseños experimentales propuestos para cada trabajo, se empleó la Metodología de la Superficie de Respuesra (RSM, por sus siglas en inlés) para evaluar y optimizar la degradación del PCT a través de los procesos Fenton y foto-Fenton/Ferrioxalato. Esta metodología es un conjunto de técnicas matemáticas y estadísticas que se emplean para modelar y analizar problemas, donde una respuesta de interés depende de varios factores. Una vez aplicada la RSM y obtenido el modelo matemático que se ajusta a los datos experimentales, se procede a evaluar la calidad de

dicho modelo, aplicando el análisis de varianza (ANOVA, del inglés *Analysis of Variance*). Finalmente, se localiza el óptimo de la variable respuesta estudiada en cada caso, en función de los niveles de los factores evaluados. En este punto, se pueden utilizar representaciones gráficas (superficies de respuesta tridimensionales) como en el caso de los resultados presentados en el **Anexo A**, o bien, utilizar resoluciones numéricas para la obtención del óptimo, como en el caso de los resultados presentados en el **Anexo E**.

3.4. Modelado de los fotorreactores de laboratorio

En la modelización de los fotorreactores empleados en la presente tesis, se adoptó una metodología que comprende la integración de tres aspectos esenciales inherentes a los modelos cinéticos basados en los primeros principios: establecer una expresión cinética que describa la degradación foto-Fenton del contaminante, plantear un balance de materia para sistemas multi-componentes, acorde al dispositivo experimental empleado, y, evaluar la distribución espacial de los fotones absorbidos en el fotorreactor a través del cálculo de la velocidad volumétrica local de absorción de fotones (LVRPA, por sus siglas en inglés).

En relación a la expresión cinética, en los **Anexos B** y **C** se propusieron mecanismos de reacción sencillos pero detallados, que contemplaron la influencia de las principales variables operacionales sobre la efectividad del proceso foto-Fenton: el flujo de radiación UV-Vis incidente en la ventana del reactor, las concentraciones del contaminante, del hierro (presente en forma de sal o unido a un ligando orgánico) y del agente oxidante (peróxido de hidrógeno), así como también la temperatura de reacción. Esto permitió que la expresión cinética presentada fuera independiente de los valores de emisión de la fuente de radiación, la configuración del reactor y las condiciones experimentales.

Luego, el balance de materia y la evaluación del campo de radiación para los fotorreactores empleados, se muestran en las siguientes secciones.

3.4.1. Balance de Materia

Para un sistema conformado por un reactor fotoquímico (con reciclo externo), que opera en forma discontinua y a temperatura constante, debe plantearse el balance de materia para una especie genérica "i", para evaluar la dependencia de la concentración de los reactivos con el tiempo. Entonces, la ecuación general de conservación de materia en sistemas de varios componentes, en una única fase (sistemas homogéneos) es la siguiente:

$$\frac{\partial C_i(\underline{x},t)}{\partial t} + \underline{\nabla} \cdot \underline{N_i}(x,t) = R_i(\underline{x},t) \qquad (3.1)$$

donde $C_i(\underline{x},t)$ es la concentración molar, $\underline{N_i}(x,t)$ es el flujo molar de materia y $R_i(\underline{x},t)$ es la velocidad de reacción, cada uno correspondiente a la especie "i" del sistema.

Integrando la ecuación del balance de materia local para la especie "i" en el volumen total del sistema (V_{tot}), y aplicando el Teorema de la Divergencia en el término correspondiente al flujo molar, resulta:

$$\int_{V_{tot}} \frac{\partial C_i(\underline{x},t)}{\partial t} dV + \int_A \underline{N_i}(\underline{x},t) \cdot n dA = \int_{V_{tot}} R_i(\underline{x},t) dV \qquad (3.2)$$

Aquí, el término correspondiente al flujo molar de materia de la especie "i" ($\underline{N_i}(\underline{x},t)$) es nulo, ya que el sistema es cerrado (no existen entradas ni salidas de materia).

La integral del primer término del lado izquierdo de la ecuación (3.2) se puede dividir en dos términos: (a) para el volumen de líquido irradiado y (b) para el volumen de líquido no irradiado. Por lo que, aplicando en el primer término de la ecuación (3.2) el Teorema del Transporte y teniendo en cuenta que la velocidad de reacción de los reactivos

en el proceso de foto-Fenton es térmica y fotoquímica, sabiendo que en el reactor (V_{irr}) tienen lugar ambas reacciones, y en el resto del dispositivo ($V_{tot} - V_{irr}$) se produce solamente la reacción térmica; el balance de materia para la especie "i", se puede escribir como:

$$\frac{d}{dt}\int_{V_{irr}} C_i(\underline{x},t)dV + \frac{d}{dt}\int_{V_{tot}-V_{irr}} C_i(\underline{x},t)dV = \int_{V_{irr}} R_i(\underline{x},t)dV + \int_{V_{tot}-V_{irr}} R_i^T(\underline{x},t)dV \quad (3.3)$$

donde $R_i^T(\underline{x},t)$ corresponde a la velocidad de reacción térmica de la especie "i".

Posteriormente, aplicando el Teorema del Valor Medio sobre todos los términos de la ecuación (3.3):

$$\langle C_i(\underline{x},t)\rangle_{V_{irr}} = \frac{1}{V_{irr}}\int_{V_{irr}} C_i(\underline{x},t)dV \quad (3.4)$$

$$\langle C_i(\underline{x},t)\rangle_{V_{tot}-V_{irr}} = \frac{1}{(V_{tot}-V_{irr})}\int_{V_{tot}-V_{irr}} C_i(\underline{x},t)dV \quad (3.5)$$

$$\langle R_i(\underline{x},t)\rangle_{V_{irr}} = \frac{1}{V_{irr}}\int_{V_{irr}} R_i(\underline{x},t)dV \quad (3.6)$$

$$\langle R_i(\underline{x},t)\rangle_{V_{tot}-V_{irr}} = \frac{1}{(V_{tot}-V_{irr})}\int_{V_{tot}-V_{irr}} R_i^T(\underline{x},t)dV = R_i^T(t) \quad (3.7)$$

Cabe aclarar que, en la ecuación (3.7) se considera que la velocidad de reacción térmica (R_i^T) no es función de la posición.

Ahora reemplazando las expresiones (3.4)-(3.7), en la ecuación (3.3) y dividiendo por el volumen total V_{tot}:

$$\frac{d}{dt}\left[\frac{V_{irr}}{V_{tot}}\left\langle C_i(\underline{x},t)\right\rangle_{V_{irr}} + \frac{(V_{tot}-V_{irr})}{V}\left\langle C_i(\underline{x},t)\right\rangle_{V_{tot}-V_{irr}}\right] = \frac{V_{irr}}{V_{tot}}\left\langle R_i(\underline{x},t)\right\rangle_{V_{irr}} + \frac{(V_{tot}-V_{irr})}{V_{tot}}R_i^T(t) \quad (3.8)$$

Si se considera además que el sistema se encuentra en condición de mezcla perfecta, el promedio de la concentración C_i coincide con el valor puntual medio en el mismo espacio, es decir:

$$\frac{d}{dt}\left\langle C_i(\underline{x},t)\right\rangle_{V_{tot}-V_{irr}} = \left.\frac{dC_i(t)}{dt}\right|_{V_{tot}-V_{irr}} \quad (3.9)$$

Además, como el volumen del fotorreactor es mucho menor que el del resto del sistema ($V_{tot} \gg V_{irr}$), entonces:

$$\frac{d}{dt}\left[\frac{V_{irr}}{V_{tot}}\left\langle C_i(\underline{x},t)\right\rangle_{V_{irr}} + \frac{(V_{tot}-V_{irr})}{V_{tot}}\left\langle C_i(\underline{x},t)\right\rangle_{V_{tot}-V_{irr}}\right] \cong \frac{dC_i(t)}{dt} \quad (3.10)$$

Finalmente, reemplazando la ecuación (3.10) en la ecuación (3.8) se obtiene:

$$\frac{dC_i(t)}{dt} = \frac{V_{irr}}{V_{tot}}\left\langle R_i(\underline{x},t)\right\rangle_{V_{irr}} + \frac{(V_{tot}-V_{irr})}{V_{tot}}R_i^T(t) \quad (3.11)$$

Por lo tanto, el balance de materia para la degradación de PCT por medio de la reacción foto-Fenton en un sistema discontinuo y con reciclo externo, como es el caso de los reactores de Placa Plana (**Anexo B**) y Anular Concéntrico (**Anexo C**), está representado por la ecuación diferencial ordinaria no lineal y de primer orden (3.11).

3.4.2. Velocidad volumétrica local de absorción de fotones (LVRPA)

El conocimiento del campo de radiación en fotorreactores es fundamental para maximizar el uso eficiente de los fotones y determinar los parámetros cinéticos intrínsecos de las reacciones fotoquímicas. Para determinar el campo de radiación, se

debe resolver la Ecuación de Transferencia Radiativa (RTE, por sus siglas en inglés). Esta describe la intensidad de radiación en cualquier posición a lo largo de un camino de rayo a través de un medio. En sistemas homogéneos (sin dispersión) en los que se puede descartar la emisión de fotones, y sólo se considera la absorción de radiación por parte de las especies presentes en el sistema reaccionante, la RTE está definida por la siguiente ecuación:

$$\frac{dI_\lambda(\mathrm{s},\underline{\Omega},t)}{ds} = -\kappa_\lambda I_\lambda(\mathrm{s},\underline{\Omega},t) \qquad (3.12)$$

Donde I_λ es la distribución espectral de intensidades de radiación, s la coordenada lineal a lo largo de la dirección $\underline{\Omega}, \Omega$ el ángulo sólido y κ_λ el coeficiente de absorción espectral.

Resolviendo la ecuación (3.12), ya considerando una posición $\underline{x}$ dentro del reactor, se obtiene la intensidad de radiación para una dada longitud de onda. De esta manera, para computar la LVRPA $\left(e_\lambda^a(\underline{x},t)\right)$, deberá resolverse la siguiente ecuación:

$$e_\lambda^a(\underline{x},t) = \kappa_\lambda \int_\Omega I_\lambda(\underline{x},\underline{\Omega},t)d\Omega \qquad (3.13)$$

En el caso de que la radiación incidente sea policromática, la ecuación (3.13) deberá ser integrada en todo el rango de longitudes de onda de interés:

$$e^a(\underline{x},t) = \int_\lambda \kappa_\lambda \int_\Omega I_\lambda(\underline{x},\underline{\Omega},t)d\Omega d\lambda \qquad (3.14)$$

La LVRPA se define como la cantidad de fotones que se absorben por unidad de tiempo y volumen de reacción. Depende de la fuente de fotones, la concentración de especies absorbentes, las propiedades ópticas del sistema y la geometría del reactor, por lo que existen diversos modelos que permiten calcular la LVRPA espectral dependiendo de la geometría del dispositivo experimental.

En el trabajo presentado en el **Anexo B**, donde se empleó un reactor de placa plana iluminado desde un solo lateral por un simulador solar, la radiación se modeló empleando un modelo unidimensional que es función únicamente de la coordenada longitudinal (x) y del tiempo de reacción (t). Dado que la radiación incidente es policromática, y que el término empleado en la resolución numérica de los balances de materia es la LVRPA promediada en el volumen del reactor ($\langle \sum_\lambda e_\lambda^a(x,t) \rangle_{V_{irr}}$), la expresión para el cálculo resulta:

$$\langle \sum_\lambda e_\lambda^a(x,t) \rangle_{V_{irr}} = \frac{\kappa_\lambda(t) \sum_\lambda q_{W,\lambda} \left[1 - exp\left(-\kappa_{T,\lambda}(t) L_R\right)\right]}{L_R \kappa_{T,\lambda}(t)} \qquad (3.15)$$

Donde κ_λ es el coeficiente de absorción volumétrico de las especies reactivas, $q_{w,\lambda}$ el flujo neto de radiación sobre la ventana del reactor, $\kappa_{T,\lambda}$ el coeficiente de absorción volumétrico total del medio reactivo, y L_R es la longitud del fotorreactor.

En el trabajo presentado en el **Anexo C**, donde se utilizó un fotorreactor anular concéntrico, se empleó un modelo de fuente lineal con emisión esférica e isotrópica (modelo LSSE, por sus siglas en inglés). Nuevamente, considerando que la radiación incidente es policromática, y que el término empleado en la resolución numérica de los balances de materia es la LVRPA promediada en el volumen del reactor, resulta:

$$\langle \sum_\lambda e_\lambda^a\left(\underline{x}, t\right) \rangle_{V_{irr}} = \frac{2\pi}{V_{irr}} \int_0^L \int_{r_{int}}^{r_{ext}} \left[\kappa_\lambda\left(\underline{x}, t\right) \frac{P_{\lambda,s}}{2\pi L_L} \int_{\theta_1}^{\theta_2} exp\left[-\frac{\kappa_{T,\lambda}\left(\underline{x}, t\right)(r_i - r_{int})}{\cos\theta} \right] d\theta \right] r \, dr \, dz \qquad (3.16)$$

Donde $P_{\lambda,s}$ es la potencia de emisión espectral de la lámpara (proporcionada por el proveedor de la lámpara), r es el radio, L_L es la longitud útil de la lámpara y r_{int} y r_{ext} son los radios interno y externo del fotorreactor anular, respectivamente. Además, θ_1 y θ_2 son

los ángulos límite de integración (definidos trigonométricamente, ecuación (3.17) necesarios para calcular la radiación absorbida en un punto genérico *I = I(r,z)* (ubicado en $\underline{x}$) dentro del reactor.

$$\theta_1 = tan^{-1}\left(\frac{r_i}{L_L - z_i}\right) \qquad \text{y} \qquad \theta_2 = tan^{-1}\left(\frac{-r_i}{z_i}\right) \tag{3.17}$$

Capítulo 4. RESULTADOS

4.1. Degradación foto-Fenton del paracetamol en un fotorreactor anular concéntrico escala planta piloto. Modelado cinético y evaluación de la citotoxicidad.

Se desarrolló un modelo cinético asociado a la degradación foto-Fenton (PFF) del PCT, así como también de sus intermediarios de reacción (HQ y BQ), en un fotorreactor anular concéntrico escala planta piloto, utilizando una fuente de radiación UV, y $FeSO_4$ como catalizador. Todas las reacciones se llevaron a cabo a pH 2.8. Los parámetros operativos evaluados fueron la concentración inicial de Fe^{2+}, la concentración inicial de HP, y presencia o ausencia de radiación. Además, se evaluó la toxicidad del efluente generado mediante ensayos de citotoxicidad con células VERO.

Inicialmente, se propuso un mecanismo de reacción simplificado para obtener las velocidades de reacción del PCT, de sus principales intermediarios (HQ y BQ) y del HP. También, teniendo en cuenta la geometría del dispositivo experimental, se calculó la LVRPA ($\langle \sum_\lambda e_\lambda^a(\underline{x}, t) \rangle_{V_{irr}}$) empleando un modelo de fuente lineal con emisión esférica e isotrópica (LSSE ecuación (3.16), **sección 3.4.2**).

Se utilizó un procedimiento de optimización no lineal para obtener los valores de las constantes cinéticas que minimizan las diferencias entre las concentraciones predichas y los valores experimentales correspondientes, para cada especie estable considerada (PCT, HP, HQ y BQ). Para ello, se resolvieron las ecuaciones diferenciales ordinarias del sistema (A.1)-(A.5) del **Anexo C** para obtener los valores de concentración teóricos de cada especie. Los parámetros cinéticos estimados fueron coherentes con la literatura

especializada, y el modelo cinético se ajustó adecuadamente a los datos experimentales, dado que los NRMSE calculados se encontraron en el mismo orden de magnitud que el error experimental: 14.30, 9.98, 1.86 y 1.61% para PCT, HP, HQ and BQ, respectivamente. Además, se realizó la validación del modelo con un set de ensayos distintos a los usados para estimar los parámetros cinéticos (**Figura 4.1**), lo que confirmó la buena capacidad del modelo cinético para predecir las variaciones temporales de las concentraciones de PCT, HP y los principales intermediarios de reacción.

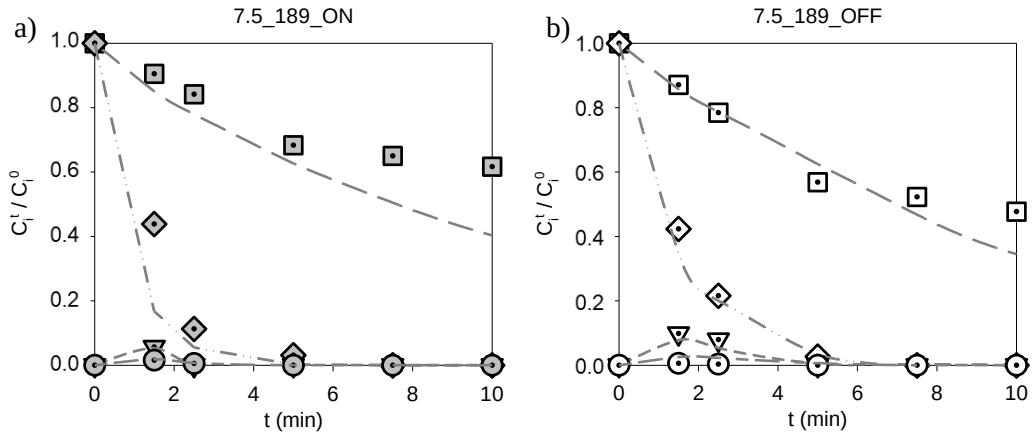

Figura 4.1. Resultados del modelo y experimentales para los compuestos PCT, HP, HQ y BQ, en concentraciones relativas, para los ensayos de validación: a) $[Fe^{2+}]^0$ = 7.5 mg L^{-1}, $[HP]^0$ = 189 mg L^{-1}, radiación: ON; b) $[Fe^{2+}]^0$ = 7.5 mg L^{-1}, $[HP]^0$ = 189 mg L^{-1}, radiación: OFF. Claves: PCT = ♦, HP = ■, HQ = ▼, BQ = ●, resultados experimentales; y PCT = línea de guion-punto, HP = línea de guion-largo, HQ = línea de guion-corto, BQ = línea corta-larga, resultados del modelo.

Los resultados experimentales mostraron que, en presencia de radiación, se alcanzaron conversiones de PCT cercanas al 100%, mientras que, en condiciones de Fenton, oscilaron entre 80.4% y 96.9%. Se observó una mejora significativa en la mineralización del TOC en presencia de radiación, con conversiones superiores al 33.5% para todas las condiciones estudiadas después de 75 minutos de reacción. Se observó que el aumento en la concentración del agente oxidante no mejoró la velocidad de degradación del PCT. Tampoco se observaron mejores resultados en la conversión final de PCT y la

remoción de sus intermediarios en reacciones Fenton (oscuras). Sin embargo, el incremento de la concentración inicial de hierro tuvo un efecto beneficioso en la degradación de los subproductos de la reacción. En particular, al utilizar la concentración máxima de hierro evaluada, se observó una reducción del 50% en el tiempo necesario para eliminar completamente dichos subproductos.

Finalmente, y con el objetivo de evaluar la toxicidad del efluente generado, se realizaron ensayos de toxicidad utilizando células VERO. Se determinó que la concentración letal media (LC_{50}) para PCT fue considerablemente alta (>1000 mg L^{-1}), lo que indica que la concentración inicial seleccionada de PCT (40 mg L^{-1}) no tiene un efecto tóxico en las células VERO. Los resultados mostraron que la viabilidad celular está influenciada principalmente por la presencia de radiación y las concentraciones iniciales de los reactivos de Fenton, con una mejora significativa en presencia de radiación y concentraciones más altas de hierro y peróxido de hidrógeno. La mayoría de las condiciones experimentales estudiadas permitieron una recuperación completa de la viabilidad celular hacia el final del proceso de degradación, incluso para bajas conversiones finales de TOC. Esto sugiere que, si bien algunos subproductos podrían tener efectos tóxicos en las células VERO, la naturaleza hidrofílica de estos compuestos podría reducir su toxicidad al limitar su capacidad de penetrar en las membranas celulares (Escher et al. 2008).

Este trabajo fue desarrollado en conjunto con investigadores de la Universidad Politécnica de Cataluña, España. Los resultados fueron publicados en el siguiente artículo de investigación: "*Kinetic model of photo-Fenton degradation of paracetamol in an annular reactor: main reaction intermediates and cytotoxicity studies*" (2022). B. Giménez, L. Conte, F. Audino, A. Schenone, M. Graells, O. Alfano, M. Pérez-Moya. Catalysis Today. Doi: https://doi.org/10.1016/j.cattod.2022.11.019. Trabajo presentado

en el **Anexo C**.

Y en los siguientes Congresos:

- VIII Congreso Argentino de la Sociedad de Toxicología y Química Ambiental, Capítulo Argentino. (2022, Argentina).
- 11th European Conference on Solar Chemistry and Photocatalysis: Environmental Applications (SPEA). (2022, Italia).

4.2. Estudio de la influencia de parámetros operacionales clave en la degradación foto-Fenton del paracetamol a pH natural. Evaluación de la toxicidad del sistema.

Teniendo en cuenta las limitaciones del PFF en condiciones ácidas, se comenzó a evaluar la degradación del PCT empleando los procesos Fenton y foto-Fenton, a pH cercano a la neutralidad, utilizando ferrioxalato como catalizador y un simulador solar como fuente de radiación (PFF/FeOxa). En una primera etapa, se desarrolló un modelo empírico empleando un diseño experimental D-optimal combinado con RSM. Además, se evaluó la toxicidad del efluente generado mediante la prueba Microtox®.

Específicamente se estudió la influencia sobre el proceso de 3 parámetros clave: temperatura (T, entre 25 y 50 °C), concentración de peróxido de hidrógeno (HP, entre 189 y 756 mg L^{-1}) y Radiación (Sin Rad, Baja Rad (31.6 W m^{-2}) y Alta Rad (57.5 W m^{-2})). Para tal fin, primero se construyó la matriz experimental utilizando el diseño D-optimal, y, luego de obtener los resultados, se empleó la RSM donde la variable respuesta a optimizar fue la conversión del PCT a los 90 min de reacción, X_{90}^{PCT}(%). Dichas X_{90}^{PCT} se ajustaron a un modelo polinomial. Posteriormente, se utilizó el análisis de regresión

múltiple para calcular los coeficientes del modelo y el análisis de varianza (ANOVA) con un nivel de confianza del 95% para validarlos, dando como resultado la siguiente expresión (ecuación (4.1):

$$\begin{aligned} \boldsymbol{X_{90,pred}^{PCT}}(\%) = {} & 75.24 + 16.02X_1 - 2.16X_2 - 36.73X_3(1) + 17.71X_3(2) \\ & + 18.47X_1X_3(1) - 10.58X_1X_3(2) - 0.35X_2X_3(1) \\ & - 1.60X_2X_3(2) - 2.15X_1^2 - 3.25X_2^2 \end{aligned} \tag{4.1}$$

Donde X_1, X_2 y X_3 representan los valores codificados de las variables en el modelo (T, HP y Rad, respectivamente). Para el modelo se obtuvieron valores satisfactorios de desviación estándar (0,74), R^2 y R^2-ajustado (0,9997 y 0,9993, respectivamente).

Las superficies de respuesta para cada nivel de radiación se presentan en la **Figura 4.2**. Para todo el rango de T y concentración de HP evaluados, las conversiones de PCT más bajas se alcanzaron para el sistema Fenton (**Figura 4.2 a**). La influencia significativa de la T en el proceso de Fenton se puede confirmar ya que, a cualquier nivel de radiación, al aumentar la T aumenta la conversión del PCT. Por otro lado, es necesario resaltar el importante efecto de la radiación en el sistema. Para todas las condiciones irradiadas, el X_{90}^{PCT} fue superior al 77% (**Figura 4.2 b y c**). Además, se observaron conversiones de PCT cercanas al 100% utilizando altos niveles de radiación.

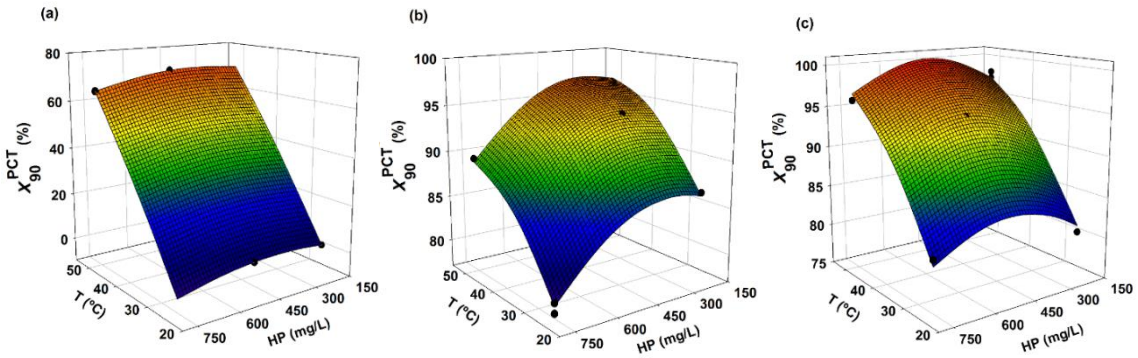

Figura 4.2. Superficies de respuesta y valores experimentales (círculos) para X_{90}^{PCT} en función de la T y la concentración de HP. a) Sin radiación (Fenton), b) Baja radiación y c) Alta radiación.

A partir del modelo desarrollado, se estimaron las condiciones óptimas de operación para maximizar la conversión de contaminante, considerando la dosis mínima de HP, obteniéndose: T = 50ºC y HP = 326,3 mg L^{-1} (Sin Rad), $X_{90,pred}^{PCT}$= 71.28%; T = 50ºC y HP = 189 mg L^{-1} (Baja Rad), $X_{90,pred}^{PCT}$= 96.75%; y T = 40ºC y HP = 189 mg L^{-1} (Alta Rad), $X_{90,pred}^{PCT}$= 92.75%. Estos resultados predichos por el modelo fueron muy similares a los valores experimentales obtenidos empleando las condiciones operacionales óptimas (75.52, 96.88 y 91.50 %, respectivamente).

En dichas condiciones óptimas, se evaluó la evolución de la toxicidad en el sistema (expresada como porcentaje de inhibición de la bioluminiscencia de cepas de bacterias de *V. fischeri* después de 15 min de incubación, I (%)). En la **Figura 4.3** se presenta el I (%) obtenido junto con la evolución experimental de PCT, y de los principales intermediarios de reacción identificados (HQ, hidroquinona y BQ, 1,4-benzoquinona) en función del tiempo, en el caso de Alta Rad.

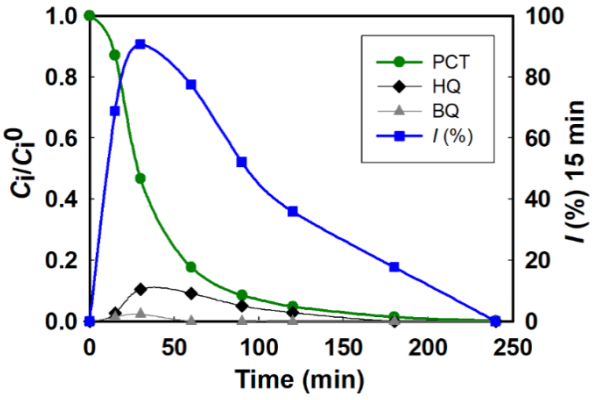

Figura 4.3. Concentraciones relativas experimentales vs. tiempo para PCT, HQ, BQ e I (%) en las condiciones óptimas para Alta Rad.

En la **Figura 4.3** se puede observar que los niveles máximos y mínimos de toxicidad encontrados en el sistema están estrechamente relacionados con las concentraciones máximas y mínimas de HQ y BQ, lográndose una reducción de la toxicidad del sistema a

medida que avanzaba la reacción. Asimismo, el comportamiento observado en los experimentos con Baja y Sin Rad fue muy similar al presentado para el caso de Alta Rad. Sin embargo, solo operando el sistema con altos niveles de radiación fue posible eliminar por completo la toxicidad del sistema (I (%) = 0) después de 240 min de reacción.

Estos resultados fueron publicados en el siguiente trabajo de investigación: "*Paracetamol removal by photo-Fenton processes at near-neutral pH using a solar simulator: Optimization by D-optimal experimental design and toxicity evaluation*" (2020). B. Giménez, L. Conte, O. Alfano, A. Schenone. Journal of Photochemistry and Photobiology A: Chemistry. Doi: https://doi.org/10.1016/j.jphotochem.2020.112584. Trabajo presentado en el **Anexo A**.

Y en los siguientes Congresos:

- 4th Iberoamerican Conference on Advanced Oxidation Technologies (IV CIPOA). (2019, Brasil).
- X Congreso Argentino de Ingeniería Química (CAIQ2019). (2019, Argentina).
- XXVI Jornadas de Jóvenes Investigadores de la Asociación de Universidades Grupo Montevideo (JJI-AUGM). (2018, Argentina).

4.3. Modelado cinético de la degradación foto-Fenton del Paracetamol a pH natural empleando un reactor de placa plana y un simulador solar.

En una etapa posterior en el estudio del PFF/FeOxa, se desarrolló un modelo cinético capaz de describir la degradación foto-Fenton del PCT a pH = 5.5, en un reactor de placa plana, empleando ferrioxalato como catalizador y un simulador solar como

fuente de radiación. Considerando los resultados alcanzados anteriormente en relación a las variables operacionales clave para el proceso estudiado (**sección 4.2**), se consideró que el modelo desarrollado debía contemplar la influencia de la concentración de peróxido de hidrógeno, la temperatura de reacción y el nivel de radiación. Además, se incluyó explícitamente el efecto de la radiación a través del cálculo de la LVRPA.

Al igual que para el modelo presentado en la **sección 4.1**, para este sistema se planteó un mecanismo de reacción simplificado, apropiado para describir la degradación Fenton y foto-Fenton/Ferrioxalato del PCT. Para los estudios cinéticos realizados en el reactor de placa plana, los balances de masa y las condiciones iniciales vienen dados por el conjunto de ecuaciones diferenciales ordinarias (EDOs) de primer orden, ecuaciones (13)-(20) presentadas en el **Anexo B**. Luego, para resolver dicho conjunto de EDOs es necesario conocer el valor de la LVRPA promediado sobre el volumen del reactor (es decir, $\langle \sum_{\lambda} e_{\lambda}^{a}(x,t) \rangle_{V_{irr}}$) donde, para calcularlo, se utilizó un modelo de radiación unidimensional (ecuación (3.15), **sección 3.4.2**).

De esta manera, a partir del modelo cinético propuesto y los datos experimentales, se estimaron los parámetros cinéticos aplicando un procedimiento de regresión no lineal. Finalmente, para probar la confiabilidad del modelo, se calculó el error cuadrático medio normalizado (NRMSE). El modelo propuesto mostró una buena concordancia con los datos experimentales, y los resultados obtenidos fueron: 14.52, 1.96, 4.36, 13.16, y 8.72 % para PCT, BQ, HQ, HP, y Oxa, respectivamente.

La **Figura 4.4** muestra los datos experimentales y los predichos por el modelo cinético de las concentraciones relativas del PCT, HQ, BQ, HP y Oxa en función del tiempo, para niveles de Alta y Baja Rad. Se puede observar que, aunque para ambas condiciones evaluadas se observaron valores de $C_{PCT}^{rel,t}$ inferiores al 5%, el ensayo

realizado con un nivel de radiación baja, requirió un tiempo de reacción mayor (120 min vs. 60 min). Además, los resultados mostrados a Baja Rad necesitaron una dosis de agente oxidante 4 veces mayor (756 mg L^{-1} vs 189 mg L^{-1}).

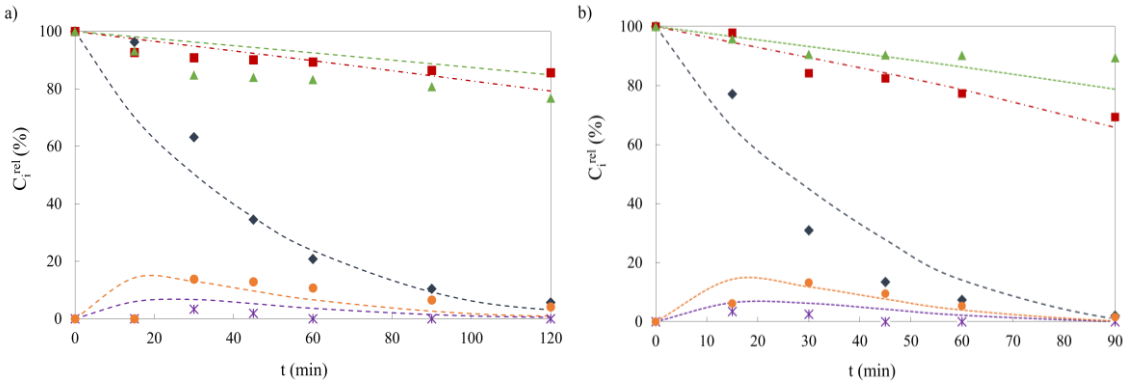

Figura 4.4. Resultados experimentales y del modelo para las concentraciones relativas de PCT, HP, Oxa, HQ y BQ. (a) Baja Rad, T = 50ºC, HP = 756 mg L^{-1}; (b) Alta Rad, T = 50ºC, HP = 189 mg L^{-1}. Claves: líneas continuas: resultados del modelo y (⧫) PCT, (■) HP, (▲) Oxa, (●) HQ, and (*) BQ, resultados experimentales.

Finalmente, en relación con el grado de mineralización alcanzado al final de la reacción (t = 180 min), se observó que el nivel de radiación más alto mejora significativamente el grado de conversión de TOC logrado. Este valor varió desde un máximo del 17.04% en el caso de los ensayos Fenton, hasta una conversión de TOC máxima de 36.84% y el 22.50% en caso de experimentos realizados con Alta y Baja Rad, respectivamente, considerando pruebas realizadas en condiciones similares.

Estos resultados fueron publicados en el siguiente trabajo de investigación: "*Reaction kinetics formulation with explicit radiation absorption effects of the photo-Fenton degradation of paracetamol under natural pH conditions*" (2021). B. Giménez, A. Schenone, O. Alfano, L. Conte. Environmental Science and Pollution Research. Doi: https://doi.org/10.1007/s11356-020-11993-5. Trabajo presentado en el **Anexo B**.

Y en el siguiente Congreso:

- 4th Iberoamerican Conference on Advanced Oxidation Technologies (IV CIPOA). (2019, Brasil).

4.4. Aplicabilidad del proceso foto-Fenton para bajas concentraciones de paracetamol, empleando ferrioxalato y un simulador solar

Se evaluó la eficiencia del PFF/FeOxa en la remoción del PCT presente en muy baja concentración, considerando los niveles del contaminante hallados en cuerpos de agua naturales. Las concentraciones iniciales de PCT, hierro y HP fueron de 500 μg L^{-1}, 1 mg L^{-1} (relación Fe/Oxa=1/10) y 2.36 mg L^{-1}, respectivamente. Se estudió el proceso variando el nivel de radiación incidente sobre el reactor, entre Sin Rad, Baja Rad (31.6 W m^{-2}) y Alta Rad (57.5 W m^{-2}).

En primer lugar, fue posible cuantificar el PCT para monitorear su degradación durante la reacción gracias a la aplicación del protocolo SPE optimizado con cartuchos comerciales C18, seguido del análisis por HPLC. Cada alícuota (15 mL) tomada a distintos tiempos de reacción fue sometida al proceso de SPE optimizado, y luego se midió la concentración de PCT en el eluido por HPLC-UV.

Luego, a partir de la cuantificación del PCT, se calcularon los valores de conversión de PCT a los 90 minutos de reacción para cada nivel de radiación, dando como resultado: 26.58%, 71.01% y 94.36% para las condiciones Sin, Baja y Alta Rad, respectivamente. De esta manera, se observó un mayor porcentaje de conversión de PCT en los ensayos con radiación, siendo más notorio el efecto en el caso de Alta radiación. Esto evidencia la importancia de la utilización de una fuente de radiación en el proceso foto-Fenton homogéneo. Teniendo en cuenta las conversiones alcanzadas, se demostró que es posible

la degradación del PCT en concentraciones en el orden de los ppb, utilizando el sistema foto-Fenton/Ferrioxalato, empleando muy bajas concentraciones de los reactivos Fenton.

Estos resultados fueron presentados en el "5th Iberoamerican Conference on Advanced Oxidation Technologies (V CIPOA)" (2022, Perú), bajo el título: "*Influence of simulated solar radiation on micropollutant removal with ferrioxalate-assisted photo-Fenton*". Este trabajo es presentado en el **Anexo D**.

4.5. Efecto de la dosificación puntual del peróxido de hidrógeno en la degradación del paracetamol a través de los procesos Fenton y foto-Fenton/Ferrioxalato en matrices complejas

Considerando la notable eficiencia del PFF/FeOxa en la remoción del PCT operando a pH natural, evitando así los ajustes de pH, y teniendo en cuenta la posibilidad de utilizar luz solar, se identificó al HP como la mayor fuente de costos del proceso. Por lo tanto, se evaluó la dosificación del agente oxidante en el sistema (PPF/FeOxa), con el objetivo de mejorar la eficiencia económica y operativa del proceso y, al mismo tiempo, reducir el consumo de HP. Se estudió la influencia de la dosificación puntual del agente oxidante sobre la eficacia del sistema foto-Fenton/Ferrioxalato para la degradación del PCT, en condiciones de pH natural y utilizando un simulador solar como fuente de radiación. Además, se analizó la interacción de esta dosificación puntual con otras variables operativas del proceso, como el nivel de radiación incidente sobre el reactor y la concentración de HP. La estrategia de dosificación del HP consistió en dos pulsos del mismo volumen de solución estándar de HP, a los 0 y 90 min de reacción. Cada pulso contribuyó con la mitad de la concentración total del HP correspondiente a cada ensayo

realizado. Asimismo, se evaluó la efectividad de la dosificación puntual del HP frente al empleo de matrices acuosas reales.

En primer lugar, respecto al nivel de HP y su impacto en la conversión del contaminante, se observó que un exceso de oxidante (por encima de 378 mg L^{-1}) produjo un efecto negativo en el sistema (consumo de HO• y auto-descomposición del HP), lo que resultó en una menor eliminación del contaminante. Sin embargo, se demostró que la estrategia de dosificación puntual pudo mitigar este efecto. La mayor influencia de la dosificación de HP se observó en las reacciones de Fenton, ya que, en estas condiciones, se lograron conversiones de PCT más altas cuando se dosificaba el agente oxidante. No obstante, se encontró una excepción en el ensayo en condiciones de oscuridad con el nivel más bajo de HP (94.5 mg L^{-1}). En este caso, la reacción comenzó con 1/4 de la concentración estequiométrica del oxidante, convirtiendo al HP en el reactivo limitante del proceso.

En segundo término, se pudo verificar que la dosificación de HP influyó positivamente en el ciclo catalítico del hierro. Se alcanzaron mayores concentraciones de Fe^{2+} en tiempos de reacción más cortos en aquellos ensayos con dosificación de HP, lo que condujo a mejores rendimientos de las reacciones de Fenton y foto-Fenton. Además, bajo la estrategia de dosificación, los intermediarios HQ y BQ desaparecieron en tiempos más cortos de reacción, respecto a los ensayos realizados sin la estrategia de dosificación. Es importante destacar que éste fue un resultado positivo desde el punto de vista toxicológico relacionado con estos subproductos, ya que poseen valores de EC_{50} (determinados en la bacteria *V. fischeri*) realmente bajos (0.04 ppm y 0.10 ppm para HQ y BQ, respectivamente).

En cuanto al modelado matemático de las reacciones Fenton y foto-Fenton, se

aplicó un diseño experimental D-óptimo, para investigar los efectos de tres variables independientes en la conversión de PCT: concentración de HP (A), dosificación de HP (B) y nivel de radiación (C). El modelo de regresión que relaciona dichas variables con la conversión del PCT a los 180 min de reacción está representado por la ecuación (4.2).

$$\boldsymbol{X_{PCT}^{180,pred}}(\%) = +77.23 - 16.51 * A + 5.90 * B + 19.10 * C + 12.94 * A * C - 2.90 * B * C - 7.76 * A^2 \quad (4.2)$$

Las condiciones operacionales óptimas predichas fueron: presencia de radiación, con dosificación, concentración total de HP = 378 mg L^{-1}.

Bajo dichas condiciones óptimas se evaluó el rendimiento del proceso en tres matrices de agua diferentes (una matriz con aniones inorgánicos, una matriz de agua subterránea real y una matriz que emula aguas residuales industriales, **Figura 4.5 a**, **b** y **c**, respectivamente). Para la matriz de aniones, se observó que la conversión de PCT lograda a los 180 minutos de reacción fue considerablemente mayor al realizar la estrategia de dosificación del agente oxidante. Además, la dosificación de HP condujo a una disminución en su consumo, lo que llevó a un uso más eficiente del agente oxidante.

En los ensayos realizados en una muestra de agua subterránea real, no se observaron diferencias significativas en las conversiones de PCT ni en los consumos de HP cuando el ensayo se realizó con o sin la estrategia de dosificación. La presencia de cationes en este tipo de muestra podría ser la causa de la ineficiencia del sistema reaccionante, ya que dichos cationes pueden formar complejos estables con oxalato, reduciendo la disponibilidad de este ligando, y, por ende, inactivando el catalizador.

Finalmente, se empleó una matriz de agua residual industrial, preparada utilizando CIP300® (detergente de pH neutro) con una concentración final en el medio de reacción de 0,1%, y PCT en forma de píldoras, que contienen almidón pre-gelatinizado, ácido

esteárico y povidona K30 como excipientes. Con esta matriz, se observó una conversión ligeramente menor de PCT al emplear la estrategia de dosificación del agente oxidante. Sin embargo, a pesar de observarse un aumento notable en el consumo de HP en comparación con las otras dos matrices acuosas evaluadas, la estrategia de dosificación redujo efectivamente el consumo improductivo del agente oxidante, demostrando la eficacia del proceso, aún en presencia de matrices de agua residual.

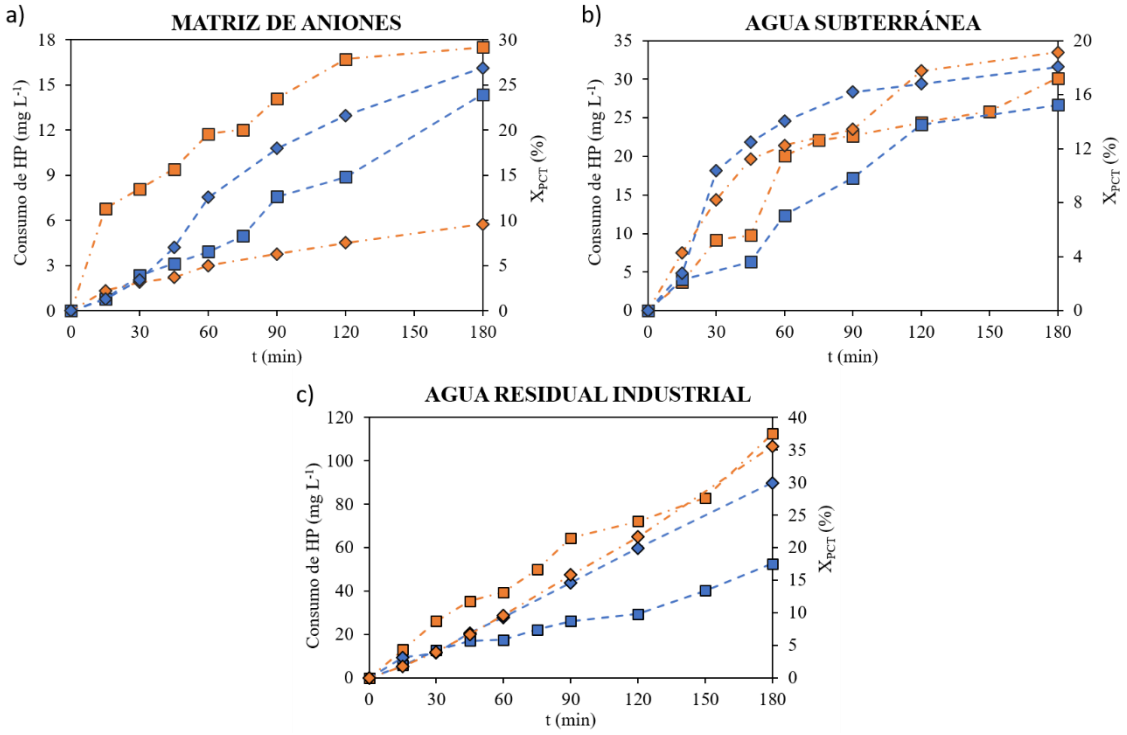

Figura 4.5. Evoluciones temporales del consumo de HP (en mg L^{-1}, símbolos = ■) y de la conversión de PCT (en %, símbolos = ♦) para ensayos realizados en diferentes matrices acuosas, RAD = ON, y HP = 378 mg L^{-1}. Los ensayos con dosificación de HP están en azul y con línea de guion-largo, y los ensayos sin dosificación de HP están en naranja y con línea guion-punto.

Estos resultados fueron publicados en el siguiente trabajo de investigación: "*Improvement of ferrioxalate assisted Fenton and photo-Fenton processes for paracetamol degradation by hydrogen peroxide dosage*" (2024). B. Giménez, L. Conte, S. Duarte, A. Schenone. Environmental Science and Pollution Research. Doi: https://doi.org/10.1007/s11356-024-32056-z. Trabajo presentado en el **Anexo E**.

Y en los siguientes Congresos:

- 11th World Congress of Chemical Engineering and II Iberoamerican Congress of Chemical Engineering - Global Symposium on Advanced Oxidation Processes (2023, Argentina).

- 5th Iberoamerican Conference on Advanced Oxidation Technologies (V CIPOA). (2022, Perú).

4.6. Estudio del rol de la dosificación continua del peróxido de hidrógeno en el proceso foto-Fenton empleando un fotorreactor de placa plana y un fotorreactor solar escala planta piloto

A partir de los resultados presentados en la **sección 4.5**, se decidió evaluar la influencia de estrategias de dosificación más complejas sobre el PFF/FeOxa. En consecuencia, se investigó el rol de la dosificación continua de peróxido de hidrógeno en la eliminación del PCT presente en diferentes matrices acuosas, utilizando el proceso foto-Fenton/Ferrioxalato solar. Se analizaron sistemáticamente diferentes parámetros en las estrategias de dosificación de HP: pulso inicial de HP, tiempo de dosificación y concentración de HP, para evaluar sus impactos en la eliminación de contaminantes (X_{PCT}), el consumo específico de oxidante ($\Upsilon^{t}_{HP/PCT}$) y los niveles de toxicidad (I(%)). El análisis involucró diferentes matrices acuosas, las cuales fueron tratadas primero en un reactor de laboratorio y, posteriormente, en un reactor solar escala planta piloto.

Los resultados a escala laboratorio mostraron que dosis bajas de HP resultaron en altas conversiones de PCT, mientras que dosis muy altas de HP condujeron a una menor conversión del PCT debido al efecto atrapador de radicales libres del agente oxidante.

Las principales diferencias operativas se encontraron en el consumo observado del agente oxidante, donde, a dosis bajas de peróxido de hidrógeno, este valor estuvo por debajo del valor requerido por estequiometría para la mineralización del PCT (4.72 mgHP $mgPCT^{-1}$), lo que resultaría en una eliminación incompleta de los intermedios de reacción. Por otro lado, para dosis medias y altas de HP, se alcanzaron consumos del agente oxidante variados, con un consumo improductivo máximo en los ensayos donde se emplearon las concentraciones máximas de HP, lo que afectó negativamente el proceso de degradación del PCT.

Teniendo en cuenta los resultados presentados anteriormente, se llevaron a cabo experimentos con muestras más complejas. Se observó que, en el caso del agua residual industrial simulada (**Figura 4.6**), la degradación del PCT fue deficiente (18.9% a los 180 min) y el consumo específico de HP fue mucho mayor que el valor estequiométrico, lo que sugiere un alto consumo improductivo del oxidante debido a la presencia de materia orgánica aportada por el detergente.

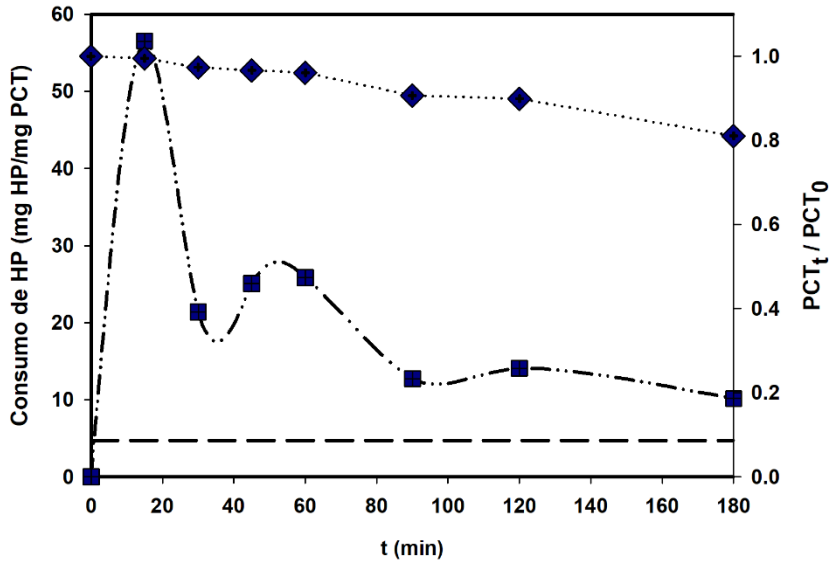

Figura 4.6. Evolución temporal del consumo específico de HP (■) y la concentración relativa de PCT (♦) para el agua residual industrial simulada con 0.1% CIP300 en el fotorreactor escala laboratorio.

En relación a los resultados a escala planta piloto, la **Figura 4.7** muestra las evoluciones asociadas a la degradación del PCT, en función de la energía acumulada en cada experimento solar. Dicha radiación acumulada ($Q_{300\text{-}550nm}$, KJ L^{-1}) se calculó según la ecuación (5) presentada en el **Anexo F.**

Los resultados mostrados en la **Figura 4.7** ilustran la eficacia del proceso estudiado.

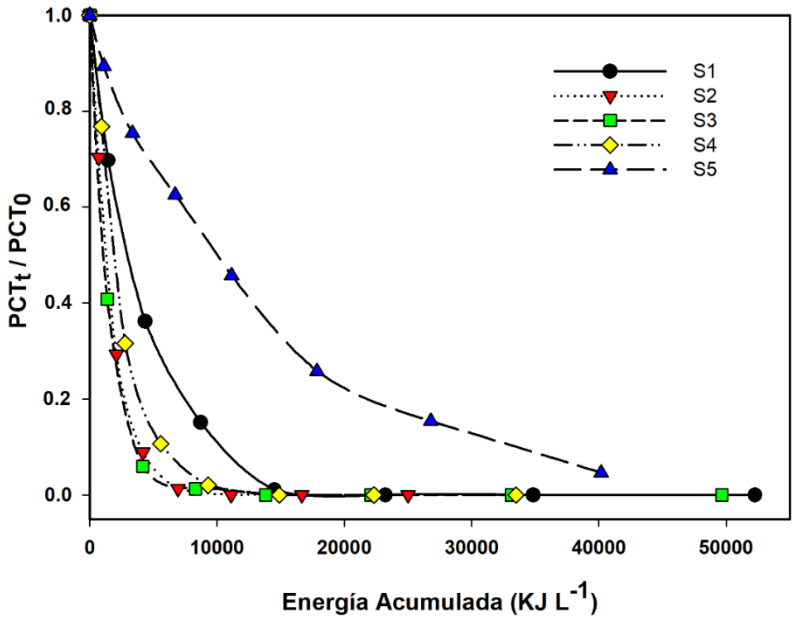

Figura 4.7. Concentraciones relativas del PCT en función de la energía acumulada (ensayos S1-S5) en los experimentos donde se empleó el reactor solar.

En primer lugar, se logró una conversión completa del PCT en solo 60 minutos de reacción para condiciones de agua ultrapura (S1 a S3). Sin embargo, al emplear dosis bajas de agente oxidante (S1), se evidenció una notable disminución en la velocidad de degradación del contaminante, a la vez que se necesitó hasta un 200% más de energía acumulada para lograr la conversión completa del contaminante en comparación con una concentración de oxidante intermedia (378 mg L^{-1}, S2). Finalmente, la dosificación de un exceso de HP (S3) no proporcionó ningún beneficio en la degradación del PCT. Notablemente, se alcanzaron altas conversiones de contaminantes (hasta un 98%) en solo

60 minutos de reacción para bajas concentraciones de detergente en el efluente simulado (S4). Sin embargo, cuando se introdujo un mayor porcentaje de detergente, empleando el mismo nivel de HP (S5), se logró una conversión del 95.4% pero a los 180 minutos, evidenciando la influencia significativa sobre el proceso de la matriz real evaluada.

Finalmente, se evaluó la toxicidad (I(%)) en el sistema (**Figura 4.8**), donde la evolución de I(%) estuvo estrechamente relacionada con la aparición y desaparición de la HQ.

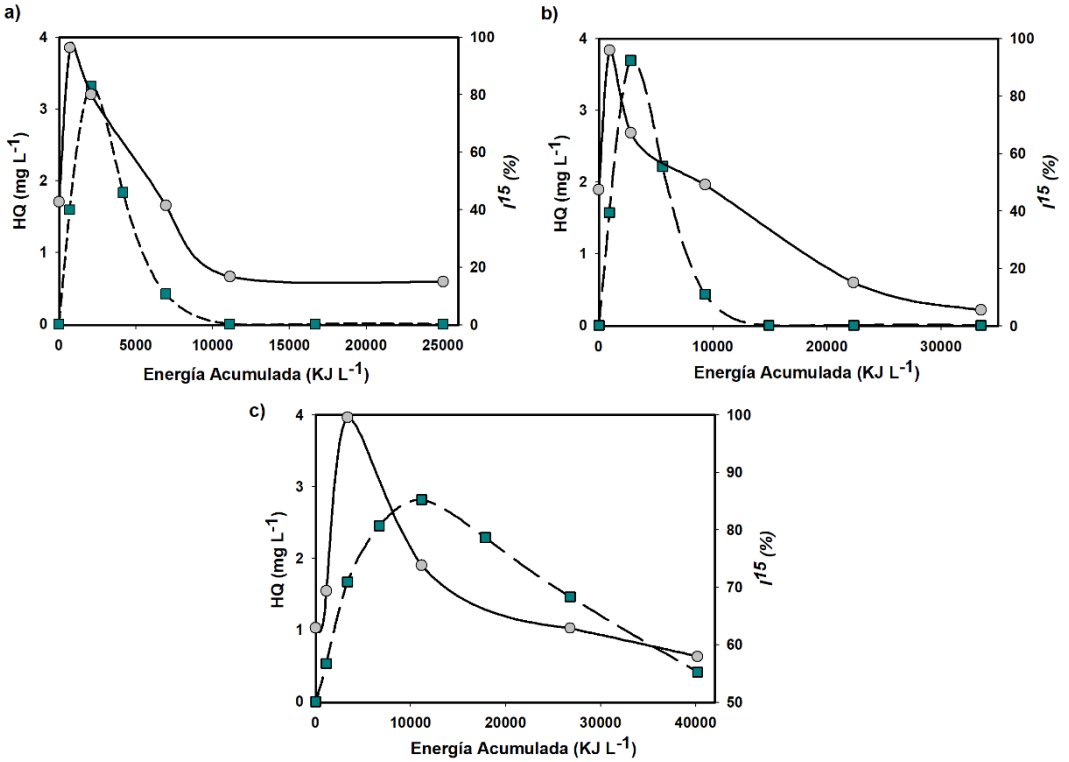

Figura 4.8. Porcentaje de inhibición de luminiscencia a los 15 min (●) y concentración de la HQ (■) vs la energía acumulada. a) Ensayo S2 (agua pura), b) Ensayo S4 (CIP300 0.01%) y c) Ensayo S5 (CIP300 0.1%). HP = 378 mg L^{-1}.

Los resultados mostraron que el 0.01% de CIP300 no representó una gran adición de toxicidad al sistema. Sin embargo, se observó una ligera desaceleración de la velocidad del proceso, ya que la HQ desapareció a un $Q_{300\text{-}550nm,t}$ mayor que en el ensayo sin CIP300, por lo que la toxicidad en el medio de reacción también persistió por más tiempo. Por otro lado, cuando el detergente se usó a una concentración del 0.1%, hubo una cantidad

adicional de toxicidad del 23.71%, causada solo por CIP300 (ensayo blanco). Además, se observó la presencia de una pequeña cantidad de HQ hacia el final de la reacción, a pesar de la gran energía acumulada, lo que provocó que el I(%) permaneciera alto, como se observa en la **Figura 4.8 c**. Esto sugiere la necesidad de implementar tiempos de reacción más largos para reducir completamente la toxicidad del sistema cuando se trabaja con aguas residuales industriales.

Estos resultados pertenecen al siguiente trabajo de investigación: "*Exploring the Role of Hydrogen Peroxide Dosage Strategies in the Photo-Fenton Process: Scaling from Lab-Scale to Pilot Plant Solar Reactor*". B. Giménez, A. Schenone, L. Conte. Chemical Engineering Journal Advances. Trabajo que se encuentra bajo revisión por pares para ser publicado, y que se presenta en el **Anexo F**.

Capítulo 5. CONCLUSIONES

En la presente tesis se modeló y optimizó la remoción del fármaco Paracetamol, empleando los procesos Fenton y foto-Fenton, particularmente el sistema foto-Fenton/Ferrioxalato, utilizando fotorreactores escala laboratorio y planta piloto activados con radiación UV-Vis simulada y solar.

El primer modelo desarrollado, fue capaz de representar satisfactoriamente la degradación foto-Fenton del PCT a pH 2.8, empleando un reactor anular concéntrico escala planta piloto. Aquí se incluyó explícitamente los efectos de la absorción de radiación en la cinética de degradación del contaminante mediante la LVRPA, calculada a partir de un modelo de radiación de fuente lineal con emisión esférica e isotrópica. Utilizando un procedimiento de optimización multiparamétrico no lineal, se demostró que el modelo presentaba una buena concordancia entre los datos experimentales y las concentraciones predichas, no sólo de paracetamol y peróxido de hidrógeno sino también de hidroquinona y 1,4-benzoquinona. Además, el modelo cinético fue validado con un nuevo conjunto de pruebas experimentales, confirmando su capacidad predictiva. Finalmente, para evaluar las consecuencias ambientales del proceso, se realizó un estudio de toxicidad con células VERO. Estos ensayos de citotoxicidad demostraron que, más allá del grado de mineralización alcanzado, el proceso foto-Fenton es efectivo para generar un efluente no tóxico bajo las variables operativas investigadas. Considerando la escala del fotorreactor empleado y los resultados de los ensayos de citotoxicidad obtenidos, se concluyó que el modelo desarrollado contribuyó significativamente al estudio de la escalabilidad del proceso para el tratamiento de aguas residuales reales.

En búsqueda de alternativas para abordar los problemas operativos asociados al sistema foto-Fenton a pH ácido, se investigó el sistema foto-Fenton/Ferrioxalato. Inicialmente, se estudió la influencia de parámetros clave sobre el PFF/FeOxa a pH natural, empleando un reactor de placa plana y un simulador solar como fuente de radiación. Dichos parámetros fueron: temperatura, concentración de HP y Radiación. Empleando la RSM se ajustó matemáticamente el comportamiento del sistema reaccionante para la degradación del paracetamol. Las variables o términos que resultaron más significativas para el sistema fueron la radiación, la temperatura y la concentración de HP, en ese orden de importancia. Al analizar los gráficos de superficies de respuesta obtenidos se concluyó que: i) los niveles de degradación alcanzados cuando se operó el sistema en ausencia de radiación, fueron menores a los obtenidos cuando se incluyó radiación en el sistema, esto para todo el rango de condiciones evaluadas; ii) un aumento de la temperatura en el rango evaluado, produjo siempre un aumento en la conversión del PCT (principalmente para el sistema Fenton) y, iii) utilizar concentraciones elevadas de HP fue desfavorable para el rendimiento del sistema en cuanto a la degradación del fármaco alcanzada, debido al efecto atrapador de HO• que posee el agente oxidante. Además, se lograron identificar dos intermediarios de reacción altamente tóxicos (hidroquinona y 1,4-benzoquinona). En efecto, a pesar de la conversión completa de PCT en a los 180 min de reacción, se observó que permanecía en solución un porcentaje de inhibición de la bioluminiscencia de la bacteria *V. fischeri*, lo cual se asoció con la presencia de estos intermediarios de reacción tóxicos. Sólo operando el sistema con altos niveles de radiación fue posible reducir completamente la toxicidad del sistema después de 240 min de reacción.

A partir de este trabajo se demostró qué variables eran las más influyentes en la degradación foto-Fenton del PCT y en qué medida cada una de ellas afectaba al proceso,

además de demostrar qué condiciones operacionales eran necesarias para generar un efluente toxicológicamente seguro.

En una segunda etapa de investigación, se desarrolló un modelo cinético capaz de describir la degradación del PCT mediante el proceso foto-Fenton/Ferrioxalato en condiciones de pH cercanas a la neutralidad, empleando un reactor de placa plana iluminado lateralmente por un simulador solar. Aquí se incorporó con éxito el efecto de la LVRPA (calculada a partir de un modelo de radiación unidimensional) en el comportamiento del sistema reaccionante. Además, se correlacionó, mediante la ecuación de Arrhenius, los cambios en los parámetros cinéticos con la temperatura. Empleando un procedimiento de optimización multiparamétrico no lineal ponderado se estimaron los parámetros desconocidos: las constantes cinéticas y el rendimiento cuántico global del ferrioxalato. Se observó que el modelo presentó una buena concordancia entre los datos predichos y los valores experimentales, demostrando su capacidad para representar el comportamiento del sistema en estudio. Este modelo brindó información valiosa para la escalabilidad del PFF/FeOxa, y facilitó la aplicación de nuevas estrategias operacionales para el proceso estudiado, así como la futura investigación en la degradación de nuevos contaminantes.

Siguiendo con los objetivos planteados en esta tesis, se pudo degradar con éxito una baja concentración de PCT (500 μg L^{-1}, acorde a los niveles encontrados en cuerpos de agua naturales) mediante el proceso foto-Fenton a pH = 5,5 utilizando una baja concentración de reactivos Fenton (Fe = 1 mg L^{-1} y HP = 2.36 mg L^{-1}), complejando al hierro con oxalato. Nuevamente, los mejores resultados en cuanto a conversión del contaminante se obtuvieron añadiendo radiación solar simulada al sistema. Este trabajo permitió verificar la eficiencia del proceso foto-Fenton en degradar muy bajas concentraciones de PCT empleando dosis reducidas de reactivos Fenton.

Finalmente, considerando que el HP es uno de los principales reactivos químicos del sistema, y su influencia sustancial en el costo de operación del proceso, se evaluaron diversas estrategias de dosificación para el agente oxidante (puntual, continua, o combinación de ambas). En primer lugar, se analizó la influencia de la dosificación puntual del HP en la eficiencia del proceso foto-Fenton/Ferrioxalato (pH 5.5), en relación a la conversión del contaminante y/o el consumo del agente oxidante, empleando un reactor de placa plana escala laboratorio, y diversas matrices acuosas. Se observó que el exceso de oxidante tuvo un efecto negativo en el sistema, sin embargo, la estrategia de dosificación puntual implementada pudo mitigar este efecto, observándose mejores conversiones del PCT cuando el HP era dosificado, tanto en presencia como en ausencia de radiación. Adicionalmente, se verificó que la dosificación del HP influyó positivamente en el ciclo catalítico del hierro, ya que se alcanzaron mayores concentraciones de Fe^{2+} en tiempos de reacción más cortos, acelerando la conversión de los subproductos de reacción (HQ y BQ), lo que condujo a mejores desempeños de los procesos Fenton y foto-Fenton, teniendo en cuenta también la toxicidad de dichos subproductos. Posteriormente, al aplicar la estrategia de dosificación del agente oxidante en diferentes matrices acuosas (una matriz artificial con aniones inorgánicos, una muestra real de agua subterránea y un agua residual industrial sintética), se observó una reducción en los efectos negativos causados por el contenido de diferentes iones y otros compuestos orgánicos. Obteniéndose mejoras significativas en el consumo de HP cuando se emplea en el tratamiento de aguas residuales más complejas.

A continuación, se analizó la dosificación continua del HP en la eliminación del PCT presente en diferentes matrices acuosas mediante el PFF/FeOxa. En este caso, los resultados preliminares de laboratorio revelaron que, en presencia de radiación, incluso con las concentraciones finales más bajas de agente oxidante se lograron altas

conversiones de PCT. Sin embargo, para estas bajas dosis de HP, el consumo específico de agente oxidante se mantuvo por debajo del valor estequiométrico requerido para la mineralización de PCT, lo que podría significar una cantidad insuficiente de HP para degradar los subproductos de la oxidación del PCT. Por otro lado, al emplear dosis elevadas de HP, aunque dosificado, se observó una disminución en la eficiencia de degradación del PCT (efecto atrapador de HO•), lo que resultó en una menor conversión del fármaco. Además, estas dosis elevadas de HP ocasionaron un consumo excesivo del oxidante, tanto debido al efecto atrapador de HO• como a la auto-descomposición del agente oxidante. Por otra parte, los experimentos realizados con agua residual industrial simulada, demostraron una degradación deficiente del PCT y un consumo excesivo de HP, sugiriendo un alto consumo improductivo del oxidante debido a la presencia de materia orgánica. Al realizar el escalado del proceso al reactor solar de planta piloto, se demostró la gran eficacia del sistema logrando una significativa conversión del contaminante en tiempos de reacción considerablemente cortos. El efecto sinérgico de la energía solar UV/visible y térmica facilitó la degradación eficiente del PCT. Esto fue especialmente evidente en muestras de aguas residuales industriales, donde, a pesar de la complejidad introducida por las matrices reales (tales como aditivos detergentes y excipientes de drogas farmacéuticas), el reactor solar exhibió un rendimiento muy superior en comparación con las pruebas a escala de laboratorio. En relación a la toxicidad del agua tratada, se observó que a medida que aumenta la concentración del detergente utilizado en el agua residual industrial simulada, mayor era la toxicidad en el efluente remanente. Dado que este detergente retarda la degradación del PCT y sus intermediarios, y que la toxicidad del sistema está estrechamente relacionada con la presencia de HQ en el sistema, se concluyó que deberían implementarse tiempos

de reacción más prolongados para reducir completamente la toxicidad del sistema al trabajar con aguas residuales industriales.

Estos trabajos de investigación demostraron que la dosificación del HP es una buena estrategia para intensificar el rendimiento del PFF/FeOxa, y sirven como una base importante para el desarrollo de estrategias más avanzadas aplicables incluso a reactores solares de mayor escala. Además, el empleo de un reactor escala planta piloto solar en combinación con matrices acuosas complejas contribuyó a reducir la brecha entre los hallazgos a escala laboratorio y las aplicaciones prácticas, proporcionando información valiosa para el desarrollo de soluciones efectivas al abordar la contaminación de las aguas residuales farmacéuticas. Se destaca la robustez del PFF/FeOxa Solar, incluso en condiciones que simulan efluentes industriales, lo que reafirma su potencial como una tecnología sostenible y escalable para el tratamiento de aguas residuales de diversas industrias.

REFERENCIAS BIBLIOGRÁFICAS

Ahile UJ, Wuana RA, Itodo AU, et al (2020) A review on the use of chelating agents as an alternative to promote photo-Fenton at neutral pH: Current trends, knowledge gap and future studies. Sci Total Environ 710:134872. https://doi.org/10.1016/j.scitotenv.2019.134872

AL Falahi OA, Abdullah SRS, Hasan HA, et al (2022) Occurrence of pharmaceuticals and personal care products in domestic wastewater, available treatment technologies, and potential treatment using constructed wetland: A review. Process Saf Environ Prot 168:1067-1088. https://doi.org/10.1016/j.psep.2022.10.082

Alfano OM, Cassano AE (2008) Photoreactor Modeling: Applications to Advanced Oxidation Processes. Int J Chem React Eng 6:. https://doi.org/10.2202/1542-6580.1617

Allen AO, Hochanadel CJ, Ghormley JA, Davis TW (1952) Decomposition of water and aqueous solutions under mixed fast neutron and gamma radiation. J Phys Chem 56:575-586. https://doi.org/10.1021/J150497A007/ASSET/J150497A007.FP.PNG_V03

Ameta R, K. Chohadia A, Jain A, Punjabi PB (2018) Fenton and Photo-Fenton Processes. En: Advanced Oxidation Processes for Waste Water Treatment. Elsevier, pp 49-87

Aparicio V, De Gerónimo E (2024) Pesticide pollution in argentine drinking water: A call to ensure safe access. Environ Challenges 14:. https://doi.org/10.1016/j.envc.2023.100808

Audino F, Campanyà G, Pérez-Moya M, et al (2019) Systematic optimization approach

for the efficient management of the photo-Fenton treatment process. Sci Total Environ 646:902-913. https://doi.org/10.1016/J.SCITOTENV.2018.07.057

Ayoub SS (2021) Paracetamol (acetaminophen): A familiar drug with an unexplained mechanism of action. Temperature 8:351-371. https://doi.org/10.1080/23328940.2021.1886392

Bah A, Chen Z, Bah A, et al (2023) Systematic literature review of solar-powered landfill leachate sanitation: Challenges and research directions over the past decade. J Environ Manage 326:116751. https://doi.org/10.1016/j.jenvman.2022.116751

Beamud SG, Fernández H, Nichela D, et al (2024) Occurrence of Pharmaceutical Micropollutants in Lake Nahuel Huapi, Argentine Patagonia. Environ Toxicol Chem 00:1-11. https://doi.org/10.1002/etc.5859

Bertrand L, Iturburu FG, Valdés ME, et al (2023) Risk evaluation and prioritization of contaminants of emerging concern and other organic micropollutants in two river basins of central Argentina. Sci Total Environ 878:. https://doi.org/10.1016/j.scitotenv.2023.163029

Carrizo JC, Vo Duy S, Munoz G, et al (2022) Suspect screening of pharmaceuticals, illicit drugs, pesticides, and other emerging contaminants in Argentinean Piaractus mesopotamicus, a fish species used for local consumption and export. Chemosphere 309:. https://doi.org/10.1016/j.chemosphere.2022.136769

Cassano AE, Martín CA, Brandi RJ, Alfano OM (1995) Photoreactor Analysis and Design: Fundamentals and Applications. Ind Eng Chem Res 34:2155-2201. https://doi.org/10.1021/ie00046a001

Chen X, Rong H, Ndagijimana P, et al (2023) Towards removal of PPCPs by advanced

oxidation processes: A review. Results Eng 20:101496. https://doi.org/10.1016/j.rineng.2023.101496

Connor R, Chaves Pacheco SM (2024) Global employment trends and the water dependency of jobs: technical paper - UNESCO Digital Library. https://unesdoc.unesco.org/ark:/48223/pf0000388410. Accessed 30 abr 2024

Conte LO, Farias J, Albizzati ED, Alfano OM (2012) Photo-fenton degradation of the herbicide 2,4-dichlorophenoxyacetic acid in laboratory and solar pilot-plant reactors. Ind Eng Chem Res 51:4181-4191. https://doi.org/10.1021/ie2023228

Conte LO, Querini P, Albizzati ED, Alfano OM (2014) Photonic and quantum efficiencies for the homogeneous photo-Fenton degradation of herbicide 2,4-D using different iron complexes. J Chem Technol Biotechnol 89:1967-1974. https://doi.org/10.1002/jctb.4284

Conte LO, Schenone A V., Alfano OM (2017) Ferrioxalate-assisted solar photo-Fenton degradation of a herbicide at pH conditions close to neutrality. Environ Sci Pollut Res 24:6205-6212. https://doi.org/10.1007/s11356-016-6400-3

Durán A, Monteagudo JM, San Martín I (2018) Operation costs of the solar photo-catalytic degradation of pharmaceuticals in water: A mini-review. Chemosphere 211:482-488. https://doi.org/10.1016/j.chemosphere.2018.07.170

Escher BI, Baumgartner R, Lienert J, Fenner K (2008) Predicting the Ecotoxicological Effects of Transformation Products. En: Handbook of Environmental Chemistry, Volume 2: Reactions and Processes. pp 205-244

Galani A, Alygizakis N, Aalizadeh R, et al (2021) Patterns of pharmaceuticals use during the first wave of COVID-19 pandemic in Athens, Greece as revealed by wastewater-

based epidemiology. Sci Total Environ 798:149014. https://doi.org/10.1016/j.scitotenv.2021.149014

Gamaralalage D, Sawai O, Nunoura T (2020) Effect of reagents addition method in Fenton oxidation on the destruction of organics in palm oil mill effluent. J Environ Chem Eng 8:103974. https://doi.org/10.1016/j.jece.2020.103974

Glaze WH, Kang JW, Chapin DH (1987) The Chemistry of Water Treatment Processes Involving Ozone, Hydrogen Peroxide and Ultraviolet Radiation. Ozone Sci Eng 9:335-352. https://doi.org/10.1080/01919518708552148

Gosset A, Wiest L, Fildier A, et al (2021) Ecotoxicological risk assessment of contaminants of emerging concern identified by "suspect screening" from urban wastewater treatment plant effluents at a territorial scale. Sci Total Environ 778:146275. https://doi.org/10.1016/j.scitotenv.2021.146275

Grčić I, Koprivanac N, Li Puma G (2021) Modeling the photocatalytic oxidation of carboxylic acids on aqueous TiO2 suspensions and on immobilized TiO2-chitosan thin films in different reactor geometries irradiated by UVA or UVC light sources. Chem Eng J 422:. https://doi.org/10.1016/j.cej.2021.130104

Hale SE, Arp HPH, Schliebner I, Neumann M (2020) Persistent, mobile and toxic (PMT) and very persistent and very mobile (vPvM) substances pose an equivalent level of concern to persistent, bioaccumulative and toxic (PBT) and very persistent and very bioaccumulative (vPvB) substances under REACH. Environ Sci Eur 32:. https://doi.org/10.1186/s12302-020-00440-4

Hernando MD, De Vettori S, Martínez Bueno MJ, Fernández-Alba AR (2007) Toxicity evaluation with Vibrio fischeri test of organic chemicals used in aquaculture. Chemosphere 68:724-730. https://doi.org/10.1016/j.chemosphere.2006.12.097

Hincapié Mejía G, Peñuela GA, Mueses MA (2022) Evaluation of a helicoidal flux photoreactor applied in the dicloxacillin degradation by UV-C/H2O2 and UV-A/photo-Fenton including the effect of photon absorption. Results Eng 15:. https://doi.org/10.1016/j.rineng.2022.100519

ISO11348-3:2007 (2022) ISO 11348-3:2007 - Water quality — Determination of the inhibitory effect of water samples on the light emission of Vibrio fischeri (Luminescent bacteria test) — Part 3: Method using freeze-dried bacteria. https://www.iso.org/standard/40518.html. Accessed 30 abr 2024

Jiménez-Bambague EM, Madera-Parra CA, Machuca-Martinez F (2023) The occurrence of emerging compounds in real urban wastewater before and after the COVID-19 pandemic in Cali, Colombia. Curr Opin Environ Sci Heal 33:100457. https://doi.org/10.1016/j.coesh.2023.100457

Khan S, Naushad M, Govarthanan M, et al (2022) Emerging contaminants of high concern for the environment: Current trends and future research. Environ Res 207:112609. https://doi.org/10.1016/j.envres.2021.112609

Kulišťáková A (2023) Removal of pharmaceutical micropollutants from real wastewater matrices by means of photochemical advanced oxidation processes – A review. J Water Process Eng 53:. https://doi.org/10.1016/j.jwpe.2023.103727

Kumari P, Kumar A (2023) ADVANCED OXIDATION PROCESS: A remediation technique for organic and non-biodegradable pollutant. Results in Surfaces and Interfaces 11:100122. https://doi.org/10.1016/J.RSURFI.2023.100122

Lajmanovich RC, Peltzer PM, Attademo AM, et al (2019) First evaluation of novel potential synergistic effects of glyphosate and arsenic mixture on Rhinella arenarum (Anura: Bufonidae) tadpoles. Heliyon 5:.

https://doi.org/10.1016/j.heliyon.2019.e02601

Lee C, Seo J, Pham ALT (2022) The Photo-Fenton System. Springer Handbooks 1719-1734. https://doi.org/10.1007/978-3-030-63713-2_59/COVER

Lee J, Von Gunten U, Kim JH (2020) Persulfate-Based Advanced Oxidation: Critical Assessment of Opportunities and Roadblocks. Environ Sci Technol 54:3064-3081. https://doi.org/10.1021/acs.est.9b07082

López-Vinent N, Cruz-Alcalde A, Lai C, et al (2022) Role of sunlight and oxygen on the performance of photo-Fenton process at near neutral pH using organic fertilizers as iron chelates. Sci Total Environ 803:149873. https://doi.org/10.1016/j.scitotenv.2021.149873

Ma D, Yi H, Lai C, et al (2021) Critical review of advanced oxidation processes in organic wastewater treatment. Chemosphere 275:130104. https://doi.org/10.1016/J.CHEMOSPHERE.2021.130104

Machado F, Teixeira ACSC, Ruotolo LAM (2023) Critical review of Fenton and photo-Fenton wastewater treatment processes over the last two decades. Springer Berlin Heidelberg

Malato S, Giménez J, Oller I, et al (2020) Removal and Degradation of Pharmaceutically Active Compounds (PhACs) in Wastewaters by Solar Advanced Oxidation Processes. En: Handbook of Environmental Chemistry. Springer, Cham, pp 299-326

Maniakova G, Kowalska K, Murgolo S, et al (2020) Comparison between heterogeneous and homogeneous solar driven advanced oxidation processes for urban wastewater treatment: Pharmaceuticals removal and toxicity. Sep Purif Technol 236:116249. https://doi.org/10.1016/j.seppur.2019.116249

Manna M, Sen S (2022) Advanced oxidation process: a sustainable technology for treating refractory organic compounds present in industrial wastewater. Environ Sci Pollut Res 30:25477-25505. https://doi.org/10.1007/s11356-022-19435-0

Mastrángelo MM, Valdés ME, Eissa B, et al (2022) Occurrence and accumulation of pharmaceutical products in water and biota of urban lowland rivers. Sci Total Environ 828:. https://doi.org/10.1016/j.scitotenv.2022.154303

Mecha AC, Onyango MS, Ochieng A, Momba MNB (2017) Ultraviolet and solar photocatalytic ozonation of municipal wastewater: Catalyst reuse, energy requirements and toxicity assessment. Chemosphere 186:669-676. https://doi.org/10.1016/j.chemosphere.2017.08.041

Ministerio de Salud (2024) Calidad del agua| Argentina.gob.ar. https://www.argentina.gob.ar/salud/ambiental/agua. Accessed 30 abr 2024

Ministerio del Interior (2024) Contaminantes de preocupación emergente | Argentina.gob.ar. https://www.argentina.gob.ar/interior/ambiente/control/productos-quimicos/contaminantes-emergentes. Accessed 30 mar 2024

Monteagudo JM, Durán A, Aguirre M, Martín IS (2010) Photodegradation of Reactive Blue 4 solutions under ferrioxalate-assisted UV/solar photo-Fenton system with continuous addition of H2O2 and air injection. Chem Eng J 162:702-709. https://doi.org/10.1016/j.cej.2010.06.029

Mukhopadhyay A, Duttagupta S, Mukherjee A (2022) Emerging organic contaminants in global community drinking water sources and supply: A review of occurrence, processes and remediation. J Environ Chem Eng 10:107560. https://doi.org/10.1016/j.jece.2022.107560

Munoz M, Pliego G, De Pedro ZM, et al (2014) Application of intensified Fenton oxidation to the treatment of sawmill wastewater. Chemosphere 109:34-41. https://doi.org/10.1016/j.chemosphere.2014.02.062

Nascimento GE do, Soares Oliveira MA, da Rocha Santana RM, et al (2020) Investigation of paracetamol degradation using LED and UV-C photo-reactors. Water Sci Technol 81:2545-2558. https://doi.org/10.2166/wst.2020.310

Nason S, Lin E, Eitzer BD, et al (2021) Traffic, Drugs, Mental Health, and Disinfectants: Changes in Sewage Sludge Chemical Signatures During a COVID-19 Community Lockdown. https://doi.org/10.26434/CHEMRXIV.13562525.V1

Nasr Esfahani K, Pérez-Moya M, Graells M (2022) Modelling of the photo-Fenton process with flexible hydrogen peroxide dosage: Sensitivity analysis and experimental validation. Sci Total Environ 839:. https://doi.org/10.1016/j.scitotenv.2022.155941

Okeke ES, Ezeorba TPC, Okoye CO, et al (2022) Environmental and health impact of unrecovered API from pharmaceutical manufacturing wastes: A review of contemporary treatment, recycling and management strategies. Sustain Chem Pharm 30:100865. https://doi.org/10.1016/j.scp.2022.100865

Oller I, Malato S (2021) Photo-Fenton applied to the removal of pharmaceutical and other pollutants of emerging concern. Curr Opin Green Sustain Chem 29:100458. https://doi.org/10.1016/j.cogsc.2021.100458

Ortega-Gómez E, Moreno úbeda JC, Álvarez Hervás JD, et al (2012) Automatic dosage of hydrogen peroxide in solar photo-Fenton plants: Development of a control strategy for efficiency enhancement. J Hazard Mater 237-238:223-230. https://doi.org/10.1016/j.jhazmat.2012.08.031

Otto B, Schleifer L (2020) Domestic Water Use Grew 600% Over the Past 50 Years | World Resources Institute. https://www.wri.org/insights/domestic-water-use-grew-600-over-past-50-years. Accessed 30 abr 2024

Pacheco-Álvarez M, Picos Benítez R, Rodríguez-Narváez OM, et al (2022) A critical review on paracetamol removal from different aqueous matrices by Fenton and Fenton-based processes, and their combined methods. Chemosphere 303:134883. https://doi.org/10.1016/j.chemosphere.2022.134883

Pandis PK, Kalogirou C, Kanellou E, et al (2022) Key Points of Advanced Oxidation Processes (AOPs) for Wastewater, Organic Pollutants and Pharmaceutical Waste Treatment: A Mini Review. ChemEngineering 6:8

Parra-Marfil A, López-Ramón M V., Aguilar-Aguilar A, et al (2023) An efficient removal approach for degradation of metformin from aqueous solutions with sulfate radicals. Environ Res 217:. https://doi.org/10.1016/j.envres.2022.114852

Peralta-Hernández JM, Brillas E (2023) A critical review over the removal of paracetamol (acetaminophen) from synthetic waters and real wastewaters by direct, hybrid catalytic, and sequential ozonation processes. Chemosphere 313:137411. https://doi.org/10.1016/j.chemosphere.2022.137411

Pérez-Moya M, Mansilla HD, Graells M (2011) A practical parametrical characterization of the Fenton and the photo-Fenton sulfamethazine treatment using semi-empirical modeling. J Chem Technol Biotechnol 86:826-831. https://doi.org/10.1002/jctb.2595

Polo-López MI, Castro-Alférez M, Oller I, Fernández-Ibáñez P (2014) Assessment of solar photo-Fenton, photocatalysis, and H2O2 for removal of phytopathogen fungi spores in synthetic and real effluents of urban wastewater. Chem Eng J 257:122-130.

https://doi.org/10.1016/j.cej.2014.07.016

Prato-Garcia D, Buitrón G (2012) Evaluation of three reagent dosing strategies in a photo-Fenton process for the decolorization of azo dye mixtures. J Hazard Mater 217-218:293-300. https://doi.org/10.1016/j.jhazmat.2012.03.036

Prieto-Rodríguez L, Oller I, Zapata A, et al (2011) Hydrogen peroxide automatic dosing based on dissolved oxygen concentration during solar photo-Fenton. Catal Today 161:247-254. https://doi.org/10.1016/j.cattod.2010.11.017

Priyadarshini M, Das I, Ghangrekar MM, Blaney L (2022) Advanced oxidation processes: Performance, advantages, and scale-up of emerging technologies. J Environ Manage 316:115295. https://doi.org/10.1016/J.JENVMAN.2022.115295

Rebolledo LP, Arana VA, Trilleras J, et al (2019) Efficiency of combined processes coagulation/solar photo Fenton in the treatment of landfill leachate. Water (Switzerland) 11:1-16. https://doi.org/10.3390/w11071351

Reichert G, Hilgert S, Fuchs S, Azevedo JCR (2019) Emerging contaminants and antibiotic resistance in the different environmental matrices of Latin America. Environ Pollut 255:. https://doi.org/10.1016/j.envpol.2019.113140

Ritchie H, Roser M (2024) Water Use and Stress - Our World in Data. https://ourworldindata.org/water-use-stress. Accessed 30 abr 2024

Rizzo L, Malato S, Antakyali D, et al (2019) Consolidated vs new advanced treatment methods for the removal of contaminants of emerging concern from urban wastewater. Sci Total Environ 655:986-1008. https://doi.org/10.1016/j.scitotenv.2018.11.265

Rodríguez-García D, Soriano-Molina P, Guzmán Sánchez JL, et al (2023) A novel control

system approach to enhance the efficiency of solar photo-Fenton microcontaminant removal in continuous flow raceway pond reactors. Chem Eng J 455:140760. https://doi.org/10.1016/j.cej.2022.140760

Saldaña-Flores KE, Flores-Estrella RA, Alcaraz-Gonzalez V, et al (2021) Regulation of hydrogen peroxide dosage in a heterogeneous photo-fenton process. Processes 9:1-12. https://doi.org/10.3390/pr9122167

Salgado Costa C, Bahl F, Natale GS, et al (2023) First evidence of environmental bioaccumulation of pharmaceuticals on adult native anurans (Rhinella arenarum) from Argentina. Environ Pollut 334:122231. https://doi.org/10.1016/j.envpol.2023.122231

Sandoval MA, Calzadilla W, Vidal J, et al (2024) Contaminants of emerging concern: Occurrence, analytical techniques, and removal with electrochemical advanced oxidation processes with special emphasis in Latin America. Environ Pollut 345:. https://doi.org/10.1016/j.envpol.2024.123397

Shokri A, Fard MS (2022) A critical review in Fenton-like approach for the removal of pollutants in the aqueous environment. Environ Challenges 7:100534. https://doi.org/10.1016/j.envc.2022.100534

Singh S, Garg A (2021) Advanced oxidation processes for industrial effluent treatment. Adv Oxid Process Effl Treat Plants 255-272. https://doi.org/10.1016/B978-0-12-821011-6.00012-8

Soares PA, Batalha M, Souza SMAGU, et al (2015) Enhancement of a solar photo-Fenton reaction with ferric-organic ligands for the treatment of acrylic-textile dyeing wastewater. J Environ Manage 152:120-131. https://doi.org/10.1016/j.jenvman.2015.01.032

Starling MCVM, Amorim CC, Leão MMD (2019) Occurrence, control and fate of contaminants of emerging concern in environmental compartments in Brazil. J Hazard Mater 372:17-36. https://doi.org/10.1016/j.jhazmat.2018.04.043

Szopińska M, Potapowicz J, Jankowska K, et al (2022) Pharmaceuticals and other contaminants of emerging concern in Admiralty Bay as a result of untreated wastewater discharge: Status and possible environmental consequences. Sci Total Environ 835:155400. https://doi.org/10.1016/J.SCITOTENV.2022.155400

Teutli-Sequeira A, Vasquez-Medrano R, Prato-Garcia D, Ibanez JG (2020) Solar photo-assisted degradation of bipyridinium herbicides at circumneutral pH: A life cycle assessment approach. Processes 8:. https://doi.org/10.3390/PR8091117

Ulvi A, Aydın S, Aydın ME (2022) Fate of selected pharmaceuticals in hospital and municipal wastewater effluent: occurrence, removal, and environmental risk assessment. Environ Sci Pollut Res 29:75609-75625. https://doi.org/10.1007/s11356-022-21131-y

United Nations (2024) The United Nations World Water Development Report 2024: water for prosperity and peace - UNESCO Digital Library. https://unesdoc.unesco.org/ark:/48223/pf0000388948?posInSet=2&queryId=N-799b083e-c6a2-4a66-a3f3-824c81a18aff. Accessed 30 abr 2024

United Nations (2023) The United Nations World Water Development Report 2023: partnerships and cooperation for water - UNESCO Digital Library. https://unesdoc.unesco.org/ark:/48223/pf0000384655. Accessed 30 abr 2024

Velo-Gala I, Pirán-Montaño JA, Rivera-Utrilla J, et al (2017) Advanced Oxidation Processes based on the use of UVC and simulated solar radiation to remove the antibiotic tinidazole from water. Chem Eng J 323:605-617.

https://doi.org/10.1016/j.cej.2017.04.102

Wilkinson JL, Boxall ABA, Kolpin DW, et al (2022) Pharmaceutical pollution of the world's rivers. Proc Natl Acad Sci 119:. https://doi.org/10.1073/pnas.2113947119

Xiangwei Y, Graells M, Miralles-Cuevas S, et al (2021) An improved hybrid strategy for online dosage of hydrogen peroxide in photo-Fenton processes. J Environ Chem Eng 9:105235. https://doi.org/10.1016/j.jece.2021.105235

Yamal-Turbay E, Graells M, Pérez-Moya M (2012) Systematic assessment of the influence of hydrogen peroxide dosage on caffeine degradation by the photo-fenton process. Ind Eng Chem Res 51:4770-4778. https://doi.org/10.1021/ie202256k

Yu X, Cabrera-Reina A, Graells M, et al (2021) Towards an Efficient Generalization of the Online Dosage of Hydrogen Peroxide in Photo-Fenton Process to Treat Industrial Wastewater. Int J Environ Res Public Health 18:13313. https://doi.org/10.3390/ijerph182413313

Yu X, Somoza-Tornos A, Graells M, Pérez-Moya M (2020) An experimental approach to the optimization of the dosage of hydrogen peroxide for Fenton and photo-Fenton processes. Sci Total Environ 743:140402. https://doi.org/10.1016/j.scitotenv.2020.140402

Ziembowicz S, Kida M (2022) Limitations and future directions of application of the Fenton-like process in micropollutants degradation in water and wastewater treatment: A critical review. Chemosphere 296:134041. https://doi.org/10.1016/j.chemosphere.2022.134041

ANEXOS

Contribuciones

Referido a los artículos incluidos en los Anexos A, B, C, D, E y F:

- Giménez, B. N., Conte, L. O., Alfano, O. M., & Schenone, A. V. (2020). Paracetamol removal by photo-Fenton processes at near-neutral pH using a solar simulator: Optimization by D-optimal experimental design and toxicity evaluation. *Journal of Photochemistry and Photobiology A: Chemistry*. https://doi.org/10.1016/j.jphotochem.2020.112584

- Giménez, B. N., Schenone, A. V., Alfano, O. M., & Conte, L. O. (2021). Reaction kinetics formulation with explicit radiation absorption effects of the photo-Fenton degradation of paracetamol under natural pH conditions. *Environmental Science and Pollution Research.* https://doi.org/10.1007/s11356-020-11993-5

- Giménez, B. N., Conte, L. O., Audino, F., Schenone, A. V., Graells, M., Alfano, O. M., & Pérez-Moya, M. (2023). Kinetic model of photo-Fenton degradation of paracetamol in an annular reactor: main reaction intermediates and cytotoxicity studies. *Catalysis Today*. https://doi.org/10.1016/j.cattod.2022.11.019

- Schenone A. V., Giménez B. N., Conte L. O., Alfano O. M.. (2022). Influence of simulated solar radiation on micropollutant removal with ferrioxalate-assisted photo-Fenton. *5th Iberoamerican Conference on Advanced Oxidation Technologies (V CIPOA)*.

- Giménez, B.N., Conte, L.O., Duarte, S.A. & Schenone, A. V. (2024). Improvement of ferrioxalate assisted Fenton and photo-Fenton processes for paracetamol

degradation by hydrogen peroxide dosage. *Environmental Science and Pollution Research.* https://doi.org/10.1007/s11356-024-32056-z

- Giménez, B.N., Schenone, A. V. & Conte, L.O. Exploring the Role of Hydrogen Peroxide Dosage Strategies in the Photo-Fenton Process: Scaling from Lab-Scale to Pilot Plant Solar Reactor. *Chemical Engineering Journal Advances.* Aceptado para su revisión por pares.

La tesista declara haber contribuido en la concepción y el diseño de los estudios realizados, en la realización del trabajo experimental y la recolección de datos, así como también en análisis de estos datos y la posterior construcción de los modelos matemáticos presentados. Por otro lado, la tesista declara haber sido la autora principal en relación a la escritura de los artículos, y en la preparación de tablas y figuras para su publicación, guiada por comentarios, sugerencias y revisiones del director, la codirectora y coautores que en cada artículo se indican. Los detalles de las contribuciones en cada artículo en particular se especifican en los apartados de "*authorship contribution statement*", incluidos en todos los trabajos de investigación presentados. Los abajo firmantes avalan esta declaración.

Dr. Leandro O. Conte

Dra. Agustina V. Schenone

ANEXO A. Paracetamol removal by photo-Fenton processes at near-neutral pH using a solar simulator: optimization by D-optimal experimental design and toxicity evaluation

El artículo presentado a continuación ha sido publicado en la revista "*Journal of Photochemistry and Photobiology A: Chemistry"*

Paracetamol removal by photo-Fenton processes at near-neutral pH using a solar simulator: optimization by D-optimal experimental design and toxicity evaluation

Bárbara N. Giménez, Leandro O. Conte, Orlando M. Alfano, Agustina V. Schenone

Instituto de Desarrollo Tecnológico para la Industria Química (INTEC), Consejo Nacional de Investigaciones Científicas y Técnicas (CONICET) and Universidad Nacional del Litoral (UNL), Ruta Nacional N◦ 168, 3000, Santa Fe, Argentina

Abstract

This study discusses the degradation of paracetamol (PCT) by Fenton and photo-Fenton reactions at circumneutral pH with the aid of ferrioxalate and a solar simulator as the light source. The influence of three main operating variables: H_2O_2 concentration (*HP*), temperature (*T*) and radiation level (*Rad*) on PCT conversion was evaluated with a D-optimal design and a response surface methodology (RSM). The analysis of variance (ANOVA) revealed that *Rad* and *T* significantly affected the studied response. The model performance was satisfactory, giving low standard deviation (0.74) and good R^2 and adjusted R^2 values (0.9997 and 0.9993, respectively). The optimal conditions found for each radiation level were tested. The obtained PCT conversions after 90 min of reaction (75.52%, 96.88% and 91.5%, respectively) were in good agreement with the predicted values (71.28%, 96.75% and 92.75%, respectively). It was observed that the maximum and minimum levels of toxicity (bioluminescence inhibition of *Vibrio fischeri* bacteria) found in the system were closely related to the maximum and minimum concentrations observed for the reaction intermediaries (hydroquinone and 1,4-benzoquinone). In addition, it was only possible to completely reduce the toxicity of the system after 240 min of reaction when high levels of radiation were applied.

Keywords: Advanced Oxidation Processes, Emerging Contaminants, Acetaminophen, Ferrioxalate Complex, Response Surface Methodology.

1. Introduction

Traditionally, researches on water quality have focused on pathogens and priority pollutants (heavy metals, pesticides, polycyclic aromatic hydrocarbons, etc.). However, new contaminants were detected in wastewater and surface water in quantities ranged from nanograms to micrograms per liter, and even at 100 μg L^{-1} [1]. The toxicological effects of these compounds are difficult to evaluate and, in some cases, the legislation regarding their discharge limits and/or concentration limits in water bodies is non-existent. These groups of so-called emerging contaminants (ECs) comprise various compounds such as human and veterinary pharmaceuticals, personal care products, industrial additives, pesticides and hormones, among others [2]. Furthermore, the effects of their transformation products or metabolites are almost unknown [3].

Several publications have demonstrated that water treatment plants do not completely remove ECs, especially biological treatments which are usually not suitable for destroying this type of organic compounds [4–6]. On the other hand, the technologies based on Advanced Oxidation Processes (AOP) are very effective in the oxidation of toxic or refractory substances because of the formation of highly reactive species, i.e. hydroxyl (HO•) and hydroperoxyl (HO_2•) radicals, which attack these pollutants with high reaction rate constants ranging from 10^6 to 10^9 M^{-1} s^{-1} [7–9]. Among the available AOPs suitable for water and wastewater treatment, Fenton and photo-Fenton processes have been widely applied to degrade ECs [10–13]. Moreover, the photo-Fenton process is particularly attractive from the economic point of view due to the possibility of using solar energy as a source of radiation [14–18].

Another option to reduce the costs of the process is to work at neutral pH avoiding its adjustment before and after the treatment. In such cases, iron needs to be complexed in order to prevent its precipitation. Thus, as an alternative to the traditional photo-Fenton

process, iron can form complexes with diverse carboxylates and poly-carboxylates which allow operating the system at a wide range of pH conditions close to neutrality [19–21]. In this sense, the use of ferrioxalate instead of ferrous ions in the UV/H_2O_2 system to accelerate the production of hydroxyl radicals has been widely applied [22–26]. In addition, it greatly improves the photocatalytic activity of the systems since the molar absorption coefficients of the ferrioxalate molecules generated under certain experimental conditions are higher than those of aqueous complexes [27–29].

In the present study, ferrioxalate assisted Fenton and photo-Fenton experiments were carried out in order to study paracetamol (PCT) degradation in water under different operating conditions. This drug, also known as acetaminophen, is classified as an anti-inflammatory and non-steroidal analgesic and is one of the pharmaceutical products considered as ECs. PCT has been found in the wastewater treatment plants [30,31]. Although it is degraded quite effectively by biological processes, appreciable concentrations of this drug can be also found in effluents of these plants which reach the natural environment [32]. Despite the low concentrations (ng L^{-1} and μg L^{-1}), the presence of this biologically active molecule in the aquatic environment may still affect aquatic organisms [33]. Industrial wastewater is another source of hazardous compounds since some pharmaceutical industries discharge wastewater without effective treatment. An example of the latter is the case of PCT, which was found in concentrations between 5.6 and 294 mg L^{-1} in wastewaters [34–37]. Furthermore, Badawy and colleagues [34] showed that PCT could not be totally removed from wastewaters generated from a pharmaceutical company by biological treatment. On the other hand, the application of Fenton process as a pre-treatment improved its removal by increasing the biodegradability of the effluent. Recently, Audino et al. [13] developed a kinetic model describing Fenton and photo-Fenton degradation of PCT at high initial concentration. In

this case, the experiments were performed at acidic pH and ferrous sulphate as iron source.

The study of the degradation of an organic compound through Fenton and photo-Fenton processes involves the evaluation of several factors, each of which influences the reaction rate in different ways. In this sense, it is very useful to apply experimental design methods because they allow maximizing the quality of the information obtained from the tests carried out, minimizing time and cost [38]. Thus, the present work proposes the application of a D-optimal design combined with a response surface methodology (RSM) to evaluate the effect of three important parameters on PCT conversion: temperature, H_2O_2 concentration and radiation level. The last step was to perform the experiments under the optimized operating conditions and evaluate the toxicity through the Microtox® test.

2. Materials and Methods

2.1. Chemicals

Analytical grade reagents were used as well as ultra-pure water (Osmoion, APEMA). PCT ($C_8H_9NO_2$, 98% purity) was obtained from Aldrich. Hydroquinone (HQ, 99% purity) and 1,4-benzoquinone (BQ, 99% purity) were purchased from Fluka. The salt $FeCl_3.6H_2O$ (Merck, pro-analysis) was used as a Fe^{3+} source and the oxalate ion was used as potassium oxalate (Carlo Erba, 99.5% purity). The potassium ferrioxalate was prepared by mixing a solution of potassium oxalate (2000 mg L^{-1}) and a solution of iron(III) chloride (500 mg Fe^{3+} L^{-1}) in the adequate quantities. Hydrogen peroxide (HP, 30%) and NaOH were obtained from Cicarelli. Finally, methanol (HPLC grade) was purchased from Sintorgan.

2.2. Experimental device

The experiments were carried out in a flat plate reactor of borosilicate glass (0.07

L) with external recycling. The reactor was connected to a storage tank containing the solution to be treated (3 L) and equipped with a pH-meter, a thermometer and a liquid sample valve. The experimental system was completed with a thermostatic bath and a centrifugal pump to provide good mixing conditions. Also, in the case of photo-Fenton reactions, the reactor was irradiated by a solar simulator (Oriel, model 9600). More details of the experimental device can be found in Conte et al. [11].

2.3. Procedure

The treated sample consisted of ultrapure water spiked with the contaminant. Initial PCT and Fe^{3+} concentrations were set at 40 mg L^{-1} and 3 mg L^{-1} (molar ratio Fe/Ox=1/10), respectively, in all the experiments. Firstly, the thermostatic bath was set at the desired temperature and the solution containing PCT and the ferric complex was added to the storage tank. pH value was then adjusted to 5.5 with concentrated NaOH solution. Finally, HP solution was added. The first sample was taken (t = 0 min) and then the lamp shutter was removed (in case of experiments performed under irradiated conditions). The total reaction time was 180 min (for most experiments) and 240 min (for experiments under optimum conditions), and samples were withdrawn at predefined time intervals (t = 15, 30, 45, 60, 90, 120, 180 and 240 min).

The PCT initial concentration was selected based on the amounts found in a real wastewater from a pharmaceutical industry (between 5.6 and 294 mg L^{-1}) [34,36,37]. In the case of iron, the concentration level was chosen considering the legal values to discharge the treated effluent into a surface water course (5 mg L^{-1}) [39]. In order to achieve a molar ratio Fe/Ox=1/10, initial concentration of oxalate was 47.5 mg L^{-1}, avoiding iron precipitation at the working pH. In previous publications, it was demonstrated that under these conditions, there is a molar fraction close to 90% of the most active ferrioxalate specie ($Fe^{(III)}(C_2O_4)_3^{3-}$), which has high molar radiation

absorption coefficients in the UV/Vis region [11,29].

2.4. Analytical determinations

Paracetamol, hydroquinone and 1,4-benzoquinone were determined by HPLC-UV/Vis (Waters) with a YMC-Triart C18 column (250 x 4.6 mm, 5 μm) and methanol:water (25:75) as mobile phase (flow rate=1 mL min^{-1}). Detection was made at 220 and 243 nm. Maximum experimental errors were 0.08, 0.15 and 0.17 mg L^{-1} for PCT, HQ and BQ, respectively. The limits of detection (LOD) for PCT, HQ and BQ were 0.18, 0.21 and 0.38 mg L^{-1}, respectively. The samples used to determine PCT, HQ and BQ were pre-treated with methanol to stop the dark reaction. An UV/Vis spectrophotometer (Lambda 35, Perkin-Elmer) was used to monitor the H_2O_2 concentration through a modified iodometric technique, measuring the absorbance of the complex formed at 350 nm. The same instrument was used for the analysis of Fe by means of the colorimetric method with 1,10-phenanthroline at 510 nm. Total organic carbon (TOC) concentration was measured with a vario TOC cube analyser (Elementar) and samples were pre-treated with sodium sulphite.

2.5. Acute toxicity test

The acute toxicity was monitored during the oxidation process. For this purpose, the inhibition of the luminescence of the bacteria *Vibrio fischeri* NRRL-B-11177 was measured after 15 min of incubation [40]. The Microtox Model 500 Toxicity Analyser (Strategic Diagnostic Inc.) was used with the aid of MicrotoxOmni® software. Adjustment of sample pH (between 6 and 8) was carried out and hydrogen peroxide was removed with a catalase solution (1500 mg L^{-1} of >2000 U/mg bovine liver) acquired from Fluka.

2.6. Experimental design and statistical analysis

Response surface methodology was used to study and optimize PCT degradation

through Fenton and photo-Fenton processes. The aim of RSM is to find the mathematical model that best fits the experimental data and establish the values of the factors that optimize the response under study [38]. The general model structure of a response surface can be described with Eq. (1):

$$Y = \beta_0 + \sum_{i=1}^{k} \beta_i X_i + \sum_{i=1}^{k} \beta_{ii} X_i^2 + \sum_{i=1}^{k} \sum_{j=1}^{k} \beta_{ij} X_i X_j + \varepsilon \qquad \text{Eq. (1)}$$

where Y denotes the selected response, i.e. the dependent variable; k represents the number of factors; i and j are the index numbers for factors; β_0 is the intercept term; $X_i...X_k$ are coded independent variables; β_i represents the linear effect of the ith factor, β_{ii} the quadratic effect of the ith factor, $\beta_{ij}$the interaction effect between the ith and jth factors, and ε is the random error [41,42].

Before applying the RSM, the process variables and their ranges must be defined, followed by the selection of an experimental design. In the present study, a D-optimal design was applied. This methodology was developed to select experimental runs minimizing the variance of the estimated regression coefficients through optimality criteria. This model creates a possible set of runs within the design space. D-optimal designs can deal with numeric and categorical factors, which is the present case. Furthermore, the selection was made considering the reduction of experiments in comparison with factorial designs (36 experiments) or central composite designs (33 experiments).

The quadratic polynomial equation of the RSM model, Eq. (1), takes into account the parameters of the process, whose levels are within -1 and 1 for numerical and categorical factors. Furthermore, the factors can have a mixed number of levels. The key process parameters studied were: temperature (*T*), hydrogen peroxide concentration (*HP*) and level of irradiation (*Rad*), which were assigned to coded model variables X_1, X_2 and

X_3, respectively. The influence of these parameters was evaluated on the observed PCT conversion at 90 min of reaction ($\boldsymbol{X}_{\mathbf{90},pred}^{\boldsymbol{PCT}}$), which was selected as the dependent variable *Y*. The experimental design matrix obtained by D-optimal, including the coded and actual values of the studied parameters, is depicted in Table 1. It consists in a total of 19 experiments: 12 model points, 3 runs to estimate the lack of fit and 4 replicates. The experiments were randomized to minimize the effects of unexpected variability in the observed responses. The obtained model (PCT conversion) was analysed statistically applying analysis of variance (ANOVA). The adequacy of the final model was verified by graphical and numerical analysis.

Regarding the range of the studied factors, the selection was made based on previous experience in related works [11,13,26]. HP concentration was varied between 189 and 756 mg L^{-1}, which are the stoichiometric value needed for the complete mineralization of 40 mg L^{-1} of PCT and four times this value, respectively. The minimum temperature level was set at 25 °C, considered as ambient temperature, and the maximum level at 50 °C, which is the temperature that the samples could reach if they were treated in a pilot-plant solar reactor [14,15]. In the case of the categorical factor (*Rad*), three levels were evaluated: No radiation, Low (*qw* = 31.6 W m^{-2}) and High (*qw* = 57.5 W m^{-2}) radiation levels. The last two levels correspond to two different local radiation fluxes averaged over the reactor window, which are comparable to the typical solar radiation levels found in Santa Fe city, Argentina (31° 39’ S, 60° 43’ W, 25 m above sea level). Both levels were obtained from the combination of filters (air, liquid and attenuation filters) that are attached to the solar simulator [11,15].

Table 1

D–optimal design matrix with three independent variables (two numeric and one categorical) expressed in coded units and actual values, and the values of the observed ($\boldsymbol{X_{90,obs}^{PCT}}$) and predicted ($\boldsymbol{X_{90,pred}^{PCT}}$) responses.

Run	Coded values			Actual values			Response	
	X_1	X_2	X_3	T (°C)	HP (mg L^{-1})	Rad	$X_{90,obs}^{PCT}$(%)	$X_{90,pred}^{PCT}$(%)
N1	1	0	{1 0}	50.0	472.5	No	70.50	70.85
N2	0	0	{-1 -1}	37.5	472.5	High	94.23	94.26
N3	1	1	{1 0}	50.0	756	No	65.30	65.09
N4	0	-0.5	{0 1}	37.5	330.75	Low	94.05	94.02
N5	1	-1	{-1 -1}	50.0	189	High	97.99	97.19
N6	-1	1	{0 1}	25.0	756	Low	78.71	78.56
N7	1	-1	{-1 -1}	50.0	189	High	97.20	97.19
N8	-1	-1	{0 1}	25.0	189	Low	86.24	85.88
N9	0	-1	{1 0}	37.5	189	No	64.87	*outlier*
N10	1	1	{1 0}	50.0	756	No	64.88	65.09
N11	-1	0	{1 0}	25.0	472.5	No	1.88	1.87
N12	-1	1	{0 1}	25.0	756	Low	77.65	78.36
N13	-1	-1	{-1 -1}	25.0	189	High	80.15	80.94
N14	1	0	{1 0}	50.0	472.5	No	71.20	70.95
N15	1	-1	{0 1}	50.0	189	Low	96.37	96.75
N16	1	1	{0 1}	50.0	756	Low	89.59	89.23
N17	-1	1	{-1 -1}	25.0	756	High	81.33	80.53
N18	-1	-1	{1 0}	25.0	189	No	1.15	1.13
N19	1	1	{-1 -1}	50.0	756	High	96.00	96.79

3. Results and Discussion

3.1. Effect of experimental variables on the PCT conversion

RSM was performed in order to statistically evaluate the degradation of PCT by a D-optimal design, which was selected due to its versatility to analyse categorical factors. Each design variable, as well as their interactions, were analysed and the model that

describes the process was determined. The surface response, which resulted from the regression analysis, fits the experimental data by the following polynomial model:

$$\boldsymbol{X_{90,pred}^{PCT}}(\%) = 75.24 + 16.02X_1 - 2.16X_2 - 36.73X_3(1) + 17.71X_3(2) + 18.47X_1X_3(1) - 10.58X_1X_3(2) - 0.35X_2X_3(1) - 1.60X_2X_3(2) - 2.15X_1^2 - 3.25X_2^2 \quad \text{Eq.(2)}$$

where X_1, X_2 and X_3 represent the coded values of the parameters of the variables (*T*, *HP* and *Rad*, respectively). Interaction between factors is represented by the combination of variables, such as X_1X_3. In the case of the categorical factor, as well as its interaction with the numerical factors, a physical interpretation is not easy, so that only a mathematical reading is possible. Namely, the coefficient for $X_3(1)$ is the difference of level 2 average (in this case, *Low Rad*) from the overall average; for $X_3(2)$ is the difference of level 3 average (*High Rad*) from the overall average [43].

ANOVA was used to evaluate the response surface models (Table 2). *F*-value of 2163.87 and *p*-value less than 0.0001 imply that the model was significant [38]. Following the same criteria, X_1, X_2, X_3, X_1X_3, X_2X_3, X_1^2 and X_2^2 were also significant ($p < 0.05$), while there was no evidence of the lack of fit (p =0.1152). X_1X_2 term was not considered due to its high *p* value. *Rad* is the most significant term (F = 3645.10), followed by the term *T* (F =3476.06) and finally by the term *HP* (F = 90.91). Satisfactory values of standard deviation (0.74), R^2 and adjusted R^2 (0.9997 and 0.9993, respectively) were obtained for the model.

Table 2

ANOVA results – model and coefficient validation: fit summary.

Source	**Sum of Squares**	**Degree of Freedom**	**Mean Square**	***F* Value**	***p*-value Prob> *F***
Model	14107.54	11	1282.50	2163.87	< 0.0001
X1 (*T*)	2060.23	1	2060.23	3476.06	< 0.0001
X2 (*HP*)	53.885	1	53.88	90.91	< 0.0001
X3 (*Rad*)	4320.82	2	2160.41	3645.10	< 0.0001
X1X2	0.32	1	0.32	0.54	0.4893
X1X3	1608.09	2	804.04	1356.60	< 0.0001
X2X3	30.41	2	15.21	25.66	0.0011
$X1^2$	4.17	1	4.17	7.04	0.0379
$X2^2$	11.19	1	11.19	18.89	0.0048
Residual	3.56	6	0.59		
Lack of Fit	2.35	2	1.17	3.89	0.1152
Pure Error	1.21	4	0.30		

The interpretation of the computed coefficients for categorical factors could be difficult since they do not have physical meaning. Thus, model results are usually analysed by means of model graphics [43].

Firstly, the residuals were analysed to confirm that the model was adequate. The normal probability plot is presented in Fig. 1a and indicates that the residuals follow a normal distribution since they are placed closely along the straight line.

Fig. 1b and 1c present the plots of the predicted responses ($\boldsymbol{X_{90,pred}^{PCT}}$) versus the actual values ($\boldsymbol{X_{90,obs}^{PCT}}$) and the residuals versus the predicted responses, respectively. The latter suggests that the variance of the data is almost constant. Furthermore, the R^2 (0.9997) indicates a satisfactory adjustment of the model to the observed responses. Therefore, the model adequately describes the system under study.

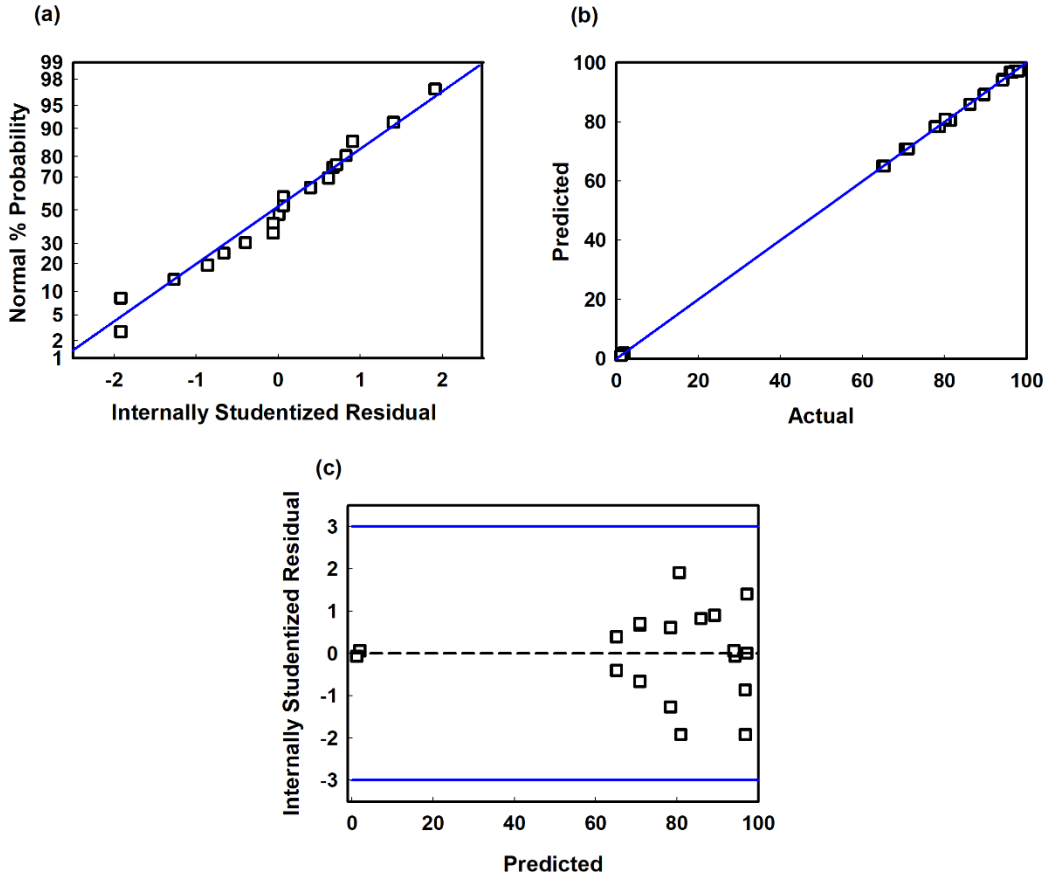

Fig. 1 Residual diagnostics of model for the prediction of PCT conversion by Fenton and photo-Fenton processes. (a) Normal probability plot, (b) observed *vs*. predicted plot, and (c) internally studentized residuals *vs*. predicted values plot.

Moreover, an interaction plot between *T* and *Rad* is presented in Figure 2. As can be observed, for *HP*=189 mg L^{-1} and increasing the *T* (from 25 to 50 ºC), a larger amplitude of PCT conversion was obtained (difference of 69.69% in the $\boldsymbol{X_{90,obs}^{PCT}}$) for dark conditions in comparison with the produced effect when the system is irradiated (difference of 10.87% in the $\boldsymbol{X_{90,obs}^{PCT}}$). Similar behaviour was observed for high radiation system (results not shown). However, for the whole range of *T* working conditions, the $\boldsymbol{X_{90}^{PCT}}$ obtained by irradiating the system was greater. Therefore, the positive and relevant significance of the *T* and *Rad* in the process was verified.

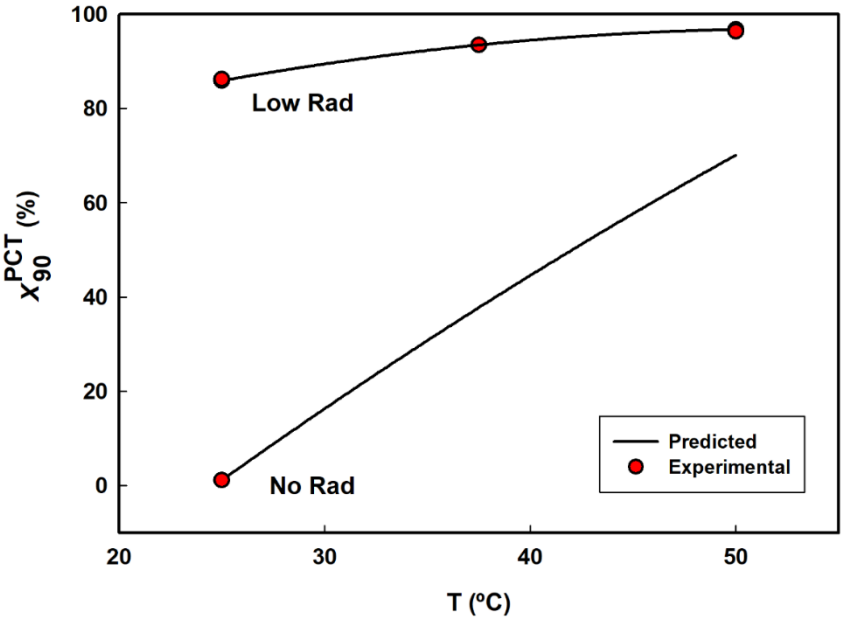

Fig. 2 Interaction plot between *T* and *Rad* for a fixed HP concentration (*HP* = 189 mg L^{-1}).

Three RSM models were developed in actual terms to describe the $\boldsymbol{X_{90,pred}^{PCT}}$ for dark conditions (M1) and using low (M2) and high (M3) radiation levels (see Eqs.(3), (4) and (5), respectively).

$$\boldsymbol{X_{90,pred}^{PCT}} = -91.333 + 3.912T + 0.031HP - 0.015T^2 - 4.162x10^{-5}HP^2 \quad \text{Eq. (3)}$$

$$\boldsymbol{X_{90,pred}^{PCT}} = 51.926 + 1.601T + 0.026HP - 0.015T^2 - 4.162x10^{-5}HP^2 \quad \text{Eq. (4)}$$

$$\boldsymbol{X_{90,pred}^{PCT}} = 38.420 + 1.843T + 0.037HP - 0.015T^2 - 4.162x10^{-5}HP^2 \quad \text{Eq. (5)}$$

Firstly, it is important to note that the signs of the terms in Eqs. (3)-(5) provide physical significance to the obtained results. For instance, larger *T* and *HP* values (terms with positive sign) would result in a higher $\boldsymbol{X_{90,pred}^{PCT}}$ validating the importance of their roles in the Fenton (M1) and photo-Fenton process (M2 and M3). However, the influence of the HP^2 term is negative since an excess of H_2O_2 produces a scavenging effect, consuming $HO^{\bullet}$ radicals available to react with PCT (Eq (6)) and thus decreasing its

degradation. Also, an excess of H_2O_2 accelerates its decomposition (Eq. (7)), producing O_2 and H_2O, but not reactive radicals [19,44]. Due to these reasons, the efficiency of the process decreases.

$$H_2O_2 + HO^{\bullet} \rightarrow HO_2^{\bullet} + H_2O \quad \text{Eq.(6)}$$

$$2H_2O_2 \rightarrow 2H_2O + O_2 \quad \text{Eq.(7)}$$

In addition, high operating temperatures (negative sign of the term T^2) promote the decomposition of the iron complex (precipitation of the catalyst). Thus, no experiments were performed using high temperatures to avoid iron precipitation [14,45,46].

The overall effect of *T* and *HP* in each model M1, M2 and M3 can be observed on the response surfaces presented in Fig. 3.

Firstly, it should be noted that for all the range of *T* and *HP* concentrations, the lowest PCT conversions were reached for the dark system (Fig. 3a). Under this *Rad* condition, the lowest levels of PCT conversion were obtained for *T* = 25ºC (runs N11 and N18, Table 1). Being the minimum value, $\boldsymbol{X_{90,obs}^{PCT}} = 1.15\%$ ($\boldsymbol{X_{90,pred}^{PCT}} = 1.13\%$) the one reached using the lowest concentration of oxidizing agent (*HP* = 189 mg L^{-1}, run N18, Table 1). In contrast, for this dark condition, and using intermediate doses of oxidizing agent (*HP* = 472 mg L^{-1}), the maximum conversion of $\boldsymbol{X_{90,obs}^{PCT}} = 71.2\%$ ($\boldsymbol{X_{90,pred}^{PCT}} = 70.95\%$) was reached for *T* = 50 °C (run N1 and its replicate run N14, Table 1).This conversion is 37.5 times higher than the one obtained by operating the system at low temperatures (run N11, *HP* = 472 mg L^{-1}, *T* = 25ºC, Table 1). Therefore, it is necessary to highlight once more the significant influence of the *T* in the process.

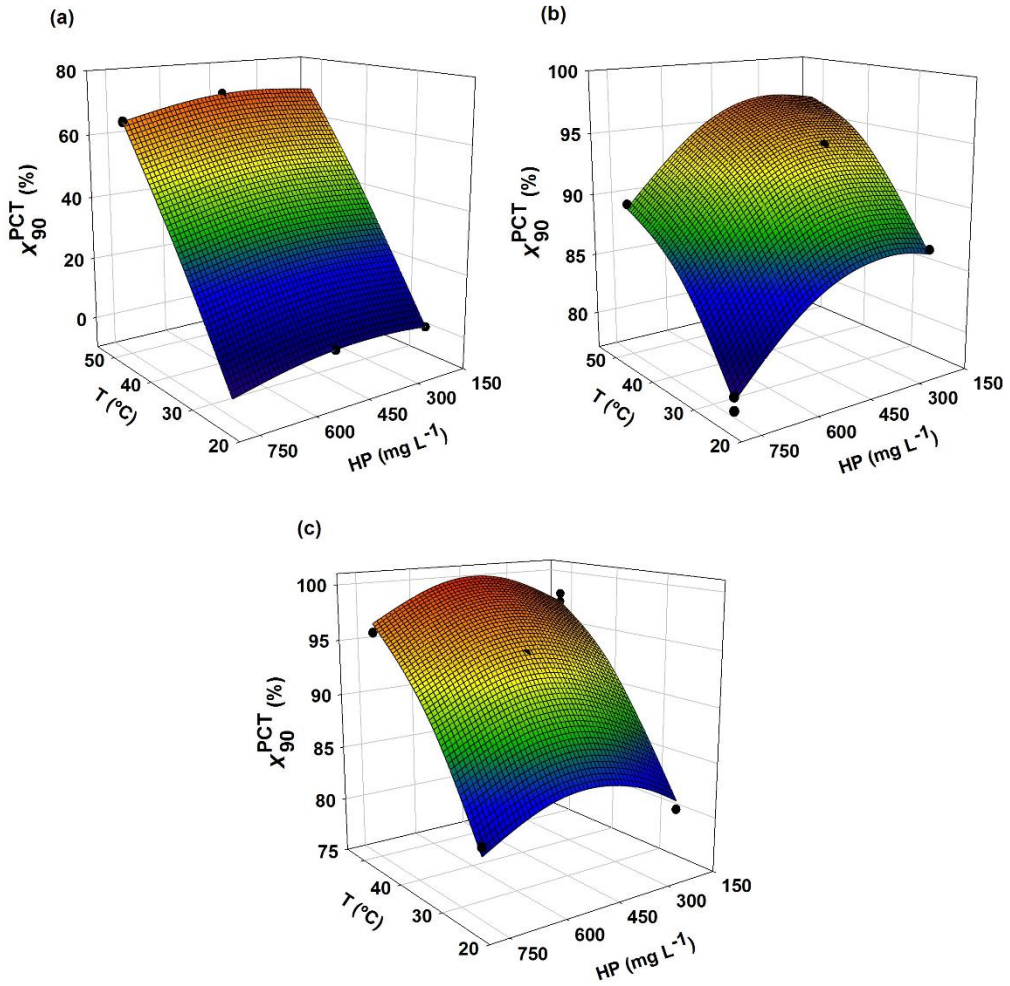

Fig. 3 Response surfaces and experimental values (circles) for $\boldsymbol{X_{90}^{PCT}}$ as a function of *T* and *HP* concentration. a) Dark conditions, b) Low Radiation, and c) High Radiation.

On the other hand, for irradiated conditions and considering the whole range of *T* and *HP*, $\boldsymbol{X_{90,obs}^{PCT}}$ higher than 77.65% ($\boldsymbol{X_{90,pred}^{PCT}}$ higher than 78.36%) were reached (run N = 12, low radiation). It should be noted, that similar values were obtained for its replicate ($\boldsymbol{X_{90,obs}^{PCT}} = 78.71\%$ and $\boldsymbol{X_{90,pred}^{PCT}} = 78.56\%$, run N = 6, Table 1). Moreover, PCT conversions close to 100% were observed using high radiation levels (N = 5, and its replicates N = 7 and N = 19). Thus, the significant influence of radiation level on the process is demonstrated.

It is also important to analyse the conversion levels achieved for TOC after 180 min of reaction ($\boldsymbol{X_{180}^{TOC}}$). Without radiation, the experimental values of $\boldsymbol{X_{180}^{TOC}}$ were very

low, being less than 17.05%. When the system was irradiated, these values increased slightly, being $\boldsymbol{X_{180}^{TOC}} = 37.84\%$ the maximum level of conversion (run N = 2, high radiation). It is worth mentioning that total mineralization is not desirable for this study since, in that case, the Fe(III)-carboxylate complex would be completely destroyed with the consequent precipitation of iron [15].

3.2. Optimized conditions and toxicity results

The criteria selected for the optimization of each evaluated model M1 (Eq. 3), M2 (Eq. 4) and M3 (Eq. 5) consisted in maximizing the conversion of the pollutant, considering a minimum consumption of oxidizing agent (aspect of economic relevance) and maintaining the operating temperature in the defined working range (between 25 and 50 ºC). Accordingly, PCT experimental conversions of 75.52%, 96.88% and 91.5% were obtained after 90 min of reaction for dark (*T*=50ºC, *HP*=326.3 mg L^{-1}), low radiation (*T*=50ºC, *HP*=189 mg L^{-1}), and high radiation (*T*=40ºC, *HP*=189 mg L^{-1}) optimized systems, respectively. These results are very close to the values predicted by M1, M2 and M3 models (71.28%, 96.75% and 92.75%, respectively), demonstrating a good agreement.

The most commonly proposed pathway for PTC decomposition is the direct hydroxyl radicals attack on the PTC molecule to form acetamide and hydroquinone, which is further oxidized to p-benzoquinone. As it was previously mentioned in this work, the primary intermediates identified were hydroquinone and 1,4-benzoquinone. Subsequently, these aromatic compounds are eventually converted into non-aromatic molecules, as proposed by Almeida et al. [47]. Finally, the complete mineralization of paracetamol would yield the final degradation products, namely NH_4^+, CO_2 and water. Taking into account these intermediates, a simplified degradation pathway of PCT was proposed, as shown in Figure 4. Furthermore, this information is useful for future

development of a reaction mechanism and a kinetic model.

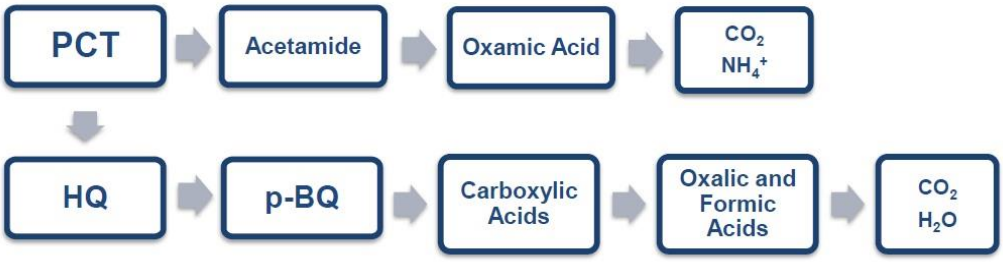

Fig. 4 Reaction pathway proposed for paracetamol degradation.

Fig. 5 shows the experimental evolution of PCT, hydroquinone and 1,4-benzoquinone as a function of time for the three optimized conditions. In addition, the figure shows in the secondary axis, the evolution of the toxicity in the system (expressed as percentage of inhibition of bioluminescence of *V. fischeri* bacteria after 15 min of incubation, *I*(%)). It should be noted that the concentrations of the reaction intermediates are related to the initial concentration of PCT.

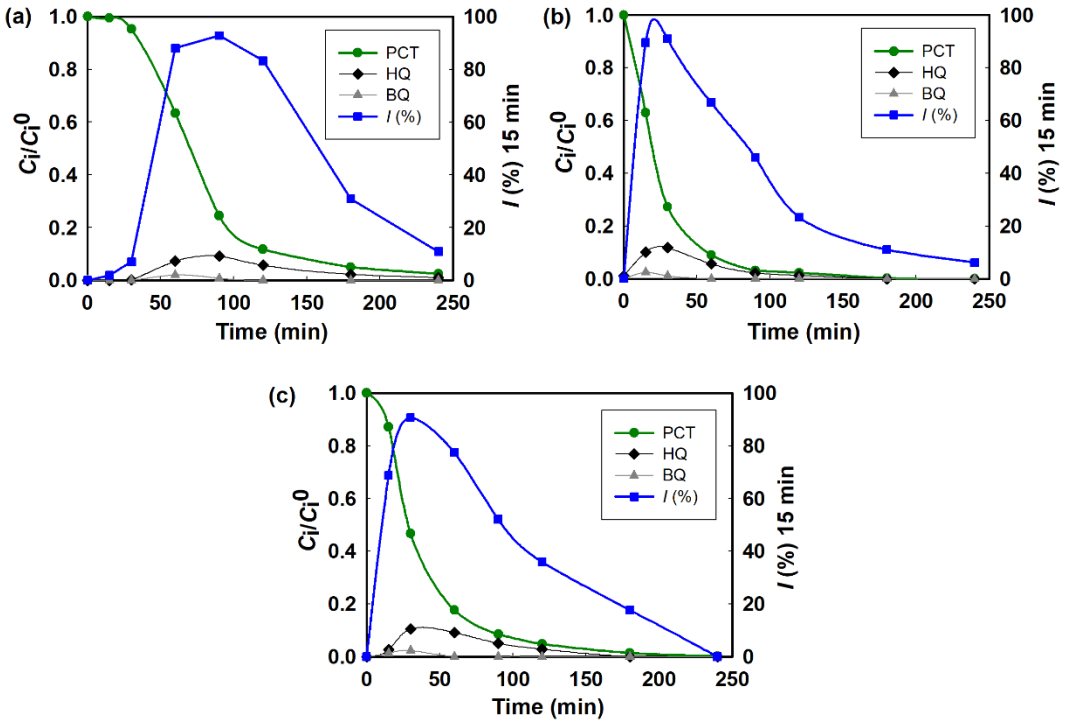

Fig. 5 Experimental relative concentrations *vs.* time for PCT, HQ, BQ and *I*(%) at the optimum conditions for a) Dark conditions, b) Low Radiation, and c) High Radiation.

Firstly, it can be observed that the maximum and minimum levels of toxicity found in the system were closely related to the maximum and minimum concentrations observed for the main reaction intermediaries (HQ and BQ). Moreover, for the initial reaction conditions, the samples did not exhibit toxicity. At this point it must be considered that EC_{50} values (concentration which causes 50% reduction of the bioluminescence) of the reaction intermediates are much lower than the values observed for the PCT (see Table 3).

On the other hand, a reduction in the toxicity of the system is observed as the reaction progresses. Being *I*(%) close to 100% for *t* = 90 min in Fig. 5a and for *t* = 30 min in Figs. 5b and c. However, only by operating the system with high levels of radiation it was possible to completely reduce the toxicity of the system (*I*(%) = 0) after 240 min of reaction (Fig. 5c).

Therefore, although PCT conversions close to 100% are reached after 180 min of reaction, longer reaction times are necessary to achieve a complete reduction of the remaining toxicity in the system.

Table 3

EC_{50} values at 15 min for *V. fischeri*.

	EC_{50} 15 min (mg L^{-1})	**References**
Paracetamol	1045.8	[48]
Hydroquinone	0.038	[48]
	0.041	[49]
1,4-Benzoquinone	0.02	[48]
	0.1	[49]

4. Conclusions

Based on the obtained results, paracetamol could be successfully degraded under

Fenton and photo-Fenton conditions at pH=5.5 using ferrioxalate as iron source. In order to study the effects of the process parameters: hydrogen peroxide concentration (*HP*), temperature (*T*) and radiation (*Rad*), a D-optimal experimental design (19 experiments: 12 model points, 3 runs to estimate the lack of fit and 4 replicates) combined with a response surface methodology was applied. A second-order quadratic model fitted the experimental data and the reported R^2 and adjusted R^2 values (0.9997 and 0.9993, respectively) were satisfactory, suggesting a good agreement between the predicted values and the experimental results. Among the studied variables, it could be seen that the largest effect on PCT conversion was due to *Rad* (the most significant term), followed by the terms *T* and finally *HP*. It was also found that an excess of H_2O_2 causes a decrease in the process efficiency.

The conversion achieved by the Fenton process at the optimal conditions (*T*=50ºC, *HP*=326.3 mg L^{-1}, $\boldsymbol{X_{90,obs}^{PCT}}$=75.52%) was lower than those obtained with low (*T*=50ºC, *HP*=189 mg L^{-1}, $\boldsymbol{X_{90,obs}^{PCT}}$=96.88%) and high (*T*=40ºC, *HP*=189 mg L^{-1}, $\boldsymbol{X_{90,obs}^{PCT}}$=91.5%) radiation levels. Moreover, the obtained results were very close to the values predicted by the quadratic models (71.28%, 96.75% and 92.75%, respectively).

Under optimum conditions, the inhibition of bioluminescence of *V. fischeri* bacteria was evaluated. Despite the complete conversion of PCT at *t*=180 min, a percentage of inhibition remaining in solution was observed. This is associated with the presence of highly toxic reaction intermediates (hydroquinone and 1,4-benzoquinone). Only by operating the system with high levels of radiation was it possible to completely reduce the toxicity of the system (*I*(%) = 0) after 240 min of reaction.

Acknowledgments

The authors are grateful to Universidad Nacional del Litoral (UNL, CAI+D PJ 50020150100028LI and CAI+D PJ 0020150100093LI), Consejo Nacional de

Investigaciones Científicas y Técnicas (CONICET, PIP 2015-2017 GI), and Agencia Nacional de Promoción Científica y Tecnológica (ANPCyT, PICT Nº 2015-2651) for financial support.

References

[1] S.D. Richardson, S.Y. Kimura, Water Analysis: Emerging Contaminants and Current Issues, Anal. Chem. 88 (2016) 546–582. https://doi.org/10.1021/acs.analchem.5b04493.

[2] C.J. Houtman, Emerging contaminants in surface waters and their relevance for the production of drinking water in Europe, J. Integr. Environ. Sci. 7 (2010) 271–295. https://doi.org/10.1080/1943815X.2010.511648.

[3] D.A. Lambropoulou, L.M.L. Nollet, Transformation Products of Emerging Contaminants in the Environment: Analysis, Processes, Occurrence, Effects and Risks, Volumes 1, John Wiley & Sons, Inc, New York, 2014. https://doi.org/10.1002/9781118339558.

[4] L. Rizzo, S. Malato, D. Antakyali, V.G. Beretsou, M.B. Đolić, W. Gernjak, E. Heath, I. Ivancev-Tumbas, P. Karaolia, A.R. Lado Ribeiro, G. Mascolo, C.S. McArdell, H. Schaar, A.M.T. Silva, D. Fatta-Kassinos, Consolidated vs new advanced treatment methods for the removal of contaminants of emerging concern from urban wastewater, Sci. Total Environ. 655 (2019) 986–1008. https://doi.org/10.1016/j.scitotenv.2018.11.265.

[5] A. Gogoi, P. Mazumder, V.K. Tyagi, G.G. Tushara Chaminda, A.K. An, M. Kumar, Occurrence and fate of emerging contaminants in water environment: A review, Groundw. Sustain. Dev. 6 (2018) 169–180. https://doi.org/10.1016/j.gsd.2017.12.009.

[6] A.M. Botero-Coy, D. Martínez-Pachón, C. Boix, R.J. Rincón, N. Castillo, L.P.

Arias-Marín, L. Manrique-Losada, R. Torres-Palma, A. Moncayo-Lasso, F. Hernández, 'An investigation into the occurrence and removal of pharmaceuticals in Colombian wastewater,' Sci. Total Environ. 642 (2018) 842–853. https://doi.org/10.1016/j.scitotenv.2018.06.088.

[7] C. Von Sonntag, Advanced oxidation processes: Mechanistic aspects, Water Sci. Technol. 58 (2008) 1015–1021. https://doi.org/10.2166/wst.2008.467.

[8] R. Ameta, A.K. Chohadia, A. Jain, P.B. Punjabi, Fenton and Photo-Fenton Processes, in: Adv. Oxid. Process. Wastewater Treat. Emerg. Green Chem. Technol., Elsevier Inc., 2018: pp. 49–87. https://doi.org/10.1016/B978-0-12-810499-6.00003-6.

[9] L. Wang, Z. Bian, Photocatalytic degradation of paracetamol on Pd–BiVO4 under visible light irradiation, Chemosphere. 239 (2020) 124815. https://doi.org/10.1016/j.chemosphere.2019.124815.

[10] M.G. Alalm, A. Tawfik, S. Ookawara, Degradation of four pharmaceuticals by solar photo-Fenton process: Kinetics and costs estimation, J. Environ. Chem. Eng. 3 (2015) 46–51. https://doi.org/10.1016/j.jece.2014.12.009.

[11] L.O. Conte, A. V. Schenone, O.M. Alfano, Photo-Fenton degradation of the herbicide 2,4-in aqueous medium at pH conditions close to neutrality, J. Environ. Manage. 170 (2016) 60–69. https://doi.org/10.1016/j.jenvman.2016.01.002.

[12] I. De la Obra, L. Ponce-Robles, S. Miralles-Cuevas, I. Oller, S. Malato, J.A. Sánchez Pérez, Microcontaminant removal in secondary effluents by solar photo-Fenton at circumneutral pH in raceway pond reactors, Catal. Today. 287 (2017) 10–14. https://doi.org/10.1016/j.cattod.2016.12.028.

[13] F. Audino, L.O. Conte, A.V. Schenone, M. Pérez-Moya, M. Graells, O.M. Alfano, A kinetic study for the Fenton and photo-Fenton paracetamol degradation in an

annular photoreactor, Environ. Sci. Pollut. Res. 26 (2019) 4312–4323. https://doi.org/10.1007/s11356-018-3098-4.

[14] L.O. Conte, J. Farias, E.D. Albizzati, O.M. Alfano, Photo-fenton degradation of the herbicide 2,4-dichlorophenoxyacetic acid in laboratory and solar pilot-plant reactors, Ind. Eng. Chem. Res. 51 (2012) 4181–4191. https://doi.org/10.1021/ie2023228.

[15] L.O. Conte, A. V. Schenone, O.M. Alfano, Ferrioxalate-assisted solar photo-Fenton degradation of a herbicide at pH conditions close to neutrality, Environ. Sci. Pollut. Res. 24 (2017) 6205–6212. https://doi.org/10.1007/s11356-016-6400-3.

[16] J.A. Sánchez Pérez, P. Soriano-Molina, G. Rivas, J.L. García Sánchez, J.L. Casas López, J.M. Fernández Sevilla, Effect of temperature and photon absorption on the kinetics of micropollutant removal by solar photo-Fenton in raceway pond reactors, Chem. Eng. J. 310 (2017) 464–472. https://doi.org/10.1016/j.cej.2016.06.055.

[17] P. Soriano-Molina, J.L. García Sánchez, S. Malato, L.A. Pérez-Estrada, J.A. Sánchez Pérez, Effect of volumetric rate of photon absorption on the kinetics of micropollutant removal by solar photo-Fenton with Fe 3+ -EDDS at neutral pH, Chem. Eng. J. 331 (2018) 84–92. https://doi.org/10.1016/j.cej.2017.08.096.

[18] A.C. Reina, A.B. Martínez-Piernas, Y. Bertakis, C. Brebou, N.P. Xekoukoulotakis, A. Agüera, J.A. Sánchez Pérez, Photochemical degradation of the carbapenem antibiotics imipenem and meropenem in aqueous solutions under solar radiation, Water Res. 128 (2018) 61–70. https://doi.org/10.1016/j.watres.2017.10.047.

[19] J.J. Pignatello, E. Oliveros, A. MacKay, Advanced oxidation processes for organic contaminant destruction based on the fenton reaction and related chemistry, Crit.

Rev. Environ. Sci. Technol. 36 (2006) 1–84. https://doi.org/10.1080/10643380500326564.

[20] A. Ruíz-Delgado, M.A. Roccamante, I. Oller, A. Agüera, S. Malato, Natural chelating agents from olive mill wastewater to enable photo-Fenton-like reactions at natural pH, Catal. Today. 328 (2019) 281–285. https://doi.org/10.1016/j.cattod.2018.10.051.

[21] S. Miralles-Cuevas, I. Oller, A. Ruíz-Delgado, A. Cabrera-Reina, L. Cornejo-Ponce, S. Malato, EDDS as complexing agent for enhancing solar advanced oxidation processes in natural water: Effect of iron species and different oxidants, J. Hazard. Mater. (2019) 129–136. https://doi.org/10.1016/j.jhazmat.2018.03.018.

[22] B.M. Souza, M.W.C. Dezotti, R.A.R. Boaventura, V.J.P. Vilar, Intensification of a solar photo-Fenton reaction at near neutral pH with ferrioxalate complexes: A case study on diclofenac removal from aqueous solutions, Chem. Eng. J. 256 (2014) 448–457. https://doi.org/10.1016/j.cej.2014.06.111.

[23] L.I. Doumic, P.A. Soares, M.A. Ayude, M. Cassanello, R.A.R. Boaventura, V.J.P. Vilar, Enhancement of a solar photo-Fenton reaction by using ferrioxalate complexes for the treatment of a synthetic cotton-textile dyeing wastewater, Chem. Eng. J. 277 (2015) 86–96. https://doi.org/10.1016/j.cej.2015.04.074.

[24] D.R. Manenti, P.A. Soares, A.N. Módenes, F.R. Espinoza-Quiñones, R.A.R. Boaventura, R. Bergamasco, V.J.P. Vilar, Insights into solar photo-Fenton process using iron(III)-organic ligand complexes applied to real textile wastewater treatment, Chem. Eng. J. 266 (2015) 203–212. https://doi.org/10.1016/j.cej.2014.12.077.

[25] J.M. Monteagudo, A. Durán, R. Culebradas, I. San Martín, A. Carnicer, Optimization of pharmaceutical wastewater treatment bysolar/ferrioxalate photo-

catalysis, J. Environ. Manage. 128 (2013) 210–219. https://doi.org/10.1016/j.jenvman.2013.05.013.

[26] A. V. Schenone, L.O. Conte, M.A. Botta, O.M. Alfano, Modeling and optimization of photo-Fenton degradation of 2,4-D using ferrioxalate complex and response surface methodology (RSM), J. Environ. Manage. 155 (2015) 177–183. https://doi.org/10.1016/j.jenvman.2015.03.028.

[27] S. Malato, P. Fernández-Ibáñez, M.I. Maldonado, J. Blanco, W. Gernjak, Decontamination and disinfection of water by solar photocatalysis: Recent overview and trends, Catal. Today. 147 (2009) 1–59. https://doi.org/10.1016/j.cattod.2009.06.018.

[28] A.G. Trovó, S.A.S. Melo, R.F.P. Nogueira, Photodegradation of the pharmaceuticals amoxicillin, bezafibrate and paracetamol by the photo-Fenton process-Application to sewage treatment plant effluent, J. Photochem. Photobiol. A Chem. 198 (2008) 215–220. https://doi.org/10.1016/j.jphotochem.2008.03.011.

[29] L.O. Conte, A. V. Schenone, B.N. Giménez, O.M. Alfano, Photo-Fenton degradation of a herbicide (2,4-D) in groundwater for conditions of natural pH and presence of inorganic anions, J. Hazard. Mater. (2019) 113–120. https://doi.org/10.1016/j.jhazmat.2018.04.013.

[30] H. Del Río, J. Suárez, J. Puertas, P. Ures, PPCPs wet weather mobilization in a combined sewer in NW Spain, Sci. Total Environ. 449 (2013) 189–198. https://doi.org/10.1016/j.scitotenv.2013.01.049.

[31] N. Hamdi El Najjar, A. Touffet, M. Deborde, R. Journel, N. Karpel Vel Leitner, Kinetics of paracetamol oxidation by ozone and hydroxyl radicals, formation of transformation products and toxicity, Sep. Purif. Technol. 136 (2014) 137–143. https://doi.org/10.1016/j.seppur.2014.09.004.

[32] N.K. Stamatis, I.K. Konstantinou, Occurrence and removal of emerging pharmaceutical, personal care compounds and caffeine tracer in municipal sewage treatment plant in Western Greece, J. Environ. Sci. Heal. - Part B Pestic. Food Contam. Agric. Wastes. 48 (2013) 800–813. https://doi.org/10.1080/03601234.2013.781359.

[33] L.H.M.L.M. Santos, A.N. Araújo, A. Fachini, A. Pena, C. Delerue-Matos, M.C.B.S.M. Montenegro, Ecotoxicological aspects related to the presence of pharmaceuticals in the aquatic environment, J. Hazard. Mater. 175 (2010) 45–95. https://doi.org/10.1016/j.jhazmat.2009.10.100.

[34] M.I. Badawy, R.A. Wahaab, A.S. El-Kalliny, Fenton-biological treatment processes for the removal of some pharmaceuticals from industrial wastewater, J. Hazard. Mater. 167 (2009) 567–574. https://doi.org/10.1016/j.jhazmat.2009.01.023.

[35] L.R. Rad, M. Irani, F. divsar, H. Pourahmad, M.S. Sayyafan, I. Haririan, Simultaneous degradation of phenol and paracetamol during photo-Fenton process: Design and optimization, J. Taiwan Inst. Chem. Eng. 47 (2015) 190–196. https://doi.org/10.1016/j.jtice.2014.10.014.

[36] G. Dalgic, F.I. TURKDOGAN, K. Yetilmezsoy, E. Kocak, Treatment of Real Paracetamol, Chem. Ind. Chem. Eng. Q. 23 (2017) 177–186.

[37] P. Pal, R. Thakura, A membrane-integrated closed loop system for treatment of pharmaceutical wastewater, in: IEEE Int. Conf. Power, Control. Signals Instrum. Eng. ICPCSI 2017, Institute of Electrical and Electronics Engineers Inc., 2018: pp. 802–810. https://doi.org/10.1109/ICPCSI.2017.8391824.

[38] R.H. Myers, D.C. Montgomery, Response Surface Methodology: Process and Product Optimization Using Designed Experiments., John Wiley & Sons, Inc, New

York, 2002.

[39] Resolution Nº 1089/82. Reglamento para el control del vertimiento de líquidos residuales: Santa Fe, Argentina., 1982. http://www.santafe.gov.ar/index.php/web/content/download/22767/111069/file/Resolución Nº 1089-82.pdf (accessed December 19, 2019).

[40] ISO, ISO 11348-3:2007 - Water quality - Determination of the inhibitory effect of water samples on the light emission of Vibrio fischeri (Luminescent bacteria test) -- Part 3: Method using freeze-dried bacteria, Switzerland, 2007. http://www.iso.org/iso/home/store/catalogue_ics/catalogue_detail_ics.htm?csnumber=40518 (accessed June 28, 2013).

[41] H. Kusic, N. Koprivanac, A.L. Bozic, Treatment of chlorophenols in water matrix by UV/ferrioxalate system: Part I. Key process parameter evaluation by response surface methodology, Desalination. 279 (2011) 258–268. https://doi.org/10.1016/j.desal.2011.06.017.

[42] A. Dean, D. Voss, D. Draguljić, Response Surface Methodology, in: 2017: pp. 565–614. https://doi.org/10.1007/978-3-319-52250-0_16.

[43] I. Grčić, D. Vujević, N. Koprivanac, The use of D-optimal design to model the effects of process parameters on mineralization and discoloration kinetics of Fenton-type oxidation, Chem. Eng. J. 157 (2010) 408–419. https://doi.org/10.1016/j.cej.2009.11.030.

[44] S. Rahim Pouran, A.R. Abdul Aziz, W.M.A. Wan Daud, Review on the main advances in photo-Fenton oxidation system for recalcitrant wastewaters, J. Ind. Eng. Chem. 21 (2015) 53–69. https://doi.org/10.1016/j.jiec.2014.05.005.

[45] J. Farias, E.D. Albizzati, O.M. Alfano, Kinetic study of the photo-Fenton degradation of formic acid. Combined effects of temperature and iron

concentration, Catal. Today. 144 (2009) 117–123. https://doi.org/10.1016/j.cattod.2008.12.027.

[46] G. Pliego, J.A. Zazo, J.A. Casas, J.J. Rodriguez, Fate of iron oxalates in aqueous solution: The role of temperature, iron species and dissolved oxygen, J. Environ. Chem. Eng. 2 (2014) 2236–2241. https://doi.org/10.1016/j.jece.2014.09.013.

[47] L.C. Almeida, S. Garcia-Segura, N. Bocchi, E. Brillas, Solar photoelectro-Fenton degradation of paracetamol using a flow plant with a Pt/air-diffusion cell coupled with a compound parabolic collector: Process optimization by response surface methodology, Appl. Catal. B Environ. 103 (2011) 21–30. https://doi.org/10.1016/j.apcatb.2011.01.003.

[48] K.L.E. Kaiser, J.M. Ribo, Photobacterium phosphoreum toxicity bioassay. II. Toxicity data compilation, Toxic. Assess. 3 (1988) 195–237. https://doi.org/10.1002/tox.2540030209.

[49] A. Santos, P. Yustos, A. Quintanilla, F. García-Ochoa, J.A. Casas, J.J. Rodriguez, Evolution of Toxicity upon Wet Catalytic Oxidation of Phenol, Environ. Sci. Technol. 38 (2004) 133–138. https://doi.org/10.1021/es030476t.

ANEXO B. Reaction kinetics formulation with explicit radiation absorption effects of the photo-Fenton degradation of Paracetamol under natural pH conditions

El artículo presentado a continuación ha sido publicado en la revista "*Environmental Science and Pollution Research"*

Reaction kinetics formulation with explicit radiation absorption effects of the photo-Fenton degradation of Paracetamol under natural pH conditions

Bárbara N. Giménez, Agustina V. Schenone, Orlando M. Alfano, Leandro O. Conte

Instituto de Desarrollo Tecnológico para la Industria Química (INTEC), Consejo Nacional de Investigaciones Científicas y Técnicas (CONICET) and Universidad Nacional del Litoral (UNL), Ruta Nacional Nº 168, 3000, Santa Fe, Argentina

Abstract

The degradation of paracetamol (PCT) in aqueous medium using the Fenton and photo-Fenton reactions was investigated. The aim of this research was the development of a kinetic model based on a reaction mechanism, which includes two main intermediates of PCT degradation and the local volumetric rate of photon absorption (LVRPA). Ferrioxalate was used as catalyst and the working pH was adjusted to 5.5 (natural pH). Experimental work was planned through a D-optimal experimental design and performed in a flat plate reactor irradiated by a solar simulator. Hydrogen peroxide (HP) concentration, reaction temperature and radiation level were the operating parameters. The photo-Fenton reaction allowed to reach a minimum relative PCT concentration of 2.01% compared to 5.04% achieved with Fenton reaction. Moreover, the photo-Fenton system required a 50% shorter reaction time and lower HP concentration than in dark conditions (90 min and 189 mg L^{-1} vs. 180 min and 334 mg L^{-1}, respectively). The experimental results were used to estimate the kinetic parameters of the proposed kinetic model employing a non-linear, multi-parameter regression method. The values obtained from the normalized root-mean-square error (14.52, 1.96, 4.36, 13.16, 8.72 % for PCT, benzoquinone, hydroquinone, HP and oxalate, respectively) showed a good agreement between the predicted and experimental data.

Keywords: Acetaminophen, Kinetic modelling, LVRPA, Ferrioxalate complex, Solar simulator, Flat-plate reactor.

Nomenclature

A_1	reparametrized Arrhenius pre-exponential factor
B_1	reparametrized Arrhenius parameter
C	concentration (mg L^{-1})
E	activation energy (kJ mol^{-1})
e^a	local volumetric rate of photon absorption (LVRPA) (Einstein cm^{-3} s^{-1})
k	kinetic constant (M^{-1} s^{-1})
L	reactor length (cm)
q	net radiation flux (Einstein cm^{-2} s^{-1})
R	reaction rate (M s^{-1})
$\Re$	ideal gas constant (kJ mol^{-1} K^{-1})
T	temperature
t	time (s)
V	volume (cm^3)
x	spatial coordinate (cm)
α	molar absorptivity (m^2 mol^{-1})
κ	volumetric absorption coefficient (m^{-1})
Φ	global quantum yield (mol $Einstein^{-1}$)
Υ	specific consumption of the oxidizing agent (mg HP/mg PCT)

Subscripts	
$(C_2O_4)^{2-}$	relative to oxalate ion
BQ	relative to 1,4-benzoquinone
exp	experimental value
$Fe^{2+}(C_2O_4)$	relative to ferrous-oxalate complex
$Fe^{3+}(C_2O_4)_3^{3-}$	relative to ferric-oxalate complex
HP	relative to hydrogen peroxide
HQ	relative to hydroquinone
i	relative to i-th specie
irr	relative to irradiated
mod	model value
PCT	relative to paracetamol
R	relative to photoreactor
W	reactor wall property

λ	dependence on wavelength
Superscripts	
0	initial condition
irr	relative to irradiated
ref	reference value
rel	relative value
T	thermal rate
t	referred to a characteristic reaction time
tot	relative to total treated volume
Special symbol	
$\langle\,\rangle_V$	volume-averaged value

1. Introduction

Anthropogenic water pollution is a global problem. Daily, a large amount of organic and inorganic products (such as pesticides, dyes, chemicals, pharmaceuticals, etc.) coming from different human activities, are released into natural waters, causing a loss in water quality for the consumption and subsistence of living beings (Montagner et al. 2019). These products are known as Emerging Contaminants (ECs), and systematic legal control over their discharge and/or environmental levels has not yet been established for most of them in many industrialized countries of the world (Reichert et al. 2019, European Community 1991). These ECs can be discharged into rivers, i.e. surface waters, which are then drinking water sources (European Community 1998 , European Commission 2018).

Within these ECs, Pharmaceutical and Personal Care Products (PPCPs) are at the top of the pollutants of most concern, since their effects on the environment are very diverse. These compounds can be persistent, bioaccumulative and can cause acute and chronic human and ecotoxicological damage (López-Pacheco et al. 2019). It is generally assumed that the release of pharmaceuticals by manufacturing industries is negligible, as these production facilities employ good manufacturing practices and seek to recover active pharmaceutical ingredients. However, this assumption is not entirely valid, because high concentrations of pharmaceutical have been detected in industrial wastewater (Cardoso et al. 2014; Balbarini et al. 2020). Particularly, in the case of Paracetamol (PCT), an anti-inflammatory and non-steroidal analgesic also known as acetaminophen, the model contaminant chosen for this research work, concentrations between 5.6 and 294 mg L^{-1} were found in effluents from pharmaceutical industries (Badawy et al. 2009; Dalgic et al. 2017; Pal and Thakura 2018). Although PCT can be degraded to some extent by conventional treatments, it can be detected (or its metabolites) in appreciable

concentrations in effluents from treatment plants, with the consequent entry into natural environments (Botero-Coy et al. 2018; Starling et al. 2019).

Currently, Advanced Oxidation Processes (AOPs) have proven to be excellent for degrading highly recalcitrant organic compounds, mainly due to the action of the hydroxyl radical (OH•), which is the second strongest oxidant after fluorine, with a high standard redox potential (E^0 = 2.80 V) (De Oliveira et al. 2015). Among the AOPs, the photo-Fenton process is one of the most efficient treatments (Maniakova et al. 2020). The addition of radiation to the system improves the conventional Fenton process (mixture of Fe^{2+} and H_2O_2), which leads to faster Fe^{2+} regeneration and production of additional amounts of OH• (Ameta et al. 2018). Another improvement that can be made is the possibility of working at a neutral pH by forming iron complexes, as was done in the present work using oxalate as organic ligand (Conte et al. 2019; Ahile et al. 2020). This, in conjunction with the possibility of using solar radiation, greatly reduces operational costs, since expensive lamps and pH adjustments before and after the photo-Fenton process would not be necessary (Clarizia et al. 2017; Conte et al. 2017; Sánchez Pérez et al. 2017).

Several investigations are reported in the literature, in which the photo-Fenton process was applied to degrade PCT in aqueous matrices. Most of these research works are focused on general experimental aspects of the reaction systems, while others are mostly focused on the effect of experimental variables on the degradation rate of PCT (and of the organic compounds formed during the reaction) (Yamal-Turbay et al. 2014; Rad et al. 2015b; Villota et al. 2016; Jamil et al. 2017; Hinojosa Guerra et al. 2019). Integral kinetic models for AOPs are an important step to evaluate the effect of process variables on the reaction system, which is essential for the design and optimization of this process (Alfano and Cassano 2008). Nevertheless, only a few contributions have

addressed the issue of reaction kinetics in their research work. In this sense, two main strategies have been proposed. On the one hand, the empirical models have a completely empirical approach to the process and are based on the use of regression models (Pérez-Moya et al. 2008). The main drawback of this approach is that the developed models do not capture the complexity and non-linear nature of the photochemical processes, and the results obtained cannot be extrapolated when the configuration of the experimental system is changed. The vast majority of research papers presented to date, which have PCT as a contaminant, follow this methodology (Rad et al. 2015a; Shokry et al. 2015; Villota et al. 2018; Audino et al. 2019b). On the other hand, there are models whereby a complete description of the chemical process is made, using information from the different reaction involved and knowledge of the generated intermediates (Castro-Alférez et al. 2017; Sánchez Pérez et al. 2017; Soriano-Molina et al. 2018; Conte et al. 2019). This approach provides an understanding of the intrinsic kinetics of the system, complemented by the radiation modelling within the photoreactor, through the evaluation of the local volumetric rate of photon absorption (LVRPA); this variable is considered fundamental within the study of kinetics and the design of photoreactors (Cassano et al. 1995; Alfano and Cassano 2008; Li Puma et al. 2010). To the best of our knowledge, only few research papers have followed this methodology using PCT as a contaminant (Cabrera Reina et al. 2015; Audino et al. 2019a).

Therefore, the main goal of this research is to develop a kinetic model based on the different reactions involved in the process, which can describe the Fenton and photo-Fenton degradation of PCT at natural pH conditions, employing ferrioxalate as catalyst. Here, the use of this iron complex allows taking advantage of a higher fraction of the visible solar radiation spectrum improving the energy efficiency of the process. Moreover, the estimation of the kinetic parameters is made by solving the mass balances

of the contaminant and the main intermediates, including the explicit radiation absorption effects through the estimation of the LVRPA.

2. Materials and methods

2.1. Reagents and analytical determinations

PCT (Aldrich, 98%) and its reaction intermediates, hydroquinone (HQ) and 1,4-benzoquinone (BQ) (both Fluka, 99%), were analysed by HPLC-UV/Vis (Waters) with a YMC-Triart C18 column (250 x 4.6 mm, 5 μm) at two wavelengths (220 and 243 nm). The eluent was a binary mixture methanol:water (25:75) (flow rate = 1 mL min^{-1}). As soon as the sample was withdrawn, methanol (HPLC grade, Sintogran) was added to prevent further degradation of the PCT, since methanol acts as a hydroxyl radical scavenger. The limits of detection (LOD) for PCT, HQ and BQ were 0.18, 0.21 and 0.38 mg L^{-1}, respectively. To determine total organic carbon (TOC) concentration, a vario TOC cube analyzer (Elementar) was employed, and the samples were previously treated with sodium sulphite and conditioned to avoid alkaline medium in the measurement. Hydrogen peroxide (Cicarrelli, 30%) and total iron were determined using a UV/Vis spectrophotometer (Lambda 35, Perkin-Elmer). For HP a modified iodometric technique was applied (measurement at 350 nm). Both the samples for total Fe (pre-treated with ascorbic acid) and Fe^{2+} were analysed by means of the colorimetric method with 1,10-phenanthroline at 510 nm. Finally, oxalate ion (Oxa, $(C_2O_4)^{2-}$) was determined by ion chromatography-conductivity detector (Waters) with an IonPac AS22 anion exchange column and an IonPac AS22 guard column (Dionex). The eluent consisted of 7.2 mM Na_2CO_3/3.2 mM NaOH (flow rate of 1 mL min^{-1}). The maximum experimental errors were 0.08, 0.15, 0.17, 1.14, 6.72 and 0.26 mg L^{-1} for PCT, HQ, BQ, TOC, HP and Fe, respectively. These global errors were estimated according to the methodology developed by Miller and Miller (2002). As required by this methodology, all measurements were

made in triplicate.

2.2. Experimental device

The employed device was a flat plate reactor of borosilicate glass (69.94 cm^3) placed inside a batch recycling system, which also comprises a storage tank equipped with a pH-meter, a thermometer and a liquid sample valve. A heat exchanger connected to a thermostatic bath and a centrifugal pump complete the system, ensuring constant temperature and good mixing conditions during the reaction. A detailed description of the employed system can be found in Conte et al. (2016). A scheme of the employed device is presented in Fig. 1.

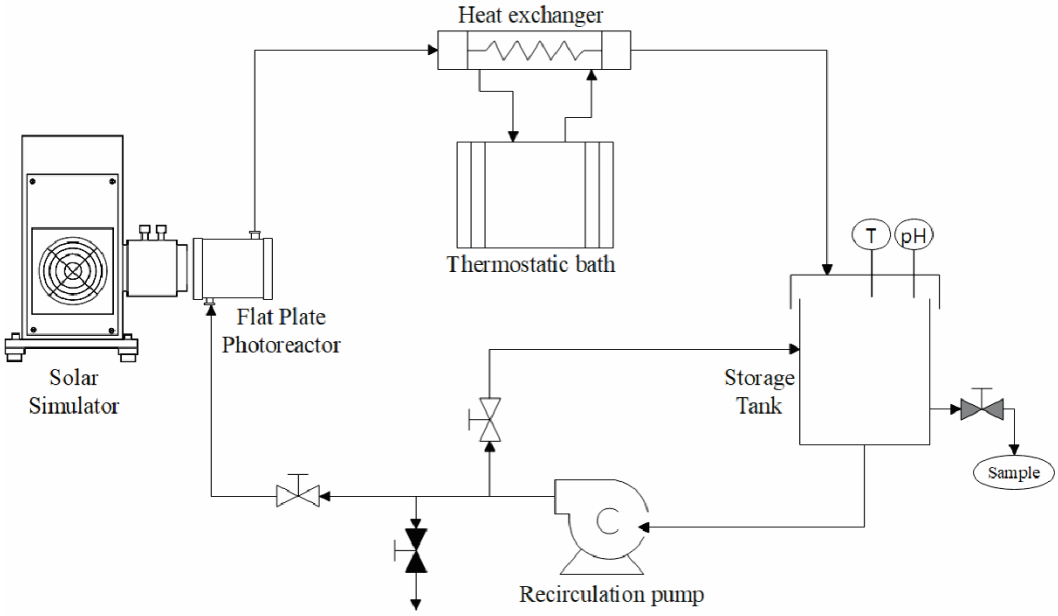

Fig. 1 Diagram of the reactor setting.

In the case of photo-Fenton experiments, the flat plate reactor was irradiated laterally by a solar simulator (Oriel, model 9600). Two different levels of radiation were used, which simulate the natural radiation conditions frequently found in Santa Fe city (Argentina, 31°39’ S, 60°43’ W, 25 m above sea level) (Conte et al. 2017). For this purpose, the following filter combinations were selected: (i) For low radiation level (F0.5D): Water filter + air mass filter AM0 + air mass filter AM1.5 Direct, q_W = 3.64 ×

10^{-8} E cm^{-2} s^{-1}; and (ii) For high radiation level (F1D): Water filter + air mass filter AM0 + air mass filter AM1 Direct, q_W = 6.58 × 10^{-8} E cm^{-2} s^{-1}.

2.3. Procedure

The set of experiments was planned through a D-optimal experimental design, which required a total of 19 experimental runs. The effect of the variables: HP concentration (between 189 and 756 mg L^{-1}), temperature (between 25 and 50 ºC) and level of radiation (F0, F0.5 and F1) on PCT degradation was assessed. Here the F0 radiation level corresponds to dark conditions. For all tests, the PCT concentration was 40 mg L^{-1}, Fe^{3+} concentration was set at 3 mg L^{-1} and oxalate concentration was 47.5 mg L^{-1}, to obtain the molar ratio Oxa/Fe=10. It was decided to set these particular operating parameters considering previous studies (Giménez et al. 2020). The potassium ferrioxalate was prepared by mixing a solution of potassium oxalate (2000 mg L^{-1}) and a solution of iron(III) chloride (500 mg Fe^{3+} L^{-1}) in the adequate quantities. It should be noted that the pH of a solution of 40 mg PCT L^{-1} is 5.5; this value was then selected as the operating pH for all the experimental tests carried out.

The details of these experiments are displayed in Table 1, along with relative concentrations of PCT remaining in the system ($C_{PCT}^{rel,t}$(%)) for each of the characteristic reaction times defined according to the radiation level (F1 = 90 min, F0.5 = 120 min, and F0 = 180 min).

Table 1. Experimental conditions and PCT relative concentration at different characteristic reaction times, for F1D, F0.5D and F0D radiation levels.

Run	T (°C)	HP (mg L^{-1})	$C_{PCT}^{rel,t}$ (%)
	F1		**90 min**
F1_27_756	27	756	18.66
F1_35_378	35	378	2.70
F1_37.5_472.5	37.5	472.5	5.77
F1_40_189	40	189	8.51
F1_50_189	50	189	2.01
F1_50_756	50	756	4.38
	F0.5		**120 min**
F0.5_25_189	25	189	5.42
F0.5_25_378	25	378	10.56
F0.5_26_756	26	756	12.90
F0.5_37.5_314	37.5	314	3.18
F0.5_50_189	50	189	1.74
F0.5_50_756	50	756	5.67
	F0		**180 min**
F0_25_189	25	189	50.09
F0_25_472.5	25	472.5	79.38
F0_37.5_189	37.5	189	8.43
F0_35_378	35	378	7.04
F0_50_334	50	334	5.04
F0_50_472.5	50	472.5	7.06
F0_50_756	50	756	8.80

The relative concentrations of PCT were calculated as follows:

$$C_{PCT}^{rel,t} = \frac{C_{PCT}^{t}}{C_{PCT}^{0}}\ 100\% \quad (1)$$

where C_{PCT}^{t} is the concentration of PCT at a characteristic reaction time (which depends on the radiation level) and C_{PCT}^{0} is the initial PCT concentration.

At the beginning of each experiment, the storage tank was filled with the aqueous

solution containing the PCT and the ferrioxalate complex in adequate concentrations. Once the thermostatic bath reached the set temperature, pH value was adjusted to 5.5 with a concentrated NaOH solution and HP solution was finally added. The first sample was then taken (t = 0 min) and the lamp shutter was removed (in the case of experiments performed under irradiated conditions). The following samples were withdrawn at predefined time intervals (15, 30, 45, 60, 90, 120 and 180 min), with a total reaction time of 180 min. The total volume of treated solution was 3000 cm^3.

3. Kinetic Model

A kinetic model was developed to describe the PCT degradation in an aqueous solution at pH = 5.5 using ferrioxalate as catalyst, including both thermal and photochemical degradation rates in the final kinetic expressions. Table 2 presents the simplified reaction scheme, which is based on different general reaction schemes proposed in the literature (Jeong and Yoon 2005; Pignatello et al. 2006; Simunovic et al. 2011) and on the reaction intermediates (HQ and BQ) generated in the conventional photo-Fenton degradation of PCT (Villota et al. 2016; Audino et al. 2019b; Giménez et al. 2020) and detected in this work.

The use of oxalate-complexed iron as a catalyst complicates the development of a kinetic model that represents the reacting system. Firstly, it must be ensured that the $Fe^{3+}(C_2O_4)_3^{3-}$ and $Fe^{2+}(C_2O_4)$ complexes are the predominant species in the system, since these species have the highest stability constants at the pH under study. Also, the $Fe^{3+}(C_2O_4)_3^{3-}$ complex has the highest molar absorption coefficients in the UV-visible region, compared to the Fe^{3+} aqueous complexes present in the traditional photo-Fenton process at pH = 2.8. In such processes, $Fe^{3+}(C_2O_4)_3^{3-}$ complex has a volumetric absorption coefficient that is approximately 60% larger than the corresponding value for the Fe^{3+} aqueous complexes (Conte et al. 2014).

Table 2. Simplified reaction scheme of PCT photo-Fenton degradation.

N°	Reaction Step	Kinetic Constant (M^{-1} s^{-1})
		$\Phi_{Fe^{2+}(C_2O_4)}$=1.20-1.26 mol Einstein^{-1} [b]
0	$Fe^{3+}(C_2O_4)_3^{3-} \xrightarrow{h\nu} Fe^{2+}(C_2O_4) + CO_2 + 1.5\ (C_2O_4)^{2-}$	$\Phi_{C_2O_4^{2-}}$ [a]
1	$Fe^{3+}(C_2O_4)_3^{3-} + H_2O_2 \xrightarrow{k_1} Fe^{2+}(C_2O_4) + 2\ (C_2O_4)^{2-} + HO^- + HO^\bullet$	$k_1 = exp[A_1 + B_1\ T^*]$* [a]
2	$Fe^{2+}(C_2O_4) + H_2O_2 + \ 2\ (C_2O_4)^{2-} \xrightarrow{k_2} Fe^{3+}(C_2O_4)_3^{3-} + HO^- + HO^\bullet$	k_2=3.10×10^4 [b]
3	$H_2O_2 + HO^\bullet \xrightarrow{k_3} O_2^{-\bullet} + H^+ + H_2O$	k_3=(3.0-4.5)×10^7 [b]
4	$PCT + HO^\bullet \xrightarrow{k_4} HQ$	k_4 [a]
5	$HQ + HO^\bullet \xrightarrow{k_5} BQ$	k_5 [a]
6	$BQ + HO^\bullet \xrightarrow{k_6} products$	k_6 [a]
7	$C_2O_4^{2-} + \ HO^\bullet \xrightarrow{k_7} products$	k_7=7.7×10^6 [b]

[a] values estimated in this research work.

[b] values taken from Conte et al. (2016).

* reparametrized Arrhenius pre-exponential factor: $\boldsymbol{A_1 = ln(k_{\infty,1}) - \frac{E_1}{\Re\, T_{ref}}}$

* reparametrized Arrhenius parameter: $\boldsymbol{B_1 = \frac{E_1}{\Re\, T_{ref}}}$

* $\boldsymbol{T^* = \left(\frac{T - T_{ref}}{T}\right)}$, $T_{ref} = 310\ °K$

For this purpose, equilibrium speciation and photochemical reactivity of the reaction system were evaluated using Visual MINTEQ version 3.1 (USEPA) software, simulating different experimental conditions. Three temperatures (25, 35 and 50 °C) and a pH range from 4.5 to 5.5 were evaluated and, in each case, the concentrations of Fe and Oxa were 3 and 47.5 mg L^{-1}, respectively (optimal value of the molar ratio Oxa/Fe = 10, previously determined). The results showed that the $Fe^{3+}(C_2O_4)_3^{3-}$ complex was the predominant species in the system, with 90.04%, 89.69% and 89.34% of initial Fe molar concentration at 25, 37.5 and 50 °C, respectively. Regarding Fe^{2+}-complex, the proportion of $Fe^{2+}(C_2O_4)$ is 72% compared to 28% associated with free Fe^{2+} (for the entire range of evaluated temperature). Furthermore, in the evaluated pH range, these percentages did not vary significantly for any of the reaction temperatures. Finally, it was found that, under all the assessed conditions, iron was completely dissolved.

In the development of the degradation rate expressions of PCT, HQ, BQ, HP and the iron complexes $Fe^{3+}(C_2O_4)_3^{3-}$ and $Fe^{2+}(C_2O_4)$, the assumptions considered by Conte et al. (2016) were adopted. Additionally, the $Fe^{2+}(C_2O_4)$ is considered the most important Fe^{2+} species in the system. This, taking into account the excess of oxalate and the pH condition used, and the significantly higher reaction rate of the $Fe^{2+}(C_2O_4)$ with the HP compared to that of free Fe^{2+} (Simunovic et al. 2011). Finally, radical–radical termination reactions are neglected compared to the propagation/consumption ones (Alfano and Cassano 1988; Savage 2000; Sterling and McCoy 2001). With these assumptions, the following reaction rates were derived (Table 3), where $\Phi_{Fe^{2+}(C_2O_4)}$ and $\Phi_{C_2O_4^{2-}}$ are the wavelength-averaged global quantum yield, and $e_\lambda^a(x,t)$ is the spectral local volumetric rate of photon absorption (LVRPA).

Table 3. Reaction rate equations for each evaluated species.

$R_{PCT}(x,t) = -k_4 C_{PCT} C_{HO\bullet}$	(2)
$R_{HP}(x,t) = (-k_3 C_{HO\bullet} - k_2 C_{Fe^{2+}(C_2O_4)} - k_1 C_{Fe^{3+}(C_2O_4)_3^{3-}}) C_{HP}$	(3)
$R_{Fe^{2+}(C_2O_4)}(x,t) = (k_1 C_{Fe^{3+}(C_2O_4)_3^{3-}} - k_2 C_{Fe^{2+}(C_2O_4)}) C_{HP} + \Phi_{Fe^{2+}(C_2O_4)} \Sigma_\lambda e_\lambda^a(x,t)$	(4)
$R_{Fe^{3+}(C_2O_4)_3^{3-}}(x,t) = -R_{Fe^{2+}(C_2O_4)}(x,t)$	(5)
$R_{HQ}(x,t) = (k_4 C_{PCT} - k_5 C_{HQ}) C_{HO\bullet}$	(6)
$R_{BQ}(x,t) = (k_5 C_{HQ} - k_6 C_{BQ}) C_{HO\bullet}$	(7)
$R_{C_2O_4^{2-}}(x,t) = -k_7 C_{C_2O_4^{2-}} C_{HO\bullet} - \Phi_{C_2O_4^{2-}} \Sigma_\lambda e_\lambda^a(x,t)$	(8)
$R_{HO\bullet}(x,t) = (k_1 C_{Fe^{3+}(C_2O_4)_3^{3-}} + k_2 C_{Fe^{2+}(C_2O_4)}) C_{HP} - (k_3 C_{HP} + k_4 C_{PCT} + k_5 C_{HQ} + k_6 C_{BQ} + k_7 C_{C_2O_4^{2-}}) C_{HO\bullet}$	(9)

Then, applying the steady-state approximation (SSA) to the radical HO• (eq. (9)), we obtain:

$$(k_1 C_{Fe^{3+}(C_2O_4)_3^{3-}} + k_2 C_{Fe^{2+}(C_2O_4)}) C_{HP} - (k_3 C_{HP} + k_4 C_{PCT} + k_5 C_{HQ} + k_6 C_{BQ} + k_7 C_{C_2O_4^{2-}}) C_{HO\bullet} = 0 \quad (10)$$

Finally, solving eq. (10) one can write:

$$C_{HO\bullet} = \frac{(k_1 C_{Fe^{3+}(C_2O_4)_3^{3-}} + k_2 C_{Fe^{2+}(C_2O_4)}) C_{HP}}{k_3 C_{HP} + k_4 C_{PCT} + k_5 C_{HQ} + k_6 C_{BQ} + k_7 C_{C_2O_4^{2-}}} \quad (11)"$$

4. Photoreactor model

4.1. Mass balances

The mass balance equations for each specie (PCT, HP, HQ, BQ, $Fe^{2+}(C_2O_4)$, $Fe^{3+}(C_2O_4)_3^{3-}$ and $(C_2O_4)^{2-}$) are given by the following set of first order, ordinary differential equations in matrix notation:

$$\frac{d\boldsymbol{C}(t)}{dt} = \boldsymbol{R^T}(t) + \frac{V_{irr}}{V_{tot}} \boldsymbol{R^{irr}}(x,t) \quad (12)$$

where the initial conditions are:

$$\mathbf{C} = \mathbf{C}^0 \qquad t = 0 \quad (13)$$

Eqs. (2-8) can be replaced in eq. (12) to obtain the ODEs system (eq. 14 - 20) to

be numerically solved applying the initial conditions shown in eq. (13).

$$\frac{dC_{PCT}(t)}{dt} = -k_4 C_{PCT} C_{HO\bullet} \quad (14)$$

$$\frac{dC_{HP}(t)}{dt} = (-k_3 C_{HO\bullet} - k_2 C_{Fe^{2+}(C_2O_4)} - k_1 C_{Fe^{3+}(C_2O_4)_3^{3-}}) C_{HP} \quad (15)$$

$$\frac{dC_{C_2O_4^{2-}}(t)}{dt} = -k_7 C_{C_2O_4^{2-}} C_{HO\bullet} - \frac{V_{irr}}{V_{tot}} \Phi_{C_2O_4^{2-}} \Sigma_\lambda e_\lambda^a(x,t) \quad (16)$$

$$\frac{dC_{Fe^{2+}(C_2O_4)}(t)}{dt} = (k_1 C_{Fe^{3+}(C_2O_4)_3^{3-}} - k_2 C_{Fe^{2+}(C_2O_4)}) C_{HP} + \frac{V_{irr}}{V_{tot}} \overline{\Phi}_{Fe^{2+}(C_2O_4)} \Sigma_\lambda e_\lambda^a(x,t) \quad (17)$$

$$\frac{dC_{Fe^{3+}(C_2O_4)_3^{3-}}(t)}{dt} = -\frac{dC_{Fe^{2+}(C_2O_4)}(t)}{dt} \quad (18)$$

$$\frac{dC_{HQ}(t)}{dt} = (k_4 C_{PCT} - k_5 C_{HQ}) C_{HO\bullet} \quad (19)$$

$$\frac{dC_{BQ}(t)}{dt} = (k_5 C_{HQ} - k_6 C_{BQ}) C_{HO\bullet} \quad (20)$$

4.2.Radiation field

To solve the ODE system, it is required to calculate the average of LVRPA over the reactor volume, so it is necessary to know the radiation field inside the photoreactor. This radiation variable will depend on the spatial distribution of photons absorbed within the flat plate reactor and, consequently, on the photochemical and geometric characteristics of the solar simulator-reactor system. In a previous paper, a three-dimensional radiation model was proposed and experimentally verified to evaluate the spectral LVRPA in a stirred tank photoreactor. Variations in the radiation field associated with the radial and angular coordinates were shown to be negligible for certain optical and geometric parameters (Alfano et al. 1985). Consequently, the following one-dimensional radiation model was proposed to calculate the spectral LVRPA as a function of the spatial coordinate (x) and the reaction time (t):

$$e_\lambda^a(x,t) = q_{W,\lambda} \kappa_\lambda(t) \, exp\left[-\kappa_{T,\lambda}(t) x\right] \quad (21)$$

Here, $q_{W,\lambda}$ is the discretized spectral radiation flux incident on the reactor wall (quantified

experimentally), κ_λ is the volumetric absorption coefficient of the reacting species and $\kappa_{T,\lambda}$ is the volumetric absorption coefficient of the medium.

To obtain the term $e_\lambda^a(x,t)$ to be finally used in the numerical solution, it is first necessary to integrate eq. (21) over the entire range of the spectrum ($\lambda_{min} = 300\ nm \leq \lambda \leq \lambda_{max} = 500\ nm$) to get the polychromatic LVRPA ($\sum_\lambda e_\lambda^a(x,t)$), since the output power of the solar simulator and the optical properties of the species are functions of the wavelengths. Second, and considering that the cross-section of the photoreactor is constant, the polychromatic LVRPA must be averaged over the entire irradiated volume, thus obtaining the following expression:

$$\langle \sum_\lambda e_\lambda^a(x,t) \rangle_{V_{irr}} = \frac{\kappa_\lambda(t) \sum_\lambda q_{W,\lambda} \left[1 - exp\left(-\kappa_{T,\lambda}(t) L_R\right)\right]}{L_R \kappa_{T,\lambda}} \tag{22}$$

where L_R is the length of the photoreactor.

Finally, considering that (i) the dominant species in system is the $Fe^{3+}(C_2O_4)_3^{3-}$ complex and (ii) the radiation absorption by H_2O_2 and ferrous complexes are negligible for wavelengths greater than 300 nm, the following equation is obtained:

$$\langle \sum_\lambda e_\lambda^a(x,t) \rangle_{V_{irr}} = \frac{1}{L_R} \sum_\lambda q_{W,\lambda} \left[1 - exp\left(-\alpha_{Fe^{3+}(C_2O_4)_3^{3-},\lambda} C_{Fe^{3+}(C_2O_4)_3^{3-}}(t) L_R\right)\right] \tag{23}$$

4.3.Kinetic parameter estimation

A nonlinear multi-parameter optimization procedure was applied in order to minimize the differences between the predicted concentrations by the theoretical model and the corresponding experimental values, for each considered species. Firstly, the obtained ODE system was numerically solved with GNU Octave (Version 5.2.0). Consequently, to estimate the parameters A_1, B_1, k_4, k_5, k_6 and $\Phi_{C_2O_4^{2-}}$, a weighted

nonlinear least-square objective function minimized with the Newton Gauss-Marquardt algorithm was used. This algorithm searched for the values that minimize the sum of squared differences between predicted and experimental PCT, BQ, HQ, HP and $(C_2O_4)^{2-}$ concentrations. It is worth mentioning that all unknown kinetic parameters were estimated/optimized simultaneously by using the complete set of experimental runs (see Table 1). Additionally, the minimum and maximum values of the kinetic parameters reported by the specific literature were taken into account (Buxton et al. 1988; Lee et al. 2003; Jeong and Yoon 2005; Simunovic et al. 2011; De Laurentiis et al. 2014).

Then, the normalized root-mean-square error (NRMSE, eq. (24)) was used to evaluate the differences between the experimental concentrations of the reactive species and the corresponding values of the proposed model.

$$NRMSE_i = \frac{\sqrt{\frac{\left(C_{i,exp} - C_{i,mod}\right)^2}{n}}}{C_i^0} * 100\% \qquad (24)$$

where $C_{i,exp}$ and $C_{i,mod}$ are the experimental data and those predicted by the model, respectively, n is the total number of samples, and C_i^0 is the initial concentration of each specie, except for HQ and BQ, where this concentration corresponds to PCT initial concentration.

5. Results and discussion

5.1. Experimental results

In terms of the achieved degradation levels (see Table 1), it can be observed that for F1 a $C_{PCT}^{rel,90}$ less than 20% was obtained in all the experiments in just 90 min of reaction (characteristic time chosen for this radiation level). The minimum concentration ($C_{PCT}^{rel,90}$ = 2.01%) was reached for conditions HP = 189 mg L^{-1} and T = 50°C, in which the reaction rate was the maximum observed. On the other hand, the characteristic time

required in the case of low radiation level (F0.5) was 120 min. The lower $C_{PCT}^{rel,120}$ under this radiation level was found in the assay F0.5_50_189 ($C_{PCT}^{rel,120}$ = 1.74%). Conversely, and for the entire range of T and HP, the conversions obtained in dark conditions (F0) were always lower than those achieved under irradiated ones. Furthermore, the characteristic time (maximum duration of the experimental test: 180 min) was 1.5 times higher than the needed time for low radiation conditions. Therefore, the significant effect of radiation on the process efficiency should be highlighted.

In the photo-Fenton degradation process of organic compounds, it is also important to evaluate the HP consumption during the treatment (economic relevance). Therefore, a useful parameter to evaluate the HP consumption is the Specific Consumption of the Oxidizing Agent ($Y_{HP/PCT}^{t}$) (Conte et al. 2019), calculated with eq. (25) at each characteristic reaction time previously defined for each radiation level.

$$Y_{HP/PCT}^{t} = \frac{C_{HP}^{0} - C_{HP}^{t}}{C_{PCT}^{0} - C_{PCT}^{t}} \quad (25)$$

Here, C_{HP}^{0} and C_{PCT}^{0} represent the initial concentrations of HP and PCT, respectively, and C_{HP}^{t} and C_{PCT}^{t} represent the concentrations of HP and PCT (respectively) at a given characteristic reaction time, all in mg L^{-1} units.

The experimental values for $C_{PCT}^{rel,t}$ and $Y_{HP/PCT}^{t}$, calculated as a function of the applied reaction conditions for F0 and F0.5 radiation levels, are presented in Fig. 2.

Firstly, it should be highlighted that in the case of dark conditions, low $C_{PCT}^{rel,180}$ values (less than 10%) were achieved only at high temperatures (T = 50° C). For low T (25 C°), $C_{PCT}^{rel,t}$ values higher than 50% were observed at 180 min (F0_25_189 and F0_25_472.5, Table 1). Therefore, it is necessary to emphasize the significance of the temperature in the process, since an increase in its value directly increases the kinetic constant k_1 (Table 2, reaction N°1). This reaction is the critical initiation step (OH• radical

generation) in the degradation process for dark conditions (Fenton).

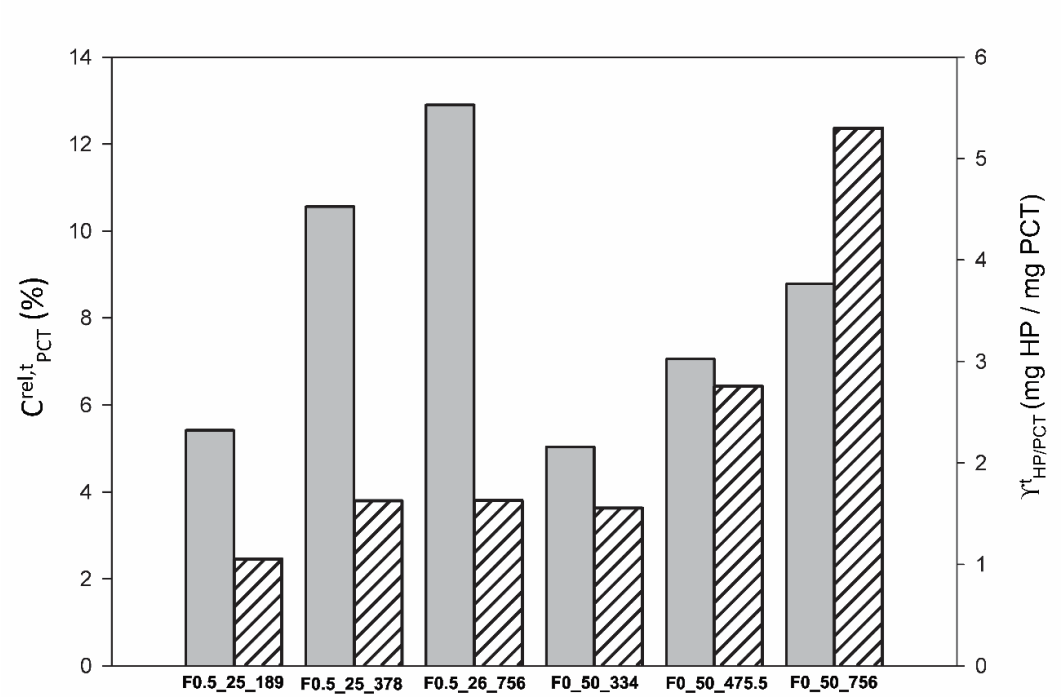

Fig. 2 Relative concentration of PCT (grey bars) and HP consumption (striped bars) for low radiation level (F0.5, t = 120 min) and dark conditions (F0, t = 180 min) as a function of the applied reaction conditions

On the other hand, in the case of both conditions (F0 and F0.5), a substantial increase in the $C_{PCT}^{rel,t}$ was observed when the dose of oxidizing agent was augmented (F0: from 334 to 756 mg L^{-1}, and F0.5: from 189 to 756 mg L^{-1}). Here, an excess of HP produces a scavenging effect consuming hydroxyl radicals (Reaction N°3, Table 2) and decreasing the PCT degradation rate (Reaction N°4, Table 2). Also, an excess of HP accelerates it self-decomposition (eq. (26)), producing O_2 and H_2O, but not reactive radicals (Pignatello et al. 2006). For these reasons, the efficiency of the process decreases.

$$2H_2O_2 \rightarrow 2H_2O + O_2 \quad (26)$$

In the analysis of the $\Upsilon^{t}_{HP/PCT}$ results (Fig. 2, right axis), it can be seen that for dark conditions, a significant increase in its values was reached when the concentration of HP was higher (excess of oxidizing agent in the system). The maximum value ($\Upsilon^{180}_{HP/PCT}$ = 5.3 mg HP/mg PCT) was obtained at the higher HP concentration (756 mg L^{-1}). On the

contrary, in the case of F0.5 tests, the estimated values of HP consumption were substantially lower (less than 1.63 mg HP/mg PCT (F0.5_26_756)). The higher HP consumption (3.2 mg HP/mg PCT) was observed at the highest dose of HP (F0.5_50_756, result not shown). On the other hand, the $\Upsilon^{90}_{HP/PCT}$ values calculated for F1 (high radiation level) were lower than 1.75 mg HP/ mg PCT for all the tested conditions, except for high doses of hydrogen peroxide (results not shown). At this point, it is worth noting the greater effectiveness in the use of reagents (expressed in terms of consumption of oxidizing agent) achieved in the irradiated tests compared to the dark ones. Therefore, this operating variable is of great significance in the economic study of the process.

5.2. Model results

Through a nonlinear multi-parameter optimization procedure the values of the kinetic parameters and global quantum yield corresponding to reaction steps N° 0, 1, 4, 5 and 6 in Table 2 were estimated and are shown in Table 4. Additionally, the NRMSE values were calculated for each evaluated species, and the obtained results were: 14.52, 1.96, 4.36, 13.16, 8.72 % for PCT, BQ, HQ, HP and Oxa, respectively.

Table 4. Estimated values of the kinetic parameters.

$\Phi_{C_2O_4^{2-}}$ (mol Einstein^{-1})	0.50
A_1 (dimensionless)	-2.04
B_1 (dimensionless)	8.65
k_4 (M^{-1} s^{-1})	1.30×10^9
k_5 (M^{-1} s^{-1})	5.89×10^9
k_6 (M^{-1} s^{-1})	1.20×10^{10}

Predicted and experimental results for Fenton and photo-Fenton experiments are

represented in Fig. 3. It shows 3-D plots of $C_{PCT}^{rel,t}$ as a function of T and HP concentration, for dark (Fig. 3a) and high radiation level (Fig. 3b) systems.

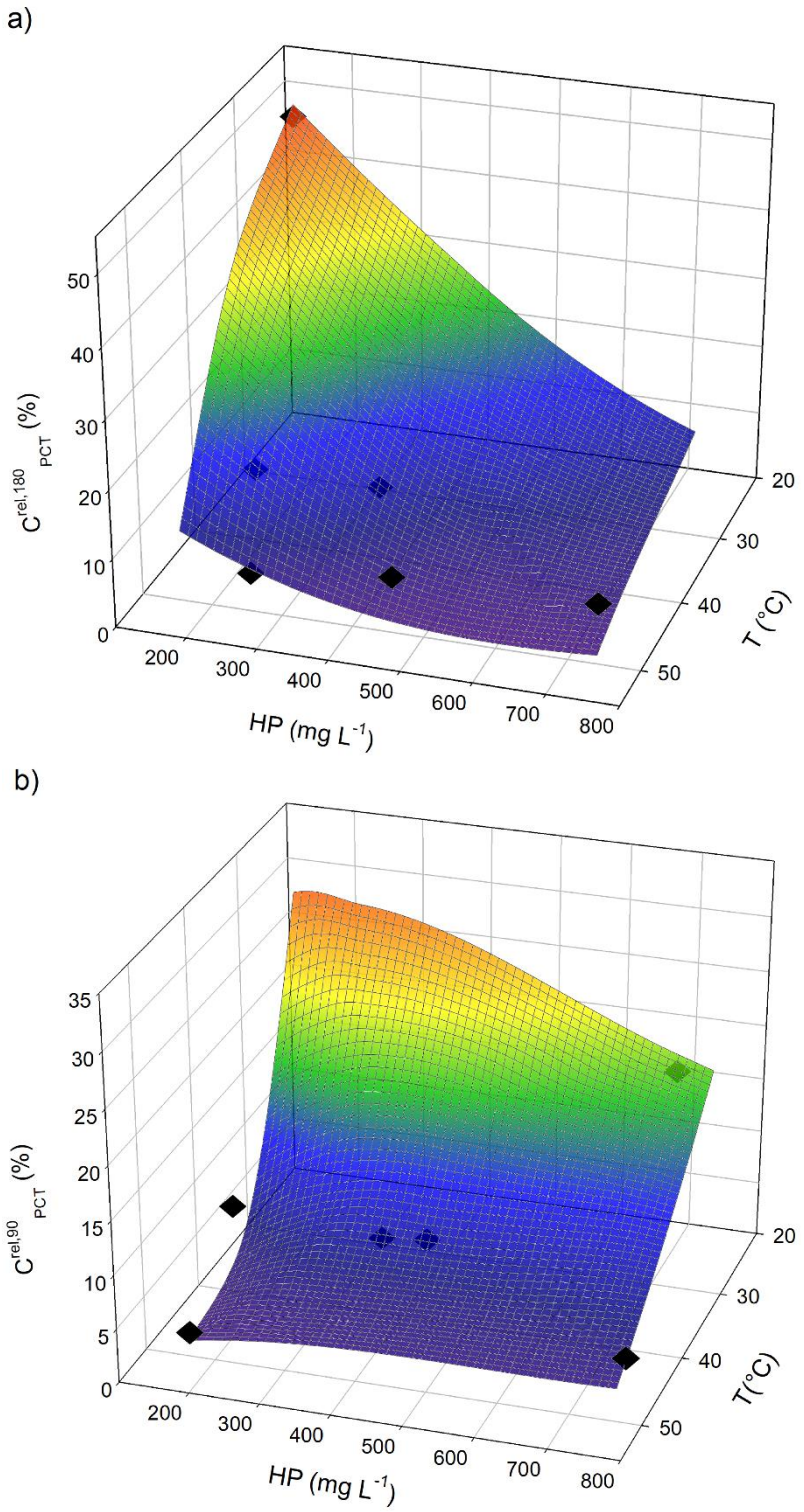

Fig. 3 Predicted (surfaces) and experimental (symbols) $C_{PCT}^{rel,t}$ as a function of reaction temperature (T) and hydrogen peroxide concentration (HP). (a) F0 (t = 180 min); (b) F1 (t = 90 min)

Firstly, the significant influence of the radiation level on the process efficiency is highlighted. For the entire range of experimental conditions (Table 1), the $C_{PCT}^{rel,t}$ values were always lower for the irradiated system. Furthermore, for a high radiation level, the characteristic time was reduced by 50% compared to the time needed when the Fenton reaction was applied (90 min vs. 180 min). Additionally, it is worth mentioning that for the dark system, $C_{PCT}^{rel,180}$ values of less than 10% were only reached when temperatures higher than 37.5 °C were assessed (for all tested HP concentrations). Once again, the significance of the temperature in the Fenton process is highlighted. Finally, it can be observed that for low temperatures, the HP concentration has a positive effect on PCT degradation, being this effect more important for the Fenton reaction.

Fig. 4 shows the experimental data and the kinetic model predictions of PCT, HQ, BQ, HP and Oxa relative concentrations as a function of time, for low and high radiation levels.

Firstly, it should be noted that although for both evaluated conditions in Fig. 4 $C_{PCT}^{rel,t}$ values lower than 5% were observed, the test performed with a lower radiation level (F0.5) required a longer reaction time (120 min vs. 60 min). Moreover, results shown at low radiation levels needed a dosage of oxidizing agent 4 times higher (756 mg L^{-1} vs. 189 mg L^{-1}).

It should also be mentioned that both analytically identified reaction intermediaries (HQ and BQ) were completely removed (not detected) only in the experiment with high radiation (Fig. 4b). This is an important aspect taking into account the associated toxicity of both intermediate compounds (EC_{50} at 15 min for *V. fischeri*: Hydroquinone 0.041 mg L^{-1} and 1,4-Benzoquinone 0.1 mg L^{-1}) (Santos et al. 2004).

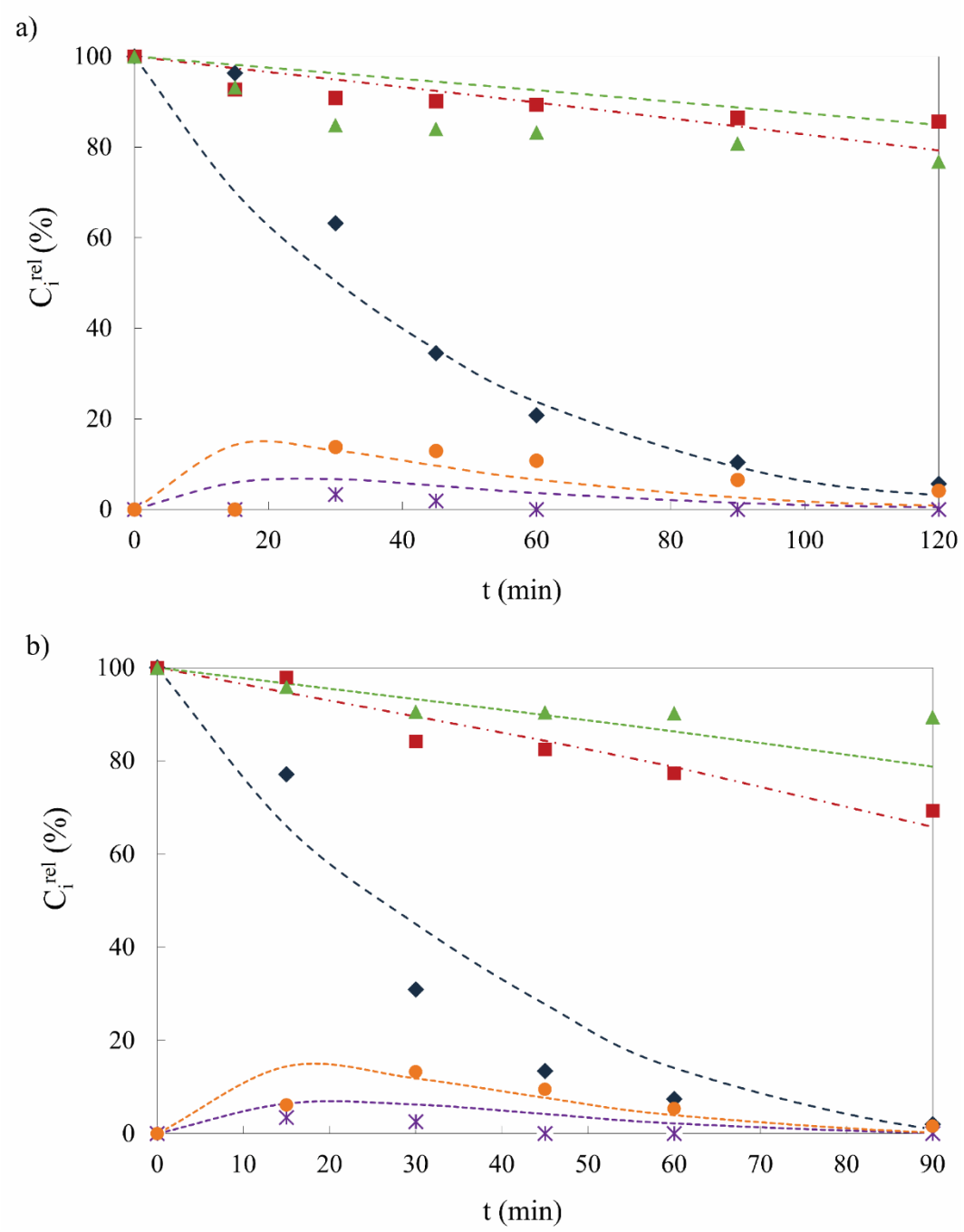

Fig. 4 Model and experimental results for PCT, HP, Oxa, HQ and BQ relative concentrations for pH=5.5. (a) F0.5, T = 50ºC, HP = 756 mg L^{-1}; (b) F1, T = 50ºC, HP = 189 mg L^{-1}. Keys: continuous lines: model results, and (♦) PCT, (■) HP, (▲) Oxa, (●) HQ, and (*) BQ, experimental results

Finally, in relation to the mineralization degree reached at the end of the reaction (t = 180 min), it was observed that the highest radiation level greatly improves the degree of TOC conversion achieved. This value varied from a maximum of 17.04% in the case of Fenton test (F0_35_378) to a TOC conversion that reached 36.84% and 22.50% in case

of experiments carried out at high (F1_35_378) and low (F0.5_25_378) radiation levels, respectively, considering tests performed at similar conditions (data not shown).

Here it is important to mention that oxalate ion contributes to TOC level in the reaction medium, but it is essential to maintain iron soluble in this particular system at pH 5.5. Hence, complete degradation of the oxalate and, therefore, total mineralization in the reaction system is not desirable.

6. Conclusions

A theoretical and experimental study was presented for the photo-Fenton degradation of the pharmaceutical PCT under pH conditions close to neutrality, using an iron complex (ferrioxalate) and a solar simulator as iron and radiation sources, respectively. The proposed kinetic model explicitly took into account the effects of radiation absorption rate on the kinetic expressions of the pollutant degradation rates.

The effect of three operating parameters (level of radiation, reaction temperature and concentration of hydrogen peroxide) on the performance of this reaction system was evaluated. Regarding the radiation level and its impact on the relative concentration of PCT remaining in the system, it was observed that when the solution was irradiated, the characteristic time for high (F1) and low (F0.5) radiation levels was reduced by 50% and 33.3% (respectively) in relation to the characteristic time required by the Fenton reaction (F0). Likewise, for the entire range of experimental conditions, the $C_{PCT}^{rel,t}$ values in dark conditions were always higher than those achieved when the system was irradiated. Also, in relation to the specific consumption of the oxidizing agent ($Y_{HP/PCT}^{t}$), it was observed that the absence of radiation produced the highest values of $Y_{HP/PCT}^{t}$ in the system. On the contrary, the highest level of radiation yielded the lowest $Y_{HP/PCT}^{t}$ values, for all evaluated conditions (except for high doses of hydrogen peroxide).

Concerning the other two operating parameters, it should first be highlighted that

temperature, in the evaluated range, always had a positive effect on the system, especially in dark conditions where large conversions were only achieved at high temperatures. In contrast, the use of very high doses of HP concentration had a negative effect on PCT degradation rates. This negative effect was also evident when the specific consumption of the oxidizing agent was analysed.

A kinetic model capable of satisfactorily represent the reaction system was developed employing a weighted nonlinear multi-parameter optimization procedure to estimate the unknown parameters: the kinetic constants and the ferrioxalate global quantum yield (A_1, B_1, k_4, k_5, k_6 and $\Phi_{C_2O_4^{2-}}$). Furthermore, the proposed model successfully incorporated the effect of the local volumetric rate of photon absorption on the photoreactor behaviour. Finally, based on the values of the normalized root-mean-square error (14.52, 1.96, 4.36, 13.16, 8.72 % for PCT, BQ, HQ, HP and Oxa, respectively), it was concluded that the model adequately predicted the concentrations of the reactive species (PCT, BQ, HQ, HP and $(C_2O_4)^{2-}$) as a function of time.

Therefore, the proposed kinetic model and the intrinsic kinetic constants obtained in this work can be used in the analysis and design of PCT degradation in large-scale photo-Fenton reactors.

Declarations

Ethics approval, consent to participate and consent for publication

Not applicable

Authors' contributions

All persons who meet authorship criteria are listed as authors, and all authors certify that they have participated sufficiently in the work to take public responsibility for the content. BNG, AVS, OMA and LOC contributed to the study conception and design. BNG, AVS

and LOC performed the experiments and data collection. BNG, AVS and LOC analysed all the data and made theoretical calculations. BNG, AVS and LOC wrote the main manuscript text and prepared the figures and tables. AVS, OMA and LOC obtained funding for the research. BNG, AVS, OMA and LOC reviewed the manuscript, made amendments and contributed with their expertise. All authors read and approved the final manuscript.

Funding information and Acknowledgments

The authors are grateful to Universidad Nacional del Litoral (UNL, CAI+D PJ 50020150100028LI, CAI+D PJ 0020150100093LI and PICT N° 2018-1415), Consejo Nacional de Investigaciones Científicas y Técnicas (CONICET, PIP 2015-2017 GI), and Agencia Nacional de Promoción Científica y Tecnológica (ANPCyT, PICT N° 2015-2651 and PICT N° 2017-0744) for financial support. Bárbara N. Giménez, particularly acknowledges to Consejo Nacional de Investigaciones Científicas y Técnicas (CONICET) for the PhD scholarship.

Competing interests

The authors declare that they have no competing interests.

Availability of data and materials

The datasets generated and analysed during the current study are available from the corresponding author on reasonable request.

References

Ahile UJ, Wuana RA, Itodo AU, et al (2020) A review on the use of chelating agents as an alternative to promote photo-Fenton at neutral pH: Current trends, knowledge gap and future studies. Sci Total Environ 710:134872. https://doi.org/10.1016/j.scitotenv.2019.134872

Alfano OM, Cassano AE (1988) Modeling of a Gas-Liquid Tank Photoreactor Irradiated from the Bottom. 1. Theory. Ind Eng Chem Res 27:1087–1095. https://doi.org/10.1021/ie00079a001

Alfano OM, Cassano AE (2008) Photoreactor Modeling: Applications to Advanced Oxidation Processes. Int J Chem React Eng 6:. https://doi.org/10.2202/1542-6580.1617

Alfano OM, Romero RL, Casano AE (1985) A cylindrical photoreactor irradiated from the bottom-I. Radiation flux density generated by a tubular source and a parabolic reflector. Chem Eng Sci 40:2119–2127. https://doi.org/10.1016/0009-2509(85)87030-5

Ameta R, Chohadia AK, Jain A, Punjabi PB (2018) Fenton and Photo-Fenton Processes. In: Advanced Oxidation Processes for Wastewater Treatment: Emerging Green Chemical Technology. Elsevier Inc., pp 49–87

Audino F, Conte LO, Schenone AV, et al (2019a) A kinetic study for the Fenton and photo-Fenton paracetamol degradation in an annular photoreactor. Environ Sci Pollut Res 26:4312–4323. https://doi.org/10.1007/s11356-018-3098-4

Audino F, Santamaria JMT, Del Valle Mendoza LJ, et al (2019b) Removal of paracetamol using effective advanced oxidation processes. Int J Environ Res Public Health 16:. https://doi.org/10.3390/ijerph16030505

Badawy MI, Wahaab RA, El-Kalliny AS (2009) Fenton-biological treatment processes for the removal of some pharmaceuticals from industrial wastewater. J Hazard Mater 167:567–574. https://doi.org/10.1016/j.jhazmat.2009.01.023

Balbarini N, Frederiksen M, Rønde V, et al (2020) Assessing the Transport of Pharmaceutical Compounds in a Layered Aquifer Discharging to a Stream. Groundwater 58:208–223. https://doi.org/10.1111/gwat.12904

Botero-Coy AM, Martínez-Pachón D, Boix C, et al (2018) 'An investigation into the occurrence and removal of pharmaceuticals in Colombian wastewater.' Sci Total Environ 642:842–853. https://doi.org/10.1016/j.scitotenv.2018.06.088

Buxton G V., Greenstock CL, Helman WP, Ross AB (1988) Critical Review of rate constants for reactions of hydrated electrons, hydrogen atoms and hydroxyl radicals (· OH/· O− in Aqueous Solution. J Phys Chem Ref Data 17:513–886. https://doi.org/10.1063/1.555805

Cabrera Reina A, Santos-Juanes L, García Sánchez JL, et al (2015) Modelling the photo-Fenton oxidation of the pharmaceutical paracetamol in water including the effect of photon absorption (VRPA). Appl Catal B Environ 166–167:295–301. https://doi.org/10.1016/j.apcatb.2014.11.023

Cardoso O, Porcher J, Sanchez W (2014) Chemosphere Factory-discharged pharmaceuticals could be a relevant source of aquatic environment contamination : Review of evidence and need for knowledge. Chemosphere 115:20–30. https://doi.org/10.1016/j.chemosphere.2014.02.004

Cassano AE, Martín CA, Brandi RJ, Alfano OM (1995) Photoreactor Analysis and Design: Fundamentals and Applications. Ind Eng Chem Res 34:2155–2201. https://doi.org/10.1021/ie00046a001

Castro-Alférez M, Polo-López MI, Marugán J, Fernández-Ibáñez P (2017) Mechanistic modeling of UV and mild-heat synergistic effect on solar water disinfection. Chem Eng J 316:111–120. https://doi.org/10.1016/j.cej.2017.01.026

Clarizia L, Russo D, Di Somma I, et al (2017) Homogeneous photo-Fenton processes at near neutral pH: A review. Appl Catal B Environ 209:358–371. https://doi.org/10.1016/j.apcatb.2017.03.011

Conte LO, Querini P, Albizzati ED, Alfano OM (2014) Photonic and quantum

efficiencies for the homogeneous photo-Fenton degradation of herbicide 2,4-D using different iron complexes. J Chem Technol Biotechnol 89:1967–1974. https://doi.org/10.1002/jctb.4284

Conte LO, Schenone A V., Alfano OM (2017) Ferrioxalate-assisted solar photo-Fenton degradation of a herbicide at pH conditions close to neutrality. Environ Sci Pollut Res 24:6205–6212. https://doi.org/10.1007/s11356-016-6400-3

Conte LO, Schenone A V., Alfano OM (2016) Photo-Fenton degradation of the herbicide 2,4-in aqueous medium at pH conditions close to neutrality. J Environ Manage 170:60–69. https://doi.org/10.1016/j.jenvman.2016.01.002

Conte LO, Schenone A V., Giménez BN, Alfano OM (2019) Photo-Fenton degradation of a herbicide (2,4-D) in groundwater for conditions of natural pH and presence of inorganic anions. J Hazard Mater 113–120. https://doi.org/10.1016/j.jhazmat.2018.04.013

Dalgic G, Turkdogan FI, Yetilmezsoy K, Kocak E (2017) Treatment of Real Paracetamol. Chem Ind Chem Eng Q 23:177–186

De Laurentiis E, Prasse C, Ternes TA, et al (2014) Assessing the photochemical transformation pathways of acetaminophen relevant to surface waters: Transformation kinetics, intermediates, and modelling. Water Res 53:235–248. https://doi.org/10.1016/j.watres.2014.01.016

De Oliveira AMD, Maniero MG, Guimarães JR (2015) Lomefloxacin degradation: Antimicrobial activity, toxicity and byproducts. J Adv Oxid Technol 18:211–220. https://doi.org/10.1515/jaots-2015-0205

European Commission (2018) Proposal for a Directive of the European Parliament and of the Council on the quality of water intended for human consumption (recast). https://eur-lex.europa.eu/resource.html?uri=cellar:8c5065b2-074f-11e8-b8f5-

01aa75ed71a1.0016.02/DOC_1&format=PDF (accessed October 31, 2020)

European Community (1991) Council Directive 91/271/EEC of 21 May 1991 concerning urban waste-water treatment. Off J Eur Communities. http://data.europa.eu/eli/dir/1991/271/oj (accessed October 31, 2020)

European Community (1998) Council Directive 98/83/EC of 3 November 1998 on the quality of water intended for human consumption. Off J Eur Communities. http://data.europa.eu/eli/dir/1998/83/oj (accessed October 31, 2020)

Giménez BN, Conte LO, Alfano OM, Schenone A V. (2020) Paracetamol removal by photo-Fenton processes at near-neutral pH using a solar simulator: Optimization by D-optimal experimental design and toxicity evaluation. J Photochem Photobiol A Chem 397:112584. https://doi.org/10.1016/j.jphotochem.2020.112584

Hinojosa Guerra MM, Oller Alberola I, Malato Rodriguez S, et al (2019) Oxidation mechanisms of amoxicillin and paracetamol in the photo-Fenton solar process. Water Res 156:232–240. https://doi.org/10.1016/j.watres.2019.02.055

Jamil TS, Roland H, Michael H, Jens-Uwe R (2017) Homogeneous photocatalytic processes for degradation of some endocrine disturbing chemicals under UV irradiation. J Water Process Eng 18:159–168. https://doi.org/10.1016/j.jwpe.2017.04.005

Jeong J, Yoon J (2005) pH effect on OH radical production in photo/ferrioxalate system. Water Res 39:2893–2900. https://doi.org/10.1016/j.watres.2005.05.014

Lee Y, Jeong J, Lee C, et al (2003) Influence of various reaction parameters on 2,4-D removal in photo/ferrioxalate/H2O2 process. Chemosphere 51:901–912. https://doi.org/10.1016/S0045-6535(03)00044-4

Li Puma G, Puddu V, Tsang HK, et al (2010) Photocatalytic oxidation of multicomponent mixtures of estrogens (estrone (E1), 17β-estradiol (E2), 17α-ethynylestradiol (EE2)

and estriol (E3)) under UVA and UVC radiation: Photon absorption, quantum yields and rate constants independent of photon absorp. Appl Catal B Environ 99:388–397. https://doi.org/10.1016/j.apcatb.2010.05.015

López-Pacheco IY, Silva-Núñez A, Salinas-Salazar C, et al (2019) Anthropogenic contaminants of high concern: Existence in water resources and their adverse effects. Sci Total Environ 690:1068–1088. https://doi.org/10.1016/j.scitotenv.2019.07.052

Maniakova G, Kowalska K, Murgolo S, et al (2020) Separation and Puri fi cation Technology Comparison between heterogeneous and homogeneous solar driven advanced oxidation processes for urban wastewater treatment : Pharmaceuticals removal and toxicity. Sep Purif Technol 236:116249. https://doi.org/10.1016/j.seppur.2019.116249

Miller JN, Miller JC (2002) Statistics and chemometrics for analytical chemistry. Pearson-Prentice Hall, New York, USA

Montagner CC, Sodré FF, Acayaba RD, et al (2019) Ten years-snapshot of the occurrence of emerging contaminants in drinking, surface and ground waters and wastewaters from São Paulo State, Brazil. J Braz Chem Soc 30:614–632. https://doi.org/10.21577/0103-5053.20180232

Pal P, Thakura R (2018) A membrane-integrated closed loop system for treatment of pharmaceutical wastewater. In: IEEE International Conference on Power, Control, Signals and Instrumentation Engineering, ICPCSI 2017. Institute of Electrical and Electronics Engineers Inc., pp 802–810

Pérez-Moya M, Graells M, Buenestado P, Mansilla HD (2008) A comparative study on the empirical modeling of photo-Fenton treatment process performance. Appl Catal B Environ 84:313–323. https://doi.org/10.1016/j.apcatb.2008.04.010

Pignatello JJ, Oliveros E, MacKay A (2006) Advanced oxidation processes for organic

contaminant destruction based on the fenton reaction and related chemistry. Crit Rev Environ Sci Technol 36:1–84. https://doi.org/10.1080/10643380500326564

Rad LR, Haririan I, Divsar F (2015a) Comparison of adsorption and photo-Fenton processes for phenol and paracetamol removing from aqueous solutions: Single and binary systems. Spectrochim Acta - Part A Mol Biomol Spectrosc 136:423–428. https://doi.org/10.1016/j.saa.2014.09.052

Rad LR, Irani M, divsar F, et al (2015b) Simultaneous degradation of phenol and paracetamol during photo-Fenton process: Design and optimization. J Taiwan Inst Chem Eng 47:190–196. https://doi.org/10.1016/j.jtice.2014.10.014

Reichert G, Hilgert S, Fuchs S, Pr C (2019) Emerging contaminants and antibiotic resistance in the different environmental matrices of Latin America *. 255:. https://doi.org/10.1016/j.envpol.2019.113140

Sánchez Pérez JA, Soriano-Molina P, Rivas G, et al (2017) Effect of temperature and photon absorption on the kinetics of micropollutant removal by solar photo-Fenton in raceway pond reactors. Chem Eng J 310:464–472. https://doi.org/10.1016/j.cej.2016.06.055

Santos A, Yustos P, Quintanilla A, et al (2004) Evolution of Toxicity upon Wet Catalytic Oxidation of Phenol. Environ Sci Technol 38:133–138. https://doi.org/10.1021/es030476t

Savage PE (2000) Mechanisms and kinetics models for hydrocarbon pyrolysis. J Anal Appl Pyrolysis 54:109–126. https://doi.org/10.1016/S0165-2370(99)00084-4

Shokry A, Audino F, Vicente P, et al (2015) Modeling and Simulation of Complex Nonlinear Dynamic Processes Using Data Based Models: Application to Photo-Fenton Process. Elsevier

Simunovic M, Kusic H, Koprivanac N, Bozic AL (2011) Treatment of simulated

industrial wastewater by photo-Fenton process: Part II. The development of mechanistic model. Chem Eng J 173:280–289. https://doi.org/10.1016/j.cej.2010.09.030

Soriano-Molina P, García Sánchez JL, Malato S, et al (2018) Effect of volumetric rate of photon absorption on the kinetics of micropollutant removal by solar photo-Fenton with Fe^{3+}-EDDS at neutral pH. Chem Eng J 331:84–92. https://doi.org/10.1016/j.cej.2017.08.096

Starling MCVM, Amorim CC, Leão MMD (2019) Occurrence, control and fate of contaminants of emerging concern in environmental compartments in Brazil. J Hazard Mater 372:17–36. https://doi.org/10.1016/j.jhazmat.2018.04.043

Sterling WJ, McCoy BJ (2001) Distribution kinetics of thermolytic macromolecular reactions. AIChE J 47:2289–2303. https://doi.org/10.1002/aic.690471014

Villota N, Lomas JM, Camarero LM (2016) Study of the paracetamol degradation pathway that generates color and turbidity in oxidized wastewaters by photo-Fenton technology. J Photochem Photobiol A Chem 329:113–119. https://doi.org/10.1016/j.jphotochem.2016.06.024

Villota N, Lomas JM, Camarero LM (2018) Journal of Photochemistry and Photobiology A : Chemistry Kinetic modelling of water-color changes in a photo-Fenton system applied to oxidate paracetamol. "Journal Photochem Photobiol A Chem 356:573–579. https://doi.org/10.1016/j.jphotochem.2018.01.040

Yamal-Turbay E, Ortega E, Conte LO, et al (2014) Photonic efficiency of the photodegradation of paracetamol in water by the photo-Fenton process. Environ Sci Pollut Res 22:938–945. https://doi.org/10.1007/s11356-014-2990-9

ANEXO C. Kinetic Model of Photo-Fenton Degradation of Paracetamol in an Annular Reactor: Main Reaction Intermediates and Cytotoxicity Studies

El artículo presentado a continuación ha sido publicado en la revista "*Catalysis Today*"

Kinetic Model of Photo-Fenton Degradation of Paracetamol in an Annular Reactor: Main Reaction Intermediates and Cytotoxicity Studies

Giménez Bárbara N.[a], Conte Leandro O.[a], Audino Francesca[b], Schenone Agustina V.[a], Graells Moisès[b], Alfano Orlando M.[a], Pérez-Moya Montserrat[b]

[a]*Instituto de Desarrollo Tecnológico para la Industria Química (INTEC), Consejo Nacional de Investigaciones Científicas y Técnicas (CONICET) and Universidad Nacional del Litoral (UNL), Ruta Nacional N◦ 168, 3000, Santa Fe, Argentina.*

[b]*Chemical Engineering Department, Universitat Politècnica de Catalunya, Escola d'Enginyeria de Barcelona Est (EEBE), Av. Eduard Maristany, 16, Barcelona 08019, Spain.*

ABSTRACT

A kinetic model derived from a simplified reaction sequence is proposed for the photo-Fenton degradation of Paracetamol (PCT), employing an annular photoreactor. The kinetic model explicitly included the effects of radiation absorption on pollutant degradation kinetics through the evaluation of the Local Volumetric Rate of Photon Absorption (LVRPA). Irradiated experiments achieved an average PCT conversion of 99.3% at 5 min of reaction, and a maximum of 69% of mineralization. Conversely, non-irradiated experiments reached an average PCT conversion of 86.6% at 5 min of reaction, and a maximum of 35% of mineralization. Kinetic parameters ($k_5 = 5.82\times10^9$, $k_6 = 3.01\times10^{10}$, $k_7 = 6.01\times10^{10}$ $M^{-1}s^{-1}$) were estimated employing a nonlinear, multi-parameter regression method, and the validated kinetic model was used to predict temporal variations of the concentrations of HP, PCT, and the main reaction intermediates: hydroquinone (HQ) and 1,4-benzoquinone (BQ). The root mean square error (RMSE) values obtained for HP, PCT, HP, HQ and BQ were 1.16×10^{-2}, 7.13×10^{-1}, 3.53×10^{-3}, 3.05×10^{-3} mM, respectively, showing a good agreement between experimental and predicted data. Moreover, the kinetic model was validated with a new set of experimental tests, confirming its predictive capacity. Beyond the degree of mineralization attained, additional cytotoxicity tests proved that the photo-Fenton process is effective in generating a non-toxic effluent under the operating variables investigated.

Keywords: *Acetaminophen, photo-Fenton, Cytotoxicity, Hydroquinone, 1-4-benzoquinone, LVRPA*

1. INTRODUCTION

For decades, new developments have been carried out to satisfy human beings' growing requirements, leading to the presence of different new chemical compounds in wastewater. The so-called “conventional” water treatments efficiently reduce the presence of N and P compounds, biological oxygen demand and pathogens, but they are not capable of degrading some of these new chemical substances [1]. Hence, these compounds (such as pharmaceuticals and personal care products (PPCPs), plasticizers, pesticides, surfactants, etc.) have been continuously introduced into natural environments for a long time, and that is why they are known collectively as Contaminants of Emerging Concern (CECs). Currently, CECs are not regulated in most of the world. Taking into account that many researchers consider that legislative intervention of governments would help to control this kind of contamination, efforts are being made in the European Union and North America to identify these CECs and reduce their release into the environment [2].

Due to the aforementioned, the need for more efficient methods for the treatment of environmental pollution has opened the field to investigate new technologies, such as Advanced Oxidation Processes (AOPs), aimed at achieving the decomposition of undesirable substances and avoiding at the same time the formation of toxic products [3]. AOPs have the potential to degrade, under environmental conditions, a wide range of hazardous compounds either partially (biodegradable products) or totally (CO_2 and H_2O). One of the most efficient AOPs is the photo-Fenton process [4]. Its mechanism is complex, but it can be described in a simplified way as the reaction between Fe^{2+} (catalyst) and H_2O_2 (oxidant), which generates Fe^{3+} and hydroxyl radicals ($HO^{\bullet}$). At pH < 3, Fe^{3+} remains dissolved and reacts with H_2O_2, generating Fe^{2+} and transforming the reaction system into an autocatalytic one. However, the reaction of Fe^{3+} with H_2O_2 occurs

very slowly compared with the oxidation of Fe^{2+} by H_2O_2 [5]. Radiation accelerates Fenton reactions, regenerating Fe^{2+} and producing more $HO^{\bullet}$ [6]. Since the photo-Fenton process can be carried out at wavelengths up to approximately 580 nm, it can be induced by solar radiation as a renewable energy source, making the process both economically and environmentally sustainable [7].

To study the intrinsic phenomena implied in the AOPs treatment technologies, particularly in the case of Fenton and photo-Fenton processes, the bibliography reports different approaches. There are a lot of empirical models (regression models), which are generally good for a given range of experimental working conditions but are not valid as predictive tools for different reactor configurations [8–10]. However, there are a small number of kinetic models that from a reaction scheme propose the resolution of the mass balance and radiative energy equations through the evaluation of the local volumetric rate of photon absorption (LVRPA) [11–13]. It is important to note that the development of these types of models is of great significance since allow not only to make predictions associated with the behaviour of reaction systems but also to extrapolate the results to larger scales of operation (pilot plant and industrial reactors).

In this work, the analgesic Paracetamol (PCT) is used as a model contaminant. It is a biologically active substance, toxic to various organisms (mainly aquatic) and even human beings, mainly due to the presence of phenolic groups [14]. Moreover, the PCT is one of the most widely used drugs to relieve fever and pain [15], and is recommended to treat mild symptoms of coronavirus disease (COVID-19) [16] causing large amounts of this compound to be discharged into water systems (low absorption in the human body) [17]. From this, different amounts of this compound were detected in effluents of hospitals, pharmaceutical industries (up to 294 mg L^{-1} [18,19]), and urban sewage treatment plants.

This work aims to improve the previous kinetic model [20] derived from a simplified reaction sequence, to study the Fenton and photo-Fenton degradation of Paracetamol (PCT) using an annular photoreactor. In this sense, the behaviour of the main reaction intermediates, hydroquinone (HQ) and 1,4-benzoquinone (BQ), was also studied. Furthermore, to assess the toxicity resulting from the generation of these reaction intermediates, cytotoxicity assays were performed with VERO cells throughout the reaction time. The proposed kinetic model explicitly considers the effects of radiation absorption on the contaminant degradation kinetics by evaluating the LVRPA. The unknown kinetic parameters (only three) were estimated by fitting the model to experimental data. Furthermore, the model was validated using a new set of experimental data.

Finally, a cytotoxicity study completes the analysis of the efficiency of the photo-Fenton degradation of the PCT. For this purpose, VERO cells (which come from an African green monkey kidney) were employed as a model system, since these cells could represent a more adequate system when evaluating the toxicity of superior organisms. Hence, the viability of VERO cells was studied not only in the final generated effluent of reaction but also during the entire process of the PCT abatement.

2. MATERIALS AND METHODS

2.1 Chemicals and reagents

Analytical grade reagents were used as well as deionised water as water matrix and milli Q grade water as HPLC mobile phases. PCT (98% purity) was purchased from Sigma-Aldrich. Hydroquinone and 1,4-benzoquinone (HQ and BQ, both 99% purity) were obtained from Fluka. Hydrogen peroxide (HP, 33% w/w) was purchased from Panreac Química SLU. The salt $Fe_2SO_4.7H_2O$ (Merck, pro-analysis) was used as a Fe^{2+} source.

Ascorbic acid (purity > 99%) and 0.2% 1,10-phenanthroline, both used to perform iron species measurements, were purchased from Riedel de Haën and Scharlab, respectively. Finally, Hydrogen chloride (HCl, 37%) or pH adjustment and methanol (HPLC grade) were obtained from J.T. Baker.

2.2 Analytical determinations

PCT and its reaction intermediates (BQ and HQ) were determined using an HPLC Agilent 1200 series with UV-DAD array detector (set at 243 nm), with an Akady 5 μm C-18 150×4.6 mm column. The eluent was a mixture of methanol:water (25:75) flowing at 0.4 mL min^{-1}, and 20 μL samples were injected by a manual injector. All the samples were treated with 0.1 M methanol, in proportion 50:50, to stop the reaction. HP, Fe^{2+} and Total Fe were determined using a UV/Vis spectrophotometer (Hitachi U-2001). In the case of iron, samples for Fe^{2+} and Total Fe were analysed by means of the colorimetric method with 1,10-phenanthroline at 510 nm. Samples for Total Fe determination were pre-treated with ascorbic acid to convert all the ferric ions to ferrous ions. HP was monitored through the measurement of the absorption at 450 nm of the complex formed after its reaction with ammonium metavanadate [21]. Samples for determination of TOC were taken and refrigerated (to slow down any further degradation of the organic matter) until their analysis through a VCHS/CSN TOC analyser (Shimadzu).

2.3 Experimental Device and Procedure

The experiments were carried out in a glass annular photoreactor (1.5 L) with external recycling, connected to a glass jacketed reservoir tank (9 L). The experimental system was completed with a pH-meter, a flowmeter, and a thermostatic bath for temperature control. A pumping system allows keeping a constant recirculation flow of 12 L min^{-1}, which ensures perfect mixing. The photoreactor was equipped with an Actinic BLTL-DK 36 W/10 1SL lamp (UVA-UVB, ⌀ = 28 mm and L = 589.8 mm). The lamp

spectral irradiance can be found in the "Supplementary Material" (Figure S2). The total reaction volume (V_{tot}) was 15 L and the irradiated one (V_{irr}) was 1.5 L (that is, 10% of the total volume). A detailed description of the experimental system can be found in Yamal-Turbay et al. [22]and in the Figure S1 provided in the "Supplementary Material. The incident photon power, E = 3.36 × 10^{-4} Einstein min^{-1} (between 300 and 420 nm) was measured using potassium ferrioxalate actinometry [22].

Each experiment began with the filling of the glass reservoir with 10 L of deionised water and then adding 4.9 L of the aqueous solution containing PCT. The pH was adjusted to 2.8 ± 0.1 with 37% hydrogen chloride (J.T. Baker Inc.) and 0.1 L of the aqueous solution containing iron sulphate was added. Then, an aliquot was taken to determine the initial concentrations of the iron species. Finally, to start the experiment, the HP solution was added. In the case of the experiments carried out with radiation, and to allow the stabilization of the emitted radiation, the lamp was turned on 10 min before adding the HP. Total reaction time was set at 75 min for all the experiments carried out.

The treated sample consisted of deionised water spiked with the contaminant. Initial PCT concentration was set at 40 mg L^{-1} in all the experiments. The effect of the following operative variables was tested on PCT degradation: Fe^{2+} initial concentration ($[Fe^{2+}]^0$, between 5 and 10 mg L^{-1}), HP initial concentration ($[HP]^0$, between 94.5 and 378 mg L^{-1}), and UV-radiation (ON or OFF). It was decided to set these particular operating parameters considering previous studies [20]. The set of experimental tests carried out, with their corresponding operating conditions of initial concentrations of catalyst and oxidant, and with or without radiation, is presented in Table 2 (see section 4.1 Experimental Results).

Finally, a set of blank assays was performed in order to identify the effect of each reagent on the degradation and mineralization of PCT. The three blank assays undertaken

correspond to only irradiation, only Fe^{2+} at a concentration of 10 mg L^{-1} and only H_2O_2 at a concentration of 756 mg L^{-1}. Results demonstrate that the reagents alone produce no PCT degradation, except in the case of H_2O_2 alone, which led to only 18% degradation after 90 min treatment. Moreover, PCT and TOC remained almost constant under UV radiation (300–420 nm) tests.

2.4 Toxicity test

The acute toxicity was monitored during the oxidation process. Cytotoxicity tests based on cell lines culture were carried out, employing VERO cells (ATCC®, Manassas, VA, USA). For this purpose, the methodology described by Audino et al. [23] was employed. In brief, aqueous samples were taken at predefined times during the treatment by Fenton and photo-Fenton processes, at different operational conditions and were evaluated at serial one-third dilutions. A control of maximum cell growth (achieved culturing the cells in medium alone), and a control to evaluate the effect of the aqueous dilution of the medium, were performed. Every sample was evaluated in triplicate, on independent plates. Cytotoxicity was assessed by measuring the viability of the cells (determined by the MTT method) [24] exposed to the contaminant and its by-products.

3. MODELLING

A kinetic model that describes the degradation of PCT and its intermediates, through the homogeneous Fenton and photo-Fenton processes, was developed. Table 1 represents the reaction mechanism proposed, based on a simplified scheme extracted from the analysis of more complex and specific reaction schemes [25,26]. The abovementioned scheme also includes the formation and degradation of two PCT reaction intermediates, 1,4-benzoquinone (BQ), and hydroquinone (HQ), which were identified and quantified in the present work [27].

Table 1. Simplified reaction scheme of PCT photo-Fenton degradation.

N°	Reaction Step	Kinetic Constant (M^{-1} s^{-1})
1	$Fe^{2+} + H_2O_2 \xrightarrow{k1} Fe^{3+} + OH^- + HO^\bullet$	$k_1 = 147.29$ [b]
2	$Fe^{3+} + H_2O_2 \xrightarrow{k2} Fe^{2+} + H^+ + HO_2^\bullet$	$k_2 = 3.16$ [b]
3	$Fe^{3+} + H_2O \xrightarrow{\Phi_{Fe^{2+}}} Fe^{2+} + H^+ + HO^\bullet$	$\Phi_{Fe^{2+}} = 0.21$ mol Einstein^{-1} [b]
4	$H_2O_2 + HO^\bullet \xrightarrow{k_4} HO_2^\bullet + H_2O$	$k_4 = 7.00\times10^7$ [b]
5	$PCT + HO^\bullet \xrightarrow{k_5} HQ$	k_5 [a]
6	$HQ + HO^\bullet \xrightarrow{k_6} BQ$	k_6 [a]
7	$BQ + HO^\bullet \xrightarrow{k_7} P_i$	k_7 [a]

[a] values estimated in this research work.

[b] values taken from Audino et al. [20].

The simplified reaction scheme was made based on a series of hypotheses [28]: i) for highly reactive radicals (i.e. HO•), the steady-state approximation (SSA) was applied; ii) the only oxidizing species considered were HO•, since radical HO_2• is far less reactive than HO• [29,30]; iii) radical–radical termination reactions are neglected compared to the propagation/consumption ones; iv) reactions of Fe^{2+} with HO• are neglected due to the low iron concentrations employed in this experimental system; v) the oxygen concentration is always in excess.

Then, these assumptions allowed to obtain the reaction rate expressions, for the following studied species (PCT, HP, Fe^{2+}, Fe^{3+}, HQ and BQ) (eqs. 1-7):

$$R_{PCT}(\underline{x},\mathrm{t}) = -k_5\,[\mathrm{PCT}]\,[HO^\bullet] \quad (1)$$

$$R_{HP}(\underline{x},\mathrm{t}) = -k_1[Fe^{2+}][\,HP] - k_2[Fe^{3+}][HP] - k_4[HP][HO^\bullet] \quad (2)$$

$$R_{Fe^{2+}}(\underline{x},\mathrm{t}) = -k_1[Fe^{2+}][HP] + k_2[Fe^{3+}]\,[HP] + \Phi_{Fe^{2+}}\sum_{\lambda} e_\lambda^a\,(\underline{x},\mathrm{t}) \quad (3)$$

$$R_{Fe^{3+}}(\underline{x},\mathrm{t}) = -R_{Fe^{2+}}(\underline{x},\mathrm{t}) \quad (4)$$

$$R_{HQ}(\underline{x},\mathrm{t}) = k_5[\mathrm{PCT}][HO^{\bullet}] - k_6[HQ]\,[HO^{\bullet}] \tag{5}$$

$$R_{BQ}(\underline{x},\mathrm{t}) = k_6[HQ][HO^{\bullet}] - k_7[\mathrm{BQ}][HO^{\bullet}] \tag{6}$$

$$\begin{aligned} R_{HO^{\bullet}}(\underline{x},\mathrm{t}) = {} & k_1[Fe^{2+}][HP] + \Phi_{Fe^{2+}} \sum_{\lambda} e_{\lambda}^{a}(\underline{x},\mathrm{t}) - k_4[HP][HO^{\bullet}] \\ & - k_5[\mathrm{PCT}][HO^{\bullet}] - k_6[HQ]\,[HO^{\bullet}] - k_7[BQ]\,[HO^{\bullet}] \end{aligned} \tag{7}$$

Here, $\Phi_{Fe^{2+}}$ is the wavelength-averaged primary quantum yield and $\sum_{\lambda} e_{\lambda}^{a}(\underline{x},\mathrm{t})$ the LVRPA in the photoreactor extended to polychromatic radiation by performing the integration over all useful wavelengths (λ: 300–420 nm).

Note that eqs. (1-7) can be generalized by using the following matrix representation:

$$\boldsymbol{R_i}(\underline{x},t) = \boldsymbol{R_i^T}(t) + \boldsymbol{R_i^{irr}}(\underline{x},t) \tag{8}$$

The first term on the right-hand side of eq. (8) corresponds to the thermal reaction rate (function only of time, t), and the second one represents the irradiated reaction rate (function of the position in the photoreactor, $\underline{x}$ and the time, t).

The mass balance for the well-stirred isothermal annular photoreactor in which the kinetic studies were carried out is represented by the following set of first order, ordinary differential equations (eq. 9) with their corresponding initial conditions (eq. 10) for all the chemical species "i" considered (PCT, HP, Fe^{2+}, Fe^{3+}, HQ and BQ):

$$\frac{d\boldsymbol{C_i}(t)}{dt} = \frac{V_{tot} - V_{irr}}{V_{tot}}\boldsymbol{R_i^T}(t) + \frac{V_{irr}}{V_{tot}}\langle \boldsymbol{R_i^{irr}}(\underline{x},t)\rangle_V \tag{9}$$

$$\boldsymbol{C_i} = \boldsymbol{C_i^0} \qquad\qquad t_0 = 0 \tag{10}$$

Applying the steady-state approximation (SSA) to the radical $HO^{\bullet}$ ($R_{HO^{\bullet}}(\underline{x},\mathrm{t}) = 0$ in eq. 7), the expression corresponding to $[HO^{\bullet}]$ is obtained. Replacing this expression into each of the equations 1 to 6, and then replacing the expressions obtained in eq. 9, the system of ordinary differential equations that models the studied system is achieved (eqs. A.1 to A.5, Appendix A).

Finally, following the assumptions adopted by Audino et al. [20], it is possible to calculate the average volumetric rate of photon absorption inside the photoreactor for polychromatic radiation ($\langle \sum_\lambda e_\lambda^a (\underline{x}, t) \rangle_{V_{irr}}$), through the numerical integration of eq. 11.

$$\langle \sum_\lambda e_\lambda^a (\underline{x}, t) \rangle_{V_{irr}} = \frac{2\pi}{V_{irr}} \int_0^L \int_{r_{int}}^{r_{ext}} e_\lambda^a (\underline{x}, t)\, r\, dr\, dz$$
$$= \frac{2\pi}{V_{irr}} \int_0^L \int_{r_{int}}^{r_{ext}} \left[\kappa_\lambda (\underline{x}, t) \frac{P_{\lambda,s}}{2\pi L_L} \int_{\Theta_1}^{\Theta_2} exp\left[-\frac{\kappa_{T,\lambda}(\underline{x}, t)(r_i - r_{int})}{\cos\theta} \right] d\theta \right] r\, dr\, dz \quad (11)$$

Here, $P_{\lambda,s}$ is the lamp spectral power emission (provided by the lamp supplier), $\kappa_\lambda(\underline{x}, t)$ the volumetric absorption coefficient of the reacting species, $\kappa_{T,\lambda}(\underline{x}, t)$ the volumetric absorption coefficient of the medium, *r* the radius, and L_L the useful length of the lamp. Also, r_{int} and r_{ext} are the internal and external radio of the annular photoreactor, respectively.

3.1 Kinetic parameter estimation

An optimization procedure was employed to provide the values of kinetic constants (k_5, k_6 and k_7) that minimize the differences between the predicted concentrations and the corresponding experimental values, for each stable species i considered (PCT, HP, HQ and BQ). The theoretical values were obtained by solving the system of ordinary differential equations (eqs.9 and 10), utilizing GNU Octave (Version 5.2.0) software. Making use of the complete set of experimental data to fit the proposed kinetic model, the three rate constants (k_5 , k_6, and k_7) were estimated, employing a nonlinear least-square objective function (Newton Gauss-Marquardt algorithm). Details about the numerical structure to obtain the kinetic parameters and the simulations of the experimental data can be found in the Figure S3 in the Supplementary Material. Finally, the root mean square error (RMSE), calculated for each chemical species i with eq. 12, was used to evaluate the model accuracy.

$$RMSE_i = \sqrt{\frac{\left(C_{i,exp} - C_{i,mod}\right)^2}{n}} \quad (12)$$

Here, $C_{i,exp}$ and $C_{i,mod}$ are the experimental data and those predicted by the model, respectively, and *n* is the total number of samples (whole set of experimental runs).

4. RESULTS

4.1 Experimental Results

Table 2 details the operating conditions (iron and hydrogen peroxide concentrations and radiation ON or OFF) for each of the experimental tests carried out (Runs 1-8 and Runs 1_V* and 2_V*). In addition, the experimental PCT conversions obtained for 5 ($X_{PCT}^{5\,min}$) and 10 ($X_{PCT}^{10\,min}$) minutes of reaction are presented, as well as the conversion levels obtained for total organic carbon (TOC) after 75 minutes of reaction ($X_{TOC}^{75\,min}$).

Table 2. Experimental conditions for each experimental run (Runs 1-8 and Runs 1_V* and 2_V*), PCT conversion at 5 (X_{PCT}^{5min}), and 10 ($X_{PCT}^{10\,min}$) min of reaction, and TOC conversion after 75 min of reaction ($X_{TOC}^{75\,min}$).

Run	$[Fe^{2+}]^0$ ($mg\ L^{-1}$)	$[HP]^0$ ($mg\ L^{-1}$)	*Radiation*	$X_{PCT}^{5\,min}$ (%)	$X_{PCT}^{10\,min}$ (%)	$X_{TOC}^{75\,min}$ (%)
#1	5	94.5	OFF	80.4	96.0	29.3
#2	5	189	OFF	84.7	96.6	30.6
#3	7.5	378	OFF	84.5	97.1	35.7
#4	10	189	OFF	96.9	100	33.3
#5	5	189	ON	97.3	100	55.2
#6	5	378	ON	100	100	69.6
#7	7.5	94.5	ON	100	100	33.6
#8	10	378	ON	100	100	68.7
#1_V*	7.5	189	ON	97.3	100	55.2
#2_V*	7.5	189	OFF	96.9	100	32.3

* Runs for model validation at central point conditions of $[Fe^{2+}]^0$ and $[HP]^0$.

Examining the experimental PCT conversion at 5 min of reaction (X_{PCT}^{5min}), all the runs carried out in the presence of radiation reached close to 100% conversion of PCT.

In contrast, runs under Fenton condition have a maximum conversion of 96.9% (run #4, 10_189_OFF) and a minimum conversion of 80.4% (run #1, 5_94.5_OFF). These results demonstrate the importance of radiation in the studied system. Additionally, if runs #2 (5_189_OFF, $X_{PCT}^{5min} =$ 84.7 %) and #5 (5_189_ON, $X_{PCT}^{5min} = 97.3$) are analysed, which have identical initial conditions of Fe^{2+} and HP concentrations, but were carried out in the absence and presence of radiation (respectively), it is observed that with the photo-Fenton system a conversion difference of almost 13% higher than with the dark reaction is achieved. Moreover, run #2 (Fenton) takes twice as many minutes in reaction time (10 min) to reach a PCT conversion ($X_{PCT}^{10min} = 96{,}6\%$) close to the X_{PCT}^{5min} of run #5 ($X_{PCT}^{5min} =$ 97,3%).

TOC conversions (X_{TOC} (%)) were also estimated after 75 min of reaction (see Table 2). In the case of reactions carried out under dark conditions (run #1 to #4), the maximum TOC conversion achieved was only 35.7% (run #3), being minimal (29.3%) for conditions of run #1 (5_94.5_OFF), where the lowest dosage of oxidizing agent and catalyst have been used.

However, in presence of radiation, it can be observed that the degree of TOC conversion achieved was higher than 33.5% for all the conditions studied after 75 min of reaction, being maximum (69.6 %) for the experimental run #6 (5_378_ON). Therefore, the performance of the process in terms of mineralization levels achieved is substantially improved by radiation.

4.2 Model Results

Firstly, it is important to note that the values of the estimated kinetic parameters: $k_5 =$ 5.82×10^9, $k_6 =$ 3.01×10^{10}, $k_7 =$ 6.01×10^{10} $M^{-1}s^{-1}$, are close to those found in the specific literature [25,31,32]. Moreover, the relatively low RMSE values obtained (in the same order of magnitude as the experimental error) using eq.12: 1.49 × 10^{-2}, 9.00 × 10^{-1},

6.33×10^{-3}, 5.62×10^{-3} mM for PCT, HP, HQ and BQ, respectively, show that the kinetic model adequately describes the behaviour of the reacting system. Furthermore, normalizing the RMSE values of the species initially present in the system (PCT and HP) according to its initial experimental concentration, low errors of 5.63 and 8.10% are reached, which again represents the efficiency of the model.

From Fig. 1a and 1b, increasing the oxidant agent concentration $[HP]^0$ from 94.5 to 189 mg L^{-1} did not cause a higher degradation rate or final conversion of both the PCT and its intermediates. For these dark Fenton reactions (run #1 and #2), an excess of HP can enhance the consumption of hydroxyl radical, according to (eq. 13) [33].

$$H_2O_2 + OH\cdot \rightarrow HO_2^- \cdot + H_2O \qquad (13)$$

Under operating conditions of Fig. 1c and 1d, with an initial HP concentration of 378 mg L^{-1}, but with different $[Fe^{2+}]^0$ (run #6: 5 mg L^{-1} and run #8: 10 mg L^{-1}), it can be observed the beneficial effect of increasing the initial concentration of iron on the by-product's degradation. Here, the time required to achieve the total removal of the intermediates is reduced by 50% when increasing $[Fe^{2+}]^0$ from 5 to 10 ppm.

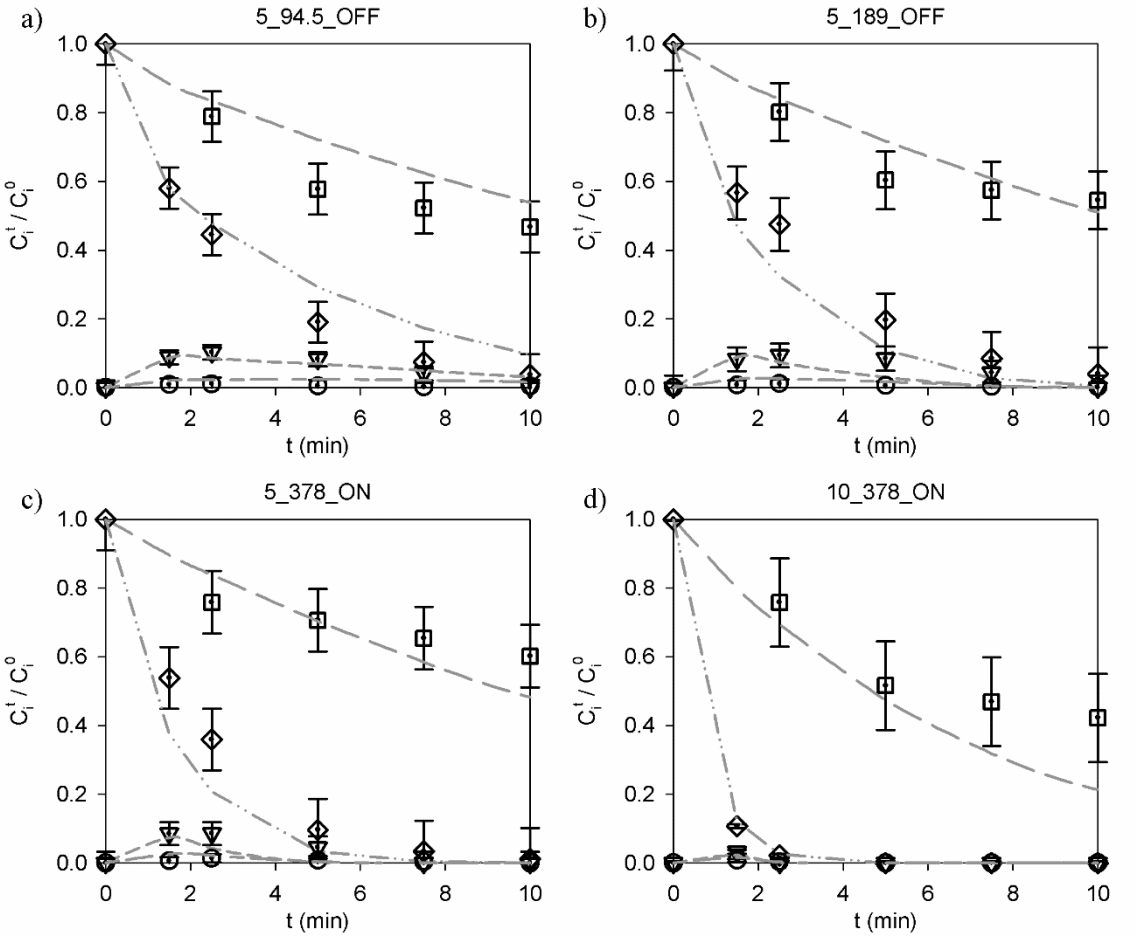

Figure 1 Experimental and model results for PCT, HP, HQ, and BQ species, in relative concentrations. a) $[Fe^{2+}]^0$ = 5 mg L^{-1}, $[HP]^0$ = 94.5 mg L^{-1}, radiation: OFF; b) $[Fe^{2+}]^0$ = 5 mg L^{-1}, $[HP]^0$ = 189 mg L^{-1}, radiation: OFF; c) $[Fe^{2+}]^0$ = 5 mg L^{-1}, $[HP]^0$ = 378 mg L^{-1}, radiation: ON; d) $[Fe^{2+}]^0$ = 10 mg L^{-1}, $[HP]^0$ = 378 mg L^{-1}, radiation: ON. Keys: PCT = diamond, HP = square, HQ = triangle down, BQ = circle, experimental results; and PCT = dash-dot line, HP = long dash line, HQ = short dash line, BQ = short-long line, model results.

Finally, a new set of experimental runs at central point conditions of $[Fe^{2+}]^0$ and $[HP]^0$ were performed to validate the kinetic model (runs #1_V and #2_V, Table 2). Fig. 2a and 2b show a good agreement between the experimental data and the predicted concentrations for validation assay conditions (RMSE values obtained: 1.16×10^{-2}, 7.13×10^{-1}, 3.53×10^{-3}, 3.05×10^{-3} mM for PCT, HP, HQ and BQ, respectively). Therefore, the proposed kinetic model is adequate to predict the temporal variations of the PCT, HP and main reaction intermediates concentrations, using the Fenton and photo-Fenton

process in the annular photoreactor.

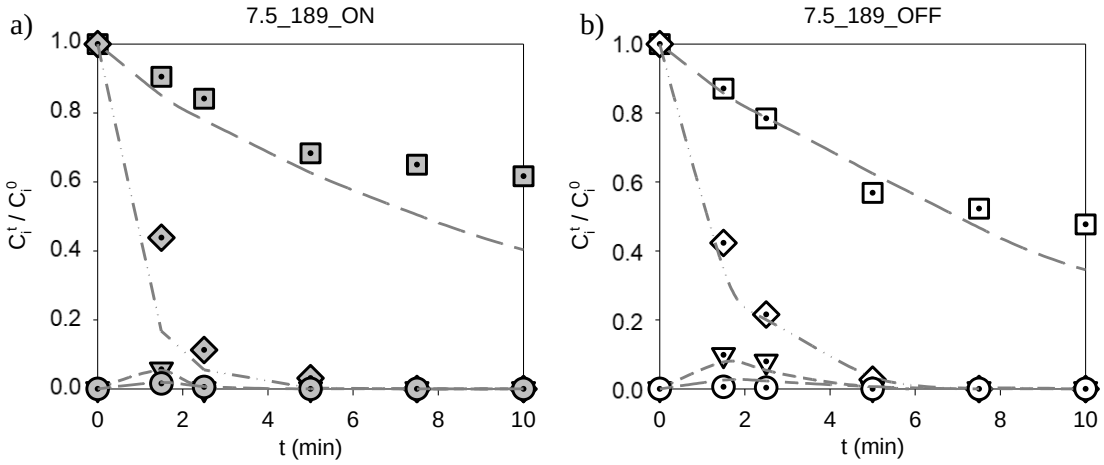

Figure 2. Experimental and model results for PCT, HP, HQ, and BQ species, in relative concentrations for the validation assays: a) $[Fe^{2+}]^0$ = 7.5 mg L^{-1}, $[HP]^0$ = 189 mg L^{-1}, radiation: ON; b) $[Fe^{2+}]^0$ = 7.5 mg L^{-1}, $[HP]^0$ = 189 mg L^{-1}, radiation: OFF. Keys: PCT = diamond, HP = square, HQ = triangle down, BQ = circle, experimental results; and PCT = dash-dot line, HP = long dash line, HQ = short dash line, BQ = short-long line, model results.

4.3 Toxicity results

Different cell types may be selected for studying toxicity. The most common options are *E. Coli* and *S. Aureus* bacteria. However, both species have been shown to be capable of metabolizing PCT and using it as a carbon source for its growth. Therefore, VERO cells were selected for performing the toxicity assays since they have shown to offer greater sensitivity to PCT and its by-products [23].

The LC_{50} value for PCT was determined and resulted to be considerably high (>1000 mg L^{-1}), showing that the selected initial concentration of PCT (40 mg L^{-1}) does not have a toxic effect on VERO cells. Fig. 3 shows the cytotoxicity results, as the temporal evolution of VERO cells viability for the entire reaction time (75 min) along with the temporal evolution of de HP concentration.

Certainly, cells viability may result from a combined toxic effect of different chemical species in the reaction media. This deserves further discussion. On one hand,

the intermediates HQ and BQ could be suggested as affecting viability. This can be discarded as it is proved (Figs. 1 and 2) that these species have a very short presence in the media, and they remain undetectable after 6 minutes. On the other hand, HP requires a deeper analysis of the data. Towards this end, Fig. 3 displays the evolution of HP concentration parallel to cell viability. All cases (a,b,c,d) show there is no HP by the end of the reaction time. They also show that HP is consumed earlier in cases c and d, because of light as it should be expected. These two cases reveal very high cell viability despite the presence or absence of HP, which allows concluding the irrelevant effect of HP to toxicity.

In Fig. 3a, a marked decrease in the viability of the cells is observed from the beginning to the end of the reaction, only recovering some viability at t = 25 min, although not 100%. Therefore, it is concluded that it is not safe to apply the proposed treatment at low concentrations of Fenton reagents without radiation.

Similarly, in Fig. 3b it can be observed that cell viability begins to decrease after 25 min of reaction, being recovered only towards the end of the process. This implies that, under these concentrations of Fenton reagents and without radiation, it would only be safe to stop the reaction after t = 60 min. Between 15 and 20 min reaction time, cell viability is also important, but if the results of TOC conversion are analysed together with this toxicity assay, in the same time lapse, the X_{TOC} achieved is 14% on average (results not shown), but at the end of the reaction (75 min) it is higher than 35% (Table 2).

For Fig. 3c the presence of radiation greatly improves the cytotoxicity profile presented by the system, where cell viability never drops to less than 20%, Furthermore, towards the end of the reaction, almost 100% viability is recovered. In addition, after 30 min of reaction, the X_{TOC} reached a plateau at the end of the reaction at a value of around 34% (Table 2).

Finally, in Fig. 3d a good cytotoxicity profile is observed throughout the reaction time and, most importantly, at the end of the degradation process, 100% recovery of cell viability is obtained. However, if we consider the X_{TOC}, it reaches a maximum value of almost 70% (Table 2) towards the end of the process (t = 75 min).

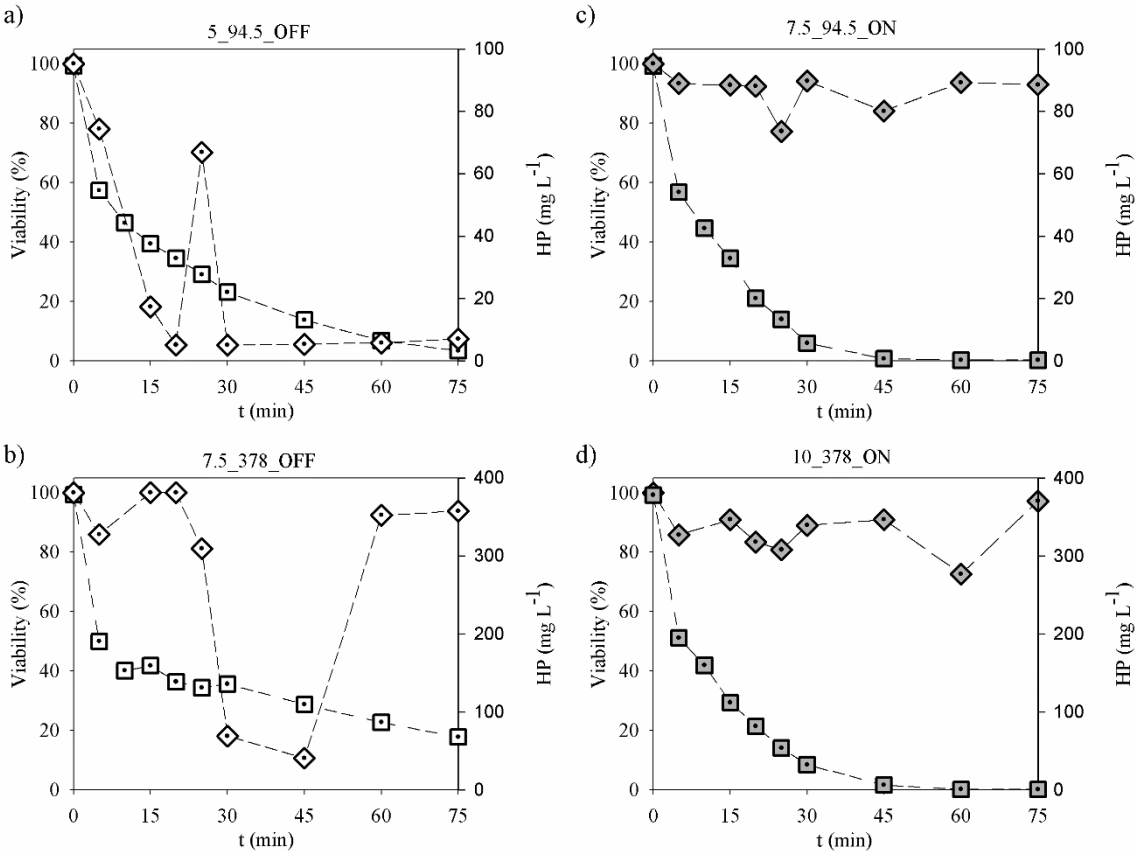

Figure 3 Cytotoxicity temporal evolution (diamond) and HP concentration (square). a) run #1: most adverse operational conditions for the reaction; b) run #3: Fenton reaction, medium $[Fe^{2+}]^0$ and high $[HP]^0$ operational conditions; c) run #7: photo-Fenton reaction, medium $[Fe^{2+}]^0$ and low $[HP]^0$ operational conditions; d) run #8: more favourable operational conditions for the reaction.

Now, analysing together the results previously stated about TOC conversion and cytotoxicity for runs #7 and #8, it can be deduced that just some of the by-products have toxic effects on VERO cells, since both experiments reached a very different X_{TOC} but very similar viability levels towards the end of the reaction. This could be explained considering the nature of the formed by-products since the oxidation of the CECs could

produce some intermediaries that are more hydrophilic than their parent compounds. This would reduce the ability of these compounds to penetrate through cell membranes, therefore resulting in less toxic for VERO cells [34].

5. CONCLUSIONS

A kinetic model was presented and experimentally validated to describe the Fenton and photo-Fenton degradation of Paracetamol and its main degradation by-products, hydroquinone, and 1-4-benzoquinone, in an annular photoreactor. The proposed kinetic model, derived from a simplified reaction sequence, explicitly included the effects of radiation absorption on the pollutant degradation kinetics through the evaluation of the Local Volumetric Rate of Photon Absorption. Using a nonlinear multi-parameter optimization procedure with only a minimum of three estimated kinetic constants, it was demonstrated that the model presented a good agreement between the experimental data and the predicted concentrations, not only of Paracetamol and hydrogen peroxide but also of hydroquinone and 1,4-benzoquinone. From a new set of experimental data, the kinetic model was validated confirming that the estimated parameters are adequate to represent the behaviour of the photo-Fenton process under the operating conditions tested.

Furthermore, to assess the environmental implications of the photo-Fenton process, a cytotoxicity study was conducted with VERO cells throughout the entire reaction time. Analysing these results, it was possible to observe that the presence of radiation in the system led to the production of a less toxic effluent compared to the non-irradiated systems, since a viability of over 95% was obtained for the photodegradation tests. Additionally, the increase in iron and hydrogen peroxide concentration produced an improvement in the cytotoxicity profiles of the system in contrast with the toxicity levels achieved in the Fenton run with the most adverse operational conditions. From the cytotoxicity results together with the experimental results of the total organic carbon

conversion, it was possible to observe that some of the by-products generated from the reaction can have toxic effects on the VERO cells. These results demonstrate the importance of evaluating the toxicity throughout the reaction time, to define when it may be convenient to stop the contaminant degradation reaction.

CRediT authorship contribution statement. Conceptualization: Ideas; formulation or evolution of overarching research goals and aims. Alfano Orlando M., Pérez-Moya Montserrat, Conte Leandro O, Graells Moisès. Methodology Development or design of methodology; creation of models. Pérez-Moya Montserrat, Conte Leandro O, Graells Moisès, Alfano Orlando M. Software Programming, software development; designing computer programs; implementation of the computer code and supporting algorithms; testing of existing code components. Conte Leandro O. Validation Verification, whether as a part of the activity or separate, of the overall replication/ reproducibility of results/experiments and other research outputs. Audino Francesca, Graells Moisès, Pérez-Moya Montserrat. Formal analysis Application of statistical, mathematical, computational, or other formal techniques to analyze or synthesize study data. Investigation Conducting a research and investigation process, specifically performing the experiments, or data/evidence collection. Audino Francesca, Pérez-Moya Montserrat, Giménez Bárbara N., Schenone Agustina V. Resources Provision of study materials, reagents, materials, patients, laboratory samples, animals, instrumentation, computing resources, or other analysis tools. Conte Leandro O., Pérez-Moya Montserrat. Data Curation Management activities to annotate (produce metadata), scrub data and maintain research data (including software code, where it is necessary for interpreting the data itself) for initial use and later reuse. Giménez Bárbara N., Schenone Agustina V., Conte Leandro O. Writing-Original Draft Preparation, creation and/or presentation of the published work, specifically writing the initial draft (including substantive translation).

Giménez Bárbara N., Conte Leandro O., Schenone Agustina V., Alfano Orlando M. Writing-Review & Editing Preparation, creation and/or presentation of the published work by those from the original research group, specifically critical review, commentary or revision – including pre-or postpublication stages. Conte Leandro O., Graells Moisès, Alfano Orlando M., Pérez-Moya Montserrat. Visualization Preparation, creation and/or presentation of the published work, specifically visualization/data presentation. Conte Leandro O., Schenone Agustina V., Giménez Bárbara N. Supervision Oversight and leadership responsibility for the research activity planning and execution, including mentorship external to the core team. Pérez-Moya Montserrat, Conte Leandro O. Project administration Management and coordination responsibility for the research activity planning and execution. Conte Leandro O., Pérez-Moya Montserrat Funding acquisition Acquisition of the financial support for the project leading to this publication. Graells Moisès, Alfano Orlando M.

Declaration of Competing Interest. The authors declare that they have no known competing financial interests or personal relationships that could have appeared to influence the work reported in this paper.

Data availability. Data will be made available on request.

Acknowledgements. This work was supported from the Spanish "Ministerio de Ciencia e Innovación" and the European Regional Development Fund, both funding the research Project CEPI (PID2020-116051RB-I00) which is fully acknowledged. The authors are also grateful to Universidad Nacional del Litoral (UNL), Consejo Nacional de Investigaciones Científicas y Técnicas (CONICET) and Agencia Nacional de Promoción Científica y Tecnológica (ANPCyT) of Argentina for the financial support.

APPENDIX A

First-order ordinary differential equations that model the well-stirred isothermal annular photoreactor used in this research work.

$$\frac{dC_{PCT}}{dt} = \left\{\frac{V_{irr}}{V_{tot}}\left[-k_5[\mathrm{PCT}]\frac{k_1[Fe^{2+}][HP] + \Phi_{Fe^{2+}}\langle\sum_\lambda e_\lambda^a\left(\underline{x},t\right)\rangle_{V_{irr}}}{k_4[HP] + k_5[\mathrm{PCT}] + k_6[HQ] + k_7[BQ]}\right]\right\} + \left\{\frac{V_{tot} - V_{irr}}{V_{tot}}\left[-k_5[\mathrm{PCT}]\frac{k_1[Fe^{2+}][HP]}{k_4[HP] + k_5[\mathrm{PCT}] + k_6[HQ] + k_7[BQ]}\right]\right\} \quad (A.1)$$

$$\frac{dC_{HP}}{dt} = \left\{\frac{V_{irr}}{V_{tot}}\left[-k_1[Fe^{2+}][HP] - k_2[Fe^{3+}][HP] - k_4[HP]\frac{k_1[Fe^{2+}]\,[HP] + \Phi_{Fe^{2+}}\langle\sum_\lambda e_\lambda^a\left(\underline{x},t\right)\rangle_{V_{irr}}}{k_4[HP] + k_5[\mathrm{PCT}] + k_6[HQ] + k_7[BQ]}\right]\right\} + \left\{\frac{V_{tot} - V_{irr}}{V_{tot}}\left[-k_1[Fe^{2+}][HP] - k_2[Fe^{3+}][HP] - k_4[HP]\frac{k_1[Fe^{2+}]\,[HP]}{k_4[HP] + k_5[\mathrm{PCT}] + k_6[HQ] + k_7[BQ]}\right]\right\} \quad (A.2)$$

$$\frac{dFe^{2+}}{dt} = -\frac{dFe^{3+}}{dt} = \frac{V_{irr}}{V_{tot}}\left\{-k_1[Fe^{2+}][HP] + k_2[Fe^{3+}][HP] + \Phi_{Fe^{2+}}\langle\sum_\lambda e_\lambda^a\left(\underline{x},t\right)\rangle_{V_{irr}}\right\} + \frac{V_{tot} - V_{irr}}{V_{tot}}\{-k_1[Fe^{2+}][HP] + k_2[Fe^{3+}][HP]\} \quad (A.3)$$

$$\frac{dC_{HQ}}{dt} = \left\{\frac{V_{irr}}{V_{tot}}\left[(k_5[\mathrm{PCT}] - k_6[\mathrm{HQ}])\frac{k_1[Fe^{2+}]\,[HP] + \Phi_{Fe^{2+}}\langle\sum_\lambda e_\lambda^a\left(\underline{x},t\right)\rangle_{V_{irr}}}{k_4[HP] + k_5[\mathrm{PCT}] + k_6[HQ] + k_7[BQ]}\right]\right\} + \left\{\frac{V_{tot} - V_{irr}}{V_{tot}}\left[(k_5[\mathrm{PCT}] - k_6[\mathrm{HQ}])\frac{k_1[Fe^{2+}][HP]}{k_4[HP] + k_5[\mathrm{PCT}] + k_6[HQ] + k_7[BQ]}\right]\right\} \quad (A.4)$$

$$\frac{dC_{BQ}}{dt} = \left\{\frac{V_{irr}}{V_{tot}}\left[(k_6[\mathrm{HQ}] - k_7[\mathrm{BQ}])\frac{k_1[Fe^{2+}][HP] + \Phi_{Fe^{2+}}\langle\sum_\lambda e_\lambda^a\left(\underline{x},t\right)\rangle_{V_{irr}}}{k_4[HP] + k_5[\mathrm{PCT}] + k_6[HQ] + k_7[BQ]}\right]\right\} + \left\{\frac{V_{tot} - V_{irr}}{V_{tot}}\left[(k_6[\mathrm{HQ}] - k_7[\mathrm{BQ}])\frac{k_1[Fe^{2+}][HP]}{k_4[HP] + k_5[\mathrm{PCT}] + k_6[HQ] + k_7[BQ]}\right]\right\} \quad (A.5)$$

REFERENCES

[1] P. Krzeminski, M.C. Tomei, P. Karaolia, A. Langenhoff, C.M.R. Almeida, E. Felis, F. Gritten, H.R. Andersen, T. Fernandes, C.M. Manaia, L. Rizzo, D. Fatta-Kassinos, Sci. Total Environ. 648 (2019) 1052–1081.

[2] A. Jurado, M. Walther, M.S. Díaz-Cruz, Sci. Total Environ. 663 (2019) 285–296.

[3] T.A. Ternes, C. Prasse, C.L. Eversloh, G. Knopp, P. Cornel, U. Schulte-Oehlmann, T. Schwartz, J. Alexander, W. Seitz, A. Coors, J. Oehlmann, Environ. Sci. Technol. 51 (2016) 308–319.

[4] G. Maniakova, K. Kowalska, S. Murgolo, G. Mascolo, G. Libralato, G. Lofrano, O. Sacco, M. Guida, L. Rizzo, Sep. Purif. Technol. 236 (2020) 116249.

[5] A. Das, M.K. Adak, Appl. Surf. Sci. Adv. 11 (2022) 100282.

[6] M. Antonopoulou, C. Kosma, T. Albanis, I. Konstantinou, Sci. Total Environ. 765 (2021) 144163.

[7] N. López-Vinent, A. Cruz-Alcalde, C. Lai, J. Giménez, S. Esplugas, C. Sans, Sci. Total Environ. 803 (2022) 149873.

[8] A. Shokry, F. Audino, P. Vicente, G. Escudero, M.P. Moya, M. Graells, A. Espuña, Modeling and Simulation of Complex Nonlinear Dynamic Processes Using Data Based Models: Application to Photo-Fenton Process, Elsevier, 2015.

[9] M. Pérez-Moya, M. Graells, P. Buenestado, H.D. Mansilla, Appl. Catal. B Environ. 84 (2008) 313–323.

[10] G.E. do Nascimento, M.A. Soares Oliveira, R.M. da Rocha Santana, B.G. Ribeiro, D.C. Silva Sales, J.M. Rodríguez-Díaz, D.C. Napoleão, M.A. da Motta Sobrinho, M.M.M.B. Duarte, Water Sci. Technol. 81 (2020) 2545–2558.

[11] A. Cabrera Reina, L. Santos-Juanes, J.L. García Sánchez, J.L. Casas López, M.I. Maldonado Rubio, G. Li Puma, J.A. Sánchez Pérez, Appl. Catal. B Environ. 166–167 (2015) 295–301.

[12] P. Soriano-Molina, J.L. García Sánchez, O.M. Alfano, L.O. Conte, S. Malato, J.A. Sánchez Pérez, Appl. Catal. B Environ. 233 (2018) 234–242.

[13] L.O. Conte, A. V. Schenone, B.N. Giménez, O.M. Alfano, J. Hazard. Mater. 372 (2019) 113–120.

[14] S. Park, S. Oh, Chemosphere 260 (2020) 127532.

[15] A. Spaltro, M.N. Pila, D.D. Colasurdo, E. Noseda Grau, G. Román, S. Simonetti, D.L. Ruiz, J. Contam. Hydrol. 236 (2021) 103739.

[16] A. Galani, N. Alygizakis, R. Aalizadeh, E. Kastritis, M.A. Dimopoulos, N.S. Thomaidis, Sci. Total Environ. 798 (2021) 149014.

[17] S. Wang, J. Wu, X. Lu, W. Xu, Q. Gong, J. Ding, B. Dan, P. Xie, Chem. Eng. J. 358 (2019) 1091–1100.

[18] G. Dalgic, F.I. TURKDOGAN, K. Yetilmezsoy, E. Kocak, Chem. Ind. Chem. Eng. Q. 23 (2017) 177–186.

[19] P. Pal, R. Thakura, IEEE Int. Conf. Power, Control. Signals Instrum. Eng. ICPCSI 2017 (2018) 802–810.

[20] F. Audino, L.O. Conte, A.V. Schenone, M. Pérez-Moya, M. Graells, O.M. Alfano, Environ. Sci. Pollut. Res. 26 (2018) 4312–4323.

[21] R.F.P. Nogueira, M.C. Oliveira, W.C. Paterlini, Talanta 66 (2005) 86–91.

[22] E. Yamal-Turbay, E. Ortega, L.O. Conte, M. Graells, H.D. Mansilla, O.M. Alfano, M. Pérez-Moya, Environ. Sci. Pollut. Res. 22 (2014) 938–945.

[23] F. Audino, J.M.T. Santamaria, L.J. Del Valle Mendoza, M. Graells, M. Pérez-Moya, Int. J. Environ. Res. Public Health 16 (2019) 505.

[24] M. Pérez-Moya, T. Kaisto, M. Navarro, L.J. del Valle, Environ. Sci. Pollut. Res. 24 (2017) 6241–6251.

[25] M. Simunovic, H. Kusic, N. Koprivanac, A.L. Bozic, Chem. Eng. J. 173 (2011)

280–289.

[26] J.J. Pignatello, E. Oliveros, A. MacKay, Crit. Rev. Environ. Sci. Technol. 36 (2006) 1–84.

[27] B.N. Giménez, L.O. Conte, O.M. Alfano, A. V. Schenone, J. Photochem. Photobiol. A Chem. 397 (2020) 112584.

[28] L.O. Conte, J. Farias, E.D. Albizzati, O.M. Alfano, Ind. Eng. Chem. Res. 51 (2012) 4181–4191.

[29] I.B.A. Falconi, | Marcela, P.G. Baltazar, D.C.R. Espinosa, | Jorge, A.S. Tenório, B.A. Falconi, (2020).

[30] J.J. Plgnatello, Environ. Sci. Technol. 26 (1992) 944–951.

[31] M.I. Litter, Environ. Photochem. Part II 2 (2005) 325–366.

[32] E. De Laurentiis, C. Prasse, T.A. Ternes, M. Minella, V. Maurino, C. Minero, M. Sarakha, M. Brigante, D. Vione, Water Res. 53 (2014) 235–248.

[33] H. Kusic, I. Peternel, S. Ukic, N. Koprivanac, T. Bolanca, S. Papic, A.L. Bozic, Chem. Eng. J. 172 (2011) 109–121.

[34] B.I. Escher, R. Baumgartner, J. Lienert, K. Fenner, Handb. Environ. Chem. Vol. 2 React. Process. 2 P (2009) 205–244.

Supplementary material

Kinetic Model of Photo-Fenton Degradation of Paracetamol in an Annular Reactor: Main Reaction Intermediates and Cytotoxicity Studies

Giménez Bárbara N.[a], Conte Leandro O.[a], Audino Francesca[b], Schenone Agustina V.[a], Graells Moisès[b], Alfano Orlando M.[a], Pérez-Moya Montserrat[b*]

[a]*Instituto de Desarrollo Tecnológico para la Industria Química (INTEC), Consejo Nacional de Investigaciones Científicas y Técnicas (CONICET) and Universidad Nacional del Litoral (UNL), Ruta Nacional N◦ 168, 3000, Santa Fe, Argentina.*

[b]*Chemical Engineering Department, Universitat Politècnica de Catalunya, Escola d'Enginyeria de Barcelona Est (EEBE), Av. Eduard Maristany, 16, Barcelona 08019, Spain.*

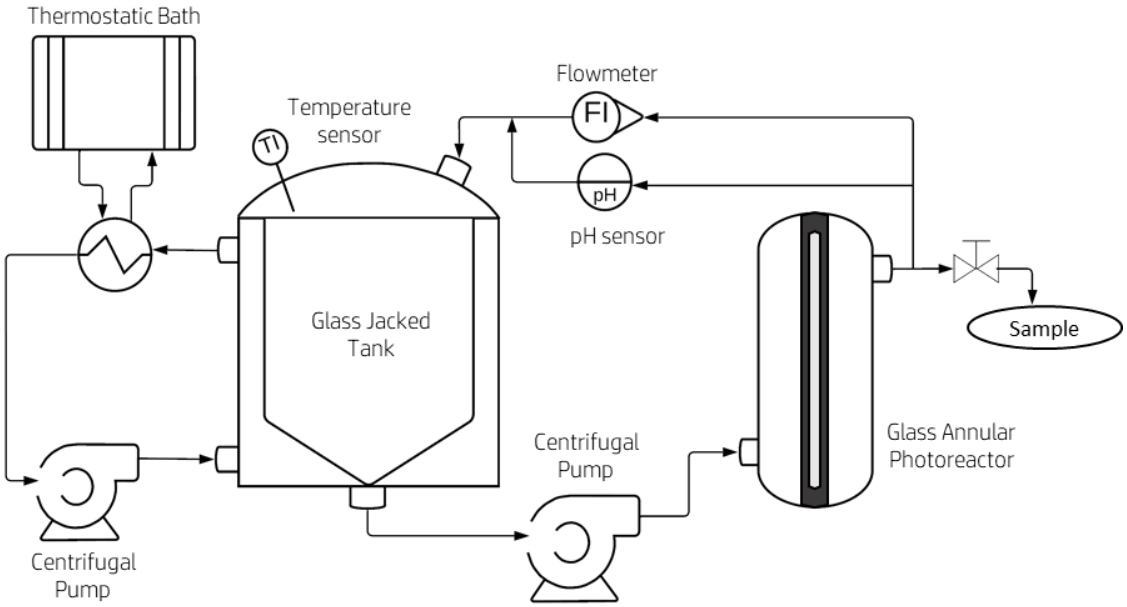

Annular reactor specifications		
Annular irradiated height		130 mm
Outer cylinder	Outer diameter	150 mm
	Inner diameter	140 mm
Inner cylinder	Outer diameter	70 mm
	Inner diameter	63.6 mm

Figure S1. Experimental device and annular photoreactor specifications.

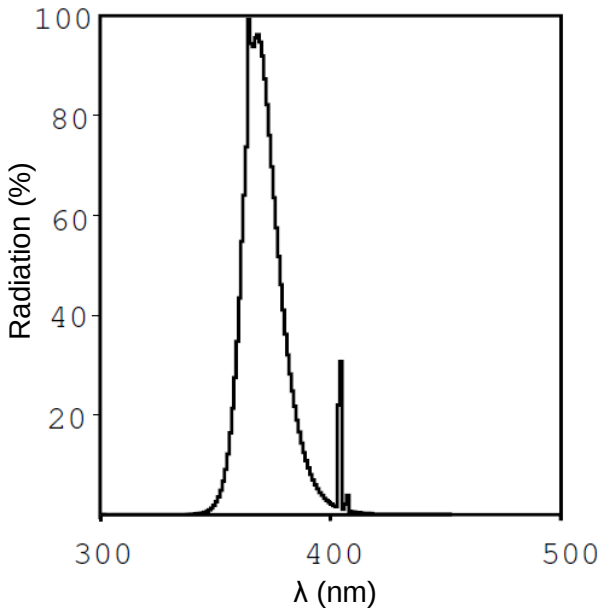

Figure S2. Spectral distribution of output power associated with Philips actinic lamp model BLTL-DK 36 W/10 1SL.

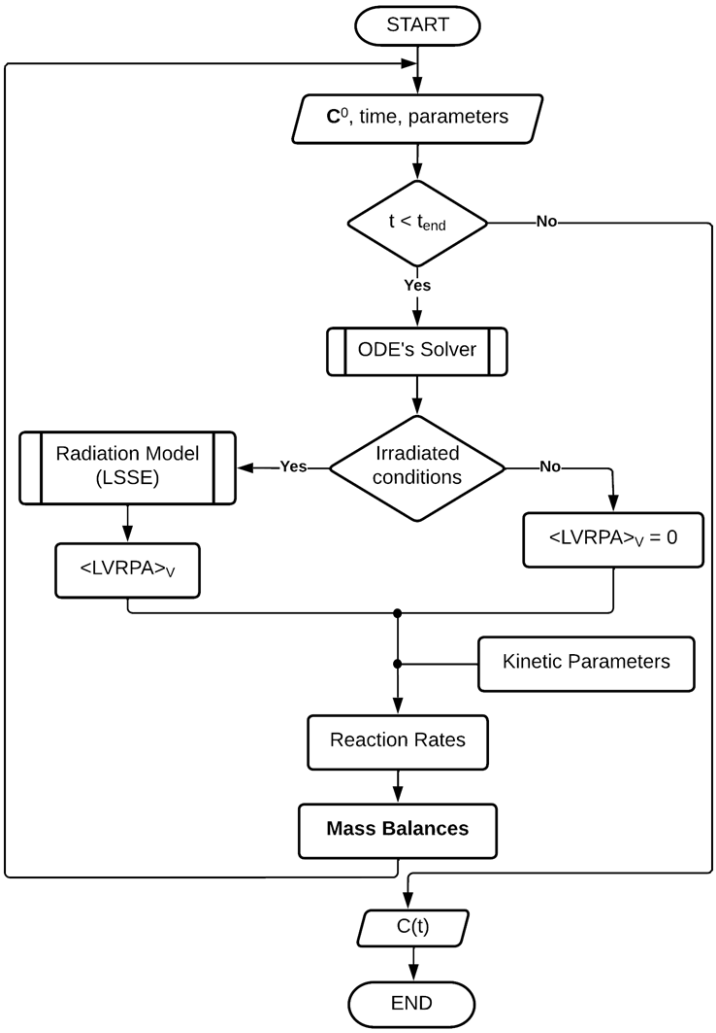

Figure S3. Flow diagram of the program used to obtain the kinetic parameters and the simulations of the experimental data.

ANEXO D. Influence of simulated solar radiation on micropollutant removal with ferrioxalate-assisted photo-Fenton

El trabajo mostrado a continuación ha sido presentado en el "*5th Iberoamerican Conference on Advanced Oxidation Technologies (V CIPOA)*"

Influence of simulated solar radiation on micropollutant removal with ferrioxalate-assisted photo-Fenton

A. Schenone[1], B. Giménez[1], L. Conte[1], O. Alfano[1].

(1) Instituto de Desarrollo Tecnológico para la Industria Química (INTEC), Universidad Nacional del Litoral (UNL) and Consejo Nacional de Investigaciones Científicas y Técnicas (CONICET). Predio Dr. A. Cassano, RN Nº 168, Santa Fe, Argentina, aschenone@intec.unl.edu.ar.

Abstract

This study is focused on the degradation of paracetamol (PTC) at µg per liter level, by photo-Fenton at near neutral pH, using ferrioxalate as iron source and simulated solar radiation. To this aim, 500 µg L^{-1} was treated with low concentration of Fenton reagents (Fe = 1 mg L^{-1} and H_2O_2 = 2.36 mg L^{-1}), and the incident irradiation was evaluated in three levels: OFF (Fenton), LOW (31.6 W m^{-2}) and HIGH (57.5 W m^{-2}). PCT was monitored during the reaction by the aid of an optimized solid phase extraction technique followed by HPLC-UV/Vis. The lowest PCT conversion after 90 min of reaction was obtained in the dark reaction, meanwhile 94.4% was achieved with the HIGH radiation level, highlighting the beneficial effect of radiation on the system. In addition, the value of oxidant consumption obtained for Fenton process was higher than the corresponding values observed for photo-Fenton system.

Introduction

In recent years, the production and consumption of a number of pharmaceuticals has increased considerably due to the growth and development of society. Among analgesics, acetaminophen or paracetamol (PCT) occupies the top of the list, which

consumption has increased during the COVID-19 pandemic in 2020/21. This drug has a high removal rate (>90%) in wastewater treatment plants (WWTPs) [1], but has still been detected in wastewater effluents at levels up to μg/L, because most WWTP are not designed to remove emerging pharmaceutical contaminants.

Among Advanced Oxidation Processes (AOPs), photo-Fenton, which involves the reaction between Fe ions and hydrogen peroxide (HP) to form reactive species capable of oxidizing different organic compounds, have been used for the removal of this type of contaminant [2]. In order to avoid the high consumption of reagents involved in operating at acidic pH, different complexing agents have been studied, which keep Fe in solution. Oxalate was used as the complexing agent in this study. This complexed iron not only allows to perform the reaction at near neutral pH, but also it greatly improves the photocatalytic activity of the system [2].

The aim of this study was to evaluate the efficiency of the ferrioxalate assisted photo-Fenton process at near neutral pH, in the removal of PCT at low concentration. As it is known, HPLC coupled to tandem mass spectrometry is the technique of choice for the determination and quantification of pharmaceuticals in environmental samples. However, this equipment is still very expensive and they are not available in many laboratories. On the other hand, almost all laboratories have HPLC systems with UV-Vis absorbance detection that may effectively be used for the analysis of pharmaceuticals in environmental samples, after an adequate pre-concentration step, which allows the detection of low concentrations and simultaneously removes the interferences. This is often performed by solid phase extraction (SPE).

Material and Methods

The experiments were carried out in a lab-flat plate photoreactor of borosilicate

glass with external recycling, irradiated from one side with a solar simulator (Oriel, model 9600) [2]. Two different filters combinations were studied, so as to simulate two solar radiation conditions. Local radiation flux averaged over the reactor window (q_W) was measured with a modular USB spectrometer (Ocean Optics), giving 31.6 and 57.5 W m^{-2}, respectively. For all tests, pH was 5.5 and temperature 25 °C, initial PCT concentration was 500 µg L^{-1}, initial HP concentration was 2.36 mg L^{-1}, Fe^{3+} concentration was set at 1 mg L^{-1} and oxalate (Oxa) concentration was 14.95 mg L^{-1}. The effect of radiation (LOW, HIGH or OFF) on PCT degradation was assessed. For the quantification of PCT during the reaction, it was firstly extracted from aqueous samples using SPE cartridges, Strata C18-U 500 mg/3 mL (Phenomenex), with the aid of a SPE Vacuum Manifold System of 12 ports. Different tests were carried out, in order to obtain a protocol to achieve the highest recovery of PCT, including matrix effect evaluation from the different reactive species present in the reaction medium. Sodium sulfite was added to the samples to stop the reaction. The cartridges were conditioned with 3 mL of methanol, followed by 3 mL of water. Then, 15 mL of sample was applied to the cartridge. Finally, after the washing step with 3 mL of water, PCT was extracted with 3 mL of acetonitrile/methanol (50:50), and injected to the HPLC system. The recovery percentage was above 97%, in all the tests, including the matrix effect study.

Results and Discussion

It was possible to quantify PCT so as to monitor its degradation during the reaction thanks to the application of the optimized SPE protocol with C18 commercial cartridges, followed by HPLC analysis.

Figure 1 shows the evolution of PCT, HP and Oxa in the three evaluated conditions. At 90 min of reaction, PCT conversions were 26.6 %, 71 % and 94.4% for OFF, LOW

and HIGH radiation levels, respectively.

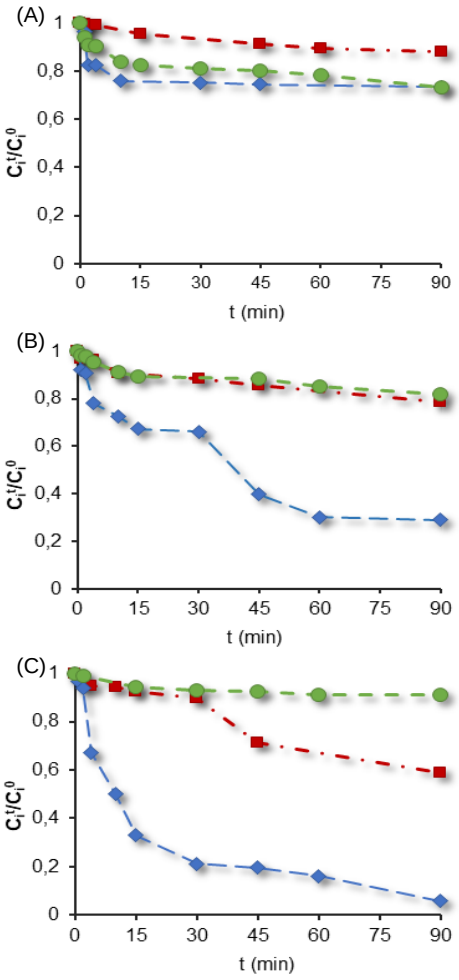

Figure 1. Experimental relative concentrations versus time for PCT (blue-diamonds), hydrogen peroxide (red-squares) and oxalate (green-circles), for (A) OFF, (B) LOW and (C) HIGH radiation level.

As can be seen, higher values were obtained in the irradiated assays, being more important at high radiation level. In this figure, it is also appreciated HP degradation, which is associated to the formation of oxidant species; and a low conversion of Oxa (the highest conversion was at HIGH radiation: 42%), which is desirable to keep iron in solution.

It is also important to mention, that the tests were carried out with a very low concentration of iron (1 mg L^{-1}), and this value was mantained in solution during the 90

min of reaction (data not shown) regarding the pH of the medium.

Finally, the consumption of HP was also evaluated at 90 min of reaction, as indicated by the following equation:

$$Y^{t}_{HP/PCT} = \frac{C^{0}_{HP} - C^{t}_{HP}}{C^{0}_{PCT} - C^{t}_{PCT}} \qquad (1)$$

The values obtained for the three conditions were 3.83, 2.13 and 3.4 mg HP/mg PCT, for OFF, LOW and HIGH radiation levels, respectively. These results highlight a less efficient consumption of H_2O_2 under nonirradiated conditions. Among the irradiated tests, a higher consumption was reached in the case of HIGH level, but it should be taken into account that only in this assay PCT is almost completely degraded after 90 minutes of reaction.

Conclusions

Low concentration of paracetamol could be successfully degraded under photo-Fenton conditions at pH=5.5 using low concentration of iron complexed with oxalate. The best results were obtained with the addition of simulated solar radiation to the system. Furthermore, the use of radiation allowed an enhancement of the process performance since a less efficient consumption of HP was observed under nonirradiated conditions.

Acknowledgments

The authors are grateful to Universidad Nacional del Litoral (UNL), Consejo Nacional de Investigaciones Científicas y Técnicas (CONICET), and Agencia Nacional de Promoción Científica y Tecnológica (ANPCyT) for financial support.

References

[1] R. Moreno-González, S. Rodriguez-Mozaz, M. Gros, D. Barceló, V.M. León.

Environmental Research, 138 (2015) 326.

[2] B. Giménez, A. Schenone, O. Alfano, L. Conte, Environmental Science and Pollution Research, 28 (2021) 23946.

ANEXO E. Improvement of ferrioxalate assisted Fenton and photo-Fenton processes for Paracetamol degradation by hydrogen peroxide dosage

El artículo presentado a continuación ha sido publicado en la revista "*Environmental Science and Pollution Research"*

Improvement of ferrioxalate assisted Fenton and photo-Fenton processes for Paracetamol degradation by hydrogen peroxide dosage

Bárbara N. Giménez[1,2], Leandro O. Conte[1,3], Sofía A. Duarte[2], Agustina V. Schenone[1,2]

[1]*Instituto de Desarrollo Tecnológico para la Industria Química (INTEC), Consejo Nacional de Investigaciones Científicas y Técnicas (CONICET) and Universidad Nacional del Litoral (UNL), Ruta Nacional Nº 168, 3000, Santa Fe, Argentina*

[2]*Facultad de Bioquímica y Ciencias Biológicas, Universidad Nacional del Litoral (UNL), Santa Fe, Argentina*

[3]*Facultad de Ingeniería y Ciencias Hídricas, Universidad Nacional del Litoral (UNL), Santa Fe, Argentina*

Abstract

This work aimed to investigate the impact of hydrogen peroxide (HP) punctual dosage on paracetamol (PCT) degradation, through Fenton and photo-Fenton processes under near-neutral pH conditions, using ferrioxalate and artificial sunlight. The assays were performed using a D-optimal experimental design, to statistically evaluate the influence of radiation (ON or OFF), HP concentration (94.5-756 mg L^{-1}), and HP dosage (YES or NO), on PCT conversion. The optimal conditions determined from the study were: HP = 378 mg L^{-1}, DOS = YES, and RAD = ON, achieving a predicted PCT conversion of 99.68% in 180 min. This result obtained from the model was very close to the experimental one (98.80%). It was verified that HP dosage positively influenced the iron catalytic cycle since higher Fe^{2+} concentrations were reached at shorter reaction times, accelerating not only PCT conversion but also its by-products hydroquinone and 1,4-benzoquinone, leading to better performances of Fenton and photo-Fenton reactions. Under optimal conditions and employing real water matrices (an artificial matrix with inorganic anions, a real groundwater sample, and a synthetic industrial wastewater), HP dosage demonstrated the ability to mitigate the negative effects caused by the content of different ions and other organic compounds and significantly improve HP consumption in challenging wastewater conditions.

Keywords: Advanced Oxidation Process; Fenton; photo-Fenton; Acetaminophen; Hydrogen Peroxide Dosage; Real Water Matrix; Ferrioxalate; Natural pH.

Introduction

The Fenton and photo-Fenton processes are very popular and effective advanced oxidation processes (AOPs) for the treatment of natural waters and wastewaters with a wide range of contaminants of emerging concern (CECs), which are difficult to treat with conventional processes (Malato et al. 2020). The photo-Fenton mechanism is based on H_2O_2 decomposition by Fe^{2+} under acidic conditions, which generates Fe^{3+} and hydroxyl radicals (HO•). The regeneration of Fe^{2+} from Fe^{3+} is considered the limiting step in the catalytic cycle. Light plays a crucial role in the photo-Fenton process as it catalytically regenerates Fe^{2+} ions, thereby accelerating the reaction (Machado et al. 2023). The photo-Fenton process could be enhanced by working with iron complexes, which allows operation at neutral pH and prevents iron precipitation (Ahile et al. 2020). Furthermore, the iron-oxalate complex allows the photo-Fenton process to occur at wavelengths up to 580 nm, opening up the possibility of using solar energy as a renewable irradiation source (Conte et al. 2019).

The detection of CECs in the water cycle is increasingly frequent, due to the uncontrolled or poorly regulated discharge of wastewater to the environment, resulting in high levels of pollution with this type of contaminants (Marson et al. 2022). Regarding pharmaceutical products, the most commonly consumed analgesic is Paracetamol (PCT) (Spaltro et al. 2021). It is extensively used to alleviate pain and fever, and it is recommended for treating COVID-19 mild symptoms (Galani et al. 2021). Consequently, large amounts of PCT and its by-products are discharged into water systems due to their low absorption in the human body (Wang et al. 2019). Accordingly, different amounts of PCT (up to 294 mg L^{-1}) were detected in hospital effluents, industrial wastewater coming from pharmaceutical plants (Dalgic et al. 2017; Pal and Thakura 2018; Eniola et al. 2022), and urban sewage treatment plants, and consequently, in groundwater, drinking and

surface water (Wang and Bian 2020; Marson et al. 2022). Although most studies indicate that pharmaceuticals are generally found in low concentrations in the environment, they can reach concentrations of mg L^{-1} in surface waters near pharmaceutical industrial facilities (Nascimento et al. 2020).

In this type of aqueous matrices, different species may be present and inhibit CECs degradation through the photo-Fenton process. Anions, such as chlorides, nitrates, bicarbonates, and sulphates, are reported to interfere with the reaction by scavenging the HO• radicals generated, thus decreasing the pollutant's degradation rate and increasing the consumption of hydrogen peroxide (among other effects) (Malato et al. 2020; Wang and Wang 2021). An alternative that would mitigate the inefficient use of the oxidizing agent in the process could be the punctual dosage of hydrogen peroxide by dividing the total supply into several doses and adding them at different reaction times (Yu et al. 2020). Furthermore, when the main focus is the cost of the process, the oxidizing agent can be considered the most expensive reactive, when the system is operated at natural pH and using solar radiation (Oller and Malato 2021). As it is known, hydrogen peroxide can limit the speed of the process if it is applied at too low concentrations. On the contrary, at very high concentrations this reagent can compete with the CECs for the generated HO•, affecting pollutants degradation rates. Additionally, HP can self-decompose into oxygen and water (Yu et al. 2021). Taking into account these drawbacks, an HP dosage strategy could have a possible beneficial effect, considering that the oxidant is one of the most important operating parameter, which affects reaction rates as well as the overall process efficiency.

In the literature, there are several works where hydrogen peroxide dosage was analysed in the photo-Fenton system, using iron sulphate salts in an acid medium (Audino et al. 2019; Yu et al. 2020; Nasr Esfahani et al. 2022; Rodríguez-García et al. 2023). On

the contrary, few articles where HP dosage is applied in the ferrioxalate-assisted photo-Fenton process are found. Monteagudo et al. (2009) evaluated the continuous addition of hydrogen peroxide and air for Orange II degradation. The analysed variables were HP and air flow rates, pH (3-6), and initial concentration of Fe(II) (0-10 mg L^{-1}) and oxalic acid (0-60 mg L^{-1}). As a result, TOC removal was greater with the continuous addition of peroxide compared to the addition of HP at the beginning of the reaction. The same authors (Monteagudo et al. 2010) studied later the same dosage strategy for Reactive Blue 4 degradation. Another strategy was evaluated by Soares et al. (2015), in which small amounts of HP were added during the treatment of textile wastewater, keeping the desired HP concentration between a range of study. Iron was complexed with oxalate, but the pH of the reaction was set at 2.8. The results showed that the strategy improved the mineralization rates minimizing the oxidant consumption rate as well.

In the present research work, the main objective was to evaluate the influence of the oxidizing agent dosage on PCT degradation. The dosage strategy consisted of two pulses and the analysis of two other important variables for the process such as: radiation level (ON or OFF) and hydrogen peroxide concentration (between 94.5 and 756 mg L^{-1}). For this purpose, a Design of Experiments (DoE) was used. This statistical tool allows following a multivariate approach, essential when the variables to be studied are not independent of each other, as the case shown in the present research. In addition, experimental designs help to reduce the number of experiments, optimizing time and cost, while maximizing the quality of the obtained information (Parra-Marfil et al. 2023). The behaviour of the Fenton and photo-Fenton systems, as regards the dosage of the oxidizing agent, was studied at a near-neutral pH (5.5) using the ferrioxalate complex as catalyst, and a solar simulator as the radiation source. To our knowledge, no publications

investigate these processes under the evaluated conditions. This artificial sunlight source serves as a preliminary step for studying the system in a solar pilot plant reactor.

Additionally, the efficiency of the process was evaluated employing real water matrices (an artificial matrix with inorganic anions, a real groundwater sample, and a synthetic industrial wastewater coming from a pharmaceutical plant) with different content of ions and other organic compounds, under the hypothesis that the dosage of the oxidizing agent can reduce the consumption of HP in the degradation process and increase contaminant degradation.

Materials and Methods

Chemicals and analytical determinations

Paracetamol (Sigma-Aldrich, 98% purity) was employed as the model pollutant. PCT,1,4-benzoquinone (BQ) and hydroquinone (HQ) (both Fluka, 99% purity) concentrations were analysed by HPLC as indicated in Giménez et al. (2020). Hydrogen peroxide (HP, Cicarrelli, 30%), Fe^{2+}, and total Fe ($FeCl_3.6H_20$, Merck, pro-analysis) were determined by colorimetric methods and oxalate ion (Oxa) was quantified by ion chromatography (Giménez et al. 2020). Finally, the achieved mineralization was monitored through TOC measurements, employing a vario TOC cube analyzer (Elementar). To prepare the ferrioxalate complex, solutions of potassium oxalate monohydrate (Carlo Erba, 99.5%) and iron(III) chloride were mixed in appropriate proportions. A reverse osmosis system (Osmoion, APEMA) was used to obtain ultrapure water (0.055 μS cm^{-1}). The maximum overall errors were 0.08, 0.15, 0.17, 1.14, 6.72 and 0.26 mg L^{-1} for PCT, HQ, BQ, TOC, HP and Fe, respectively (Miller et al. 2018).

Procedure and Experimental Device

All the experiments were performed using a lab-scale photoreactor irradiated by a solar simulator. Details of this experimental system can be found elsewhere (Giménez et

al. 2021). The averaged local radiation flux over the reactor window (q_W) was 92.80 W m^{-2} (32.2 nE cm^{-2} s^{-1}), within the wavelength range of 300 to 500 nm (USB spectrometer, Ocean Optics, USB2000).

The treated samples (total volume 3 L) consisted of: a) ultrapure water, b) artificial matrix (anions in ultrapure water), c) real groundwater, all spiked with the contaminant, and d) synthetic industrial wastewater coming from a pharmaceutical plant. Initial PCT, Oxa, and Fe concentrations were set at 40 mg L^{-1}, 47.5 mg L^{-1}, and 3 mg L^{-1} (molar ratio Fe/Oxa=1/10), respectively, in all the experiments. To reach a pH value of 5.5, concentrated NaOH or H_2SO_4 solutions were used, and the temperature was set to 25 °C. The concentration of iron was selected based on the permissible discharge values into a surface water course (5 mg L^{-1}) as specified in Resolución n° 1089/82 (1982). The selection of Oxa as a chelating agent was not only for its ability to keep iron in solution even at pH close to neutrality and for its good optical absorption properties but also taking into account that it is a natural low molecular weight organic acid. In addition, it is also a non-recalcitrant and non-toxic compound (Ahile et al. 2020, 2021; Conte et al. 2022b). Moreover, oxalate-associated toxicity expressed as EC_{50} at 15 min for *V. fischeri* is more than 450 mg L^{-1} (Santos et al. 2004). Finally, it is important to note that Oxa is produced and released to the environment in significant amounts by microorganisms and plants (Palmieri et al. 2019).

The oxidant dosage strategy consisted of two pulses of the same volume of HP standard solution, at reaction times 0 and 90 min. Each pulse contributed half of the total HP concentration of each run to the reaction medium.

An artificial sample with NaCl, Na_2SO_4 and $NaHCO_3$ (Cicarelli) was prepared. The final concentrations of each anion in the reaction volume (3 L) were: 80, 50, and 100 mg L^{-1}, for Cl^-, SO_4^{2-}, and HCO_3^-, respectively. The main characteristics of the real

groundwater sample and its composition are shown in Table 1. The synthetic industrial effluent was prepared using CIP300®, a neutral pH detergent, with a final concentration in the reaction medium of 0.1% (TOC = 54.74 mg C L^{-1}) and PCT pharmaceutical drug (LIF, Cert. ANMAT Nº 54.235), which contains pre-gelatinized starch, stearic acid, and povidone K30 as excipients. The drug solution was diluted to obtain an initial PCT concentration of 40 mg L^{-1} (TOC = 30.54 mg C L^{-1}).

Table 1. Main characteristics and components of groundwater

Parameter	*Value*	***Composition***	*Value (*mg L^{-1})
Conductivity	232 µs.cm^{-1}	**Bicarbonates**	112.1
pH	6.67	**Chlorides**	8.7
Total Alkalinity	92 mg L^{-1}	**Sulphates**	13.5
Total Hardness	101.4 mg L^{-1}	**Calcium**	28.4
Total Organic Carbon (TOC)	8.88 mg L^{-1}	**Magnesium**	7.4
Aerobic mesophilic bacteria	65 CFU/mL	**Sodium**	12.0
Gram negative bacteria	Absence	**Potassium**	2.7
		Total Iron	0.13

Experimental design and statistical analysis

A D-Optimal experimental design built from candidate points was employed. In particular, it was chosen because it can deal with numerical and categorical factors, with a mixed number of levels. The impact of HP concentration, HP dosage (DOS), and radiation level (RAD), represented as model variables *A*, *B*, and *C*, respectively, was evaluated on the pharmaceutical conversion. For two categorical variables (with two levels each) and one numerical variable (with continuous range), 24 experiments were performed including 8 model points, 12 runs to estimate the lack of fit, and 4 replicates. All the proposed experiments, as well as the coded and actual values of the parameters, can be found in Table 2 (Results and Discussion section). The levels of the mentioned factors were: NO and YES for DOS, OFF and ON for RAD, and a range between 94.5

and 756 mg L^{-1} for HP. These levels in coded values were marked as -1 and +1 for low and high levels, respectively. The response factor chosen was the percentage of PCT conversion after 180 minutes of reaction ($X_{PCT}^{180,exp}(\%)$).

The concentration of the oxidizing agent varied between 94.5 and 756 mg L^{-1}, which are the half of stoichiometric value needed for the complete mineralization of 40 mg L^{-1} of PCT and four times this value, respectively. The upper value was selected considering that higher conversion levels could be achieved in a shorter time when the concentration of hydrogen peroxide exceeds the stoichiometric requirement.

Once the experimental results of $X_{PCT}^{180,exp}(\%)$ were obtained, a mathematical model was developed. The following equation (1) (Giménez et al. 2020) represents the behaviour of the system:

$$Y = \beta_0 + \sum_{i=1}^{k} \beta_i X_i + \sum_{i=1}^{k} \beta_{ii} X_i^2 + \sum_{i=1}^{k} \sum_{j=1}^{k} \beta_{ij} X_i X_j + \varepsilon \quad (1)$$

In equation (1), *Y* represents the dependent variable or the selected response; *k* denotes the number of factors; *i* and *j* are the index numbers for factors; β_0 is the intercept term; $X_i...X_k$ are coded independent variables; the linear effect of the *i*th factor is represented by β_i, β_{ii} is the quadratic effect of the *i*th factor, β_{ij} represents the interaction effect between the *i*th and *j*th factors, and ε is the random error. The model obtained for PCT conversion was then statistically evaluated using an analysis of variance (ANOVA). It is worth noting that the experiments were done in random order to diminish the impact of unexpected variability in the observed response.

Results and Discussion

A D-optimal experimental design was applied to investigate the effects of three independent variables (one numerical and two categorical factors) on PCT conversion.

The complete set of experiments (24 runs), including: ranges of the variables, PCT experimental conversion, and PCT modelled conversion, are shown in Table 2.

The criterion adopted for the oxidizing agent dosage strategy considered the simplicity of its execution. Therefore, only one extra punctual addition was considered. The time selected to carry out this additional pulse was defined at 90 minutes of reaction. It was the most representative (in terms of system degradation efficiency) over different times (shorter and longer) analysed. It is worth mentioning that, in all the DoE experiments, no precipitation of the catalyst was observed during the entire reaction time (180 min). Then the total iron concentration present in the system was constant (Fe = 3 mg L^{-1}).

The conversion was defined as the disappearance of the reactant during the reaction and can be calculated with the following expression (Eq. 2) (Conte et al. 2022a):

$$X_i = \frac{C_i(t=0) - C_i(t)}{C_i(t=0)} * 100\% = \left(1 - \frac{C_i(t)}{C_i(t=0)}\right) * 100\% \quad (2)$$

PCT conversion was calculated at 180 min of reaction. This time was selected since the most significant differences were observed when the set of assays were compared (dark and irradiated test). Furthermore, at this time maximum conversions were achieved, not only for PCT but also for two main by-products (hydroquinone and p-benzoquinone).

Influence of the studied variables on PCT conversion

PCT conversions at 180 min of reaction ($X_{PCT}^{180,exp}$) are presented in Fig. 1, under all the studied conditions. Firstly, it is remarkable the differences in the conversions achieved when the variable radiation was studied. In the photo-Fenton reactions (Fig. 1b), these values were always higher than the obtained ones in dark conditions (Fig. 1a), for all HP concentrations. Moreover, in the presence of radiation, no run had a PCT conversion

below 80%, meanwhile in the Fenton assays only one combination of conditions exceeded this percentage (run #13, $X_{PCT}^{180,exp}$ = 83.21%, Table 2).

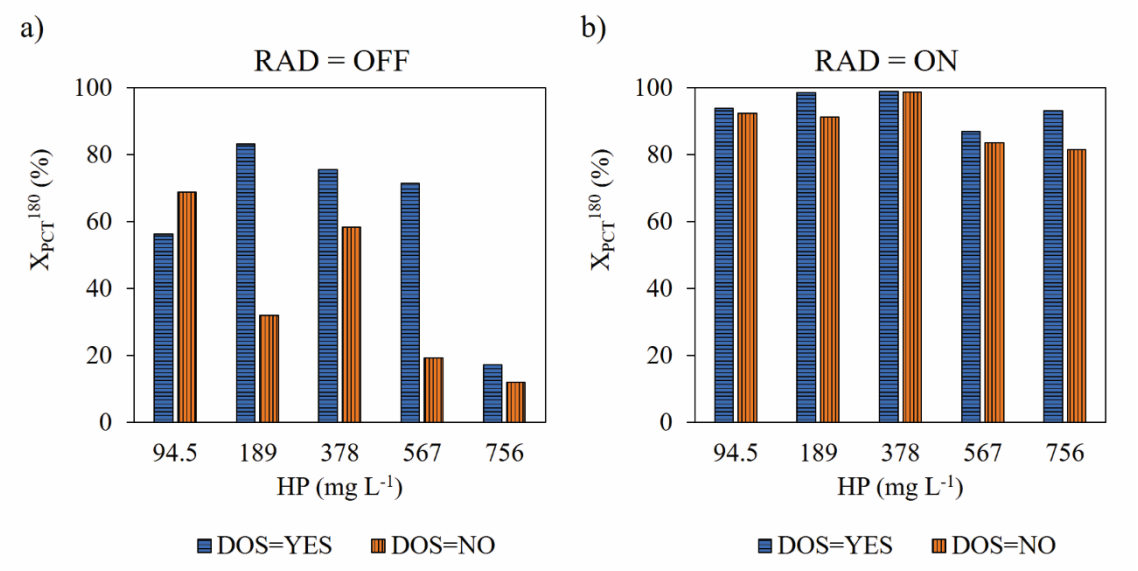

Fig. 1 Conversion of PCT at 180 min of reaction ($X_{PCT}^{180,exp}$) for all performed experiments: a) Fenton and b) photo-Fenton reactions. Runs with HP dosage are in blue and horizontal stripes and runs with no HP dosage are in orange and vertical stripes. Average results are shown for duplicated runs

Under all the studied conditions, for HP concentrations above 378 mg L^{-1}, a decrease in PCT conversion was observed. The consumption of HO• radicals by a HP excess also known as the scavenger effect of HP (Eq. (3), Yu et al. 2020) could be the cause or reason. Furthermore, higher quantities of HP promotes its decomposition (Eq. (4), Giménez et al. 2020), without the production of radicals, but generating O_2 and H_2O.

$$H_2O_2 + HO^{\bullet} \rightarrow HO_2^{\bullet -} + H_2O \quad (3)$$

$$2H_2O_2 \rightarrow 2H_2O + O_2 \quad (4)$$

Table 2. D-optimal experimental design for the homogeneous Fenton and photo-Fenton degradation of PCT

Name[a]	Run	Coded values			Actual values			$X_{PCT}^{180,exp}$	$X_{PCT}^{180,pred}$
	#	**A**	**B**	**C**	**HP**	**DOS**	**RAD**	(%)	(%)
RadON_189	1	-0.71	{ -1 }	{ 1 }	189	NO	ON	91.12	91.93
RadOFF_567_D	2	0.43	{ 1 }	{ -1 }	567	YES	OFF	71.36	52.89
RadOFF_94.5_D	3	-1	{ 1 }	{ -1 }	94.5	YES	OFF	56.23	88.62
RadOFF_756	4	1	{ -1 }	{ -1 }	756	NO	OFF	17.03	12.12
RadOFF_567	5	0.43	{ -1 }	{ -1 }	567	NO	OFF	20.04	35.28
RadON_756	6	1	{ -1 }	{ 1 }	756	NO	ON	81.52	82.00
RadOFF_378_D	7	-0.14	{ 1 }	{ -1 }	378	YES	OFF	75.48	70.98
RadON_378	8	-0.14	{ -1 }	{ 1 }	378	NO	ON	98.68	93.69
RadON_94.5_D	9	-1	{ 1 }	{ 1 }	94.5	YES	ON	93.72	95.14
RadON_189_D	10	-0.71	{ 1 }	{ 1 }	189	YES	ON	99.38	97.92
RadON_756_D	11	1	{ 1 }	{ 1 }	756	YES	ON	98.00	87.99
RadON_567_D	12	0.43	{ 1 }	{ 1 }	567	YES	ON	87.07	96.37
RadOFF_189_D	13	-0.71	{ 1 }	{ -1 }	189	YES	OFF	83.21	84.01
RadOFF_189	14	-0.71	{ -1 }	{ -1 }	189	NO	OFF	31.84	66.40
RadOFF_756_R	15	1	{ -1 }	{ -1 }	756	NO	OFF	6.99	12.12
RadON_567	16	0.43	{ -1 }	{ 1 }	567	NO	ON	83.56	90.38
RadOFF_756_D	17	1	{ 1 }	{ -1 }	756	YES	OFF	26.03	29.73
RadOFF_756_D_R	18	1	{ 1 }	{ -1 }	756	YES	OFF	8.48	29.73
RadON_378_D	19	-0.14	{ 1 }	{ 1 }	378	YES	ON	98.80	99.68
RadOFF_378	20	-0.14	{ -1 }	{ -1 }	378	NO	OFF	58.26	53.37
RadON_94.5	21	-1	{ -1 }	{ 1 }	94.5	NO	ON	92.25	89.15
RadOFF_94.5	22	-1	{ -1 }	{ -1 }	94.5	NO	OFF	67.78	71.01
RadOFF_94.5_R	23	-1	{ -1 }	{ -1 }	94.5	NO	OFF	69.55	71.01
RadON_756_D_R	24	1	{ 1 }	{ 1 }	756	YES	ON	88.13	87.99

[a]Outliers: #2, #3, #5, #14 y #18. D: dosage. R: replica.

Regarding HP dosage influence, in all the experiments, PCT abatement was higher in the runs where the oxidizing agent was dosed, comparing with the same conditions but when the full dose of HP was added at the beginning of the reaction. An exception was found under conditions RAD OFF and HP = 94.5 mg L^{-1} (run #3). This behaviour could be because when this level of HP was divided into two doses, the concentration at the beginning of the reaction was 1/4 the stoichiometric relationship between HP and PCT, making the oxidant act as the limiting reactant. Then, its performance was worse against the run where HP was not dosed (run #22) (Yu et al. 2020).

The difference in the system efficiency between runs with and without HP dosage was much more evident in Fenton reactions. In the case of Fenton reactions without the dosing strategy, when HP concentration increased from 378 to 756 mg L^{-1}, the conversion percentage decreased from 58.3 to 17.0% (runs #20 and #4, respectively). However, in the same conditions but with HP dosage ($X_{PCT}^{180,exp}$ = 75.5% and 26.0% for runs #7 and #17, respectively), better results were achieved. Moreover, for HP = 576 mg L^{-1}, there was a difference in PCT conversion greater than 50% in the case of HP dosage (run #2 $X_{PCT}^{180,\,exp}$= 71.36%; and run #5 $X_{PCT}^{180,\,exp}$ = 20.04%). In this sense, the highest PCT conversion achieved in dark conditions was 83.21% (run #13, HP = 189 mg L^{-1} and dosed), being similar to the worst conversion achieved in the presence of radiation (run #16, $X_{PCT}^{180,\,exp}$ = 83.56%, HP = 567 mg L^{-1}, without dosage).

In the photo-Fenton runs with 756 mg L^{-1} of HP, when the oxidant was divided in two doses better $X_{PCT}^{180,exp}$were achieved, from 81.5% to 98.0% without (run #6) and with HP dosage (run #11), respectively. The same behaviour was obtained with 567 mg L^{-1} of oxidant (run #16, $X_{PCT}^{180,exp}$ = 83.56%; and run #12, $X_{PCT}^{180,exp}$ = 87.07%).

Influence of HP dosing on the iron catalytic cycle

An important impact of HP dosing was observed in the Fe^{2+} temporal evolution. This effect is illustrated in Fig. 2 and could be the reason of the system performance improvement. As it can be seen, in all the presented runs (except for RAD ON and HP = 378 mg L^{-1}), higher Fe^{2+}concentrations were reached at shorter reaction times in those tests with HP dosage, for both operational conditions (with and without radiation).

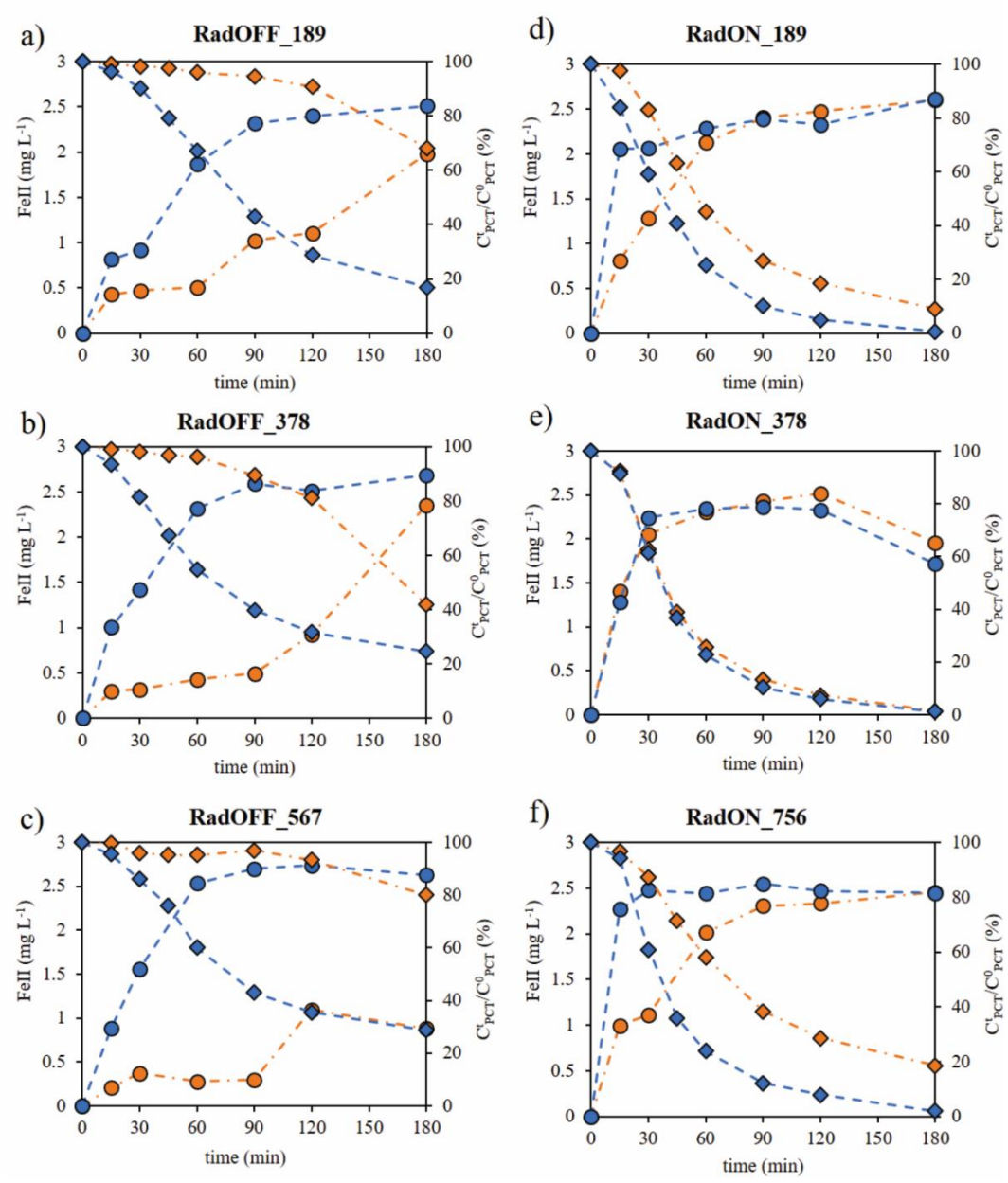

Fig. 2 Temporal evolutions of Fe^{2+} (in mg L^{-1}, symbols = circles) and PCT (in relative concentration %, symbols = diamonds) for: a) Rad = OFF and HP = 189 mg L^{-1}; b) Rad = OFF and HP = 378 mg L^{-1}; c) Rad = OFF and HP = 567 mg L^{-1}; d) Rad = ON and HP = 189 mg L^{-1}; e) Rad = ON and HP = 378 mg L^{-1}; f) Rad = ON and HP = 756 mg L^{-1}. Runs with HP dosage are in blue and long dash line and runs with no HP dosage are in orange and dash-dot line

When PCT temporal evolution was analysed in the Fenton reactions (Fig. 2 a, b, and c), a wide difference in the system efficiency (PCT in relative concentration) was observed considering whether the oxidizing agent was dosed. Here, the difference between the PCT relative concentrations (%) with and without HP dosage were 51.37, 17.22 and 52.22% for HP = 189 (runs #14 vs. #13), 378 (runs #20 vs. #7) and 567 (runs #5 vs. #2) mg L^{-1}, respectively.

In the conditions depicted in Fig. 2e (RAD ON and HP = 378 mg L^{-1}), Fe^{+2} profiles are very similar, which leads to the fact that there were no significant differences in PCT conversion towards the end of the reactions. For the other two photo-Fenton presented runs, more (Fig. 2f) and less (Fig. 2d) important differences were observed in the time profiles of Fe^{2+}, which directly affected the differences in the achieved PCT conversions.

Moreover, the temporal evolution profiles of HQ and BQ were also studied. Fig. 3 illustrates three photo-Fenton runs with HP = 189, 378, and 756 mg L^{-1}, respectively. These HP conditions are the same as those presented for the temporal evolution of Fe^{2+} (Fig. 2d-f).

Under the dosage strategy, the intermediates appeared and disappeared earlier than in the runs without HP dosage. The most noticeable difference was found in the presence of radiation and 756 mg L^{-1} of HP, in which the by-products were eliminated towards the end of the reaction when HP was dosed. However, the same conditions but without dosage, there was still an important quantity of HQ before the end of the process. In the case of Fenton reactions, the same behaviour was observed (data not shown). The intermediates removal is a favourable result considering the knowledge of their toxicity. Qutob et al. (2022) studied and summarized PCT degradation pathways, their by-products and biotoxicity, considering HQ and BQ as harmful.

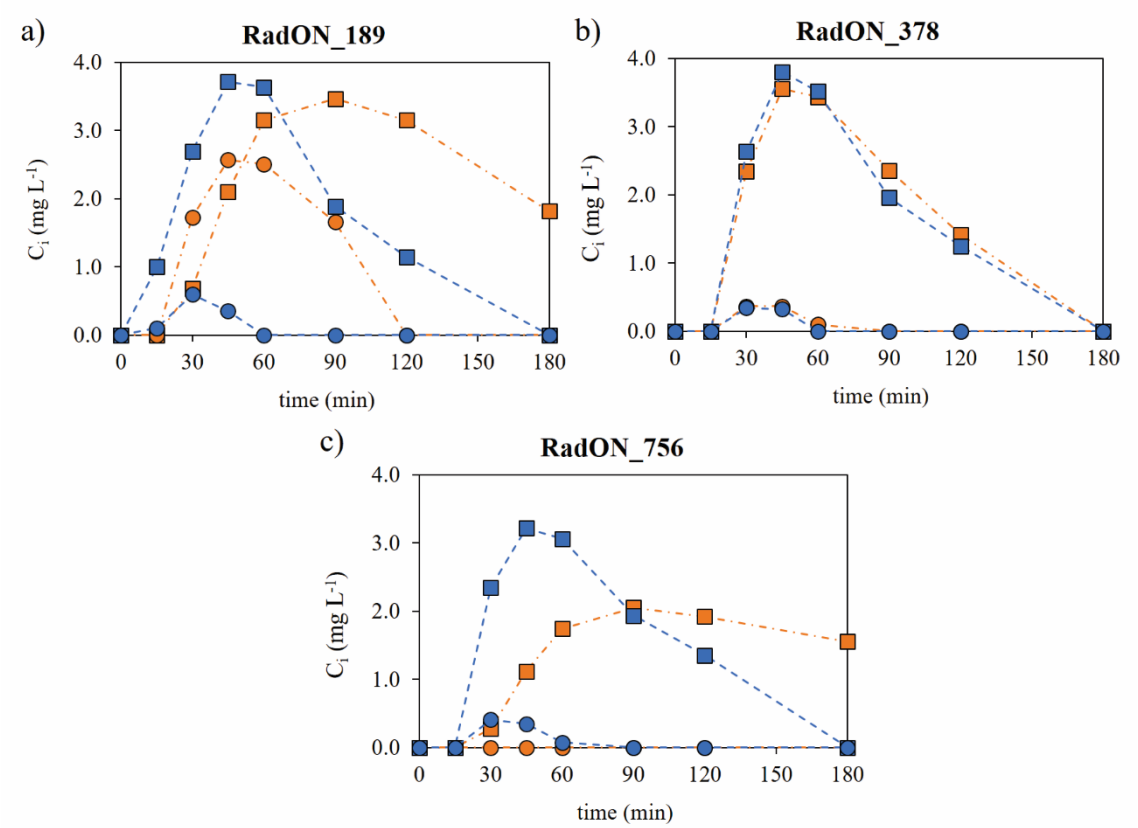

Fig. 3 Experimental concentrations vs. time for HQ (symbols = squares) and BQ (symbols = circles) in photo-Fenton runs, for three different HP concentrations: a) 189 mg L^{-1}, b) 378 mg L^{-1} and c) 756 mg L^{-1}. Runs with HP dosage are in blue and long dash line, and runs with no HP dosage are in orange and dash-dot line

Therefore, these results demonstrated the positive effect of the HP dosage strategy over the iron catalytic cycle, leading to better performances of Fenton and photo-Fenton reactions. Here, and from the kinetic model developed and validated by Giménez et al. (2021) (Eq. (5-11)); the hydroxyl production is strongly affected by the low dark reaction rate of ferrioxalate with the oxidizing agent (Fe^{2+} regeneration, Eq. (6)), which is considered the limiting step of the system. At this point, the radiation favours the reduction of ferrioxalate (Eq. (5)), improving the production of hydroxyl radicals. These hydroxyl radicals are then responsible for producing the oxidation of PCT (Eq. (8)) and its by-products HQ (Eq. (9)) and BQ (Eq. (10)). However, at the same time, the hydroxyl radical undergoes unproductive consumption reactions (Eq. (3) and (11)), being the reaction with the oxidizing agent (Eq. (3)) the main responsible for the loss of efficiency

in the system. Thus, the amounts of Fe^{2+} and HP in the system dominate the oxidative process. There is a compromise between not limiting the degradation process due to a very low HP concentration and not reaching an excess of oxidant. Thus, the dosage is then a critical point in the system (Yu et al. 2021).

$$Fe^{3+}(C_2O_4)_3^{3-} \overset{h\nu}{\rightarrow} Fe^{2+}(C_2O_4) + CO_2 + 1.5\,(C_2O_4)^{2-} \quad (5)$$

$$Fe^{3+}(C_2O_4)_3^{3-} + H_2O_2 \overset{k_1}{\rightarrow} Fe^{2+}(C_2O_4) + 2\,(C_2O_4)^{2-} + HO^- + HO^\bullet \quad (6)$$

$$Fe^{2+}(C_2O_4) + H_2O_2 + 2\,(C_2O_4)^{2-} \overset{k_2}{\rightarrow} Fe^{3+}(C_2O_4)_3^{3-} + HO^- + HO^\bullet \quad (7)$$

$$PCT + HO^\bullet \overset{k_4}{\rightarrow} HQ \quad (8)$$

$$HQ + HO^\bullet \overset{k_5}{\rightarrow} BQ \quad (9)$$

$$BQ + HO^\bullet \overset{k_6}{\rightarrow} products \quad (10)$$

$$C_2O_4^{2-} + HO^\bullet \overset{k_7}{\rightarrow} products \quad (11)$$

As regards TOC conversion after 180 min of reaction (X_{TOC}^{180}), only for irradiated tests the reached values were higher than 10%. The addition of Oxa in the system was essential to avoid iron precipitation at a pH value of 5.5. The ligand concentration contributes with 12.96 mgC L^{-1} of the total TOC value. For this reason, complete TOC conversion with the consequent oxalate degradation, was not desirable. As an example, in runs RadOFF_378_D and RadON_189_D, the final oxalate concentration at 180 min (expressed as mg of C L^{-1}) represented 33 and 35% of the final TOC. Considering that fact in both runs, at the end of the reaction, neither HQ nor BQ were detected (Fig. 3 a and c), the rest of the TOC content that was not oxalate was believed to be short chain carboxylic acids. This assumption was made considering the PCT reaction mechanism

(Giménez et al. 2020; Pacheco-Álvarez et al. 2022), and the chromatographic profiles obtained from the samples at 180 min of reaction (data not shown).

Process optimization

Based on the experimental results obtained from the execution of the proposed D-optimal design (Table 2), it was possible to establish a regression model that relates the different evaluated levels of each factor, as well as their interactions, with the studied response ($X_{PCT}^{180}(\%)$). The model coefficients were calculated with a multiple regression method, resulting in the following expression, in coded variables:

$$\boldsymbol{X_{PCT}^{180,pred}}(\%) = +77.23 - 16.51 * A + 5.90 * B + 19.10 * C + 12.94 * A * C - 2.90 * B * C - 7.76 * A^2 \quad (12)$$

in which *A*, *B*, and *C* represent the coded values for HP, DOS, and RAD, respectively. The interactions between factors are denoted with the combination of variables, such as *AC* and *BC*. In the case of categorical factors and their interaction among them or with numerical factors, the physical interpretation is not simple and may even be impossible, so only a mathematical reading is possible (Amiri and Behin 2020).

The analysis of variance (ANOVA) with a 95% confidence level was performed to evaluate the presented model and to validate its coefficients. The model was statistically significant, according to the calculated *F* (70,92) and the low *p* value ($p < 0{,}0001$). Furthermore, the lack of fit was non-significant (p=0,5737). The regression analysis resulted in high coefficients, with: R^2= 0.9726, Adjusted-R^2= 0.9589 and coefficient of variation: 7.70%. The ANOVA analysis yielded values of $p < 0.05$ for all the effects considered by the model (HP, DOS, Rad, HP*RAD, DOS*RAD, and HP^2), indicating that they were significant at the 95% confidence level. It is important to mention that experiments N°=2, 3, 5, 14, and 18 were considered outliers, so they were removed for

the elaboration of this model. Fig. 4 depicts: a) the residuals as a function of the predicted responses, and b) the normal probability plot of the residuals. In the former, all the experimental points exhibited similar variances, and the residuals were randomly distributed around zero. Therefore, it can be concluded that the data satisfy the assumption of homoscedasticity. Moreover, the residuals followed a straight line in the normal probability plot, indicating a normal distribution (Fig. 4b).

Overall, the results from the analysis of the D-optimal design supported the regression model, demonstrating its statistical significance and adequacy in explaining the relationship between the factors (HP, DOS, RAD) and the response variable.

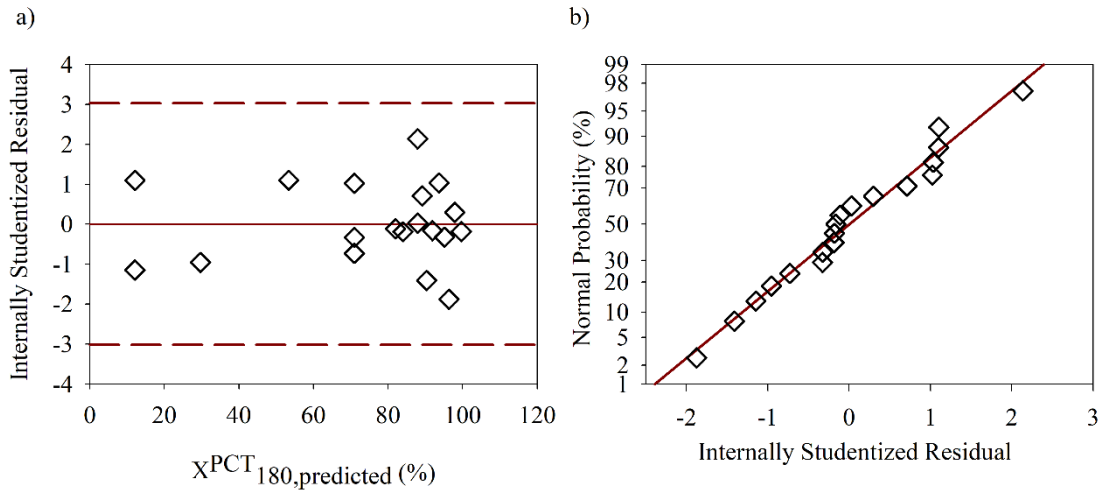

Fig. 4 Diagnostics plots for the prediction of PCT conversion. a) Internally studentized residuals vs. predicted values plot and b) normal probability plot

Finally, the optimization step was assessed to find the values of the operational variables that maximize PCT conversion. The model predicted that the optimal conditions were as follows: HP = 378 mg L^{-1}, DOS = YES, and RAD = ON. The optimization process aimed to maximize the response, while keeping the factors HP, DOS, and RAD within the range of study. Based on the model's predictions, the pharmaceutical conversion $X_{PCT}^{180,\,pred}$ was estimated to be 99.68%, a value very close to the one experimentally obtained ($X_{PCT}^{180,\,exp}$ = 98.80%)

Application of the optimized conditions in real water matrices

The performance of the system under optimal conditions (RAD ON, HP = 378 mg L^{-1}, DOS YES) in three different water matrices (artificial matrix with inorganic anions, real groundwater sample and a synthetic industrial wastewater) was evaluated. Although optimal conditions were found to be with the HP dosing strategy, the same experiments were performed without dosage to compare the results.

Firstly, the system efficiency was analysed using an artificial matrix with inorganic anions, which were selected based on the most common species present in groundwater: chloride (80 mg L^{-1}), bicarbonate (100 mg L^{-1}), and sulphate (50 mg L^{-1}), at typical concentrations ranges that are usually found in this type of water (Dişli and Gülyüz 2020). Here, the temporal PCT conversions and consumption of oxidizing agent (with and without dosing) are presented in Fig. 5.

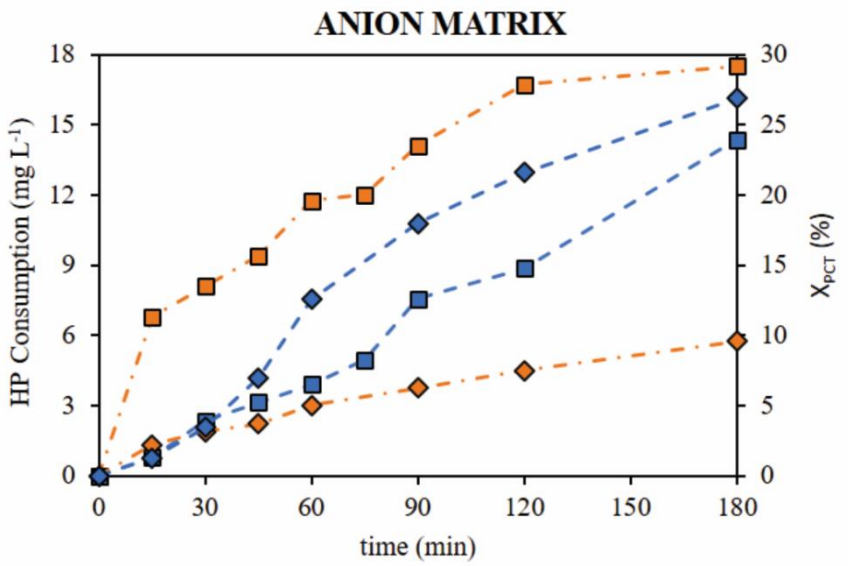

Fig. 5 Temporal evolutions of HP consumption (in mg L^{-1}, symbols = squares) and PCT conversion (in %, symbols = diamonds) for assays carried out in the presence of anions, RAD = ON, and HP = 378 mg L^{-1}. Runs with HP dosage are in blue and long dash line, and runs with no HP dosage are in orange and dash-dot line

As it can be seen, the PCT degradation rate achieved was considerably lower without performing the dosing of the oxidizing agent. Moreover, the $X_{PCT}^{180,exp}$ was

considerably higher when performing HP dosage ($X_{PCT}^{180,exp}$ = 26.90% vs. $X_{PCT}^{180,exp}$ = 6.50 %). However, these conversions were lower than the values obtained in the same conditions (HP = 378 mg L^{-1} and RAD ON) but with ultrapure water ($X_{PCT}^{180,exp}$ = 98.68%, run #8; and $X_{PCT}^{180,exp}$ = 98.90%, run #19, Table 2). On the other hand, the consumption of oxidizing agent obtained without dosing was considerably higher than the one obtained by dosing the oxidizing agent, thus reducing its unproductive depletion. Although the presence of anions in the reaction medium significantly decreased the efficiency of the process by trapping hydroxyl radicals and generating less reactive inorganic radicals (i.e. Cl•, Cl_2• or, SO_4•), the dosage of the oxidizing agent mitigated this negative effect.

Secondly, a real groundwater sample was used to analyse the effectiveness of the ferrioxalate-assisted photo-Fenton process. The composition and characteristics of the sample were presented in section 2, "Materials and Methods" (Table 1). The temporal PCT conversions and consumption of oxidizing agent (with and without dosage) are presented in Fig. 6.

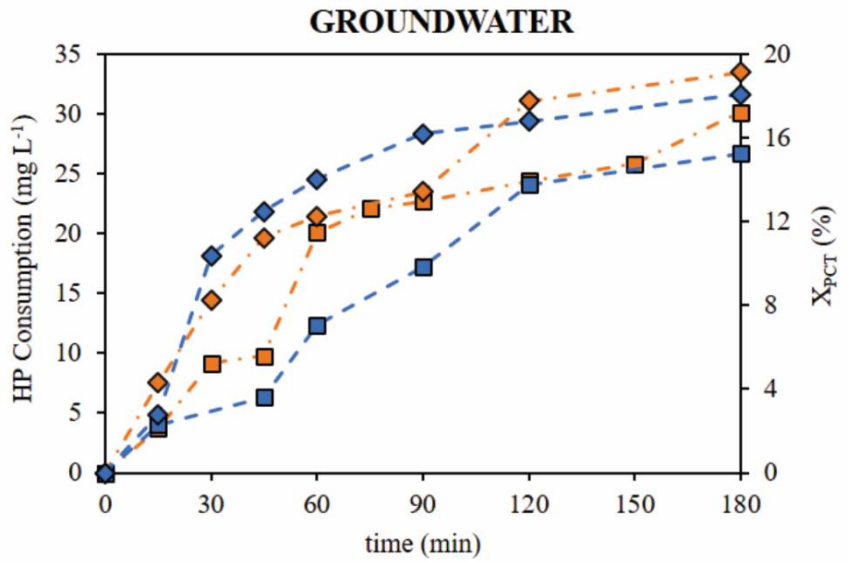

Fig. 6 Temporal evolutions of HP consumption (in mg L^{-1}, symbols = squares) and PCT conversion (in %, symbols = diamonds) for assays carried out in real groundwater, RAD = ON, and HP = 378 mg L^{-1}. Runs with HP dosage are in blue and long dash line, and runs with no HP dosage are in orange and dash-dot line

No significant differences were observed in the behaviour of the system (PCT conversion and HP consumption) performing or not the oxidizing agent dosage strategy with this type of water. Under such conditions, the pollutant conversion $X_{PCT}^{180,exp}$ = 19.13% (without dosing) and $X_{PCT}^{180,exp}$ = 18.06% (with dosing) were considerably lower than in the experiments in ultrapure water ($X_{PCT}^{180,exp}$ = 98.68%, run #8; and $X_{PCT}^{180,exp}$ = 98.90%, run #19, Table 2). Although the quantity of anions in this real matrix (Table 1) is lower than the concentrations used in the artificial sample, different cations such as Ca, Mg, Na, and K are present. These cations can also form stable complexes with oxalate, being calcium the most problematic since it is at higher concentration. Then, the organic ligand (oxalate) availability is reduced and can decrease the oxidation efficiency through iron inactivation. Therefore, the presence of anions and cations might also have significant negative effects on the photo-Fenton process (Smith and Martell 1987; Wang and Wang 2021).

Finally, a synthetic industrial wastewater was employed to assess the efficiency of the ferrioxalate-assisted photo-Fenton process. The composition of this wastewater was outlined in section 2, "Materials and Methods." Temporal PCT conversions and the consumption of the oxidizing agent (with and without dosing) are shown in Figure 7.

A slightly lower PCT conversion was reached when employing the oxidizing agent dosing strategy with this specific wastewater type. Nevertheless, the pollutant conversions 35.59% (without dosing) and 29.96% (with dosing) were lower compared to experiments conducted in ultrapure water (98.68%, run #8; and 98.90%, run #19, Table 2).

Conversely, the observed HP consumptions were substantially greater than the

consumptions obtained with the other two matrices under evaluation, whether performing or not the oxidizing agent dosage strategy. In any case, the consumption of the oxidizing agent at 180 min without dosing was notably higher (112.54 mg HP L^{-1}) than when the dosing strategy was employed (52.64 mg HP L^{-1}). Despite the noticeable increase in HP consumption, the dosing strategy reduced its unproductive depletion, even in the presence of the additional organic load from CIP300® and the drug´s excipients.

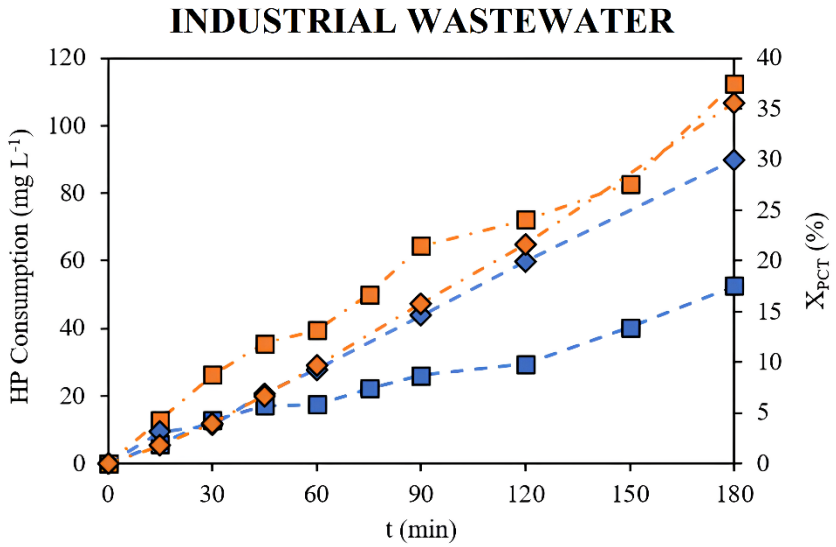

Figure 7. Temporal evolutions of HP consumption (in mg L^{-1}, symbols = squares) and PCT conversion (in %, symbols = diamonds) for assays carried out in a synthetic industrial wastewater, Rad = ON and HP = 378 mg L^{-1}. Runs with HP-dosage are in blue and long dash line, and runs with no HP-dosage are in orange and dash-dot line.

Conclusions

PCT degradation through Fenton and photo-Fenton processes at circumneutral pH was investigated, using ferrioxalate and a solar simulator. The influence of the incident radiation, HP concentration, and mainly, the dosage of the oxidizing agent was evaluated.

The results showed that radiation significantly enhanced PCT conversion, with all the photo-Fenton experiments achieving over 80% conversion.

As regards HP concentration, excessive oxidant levels (above 378 mg L^{-1}) produced a negative effect on contaminant removal. Additionally, it was possible to verify that HP

dosage positively influenced the iron catalytic cycle, resulting in higher Fe^{2+} concentrations at shorter reaction times and faster disappearance of the intermediates HQ and BQ, which is favourable from a toxicological point of view.

A mathematical model employing a D-optimal experimental design (8 model points, 12 runs to estimate the lack of fit and 4 replicates) with three independent variables (radiation level, HP concentration, and HP dosage) yielded a good-quality model with R^2 and adjusted R^2 values of 0.9726 and 0.9589, respectively.

Under optimal conditions (HP = 378 mg L^{-1}, DOS = YES, and RAD = ON), the process was evaluated in different water matrices. In an inorganic anion matrix, PCT conversion was considerably higher with the oxidizing agent dosage strategy, leading to more efficient HP use. However, in a real groundwater sample, no significant differences in PCT conversion or HP consumption were observed, possibly due to the presence of cations that form stable complexes with oxalate, reducing the availability of this ligand and inactivating the catalyst. Finally, in the synthetic industrial wastewater, a slightly lower PCT conversion was observed when employing the oxidizing agent dosing strategy. Despite a noticeable increase in HP consumption when compared with the other two evaluated aqueous matrices, the dosing strategy effectively reduced the unproductive depletion of the oxidizing agent, demonstrating the process's efficacy in challenging wastewater conditions.

The HP dosage strategy introduced in this study serves as an important basis for the development of more advanced strategies applicable to pilot plant solar reactors.

Statements and Declarations

Acknowledgments

Bárbara N. Giménez particularly acknowledges to Consejo Nacional de Investigaciones Científicas y Técnicas (CONICET) for the PhD scholarship. Dr. Maia

Raquel Lescano and Dr. Silvia Mercedes Zacarías are thanked for their contribution in the revision of this research work.

Authors' contributions

All persons who meet authorship criteria are listed as authors, and all authors certify that they have participated sufficiently in the work to take public responsibility for the content. Bárbara N. Giménez, Leandro O. Conte, Sofía A. Duarte, and Agustina V. Schenone contributed to the study conception and design. Bárbara N. Giménez, Sofía A. Duarte and Agustina V. Schenone performed the experiments and data collection. Bárbara N. Giménez, Leandro O. Conte and Agustina V. Schenone analysed all the data and made theoretical calculations. Bárbara N. Giménez, Leandro O. Conte and Agustina V. Schenone wrote the main manuscript text and prepared the figures and tables. Leandro O. Conte and Agustina V. Schenone obtained the funding for the research. All authors reviewed the manuscript, made amendments and contributed with their expertise. All authors read and approved the final manuscript.

Funding

The authors are grateful to Universidad Nacional del Litoral (UNL, CAI+D 2020 50620190100040LI), Consejo Nacional de Investigaciones Científicas y Técnicas (CONICET, PIBAA 28720210100303CO and PIBAA 28720210100301CO), Agencia Nacional de Promoción Científica y Tecnológica (ANPCyT, PICT N° 2018-2346), and Secretaría de Ciencia, Tecnología e Innovación de la Provincia de Santa Fe (PEICID-2022-161) for financial support.

Availability of data and materials

The datasets generated and analysed during the current study are available from the corresponding author on reasonable request.

Competing interests

The authors have no relevant financial or non-financial interests to disclose.

Ethics approval, consent to participate and consent for publication

Not applicable

References

Ahile UJ, Wuana RA, Itodo AU, et al (2020) A review on the use of chelating agents as an alternative to promote photo-Fenton at neutral pH: Current trends, knowledge gap and future studies. Sci Total Environ 710:134872. https://doi.org/10.1016/j.scitotenv.2019.134872

Ahile UJ, Wuana RA, Itodo AU, et al (2021) Are iron chelates suitable to perform photo-Fenton at neutral pH for secondary effluent treatment? J Environ Manage 278:111566. https://doi.org/10.1016/j.jenvman.2020.111566

Amiri P, Behin J (2020) Assessment of wastes recycling for deinking purposes in ozone assisted green process. Environ Sci Pollut Res 27:21859–21871. https://doi.org/10.1007/s11356-020-08457-1

Audino F, Campanyà G, Pérez-Moya M, et al (2019) Systematic optimization approach for the efficient management of the photo-Fenton treatment process. Sci Total Environ 646:902–913. https://doi.org/10.1016/J.SCITOTENV.2018.07.057

Conte LO, Cotillas S, Sánchez-Yepes A, et al (2022a) LED visible light assisted photochemical oxidation of HCHs in aqueous phases polluted with DNAPL. Process Saf Environ Prot 168:434–442. https://doi.org/10.1016/j.psep.2022.10.015

Conte LO, Dominguez CM, Checa-Fernandez A, Santos A (2022b) Vis LED Photo-Fenton Degradation of 124-Trichlorobenzene at a Neutral pH Using Ferrioxalate as Catalyst. Int J Environ Res Public Health 19:. https://doi.org/10.3390/ijerph19159733

Conte LO, Schenone A V., Giménez BN, Alfano OM (2019) Photo-Fenton degradation of a herbicide (2,4-D) in groundwater for conditions of natural pH and presence of inorganic anions. J Hazard Mater 372:113–120. https://doi.org/10.1016/j.jhazmat.2018.04.013

Dalgic G, TURKDOGAN FI, Yetilmezsoy K, Kocak E (2017) Treatment of Real Paracetamol. Chem Ind Chem Eng Q 23:177–186

Dişli E, Gülyüz N (2020) Hydrogeochemical investigation of an epithermal mineralization bearing basin using multivariate statistical techniques and isotopic evidence of groundwater: Kestanelik Sub-Basin, Lapseki, Turkey. Chemie der Erde 80:125661. https://doi.org/10.1016/j.chemer.2020.125661

Eniola JO, Kumar R, Barakat MA, Rashid J (2022) A review on conventional and advanced hybrid technologies for pharmaceutical wastewater treatment. J Clean Prod 356:131826. https://doi.org/10.1016/j.jclepro.2022.131826

Galani A, Alygizakis N, Aalizadeh R, et al (2021) Patterns of pharmaceuticals use during the first wave of COVID-19 pandemic in Athens, Greece as revealed by wastewater-based epidemiology. Sci Total Environ 798:149014. https://doi.org/10.1016/j.scitotenv.2021.149014

Giménez BN, Conte LO, Alfano OM, Schenone A V. (2020) Paracetamol removal by photo-Fenton processes at near-neutral pH using a solar simulator: Optimization by D-optimal experimental design and toxicity evaluation. J Photochem Photobiol A Chem 397:112584. https://doi.org/10.1016/j.jphotochem.2020.112584

Giménez BN, Schenone A V., Alfano OM, Conte LO (2021) Reaction kinetics formulation with explicit radiation absorption effects of the photo-Fenton

degradation of paracetamol under natural pH conditions. Environ Sci Pollut Res 28:23946–23957. https://doi.org/10.1007/s11356-020-11993-5

Machado F, Teixeira ACSC, Ruotolo LAM (2023) Critical review of Fenton and photo-Fenton wastewater treatment processes over the last two decades. Springer Berlin Heidelberg

Malato S, Giménez J, Oller I, et al (2020) Removal and Degradation of Pharmaceutically Active Compounds (PhACs) in Wastewaters by Solar Advanced Oxidation Processes. Handb Environ Chem 108:299–326. https://doi.org/10.1007/698_2020_688

Marson EO, Paniagua CES, Gomes Júnior O, et al (2022) A review toward contaminants of emerging concern in Brazil: Occurrence, impact and their degradation by advanced oxidation process in aquatic matrices. Sci Total Environ 836:. https://doi.org/10.1016/j.scitotenv.2022.155605

Miller JN, Miller JC, Miller RD (2018) Statistics and Chemometrics for Analytical Chemistry, Seventh. Pearson, London

Monteagudo JM, Durán A, Aguirre M, Martín IS (2010) Photodegradation of Reactive Blue 4 solutions under ferrioxalate-assisted UV/solar photo-Fenton system with continuous addition of H2O2 and air injection. Chem Eng J 162:702–709. https://doi.org/10.1016/j.cej.2010.06.029

Monteagudo JM, Durán A, San Martín I, Aguirre M (2009) Effect of continuous addition of H2O2 and air injection on ferrioxalate-assisted solar photo-Fenton degradation of Orange II. Appl Catal B Environ 89:510–518. https://doi.org/10.1016/J.APCATB.2009.01.008

Nascimento GE do, Soares Oliveira MA, da Rocha Santana RM, et al (2020) Investigation of paracetamol degradation using LED and UV-C photo-reactors. Water Sci Technol 81:2545–2558. https://doi.org/10.2166/wst.2020.310

Nasr Esfahani K, Pérez-Moya M, Graells M (2022) Modelling of the photo-Fenton process with flexible hydrogen peroxide dosage: Sensitivity analysis and experimental validation. Sci Total Environ 839:. https://doi.org/10.1016/j.scitotenv.2022.155941

Oller I, Malato S (2021) Photo-Fenton applied to the removal of pharmaceutical and other pollutants of emerging concern. Curr Opin Green Sustain Chem 29:100458. https://doi.org/10.1016/j.cogsc.2021.100458

Pacheco-Álvarez M, Picos Benítez R, Rodríguez-Narváez OM, et al (2022) A critical review on paracetamol removal from different aqueous matrices by Fenton and Fenton-based processes, and their combined methods. Chemosphere 303:. https://doi.org/10.1016/j.chemosphere.2022.134883

Pal P, Thakura R (2018) A membrane-integrated closed loop system for treatment of pharmaceutical wastewater. IEEE Int Conf Power, Control Signals Instrum Eng ICPCSI 2017 802–810. https://doi.org/10.1109/ICPCSI.2017.8391824

Palmieri F, Estoppey A, House GL, et al (2019) Oxalic acid, a molecule at the crossroads of bacterial-fungal interactions, 1st edn. Elsevier Inc.

Qutob M, Hussein MA, Alamry KA, Rafatullah M (2022) A review on the degradation of acetaminophen by advanced oxidation process: pathway, by-products, biotoxicity, and density functional theory calculation †. https://doi.org/10.1039/d2ra02469a

Resolución n° 1089/82 (1982) Reglamento para el control del vertimiento de líquidos residuales. Dirección Provincial de Obras Sanitarias. Provincia de Santa Fe. http://www.santafe.gov.ar/index.php/web/content/download/22767/111069/file/Resolución Nº 1089-82.pdf. Accessed 28 Nov 2023

Rodríguez-García D, Soriano-Molina P, Guzmán Sánchez JL, et al (2023) A novel control system approach to enhance the efficiency of solar photo-Fenton microcontaminant removal in continuous flow raceway pond reactors. Chem Eng J 455:. https://doi.org/10.1016/j.cej.2022.140760

Santos A, Yustos P, Quintanilla A, et al (2004) Evolution of Toxicity upon Wet Catalytic Oxidation of Phenol. Environ Sci Technol 38:133–138. https://doi.org/10.1021/es030476t

Smith RM, Martell AE (1987) Critical stability constants, enthalpies and entropies for the formation of metal complexes of aminopolycarboxylic acids and carboxylic acids. Sci Total Environ 64:125–147. https://doi.org/10.1016/0048-9697(87)90127-6

Soares PA, Batalha M, Souza SMAGU, et al (2015) Enhancement of a solar photo-Fenton reaction with ferric-organic ligands for the treatment of acrylic-textile dyeing wastewater. J Environ Manage 152:120–131. https://doi.org/10.1016/j.jenvman.2015.01.032

Spaltro A, Pila MN, Colasurdo DD, et al (2021) Removal of paracetamol from aqueous solution by activated carbon and silica. Experimental and computational study. J Contam Hydrol 236:103739. https://doi.org/10.1016/j.jconhyd.2020.103739

Wang J, Wang S (2021) Effect of inorganic anions on the performance of advanced oxidation processes for degradation of organic contaminants. Chem Eng J 411:128392. https://doi.org/10.1016/J.CEJ.2020.128392

Wang L, Bian Z (2020) Photocatalytic degradation of paracetamol on Pd–BiVO4 under visible light irradiation. Chemosphere 239:124815. https://doi.org/10.1016/j.chemosphere.2019.124815

Wang S, Wu J, Lu X, et al (2019) Removal of acetaminophen in the Fe2+/persulfate system: Kinetic model and degradation pathways. Chem Eng J 358:1091–1100. https://doi.org/10.1016/j.cej.2018.09.145

Yu X, Cabrera-Reina A, Graells M, et al (2021) Towards an Efficient Generalization of the Online Dosage of Hydrogen Peroxide in Photo-Fenton Process to Treat Industrial Wastewater. Int J Environ Res Public Heal 2021, Vol 18, Page 13313 18:13313. https://doi.org/10.3390/IJERPH182413313

Yu X, Somoza-Tornos A, Graells M, Pérez-Moya M (2020) An experimental approach to the optimization of the dosage of hydrogen peroxide for Fenton and photo-Fenton processes. Sci Total Environ 743:140402. https://doi.org/10.1016/j.scitotenv.2020.140402

ANEXO F. Exploring the Role of Hydrogen Peroxide Continuous Dosage in the photo-Fenton process: Comparative study between Lab-Scale and Solar Reactor Experiments

El artículo presentado a continuación ha sido aceptado para su revision por pares en la revista "*Chemical Engineering Journal Advances"*

Exploring the Role of Hydrogen Peroxide Dosage Strategies in the Photo-Fenton Process: Scaling from Lab-Scale to Pilot Plant Solar Reactor

Bárbara N. Giménez[1,2], Agustina V. Schenone[1,2], Leandro O. Conte[1,3]

[1]*Instituto de Desarrollo Tecnológico para la Industria Química (INTEC), Consejo Nacional de Investigaciones Científicas y Técnicas (CONICET) and Universidad Nacional del Litoral (UNL), Ruta Nacional Nº 168, 3000, Santa Fe, Argentina*

[2]*Facultad de Bioquímica y Ciencias Biológicas, Universidad Nacional del Litoral (UNL), Santa Fe, Argentina*

[3]*Facultad de Ingeniería y Ciencias Hídricas, Universidad Nacional del Litoral (UNL), Santa Fe, Argentina*

Abstract

This study aims to investigate the role of hydrogen peroxide (HP) continuous dosage in removing Paracetamol (PCT) from different water matrices using the solar photo-Fenton process. Different parameters in the HP dosage strategies (initial HP pulse, dosing time, and HP concentration) were systematically analysed to assess their impacts on pollutant removal (X_{PCT}), oxidant specific consumption ($\Upsilon^{t}_{HP/PCT}$), and toxicity levels (I(%)). The analysis involved various water matrices (ultrapure water UW, groundwater GW, anion matrix AW, and synthetic pharmaceutical wastewater IW0.01 or IW0.1), which were firstly treated in a laboratory reactor and subsequently scaled up to a solar prototype. After laboratory testing, the most effective reaction configuration (maximum X_{PCT} and $\Upsilon^{t}_{HP/PCT}$ close to the stoichiometric one) was chosen as the starting point for scaling up the reaction system. Using the solar reactor setup, complete PCT conversion was achieved within just 60 minutes of reaction time (UW matrix). However, under IW0.1 condition and employing the same HP dosing strategy, a X_{PCT} of 95.4% was attained but at 180 minutes of reaction, highlighting the significant influence of the real matrix. Additionally, the I(%) remained high towards the end of the reaction (close to 60%), attributed to the presence of hydroquinone in the system, demanding longer reaction times to completely reduce the toxicity when working with industrial wastewater. This comprehensive approach aims to close the gap between lab results and practical applications, offering crucial insights to address pharmaceutical wastewater pollution.

Keywords: Solar Photo-Fenton, Pilot Plant Reactor, Ferrioxalate, Natural pH, Hydrogen Peroxide Dosage Strategies, Pharmaceutical Wastewater

1. Introduction

The growing concern over Emerging Contaminants (ECs) is evident, particularly with substances such as pharmaceuticals and personal care products (PPCPs), pesticides, dyes, antibiotics, and antibiotic-resistant genes (ARGs) [1]. These pollutants have diverse sources, including industrial wastewater, domestic sewage, livestock and poultry wastewater, and hospital wastewater [2], having potential risks to both ecological environments and human health [3]. PPCPs have become pervasive in the environment due to their extensive production and use [4]. Specifically, substantial quantities of Paracetamol (PCT) were discharged into water systems because of its widespread use, inadequate disposal practices by manufacturers, limited metabolic breakdown in the human body, and their biologically active structures [5]. High concentrations of PCT (up to 300 mg L^{-1}, [6]) were detected in hospital effluents [7], pharmaceutical industry wastewater [8], and urban sewage treatment plants [9]. It is, therefore, unsurprising that pharmaceuticals are identified in receiving surface water [10], groundwater [11] and in some instances, even in drinking water [12].

The standard technologies implemented by wastewater treatment plants (WWTPs) are often ineffective in efficiently removing these contaminants of emerging concern [13]. Similarly, other water treatment methods such as reverse osmosis [14], and carbon adsorption [15], primarily shift these pharmaceutical pollutants from one phase to another but do not effectively remove them [16]. Advanced Oxidation Processes (AOPs), with a particular focus on the Fenton and photo-Fenton systems, have gained significant attention. These well-established and highly efficient technologies are widely utilized for treating both natural waters and wastewater. They exhibit the capability to eliminate a broad spectrum of contaminants, a task that conventional treatment methods often find challenging to address [17]. The photo-Fenton process is a photocatalytic method that

generates highly reactive hydroxyl radicals (HO•) by combining chemical reagents (Fe(II)/Fe(III) salt/complex and hydrogen peroxide, HP) with UV-Vis irradiation, resulting in a synergistic effect that accelerates the production of hydroxyl radicals. Nonetheless, there are significant limitations associated with this "traditional" process approach [18]. Firstly, the regeneration of Fe(II) from Fe(III) was identified as the step that limits the rate of the process. In this context, light plays a crucial role, serving as an "activator" for the regeneration of Fe(II) and, consequently, accelerates the overall reaction [19]. Here, the use of iron complexes proves to be advantageous, allowing operation at a neutral pH, preventing iron precipitation, and expanding the application range of the process to the visible region of the solar spectrum [20]. Secondly, hydroxyl radicals are highly unstable and non-selective, making them prone to unwanted secondary reactions, some of which involve HP consumption, reducing the process efficiency [21]. Moreover, an oversupply of hydrogen peroxide can undergo spontaneous decomposition into oxygen and water [22]. Consequently, it is crucial to control the reaction conditions by adjusting the oxidant dosage, which is frequently the most costly reagent, to achieve the complete degradation of the target compound [23]. Then, a balance between the low decontamination efficiency of the process, caused by insufficient hydrogen peroxide dosage, and the additional expenses linked to an excess of it, need to be established. To address this issue, researchers have explored the use of different HP dosage strategies to enhance the performance of the photo-Fenton process [23–25].

In recent years, solar technology has transformed the photo-Fenton process into a cost-effective and competitive method for chemical degradation of organic pollutants. Solar reactors offer an intriguing alternative for effluent treatment, eliminating expenses associated with UV lamps installation and maintenance, and reducing electrical power consumption [26]. The literature specifically highlights the application of the solar photo-

Fenton process in remediating water containing ECs, including PPCPs [27], pesticides [28], dyes [29], antibiotic [30], ARGs [31], effluents from municipal treatment plants [32] and hospitals [33]. However, cost considerations, particularly regarding the oxidizing agent, are important to address. In systems operating at natural pH and utilizing solar radiation, the oxidizing agent can be one of the most expensive reagents [34]. The pursuit of automating the photo-Fenton process is driven by the goal of improving its performance, with a focus on decreasing hydrogen peroxide consumption compared to manual operation. This objective is directed at lowering both the economic cost and process time, ultimately enhancing resource use efficiency.

It is important to highlight that a considerable number of scientific articles focus only on studying the degradative behaviour of PPCPs in ideal water matrices. However, in real aqueous environments, a range of substances may coexist, posing potential obstacles to the breakdown of these contaminants via the photo-Fenton process. Anions (chlorides, nitrates, bicarbonates, and sulphates) are recognized for interfering in the reaction, as they act as scavengers for the HO• produced [35]. Cations (mainly, calcium and magnesium) can interfere with the Fe(III)/Oxalate equilibrium/precipitation reactions, affecting the photochemical activity of the system [58]. Furthermore, in real pharmaceutical industry effluents, many agents (such as detergents), are employed to clean the formulation reactors. Thus, all these interferences contribute to a reduction in the pollutants degradation rates and an increase in the HP consumption [36,37].

Indeed, the assessment of purification technologies like the photo-Fenton process in real-world scenarios is crucial for addressing the challenges posed by persistent contaminants in complex effluents. In this context, the current research aims to address the removal of Paracetamol (PCT) from complex pharmaceutical wastewater effluent. The chosen approach involves harnessing the solar photo-Fenton reaction, operating at a

near-neutral pH and incorporating oxalate as a complexing agent to form ferrioxalate (Fe-Ox). A fundamental aspect of this research lies in investigating different parameters in the HP dosage strategies (initial HP pulse, dosing time, and HP concentration), which play vital roles in determining the efficiency of the process, including considerations regarding toxicity levels. Through systematic experimentation and analysis, the research aims to optimize the dosing strategy to maximize pollutant removal while minimizing operational costs and environmental impacts.

2. Material and methods

2.1 Experimental Devices

In this investigation the experiments were conducted employing two different photoreactors. The first one was a batch lab-scale reactor irradiated by a solar simulator. This unit operates under perfect mixing conditions and at a constant temperature. Details of this experimental system can be referenced elsewhere [38]. Here, the local radiation flux averaged over the reactor window (q_W) was 92.80 W m^{-2} (32.2 nE cm^{-2} s^{-1}), within the wavelength range of 300 to 500 nm (USB spectrometer, Ocean Optics, USB2000). The total volume of the treated solution was 3 L.

The second reactor utilized in this study was a pilot-plant non-concentrating solar photoreactor, specifically designed to capture UV/visible and near-infrared solar radiation (patent INPI P-080103697). The entire reaction system operates within a closed recirculating circuit, which is facilitated by a high flow rate centrifugal pump and a well-stirred storage tank. The storage tank is equipped with a pH-meter and an OD sensor from HANNA Instruments. Additionally, type J thermocouples are employed to monitor temperature variations at different positions in the system over time. To measure the UV and total broadband solar radiation fluxes incident on the two-plate reactor window, CUV3 and CM11 Kipp and Zonen radiometers were employed. The irradiated reactor

volume was 6.1 L, while the total volume of the treated solution was 35 L. For further detailed information regarding this solar photoreactor, please refer to [28]. Finally, both experimental setups (laboratory and pilot plant units) were equipped with a diaphragm dosing pump (Acquatron® MA-CP series) for the automatic addition of the oxidizing agent.

2.2 Analytical determinations

Paracetamol (Sigma-Aldrich, 98% purity) served as the model pollutant. The concentrations of PCT and its main reaction intermediate, hydroquinone (HQ) (Fluka, 99% purity), were analysed by HPLC-DAD (Waters) following the methodology outlined in Giménez et al [39]. The mineralization achieved was monitored via TOC measurements employing a Vario TOC cube analyzer (Elementar). Hydrogen peroxide (HP, Cicarrelli, 30%), Fe^{2+}, and Total Fe ($FeCl_3.6H_20$, Merck, pro-analysis) were determined through colorimetric methods, while oxalate ion (Oxa) was quantified using ion chromatography [38]. For the preparation of the ferrioxalate complex, a solution of potassium oxalate monohydrate (Carlo Erba, 99.5%) and a solution of iron(III) chloride were mixed in appropriate proportions. Ultrapure water was obtained using a reverse osmosis system (Osmoion, APEMA).

A Microtox Model 500 Toxicity Analyser (Strategic Diagnostic Inc.) was utilized to assess acute toxicity of the samples throughout the oxidation process. Toxicity was computed as the percentage of light emission inhibition by the *Vibrio fischeri* NRRL-B-11177 bacteria following a 15-minute incubation period. Light inhibition measurements were conducted without sample dilution. Prior to toxicity assessments, sample pH was adjusted within the range of 6 to 7 and any residual hydrogen peroxide in the aqueous sample was decomposed into water and oxygen using a catalase solution (1500 mg L^{-1} of >2000 U/mg bovine liver, Fluka)

2.3 Experimental procedure

For the tests conducted in the pilot plant solar reactor, each experimental assay begins with the introduction of PCT and ferrioxalate solutions into the storage tank of the system. At the beginning of these experiments, a solar-opaque plate protects the reactor window to prevent solar radiation entry. In all cases, the medium pH is adjusted to 5 using either a concentrated sodium hydroxide solution (3 mol L^{-1}, Cicarelli) or sulphuric acid (3 mol L^{-1}, Cicarelli), depending on the initial pH of the solution under treatment. The oxidizing agent is added according to the evaluated dosing strategy, and upon addition, the first sample is taken, and the reactor cover is removed to initiate the photochemical reaction. The solar experiments begins at 10.0 LST and the reaction progress is monitored over 180 minutes, taking samples at predefined times for various analyses and parameter assessments. An analogous procedure is performed when operating the laboratory-scale reactor, although a constant temperature of 25°C is maintained throughout the reaction time. More details of the experimental procedure can be found in [28].

Specifically, regarding the dosage of HP, two strategies were evaluated: 1) starting with an initial pulse of reagent, followed by a continuous additional dosage of HP until 75 or 150 minutes of reaction; 2) beginning the test without an initial pulse of reagent, instead, starting with a continuous dosage of the oxidizing agent until 75 or 150 minutes of reaction (see Table 1 and Table 2, Results and Discussion section).

Finally, the treated samples consisted of: a) ultrapure water (UW), b) an artificial matrix of anions in ultrapure water (AW), c) real groundwater (GW), all spiked with PCT (standard drug), and d) synthetic industrial wastewater coming from a pharmaceutical plant (IW0.01 or IW0.1). In all the experiments, initial PCT, Oxa, and Fe concentrations were set at 40 mg L^{-1}, 47.5 mg L^{-1}, and 3 mg L^{-1} (molar ratio Fe/Oxa=1/10), respectively, based on prior studies [39].

The AW matrix was prepared so that the final concentrations of each anion in the reaction volume were: 80, 50, and 100 mg L^{-1}, for Cl^-, SO_4^{2-}, and HCO_3^-, respectively. For this, NaCl, Na_2SO_4 and $NaHCO_3$ obtained from Cicarelli were used. The main characteristics of the GW sample and its composition can be found elsewhere [40]. Lastly, IW0.01 or IW0.1 were formulated using CIP300® (neutral pH detergent), with a final concentration of 0.01 or 0.1% in the reaction medium (TOC = 54.74 mgC L^{-1} for a solution of CIP 0.1%). Here, PCT pharmaceutical drug (LIF, Cert. ANMAT Nº 54.235), comprising pre-gelatinized starch, stearic acid, and povidone K30 as excipients, was incorporated. The drug solution was diluted to achieve an initial PCT concentration of 40 mg L^{-1} (TOC = 30.54 mgC L^{-1} for diluted drug solution). Then, the simulated effluent (IW0.1) contributed with a total amount of 85.28 mgC L^{-1}.

3. Results and Discussion

Two different photoreactors were utilized in this study: a batch lab-scale and a pilot plant solar reactor. These reactors were employed to assess the scalability and efficiency of hydrogen peroxide dosage in PCT photo-Fenton degradation.

3.1 Lab-scale reactor

Table 1 lists the set of experiments carried out in the lab-scale reactor in different matrices.

The HP dosage consisted of whether or not to carry out an initial punctual dosage (47.25 mg L^{-1}), followed by a continuous addition until 75 or 150 min of reaction, using different dosing rates (mg min^{-1} HP), in which the theoretical target/final oxidizing agent concentration was reached (HP).

Table 1. Experimental conditions and PCT conversion (X_{PCT}^{180} (%)) after 180 min of reaction for lab-scale reactor.

Run	ID	Rad	HP (mg L^{-1})	Dosing time (min)	Flow (mgHP min^{-1})	Matrix[a]	X_{PCT}^{180}(%)
N1*	378_IP_150_OFF	OFF	378	150	8.41	UW	3.5
N2	47.25_75_ON	ON	47.25	75	2.13	UW	96.0
N3	94.5_75_ON	ON	94.5	75	4.81	UW	94.3
N4*	189_IP_150_ON	ON	189	150	3.61	UW	93.3
N5	189_150_ON	ON	189	150	4.81	UW	93.9
N6*	378_IP_150_ON	ON	378	150	8.41	UW	90.7
N7	378_75_ON	ON	378	75	14.88	UW	85.9
N8*	378_IP_75_ON	ON	378	75	16.63	UW	87.8
N9	756_75_ON	ON	756	75	34.03	UW	79.0
N10	378_75_ON_GW	ON	378	75	16.63	GW	99.5
N11	189_75_ON_AW	ON	189	75	8.51	AW	97.7
N12	378_75_ON_IW	ON	378	75	16.63	IW0.1	18.9

[a] UW: ultrapure water; GW: ground water; AW: artificial anion matrix; IW0.1: simulated industrial wastewater with 0.1% CIP300.

* Runs with an asterisk are those that were carried out with an Initial Pulse (IP) of HP = 47.25 mg L^{-1}

The influence of radiation on the system is significant. Under dark conditions, using UW matrix (Run N1), PCT conversion only reached 3.5% after 180 min of reaction. In contrast, a minimum conversion of 79.0% was obtained under irradiated conditions (Fig. 1d, Run N9), where an excess of oxidizing agent was present in the system. Moreover, when radiation was applied, even at the lowest final concentrations of oxidizing agent (Fig 1c, HP = 47.5 mg L^{-1}, Run N2, and HP = 94.5 mg L^{-1}, Run N3), high PCT conversions were still achieved (greater than 94%).

In second place, it can be observed that the influence of the initial pulse of HP was not significant in the achieved contaminant conversion levels (Fig. 1c, Run N4 *vs*. Run N5, and Fig. 1d, Run N7 *vs*. Run N8). There were also no substantial differences between contaminant conversion for a dosing time of 75 min (Run N7) *vs.* 150 min (Run N6). However, the main operational differences were found in the observed oxidizing agent consumption ($Y^t_{HP/PCT}$). At this point, the specific consumption of HP was defined as the difference between the mass of HP added to the reaction medium (HP^t_{dosed}) and the mass of HP quantified experimentally in the system ($HP^t_{measured}$), as a function of the mass of PCT converted (Eq. (1), [38]).

$$Y^t_{HP/PCT} = \frac{\sum_0^t (HP^t_{dosed} - HP^t_{measured})}{PCT^0 - PCT^t} \quad (1)$$

The specific consumptions of oxidizing agent and PCT evolution are depicted in Fig. 1. For low doses of hydrogen peroxide (Fig. 1a, Runs N2 to N5), regardless of the reagent dosing rate used (75 or 150 min), the consumption of oxidizing agent remained below the stoichiometric value required for the mineralization of PCT (4.72 mgHP mgPCT^{-1}, Eq. (2)). Considering that a consumption value close to the stoichiometric one is associated with the complete removal of reaction intermediates, the studied dosing conditions were not sufficient to degrade the generated by-products [41].

$$C_8H_9NO_2 + 21H_2O_2 \rightarrow 8CO_2 + 25H_2O + H^+ + NO_3^- \quad (2)$$

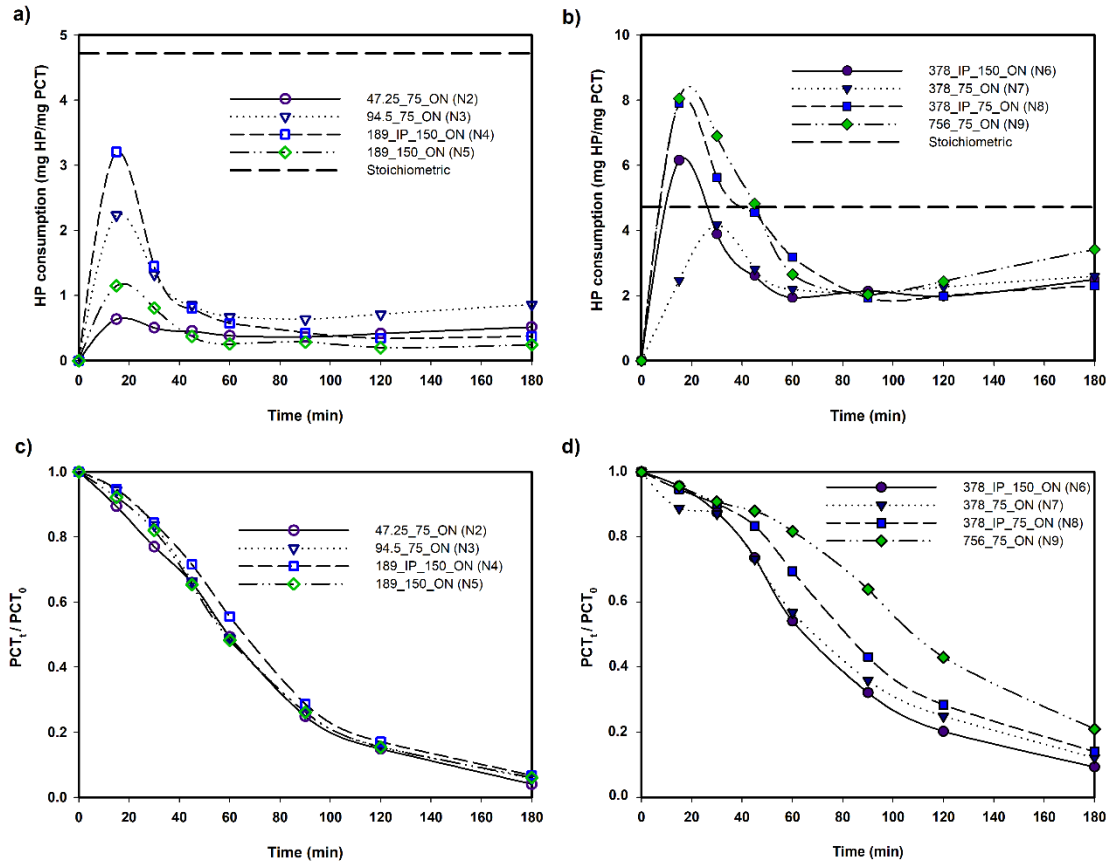

Fig. 1. Specific consumption of hydrogen peroxide for a) low HP concentrations (Runs N2 - N5) and b) medium and high HP concentrations (Runs N6 - N9); c) relative PCT concentrations for low HP conditions (Runs N2 - N5); d) relative PCT concentrations for medium and high HP concentrations (Runs N6 - N9).

In the case of medium and high HP doses (Fig. 1b, Runs N6 to N9), variable levels of oxidizing agent consumption were observed. Using maximum HP concentrations and HP dosage rates (Run N9), the specific unproductive consumption reached its maximum value (8.05 mgHP mgPCT^{-1} for 15 min of reaction). This excess of HP, besides interfering in the PCT degradation process, leads to excessive and nonspecific consumption of the oxidizing agent itself. This phenomenon arises from the reaction of HP with HO• radicals (Eq. (3)) or the self-decomposition of HP (Eq. (4)) [40]. However, for medium HP concentrations and dosage rates (Runs N6 and N7), this unproductive consumption decreased. In the conditions of Run N8, this value was close to the stoichiometric one,

which will be considered as the starting point for pilot plant scale tests.

$$H_2O_2 + HO^{\bullet} \rightarrow HO_2^{\bullet -} + H_2O \quad (3)$$

$$2H_2O_2 \rightarrow 2H_2O + O_2 \quad (4)$$

Based on these results, the experiments with more complex matrices were carried out with continuous addition of HP until 75 min of reaction, without initial punctual dosage (Runs N10 to N12). PCT temporal evolution and calculated HP consumptions can be analysed in Fig. 2.

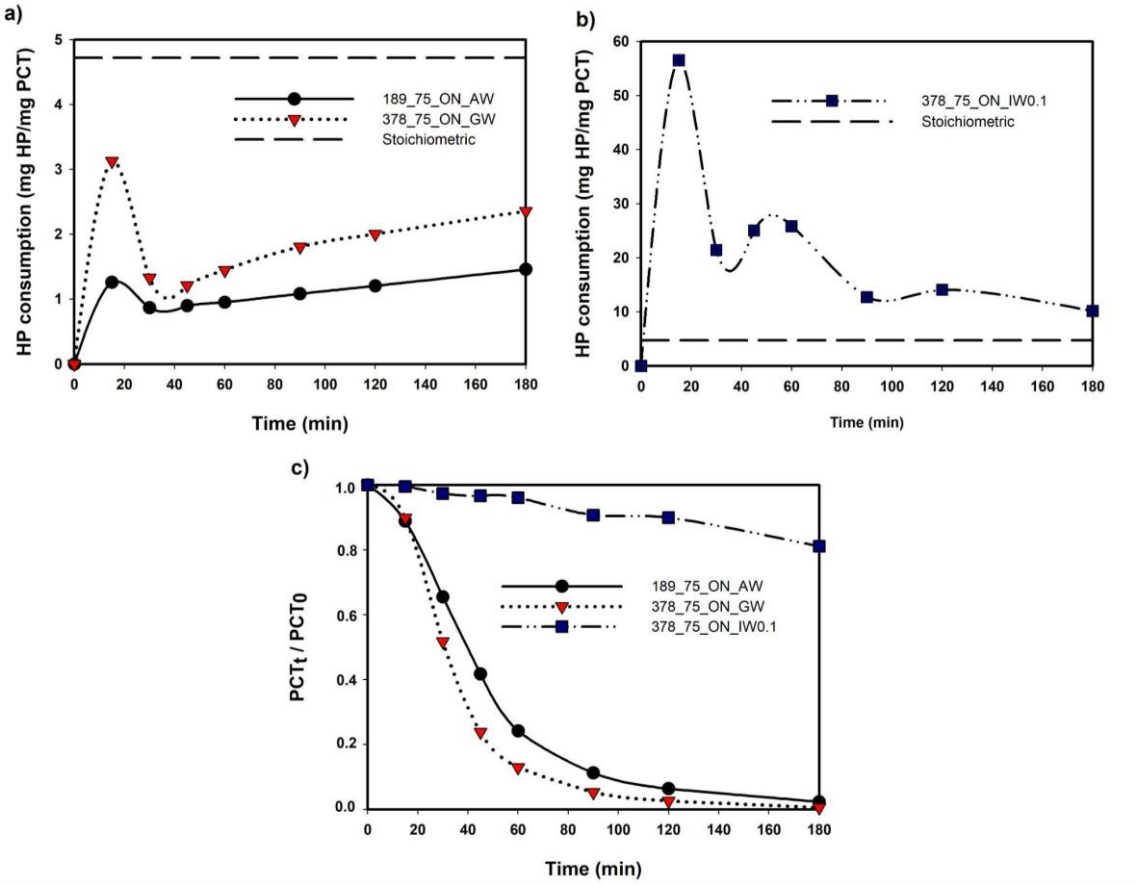

Fig. 2. a) and b) Specific consumption of hydrogen peroxide and c) relative PCT concentrations for complex matrices in the lab-scale reactor. GW: groundwater (Run N10, HP=378 mg L^{-1}); AW: artificial anion matrix (Run N11, HP=189 mg L^{-1}); IW0.1: simulated industrial wastewater with 0.1% CIP300 (Run N13, HP=378 mg L^{-1})

In the case of AW and GW matrices, although high conversion levels of the pharmaceutical were achieved (Fig. 2c), the oxidizing agent consumptions were lower than the stoichiometric amount (Fig. 2a), indicating the formation of reaction

intermediates [41]. Conversely, when evaluating synthetic industrial wastewater, PCT was poorly degraded (Fig. 2c, 18.9% at 180 min) and the specific consumption was much greater than 4.72 mg HP mg PCT^{-1}, demonstrating a high unproductive consumption of the oxidant (Fig. 2b). Both effects can be associated with the contribution of organic matter to the reaction medium due to the components of CIP300® and the excipients in the pills of PCT. Furthermore, even though the composition of the detergent is not informed, it is known that anionic surfactants can form complexes with Fe ions, interfering with the catalytic cycle and the performance of the process [42].

3.2 Pilot plant solar reactor

Table 2 presents the operating conditions of the runs performed in the solar reactor. The temperature increment, the total accumulated energy (between 300 and 550 nm) and PCT conversions were monitored for 180 min of reaction. For all the tests carried out and considering the results obtained in the laboratory tests, the dosing time of the oxidizing agent was set at 75 min and no initial HP pulse was employed.

Table 2. Experimental conditions in the pilot plant solar reactor.

Run	HP (mg L^{-1})	T^{t0} (°C)	T^{t180} (°C)	Accumulated energy[a] (KJ L^{-1})	Flow (mgHP min^{-1})	Matrix[b]	X_{PCT}[c] (%)
S1	47.25	23.8	38.9	5.23E+04	21.88	UW	98.90 (60 min)
S2	378	25.8	35.9	2.50E+04	175	UW	98.70 (60 min)
S3	756	26.2	41.9	4.97E+04	350	UW	98.90 (45 min)
S4	378	28.0	39.9	3.35E+04	175	IW0.01	97.90 (60 min)
S5	378	29.0	44.2	4.02E+04	175	IW0.1	95.40 (180 min)

[a] Calculated at 180 min reaction time.
[b] UW: ultrapure water; IW0.01: simulated industrial wastewater with 0.01% CIP300; IW0.1: simulated industrial wastewater with 0.1% CIP300.
[c] Between parenthesis: time (min) at which the conversion value was reached.

Firstly, it's important to note that for each of the tests outlined in Table 2 (Runs S1 to S5), variable values of accumulated energy and temperature increase were recorded due to the environmental conditions encountered during each experimental test. Therefore, the accumulated radiation ($Q_{300-550nm,t}$, KJ L^{-1}) in each experiment with solar radiation was calculated according to Eq. (5), [43]:

$$Q_{300-550nm,t} = Q_{300-550nm,t-1} + \Delta t_t \overline{RAD}_{300-550nm,t} \frac{A_r}{V_t} \quad (5)$$

where $Q_{300-550nm,t}$ is the total accumulated radiation (KJ L^{-1}), Δt represents the time interval (s), $\overline{RAD}_{300-550nm,t}$ is the average total radiation (W m^{-2}), A_r is the irradiated area (0.24 m2), and V_t is the total volume of treated wastewater (35 L). The accumulated radiation was calculated between 300 and 550 nm, considering the photochemical characteristics of the employed ferrioxalate complex [44], which enables the utilization of both, UV and visible radiation. Therefore, this accumulated radiation represents the energy required for the photochemical activation of the process.

Fig. 3 shows the evolutions associated with PCT degradation, as a function of accumulated energy.

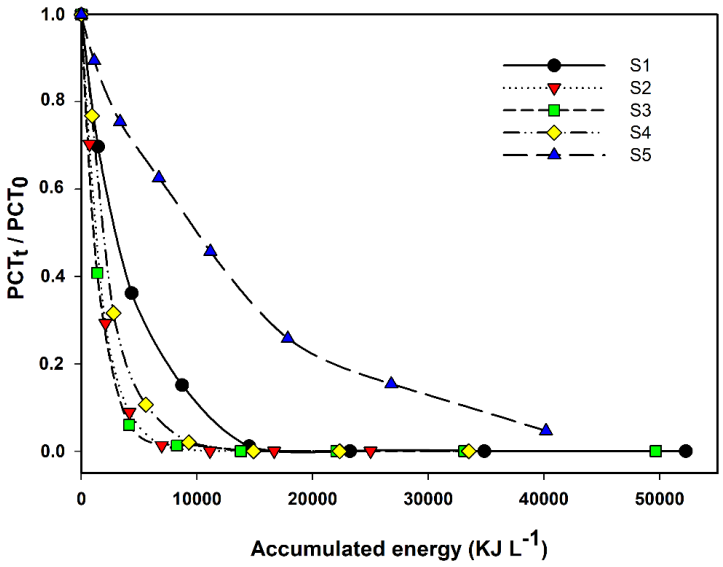

Fig. 3. Relative PCT concentration as a function of accumulated energy (Runs S1-S5) in the solar reactor experiments.

The results presented in Table 2 and Fig. 3 illustrate the efficacy of the examined process. First, complete conversion of PCT was attained within just 60 minutes of reaction (Runs S1 to S3) for UW conditions. However, when employing low doses of oxidizing agent (Run S1), a notable decrease in the rate of contaminant degradation was evident. In fact, up to 200% more accumulated energy was needed (5.23×10^4 KJ L^{-1} vs. 2.50×10^4 KJ L^{-1}) to achieve complete conversion of the contaminant compared to an intermediate oxidant concentration of 378 mg L^{-1} (Run S2). Finally, dosing an excess of HP (Run S3) did not lead to any benefit in the degree of PCT degradation.

It is noteworthy to emphasize the effectiveness of the investigated process even under conditions that simulate an industrial effluent (IW0.01 and IW0.1). Remarkably high contaminant conversions (up to 98%) were achieved within just 60 minutes of reaction for low detergent concentrations (Run S4, IW0.01). However, when a higher detergent percentage was introduced under the same HP level (Run S5, IW0.1), a conversion of 95.4% was attained but at 180 minutes, indicating the significant influence of the real matrix (and consequent consumption of hydroxyl radicals). It's important to note that despite using the same hydrogen peroxide (HP) concentration (378 mg L^{-1}) and dosing strategy, the combined effect of UV/visible and thermal sunlight was able to almost completely degrade PCT after 180 minutes of reaction in the simulated industrial wastewater (Run S5). This contrasts with the conversion value of 18.9% achieved in the lab-scale reactor (Run N12, Table 1).

Dissolved oxygen (DO) profiles were monitored throughout the reaction as an easily quantifiable variable associated with the evolution of the photo-Fenton process and its efficiency [45]. Fig. 4a illustrates the evolution of DO as a function of accumulated energy for Runs S1 (HP deficit) and S3 (HP excess). Under the conditions of run S1, a constant decay in the DO concentration was observed (up to 40% of the saturation value

of 7.10 mg L^{-1}) during the progress of the reaction. This observation suggests a Dorfman-type mechanism in the system, where dissolved oxygen actively participates in the oxidative process [22].

However, using an excess of oxidizing agent (Run S3), two distinct behaviours were observed in the evolution of the DO. Initially, for low reaction times, the amount of the oxidizing agent (Fig. 4 b) was insufficient. Considering the high initial reaction rate of the system, a DO consumption of up to 75% of the saturation value was reached. In a subsequent stage, hydrogen peroxide accumulated in the system and began to be in excess (up to 250 mgrL^{-1}). At this point, it initiated parallel reactions, such as self-decomposition and reaction with free radicals, resulting in the production of O_2 and subsequent increase in the DO profile up to 130% of the saturation value (Eq. (3) and Eq. (4)) [25].

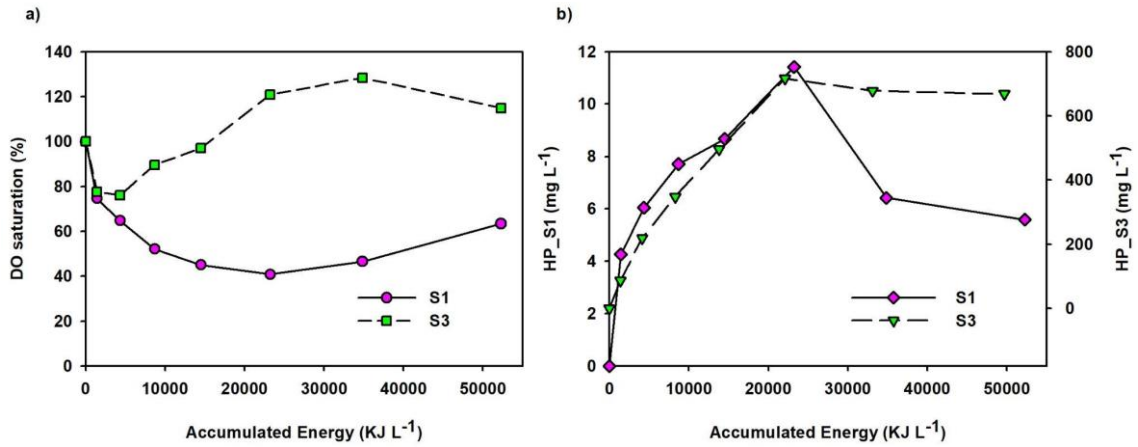

Fig. 4. Evolution of a) DO in percentage of saturation and b) HP concentration vs. accumulated energy.

Analysing the achieved TOC conversion is crucial for assessing the overall effectiveness of the degradation process. In the case of pure water samples (Runs S1-S3), the relative TOC concentration (Fig. 5) values obtained at 180 min ranged between 32.7% and 38.7% (corresponding to conversions between 61.3% and 67.3%). However, an analysis of the system mineralization as a function of accumulated energy reveals that the

presence of detergent and the drug excipients (Run S4 and S5) negatively affected the rate and final conversion of TOC (Fig. 5), only reaching 10% mineralization for the conditions of Run S5 (IW0.1). Indeed, the performance of the photo-Fenton process in the solar pilot plant device surpassed that observed in the laboratory-scale test. The laboratory reactor achieved maximum TOC conversions close to 20% (Run N6), whereas the solar system exhibited enhanced efficiency (up to 67.3% conversion of TOC, Run S2).

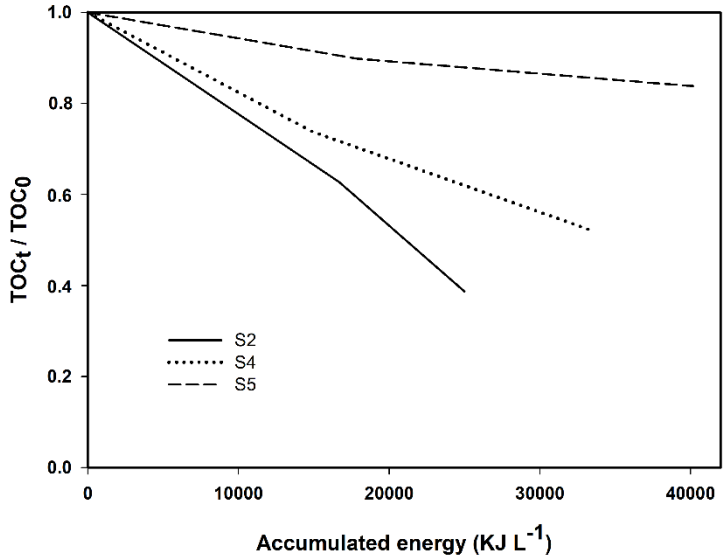

Fig. 5. Relative TOC concentration as a function of accumulated energy (Runs S2, S4 and S5) in the solar reactor experiments.

Finally, the toxicity in the system was evaluated. Fig. 6 depicts the changes in the percentage of inhibition of bioluminescence of *V. fischeri* bacteria after 15 min of incubation (*I(%)*) together with the concentration of HQ (main reaction intermediate detected and quantified) as a function of the accumulated energy.

In each case, the evolution of toxicity in the system was closely linked to the appearance and disappearance of HQ, reaching the maximum *I(%)* when the concentration of HQ in the reaction medium was the highest.

It's noteworthy that for the conditions depicted in Fig. 6a, a significant reduction in the toxicity of the system is observed after only 60 min of reaction (accumulated energy exceeding 1.10E+04 KJL^{-1}). Secondly, it can be seen that IW0.01 matrix did not represent a great addition of the initial toxicity to the system (Fig. 6b). However, a slight slowdown of the reaction was observed, since HQ disappeared at a higher accumulated energy than in the Run S1, which implied that the toxicity in the reaction medium also lasted longer. On the other hand, when the detergent was used at a concentration of 0.1%, there was an extra addition on the initial toxicity of 23.71% caused by only CIP300 at that quantity (blank test). Here, the presence of HQ at the end of the reaction, despite the great accumulated energy, caused that *I(%)* remained high (close to 60%).

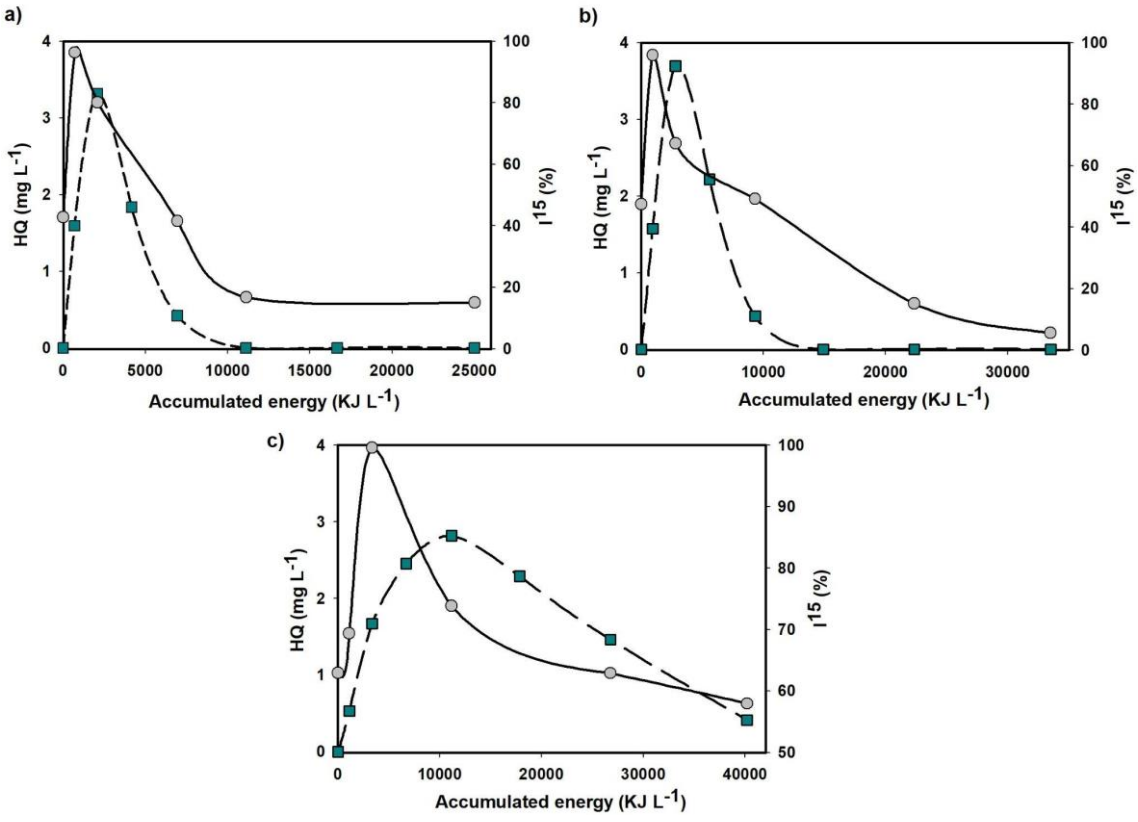

Fig. 6. Percentage of luminescence inhibition at 15 min (●) and HQ concentration (■) vs accumulated energy. a) Run S2 (UW); b) Run S4 (IW0.01) and c) Run S5 (IW0.1). HP = 378 mg L^{-1}.

The HPLC chromatograms are shown in Fig. 7 for Runs S2 and S5, registered at 243 nm (wavelength used to quantify PCT). The disappearance of PCT can be seen (t_r = 7.29 min) and some peaks can be distinguished as reaction intermediates, of which only HQ was identified (t*r* = 5.23 min). Here, the difference between working with ideal and real matrices is also noted. In the case of pure water, PCT and HQ were completely degraded at near 60 min of reaction, while in the simulated effluent there were still low quantities of both analytes at 180 min. Taking into account the low EC_{50} value of HQ (0.04 mg L^{-1}) for *V. fischeri* [46] and the presence of no identified peaks (between 1.5 and 3.3 min), it might be necessary to implement longer reaction times so as to completely reduce the toxicity when working with industrial wastewater.

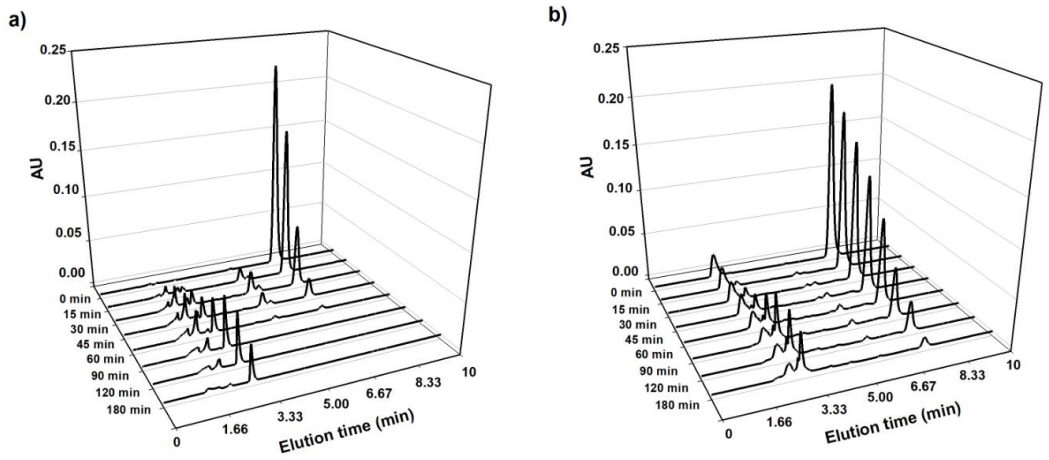

Fig. 7. HPLC chromatograms at 243 nm for solar experiments. a) Run S2 in ultrapure water; b) Run S5 in simulated industrial wastewater with 0.1% CIP300. HP= 378 mgL^{-1}.

4. Conclusions

This study highlights the crucial role of hydrogen peroxide dosing strategies in optimizing the ferrioxalate-assisted solar photo-Fenton process to remove Paracetamol. Through systematic analysis of various dosing methods, this research provides significant insights into their impact on pollutant removal efficiency, oxidant consumption, and toxicity levels across diverse water matrices.

The lab-scale reactor experiments highlighted the role of radiation and the initial point dose of HP on the contaminant conversion efficiency. In particular, irradiation conditions significantly improved the process compared to dark conditions, with high conversion rates. However, excessive doses of HP led to unproductive consumption, which hindered the degradation of contaminants and generated unwanted reaction by-products.

The transition from lab-scale experiments to a pilot plant solar prototype demonstrated the scalability and effectiveness of the photo-degradation process. Nonetheless, challenges emerged when confronting real industrial effluents, demanding extended reaction times to attain comparable conversion rates. The combined effect of UV/visible and thermal sunlight was able to almost completely degrade PCT after 180 minutes of reaction in the case of simulated industrial effluent treated in the solar reactor. However, the persistence of high toxicity levels (IW0.1 matrix) underscores the need for continued research on mitigation strategies for harmful by-products, such as hydroquinone, to ensure the environmental sustainability of wastewater treatment processes.

Overall, this comprehensive approach bridges the gap between laboratory findings and practical applications, providing valuable insights for the development of effective solutions to address pharmaceutical wastewater pollution. The robustness of the solar photo-Fenton process, even under conditions simulating industrial effluents, reaffirms its potential as a sustainable and scalable technology for wastewater treatment in pharmaceutical industries.

Acknowledgments

Bárbara N. Giménez particularly acknowledges to Consejo Nacional de Investigaciones Científicas y Técnicas (CONICET) for the PhD scholarship.

The authors are grateful to Universidad Nacional del Litoral (UNL, CAI+D 2020

50620190100040LI), Consejo Nacional de Investigaciones Científicas y Técnicas (CONICET, PIBAA 28720210100303CO, PIBAA 28720210100301CO and PIP11220210100060CO), and Secretaría de Ciencia, Tecnología e Innovación de la Provincia de Santa Fe (PEICID-2022-161) for financial support.

Authors' contributions

Bárbara N. Giménez: Conceptualization, Formal analysis, Investigation, Methodology, Validation, Visualization, Writing – original draft, Writing – review & editing.

Agustina V. Schenone: Formal analysis, Funding acquisition, Investigation, Methodology, Project administration, Resources, Supervision, Validation, Visualization, Writing – original draft, Writing – review & editing.

Leandro O. Conte: Conceptualization, Formal analysis, Funding acquisition, Project administration, Resources, Supervision, Validation, Writing – original draft Writing – review & editing.

5. References

[1] J. Wang, L. Chu, L. Wojnárovits, E. Takács, Occurrence and fate of antibiotics, antibiotic resistant genes (ARGs) and antibiotic resistant bacteria (ARB) in municipal wastewater treatment plant: An overview, Sci. Total Environ. 744 (2020) 140997. https://doi.org/10.1016/J.SCITOTENV.2020.140997.

[2] P. Chaturvedi, P. Shukla, B.S. Giri, P. Chowdhary, R. Chandra, P. Gupta, A. Pandey, Prevalence and hazardous impact of pharmaceutical and personal care products and antibiotics in environment: A review on emerging contaminants, Environ. Res. 194 (2021) 110664. https://doi.org/10.1016/J.ENVRES.2020.110664.

[3] A. Ziylan-Yavas, D. Santos, E.M.M. Flores, N.H. Ince, Pharmaceuticals and personal care products (PPCPs): Environmental and public health risks, Environ. Prog. Sustain. Energy. 41 (2022) e13821. https://doi.org/10.1002/EP.13821.

[4] R. Silori, V. Shrivastava, A. Singh, P. Sharma, M. Aouad, J. Mahlknecht, M. Kumar, Global groundwater vulnerability for Pharmaceutical and Personal care

products (PPCPs): The scenario of second decade of 21st century, J. Environ. Manage. 320 (2022) 115703. https://doi.org/10.1016/J.JENVMAN.2022.115703.

[5] H.B. Hawash, A.A. Moneer, A.A. Galhoum, A.M. Elgarahy, W.A.A. Mohamed, M. Samy, H.R. El-Seedi, M.S. Gaballah, M.F. Mubarak, N.F. Attia, Occurrence and spatial distribution of pharmaceuticals and personal care products (PPCPs) in the aquatic environment, their characteristics, and adopted legislations, J. Water Process Eng. 52 (2023) 103490. https://doi.org/10.1016/J.JWPE.2023.103490.

[6] J.M. Peralta-Hernández, E. Brillas, A critical review over the removal of paracetamol (acetaminophen) from synthetic waters and real wastewaters by direct, hybrid catalytic, and sequential ozonation processes, Chemosphere. 313 (2023) 137411. https://doi.org/10.1016/J.CHEMOSPHERE.2022.137411.

[7] A. Ulvi, S. Aydın, M.E. Aydın, Fate of selected pharmaceuticals in hospital and municipal wastewater effluent: occurrence, removal, and environmental risk assessment, Environ. Sci. Pollut. Res. 29 (2022) 75609-75625. https://doi.org/10.1007/s11356-022-21131-y.

[8] E.S. Okeke, T.P.C. Ezeorba, C.O. Okoye, Y. Chen, G. Mao, W. Feng, X. Wu, Environmental and health impact of unrecovered API from pharmaceutical manufacturing wastes: A review of contemporary treatment, recycling and management strategies, Sustain. Chem. Pharm. 30 (2022) 100865. https://doi.org/10.1016/J.SCP.2022.100865.

[9] E.M. Jiménez-Bambague, C.A. Madera-Parra, F. Machuca-Martinez, The occurrence of emerging compounds in real urban wastewater before and after the COVID-19 pandemic in Cali, Colombia, Curr. Opin. Environ. Sci. Heal. 33 (2023) 100457. https://doi.org/10.1016/J.COESH.2023.100457.

[10] X. Chen, L. Lei, S. Liu, J. Han, R. Li, J. Men, L. Li, L. Wei, Y. Sheng, L. Yang,

B. Zhou, L. Zhu, Occurrence and risk assessment of pharmaceuticals and personal care products (PPCPs) against COVID-19 in lakes and WWTP-river-estuary system in Wuhan, China, Sci. Total Environ. 792 (2021) 148352. https://doi.org/10.1016/J.SCITOTENV.2021.148352.

[11] A. Jurado, E. Pujades, M. Walther, M.S. Diaz-Cruz, Occurrence, fate, and risk of the organic pollutants of the surface water watch List in European groundwaters: a review, Environ. Chem. Lett. 20 (2022) 3313-3333. https://doi.org/10.1007/s10311-022-01441-w.

[12] S.Y. Wee, N.A.H. Ismail, D.E.M. Haron, F.M. Yusoff, S.M. Praveena, A.Z. Aris, Pharmaceuticals, hormones, plasticizers, and pesticides in drinking water, J. Hazard. Mater. 424 (2022) 127327. https://doi.org/10.1016/J.JHAZMAT.2021.127327.

[13] M. Kumar, R. Silori, P. Mazumder, S.M. Tauseef, Screening of pharmaceutical and personal care products (PPCPs) along wastewater treatment system equipped with root zone treatment: A potential model for domestic waste leachate management, J. Environ. Manage. 335 (2023) 117494. https://doi.org/10.1016/J.JENVMAN.2023.117494.

[14] J. Liu, L. Duan, Q. Gao, Y. Zhao, F. Gao, Removal of Typical PPCPs by Reverse Osmosis Membranes: Optimization of Treatment Process by Factorial Design, Membr. 2023, Vol. 13, Page 355. 13 (2023) 355. https://doi.org/10.3390/MEMBRANES13030355.

[15] T. Wang, J. He, J. Lu, Y. Zhou, Z. Wang, Y. Zhou, Adsorptive removal of PPCPs from aqueous solution using carbon-based composites: A review, Chinese Chem. Lett. 33 (2022) 3585-3593. https://doi.org/10.1016/J.CCLET.2021.09.029.

[16] A. Shah, A. Arjunan, A. Baroutaji, J. Zakharova, A review of physicochemical and

biological contaminants in drinking water and their impacts on human health, Water Sci. Eng. 16 (2023) 333-344. https://doi.org/10.1016/J.WSE.2023.04.003.

[17] X. Chen, H. Rong, P. Ndagijimana, F. Nkinahamira, A. Kumar, D. Guo, B. Cui, Towards removal of PPCPs by advanced oxidation processes: A review, Results Eng. 20 (2023) 101496. https://doi.org/10.1016/J.RINENG.2023.101496.

[18] S. Ziembowicz, M. Kida, Limitations and future directions of application of the Fenton-like process in micropollutants degradation in water and wastewater treatment: A critical review, Chemosphere. 296 (2022) 134041. https://doi.org/10.1016/J.CHEMOSPHERE.2022.134041.

[19] F. Machado, A.C.S.C. Teixeira, L.A.M. Ruotolo, Critical review of Fenton and photo-Fenton wastewater treatment processes over the last two decades, Springer Berlin Heidelberg, 2023. https://doi.org/10.1007/s13762-023-05015-3.

[20] L.O. Conte, A. V. Schenone, B.N. Giménez, O.M. Alfano, Photo-Fenton degradation of a herbicide (2,4-D) in groundwater for conditions of natural pH and presence of inorganic anions, J. Hazard. Mater. 372 (2019) 113-120. https://doi.org/10.1016/j.jhazmat.2018.04.013.

[21] A. Gabet, H. Métivier, C. de Brauer, G. Mailhot, M. Brigante, Hydrogen peroxide and persulfate activation using UVA-UVB radiation: Degradation of estrogenic compounds and application in sewage treatment plant waters, J. Hazard. Mater. 405 (2021) 124693. https://doi.org/10.1016/j.jhazmat.2020.124693.

[22] X. Yu, A. Cabrera-Reina, M. Graells, S. Miralles-Cuevas, M. Pérez-Moya, Towards an Efficient Generalization of the Online Dosage of Hydrogen Peroxide in Photo-Fenton Process to Treat Industrial Wastewater, Int. J. Environ. Res. Public Health. 18 (2021) 13313. https://doi.org/10.3390/ijerph182413313.

[23] D. Rodríguez-García, P. Soriano-Molina, J.L. Guzmán Sánchez, J.L. García

Sánchez, J.L. Casas López, J.A. Sánchez Pérez, A novel control system approach to enhance the efficiency of solar photo-Fenton microcontaminant removal in continuous flow raceway pond reactors, Chem. Eng. J. 455 (2023) 140760. https://doi.org/10.1016/j.cej.2022.140760.

[24] K. Nasr Esfahani, M. Pérez-Moya, M. Graells, Modelling of the photo-Fenton process with flexible hydrogen peroxide dosage: Sensitivity analysis and experimental validation, Sci. Total Environ. 839 (2022). https://doi.org/10.1016/j.scitotenv.2022.155941.

[25] Y. Xiangwei, M. Graells, S. Miralles-Cuevas, A. Cabrera-Reina, M. Pérez-Moya, An improved hybrid strategy for online dosage of hydrogen peroxide in photo-Fenton processes, J. Environ. Chem. Eng. 9 (2021). https://doi.org/10.1016/j.jece.2021.105235.

[26] I. Oller, S. Malato, Photo-Fenton applied to the removal of pharmaceutical and other pollutants of emerging concern, Curr. Opin. Green Sustain. Chem. 29 (2021) 100458. https://doi.org/10.1016/j.cogsc.2021.100458.

[27] N.A. Khan, A.H. Khan, P. Tiwari, M. Zubair, M. Naushad, New insights into the integrated application of Fenton-based oxidation processes for the treatment of pharmaceutical wastewater, J. Water Process Eng. 44 (2021) 102440. https://doi.org/10.1016/J.JWPE.2021.102440.

[28] L.O. Conte, A. V. Schenone, O.M. Alfano, Ferrioxalate-assisted solar photo-Fenton degradation of a herbicide at pH conditions close to neutrality, Environ. Sci. Pollut. Res. 24 (2017) 6205-6212. https://doi.org/10.1007/s11356-016-6400-3.

[29] R.M.R. Santana, D.C. Napoleão, S.G. dos Santos Júnior, R.K.M. Gomes, N.F.S. de Moraes, L.E.M.C. Zaidan, D.R.M. Elihimas, G.E. do Nascimento, M.M.M.B.

Duarte, Photo-Fenton process under sunlight irradiation for textile wastewater degradation: monitoring of residual hydrogen peroxide by spectrophotometric method and modeling artificial neural network models to predict treatment, Chem. Pap. 75 (2021) 2305-2316. https://doi.org/10.1007/s11696-020-01449-y.

[30] P. Soriano-Molina, S. Miralles-Cuevas, B. Esteban García, P. Plaza-Bolaños, J.A. Sánchez Pérez, Two strategies of solar photo-Fenton at neutral pH for the simultaneous disinfection and removal of contaminants of emerging concern. Comparative assessment in raceway pond reactors, Catal. Today. 361 (2021) 17-23. https://doi.org/10.1016/j.cattod.2019.11.028.

[31] P.B. Vilela, M.C. Maria, R.P. Mendonça Neto, F.A.R. de Souza, G.F.F. Pires, C.C. Amorim, Solar photo-Fenton mediated by alternative oxidants for MWWTP effluent quality improvement: Impact on microbial community, priority pathogens and removal of antibiotic-resistant genes, Chem. Eng. J. 441 (2022) 136060. https://doi.org/10.1016/J.CEJ.2022.136060.

[32] E. Gualda-Alonso, P. Soriano-Molina, J.L. Casas López, J.L. García Sánchez, P. Plaza-Bolaños, A. Agüera, J.A. Sánchez Pérez, Large-scale raceway pond reactor for CEC removal from municipal WWTP effluents by solar photo-Fenton, Appl. Catal. B Environ. 319 (2022) 121908. https://doi.org/10.1016/J.APCATB.2022.121908.

[33] G. Lofrano, M. Faiella, M. Carotenuto, S. Murgolo, G. Mascolo, L. Pucci, L. Rizzo, Thirty contaminants of emerging concern identified in secondary treated hospital wastewater and their removal by solar Fenton (like) and sulphate radicals-based advanced oxidation processes, J. Environ. Chem. Eng. 9 (2021) 106614. https://doi.org/10.1016/j.jece.2021.106614.

[34] A. Durán, J.M. Monteagudo, I. San Martín, Operation costs of the solar photo-

catalytic degradation of pharmaceuticals in water: A mini-review, Chemosphere. 211 (2018) 482-488. https://doi.org/10.1016/j.chemosphere.2018.07.170.

[35] L.O. Conte, C.M. Dominguez, A. Checa-Fernandez, A. Santos, Vis LED Photo-Fenton Degradation of 124-Trichlorobenzene at a Neutral pH Using Ferrioxalate as Catalyst, Int. J. Environ. Res. Public Health. 19 (2022). https://doi.org/10.3390/ijerph19159733.

[36] G.D. Silva, E.O. Marson, L.L. Batista, C. Ueira-Vieira, M.C.V.M. Starling, A.G. Trovó, Contrasting the performance of photo-Fenton at neutral pH in the presence of different organic iron-complexes using hydrogen peroxide or persulfate as oxidants for naproxen degradation and removal of antimicrobial activity, Process Saf. Environ. Prot. 147 (2021) 798-807. https://doi.org/10.1016/j.psep.2021.01.005.

[37] M. Pacheco-Álvarez, R. Picos Benítez, O.M. Rodríguez-Narváez, E. Brillas, J.M. Peralta-Hernández, A critical review on paracetamol removal from different aqueous matrices by Fenton and Fenton-based processes, and their combined methods, Chemosphere. 303 (2022) 134883. https://doi.org/10.1016/j.chemosphere.2022.134883.

[38] B.N. Giménez, A. V. Schenone, O.M. Alfano, L.O. Conte, Reaction kinetics formulation with explicit radiation absorption effects of the photo-Fenton degradation of paracetamol under natural pH conditions, Environ. Sci. Pollut. Res. 28 (2021) 23946-23957. https://doi.org/10.1007/s11356-020-11993-5.

[39] B.N. Giménez, L.O. Conte, O.M. Alfano, A. V. Schenone, Paracetamol removal by photo-Fenton processes at near-neutral pH using a solar simulator: Optimization by D-optimal experimental design and toxicity evaluation, J. Photochem. Photobiol. A Chem. 397 (2020) 112584.

https://doi.org/10.1016/j.jphotochem.2020.112584.

[40] B.N. Giménez, L.O. Conte, S.A. Duarte, A. V Schenone, Improvement of ferrioxalate assisted Fenton and photo-Fenton processes for paracetamol degradation by hydrogen peroxide dosage, Environ. Sci. Pollut. Res. 31 (2024) 13489-13500. https://doi.org/10.1007/s11356-024-32056-z.

[41] F. Audino, L.O. Conte, A.V. Schenone, M. Pérez-Moya, M. Graells, O.M. Alfano, A kinetic study for the Fenton and photo-Fenton paracetamol degradation in an annular photoreactor, Environ. Sci. Pollut. Res. 26 (2018) 4312-4323. https://doi.org/10.1007/s11356-018-3098-4.

[42] E. Ono, M. Tokumura, Y. Kawase, Photo-Fenton degradation of non-ionic surfactant and its mixture with cationic or anionic surfactant, J. Environ. Sci. Heal. Part A. 47 (2012) 1087-1095. https://doi.org/10.1080/10934529.2012.668034.

[43] M.C.V.M. Starling, P.H.R. dos Santos, F.A.R. de Souza, S.C. Oliveira, M.M.D. Leão, C.C. Amorim, Application of solar photo-Fenton toward toxicity removal and textile wastewater reuse, Environ. Sci. Pollut. Res. 24 (2017) 12515-12528. https://doi.org/10.1007/s11356-016-7395-5.

[44] L.O. Conte, P. Querini, E.D. Albizzati, O.M. Alfano, Photonic and quantum efficiencies for the homogeneous photo-Fenton degradation of herbicide 2,4-D using different iron complexes, J. Chem. Technol. Biotechnol. 89 (2014) 1967-1974. https://doi.org/10.1002/jctb.4284.

[45] R. Poblete, J. Bakit, Technical and economical assessment of the treatment of vinasse from Pisco production using the advanced oxidation process, Environ. Sci. Pollut. Res. 30 (2023) 70213-70228. https://doi.org/10.1007/s11356-023-27390-7.

[46] A. Santos, P. Yustos, A. Quintanilla, F. García-Ochoa, J.A. Casas, J.J. Rodriguez, Evolution of Toxicity upon Wet Catalytic Oxidation of Phenol, Environ. Sci.

Technol. 38 (2004) 133-138. https://doi.org/10.1021/es030476t.

Doctorado en Ingeniería
mención Ambiental

Título de la obra:

Degradación de Contaminantes Emergentes Presentes en Aguas Reales Empleando Reactores Solares a Escala Planta Piloto

Autor: Bárbara Natalí Giménez

Lugar: Santa Fe, Argentina

Palabras Claves:

Procesos Avanzados de Oxidación,
Reacción foto-Fenton,
Modelado cinético,
Velocidad volumétrica local de absorción de fotones,
Ferrioxalato,
Fotoreactores Solares,
Descontaminación,
Contaminantes Emergentes,
Paracetamol.